UNIVERSITÉ DU QUÉBEC EN ABITIBI-TÉMISCAMINGUE

IMPACT DES GELÉES PRINTANIÈRES SUR LE DÉVELOPPEMENT DES JEUNES PLANTATIONS D'ÉPINETTES BLANCHES, NOIRES ET DE NORVÈGE À L'ÉCOTONE DE LA FORÊT TEMPÉRÉE ET BORÉALE DE L'OUEST DU QUÉBEC

THÈSE
PRÉSENTÉE
COMME EXIGENCE PARTIELLE
DU DOCTORAT EN SCIENCES DE L'ENVIRONNEMENT

PAR
BENJAMIN MARQUIS

DÉCEMBRE 2020

AVANT-PROPOS

Les travaux de recherche présentés dans le cadre de ma thèse de doctorat en sciences de l'environnement effectuée à l'Université du Québec en Abitibi-Témiscamingue s'inscrivent dans un vaste projet qui s'intitule *Établissement de plantations pures et mixtes d'essences améliorées Peupliers hybrides-Épinettes en Abitibi-Témiscamingue.* Ce projet de recherche a, entre autres, comme objectif d'identifier les provenances de peupliers hybrides et d'épinettes qui sont les mieux adaptées aux conditions climatiques (présentes et futures), aux conditions de sol et aux épidémies d'insectes survenant en Abitibi-Témiscamingue. Ce projet a été développé au sein du programme d'infrastructure régionale stratégique pour l'Abitibi-Témiscamingue, dans le volet ressource forestière, du programme de Développement Économique Canada. Le volet analysant la génétique des provenances améliorées est dirigé par la professeure Francine Tremblay, présentement doyenne à la recherche et à la création de l'Université du Québec en Abitibi-Témiscamingue. C'est donc la professeure Tremblay qui a développé et installé, en 2002, les deux dispositifs expérimentaux (plantations) qui ont servi de sites d'étude pour les chapitres un à trois de ma thèse. De plus, la professeure Tremblay a aussi participé au développement des méthodes d'échantillonnage ainsi qu'à la rédaction finale du chapitre quatre. Puisqu'elle a contribué de manière significative au contenu scientifique, elle est coauteur de chacun des articles formant ma thèse.

Mes recherches s'inscrivent aussi à l'intérieur de la Chaire industrielle CRSNG-UQAT-UQAM en aménagement forestier durable, qui est dirigée par mon directeur de recherche, le professeur Yves Bergeron, et concernent spécifiquement l'effet néfaste du gel survenant durant la saison de croissance sur le développement des épinettes en plantation sur la ceinture d'argile de l'ouest du Québec. Mon directeur a contribué de manière importante à toutes les étapes (développement des hypothèse, développement des méthodes d'échantillonnage, analyses et interprétation) déterminantes de mon passage au doctorat, il est donc coauteur de chacun des articles de ma thèse. Puisque mon codirecteur de recherche, le professeur Martin Simard de l'Université Laval, est, entre-autres, spécialisé dans la quantification de l'impact du gel tardif sur le développement des épinettes par l'utilisation de méthodes dendroécologiques (identification des cernes de gel) et parce qu'il est également cochercheur avec la professeure Tremblay sur un projet de recherche provenant d'un programme de subvention de recherche et de développement coopératif (RDC-CRSNG) intitulée *Caractérisation de provenances sélectionnées d'arbres forestiers et identification des causes de la stagnation des plantations établies sur la ceinture d'argile en milieu boréal,* il a, de par le partage de ses connaissances, contribué de manière considérable à l'amélioration du contenu scientifique présenté dans chacun des articles formant ma thèse, c'est pourquoi il figure aussi comme coauteur de chacun des articles. Le projet de recherche a aussi été financé par la compagnie Ryam et la forêt d'enseignement et de recherche du Lac Duparquet.

Un des membres de mon comité d'évaluation, Nelson Thiffault, présentement chercheur à Ressources Naturelles Canada, a été particulièrement intéressé par le quatrième chapitre de ma thèse de doctorat, qui fait état de l'importance des évènements de gel durant la saison de croissance pour expliquer le phénomène de la stagnation de la croissance des plantations d'épinettes à l'échelle du paysage régional de l'Abitibi-Ouest. Comme il a particulièrement aidé à l'élaboration des analyses statistiques ainsi qu'à la rédaction de ce chapitre il en est aussi coauteur.

Le technicien forestier Philippe Duval est coauteur du chapitre quatre parce qu'il a participé activement à la réalisation de l'échantillonnage, à la saisie des données ainsi qu'à sa rédaction finale.

Enfin, j’ai été au cœur de toutes les étapes de mon projet de doctorat, de l’élaboration du cadre conceptuel et des hypothèses jusqu’à la rédaction finale, en passant par la conception des méthodes d’échantillonnage sur le terrain ainsi qu’à la collecte (observation des différents stades de la séquence de débourrement des bourgeons, de l’identification des cernes de gel, de la gestion des capteurs de température de l’air et de la prise de mesure terrain du quatrième chapitre), la saisie des données et les analyses statistiques.

REMERCIEMENTS

J’aimerais d’abord remercier les membres de mon entourage, familles et amis, qui m’ont soutenu et encouragé lors des moments stressants de mon parcours doctoral. C’est grâce à votre soutien quotidien que j’ai pu finalement, au terme de quatre années, déposer une thèse dont je suis fier.

J’aimerais aussi souligner l’importance que mes deux assistantes terrains Lawrence Gervais et Ralitsa Mincheva ont eue dans ce projet. Elles m’ont aidé à installer les capteurs de la température de l’air, mesurer la hauteur des arbres, identifier les stades de la séquence du débourrement des bourgeons, former le dispositif de butte pour analyser l’effet de la microtopographie sur la température de l’air, sabler les galettes d’arbres et saisir les données qui ont été amassées lors des deux campagnes terrains nécessaires à l’accomplissement de ce projet de recherche.

Je tiens à remercier le forestier Philippe Duval qui m’a aidé à identifier les différents stades de la séquence de débourrement des bourgeons des épinettes et qui a effectué, en partie avec moi, l’inventaire terrain et la saisie des données qui ont servie dans mon quatrième chapitre. Il a aussi coupé les arbres qui ont été utilisés pour le développement des séries de cernes de gel.

J’adresse aussi mes remerciements à tous les membres de l’Université du Québec en Abitibi-Témiscamingue, particulièrement à Danièle Laporte ainsi qu’à Marie-Hélène Longpré pour leur aide logistique et administrative. Je suis aussi reconnaissant envers les membres du Centre d’étude de la forêt: Danielle Charron, pour son aide logistique lors du terrain, Mélanie Desrochers, pour son aide avec les données géospatiales, Daniel Lesieur, pour son aide à monter ma base de données, ainsi que François Rousseau pour ses conseils pour les analyses statistiques entreprises dans ma thèse. Je remercie aussi le personnel de la Forêt d’enseignement et de recherche du lac

Duparquet, Raynald Julien et Marie Robin, ainsi que tous les étudiants qui ont séjourné à la station de recherche lorsque j'y étais, plus particulièrement Alexandre Nolin et Samuel Proulx, pour leurs échanges, leurs discussions et les parties enlevantes de soccer sur table que nous avons jouées.

Je remercie mon directeur, Yves Bergeron, pour son apport scientifique toujours très avisé, pour sa grande implication, pour ses encouragements qui m'ont permis d'aller jusqu'au bout de ce projet de recherche, et pour m'avoir intégré dans la grande et dynamique équipe de recherche de l'Institut de recherche sur les forêts et de la Forêt d'enseignement et de recherche du lac Duparquet. Je remercie mon co-directeur Martin Simard de l'université Laval pour le partage de ses connaissances, surtout au niveau de l'écriture de texte scientifique.

DÉDICACE

À mon amoureuse, Audrey Boisvert,
qui par ses encouragements, son écoute et son soutien moral, m’a aidé à compléter mon cheminement aux études supérieures.

Son impressionnante force de caractère lui a permis de tenir le fort familial lors de moments d’éloignement.

Pour témoigner de mon amour et pour te remercier de tous les efforts que tu as fournis durant mon parcours au doctorat, je te dédie ce présent ouvrage, que tu connais par cœur de toute façon, m’ayant écouté des heures durant réfléchir tout haut sur des sujets qui me passionnent, dont l’effet du gel printanier sur la séquence de débourrement des bourgeons.

Je t’aime et te remercie de partager ta vie avec la mienne

TABLE DES MATIÈRES

LISTE DES FIGURES

LISTES DES TABLEAUX

LISTES DES ABRÉVIATIONS, DES SYGLES ET DES ACRONYMES

Abréviation	Définition
am	*Ante meridiem*
a.s.l.	Above seas level
CDM	Continuous developmental model
CRSNG	Conseil de recherches en sciences naturelles et en génie
Daily max temp.	Daily maximum temperature in °C
Daily mean temp.	Daily mean temperature in °C
Daily min temp.	Daily minimum temperature in °C
DOY	Day of year
Frost prob.	Frost probability
GS	Growing season
IPCC	Intergovernmental panel on climate change
MAT	Mean annual temperature
NSERC	Natural Sciences and Engineering Research Council of Canada
RDC	Recherche et développement coopératif
UQAM	Université du Québec à Montréal
UQAT	Université du Québec en Abitibi-Témiscamingue

LISTES DES SYMBOLES ET DES UNITÉS

AICc	Corrected Akaike's information criteria
AICc Wt.	Corrected Akaike's weight
cm	Centimètre
cm y^{-1}	Cm per year
Conditional pseudo-R^2	Amount of explained variance by both fixed and random effects
Cum. Wt.	Cumulative weight
°C	Degrés celsius
°C days	Degree celsius per day
°E	Longitude in degree East
°N	Latitude in degree North
°W	Longitude in degree West
GDD	Growing degree-days
GDD max	Growing degree-days calculate using the maximum daily temperature with a base temperature of 0 °C
GDD mean	Growing degree-days calculate using the mean daily temperature with a base temperature of 0 °C
ha	Hectare
Km	Kilomètre

Marginal pseudo-R^2	Amount of explained variance by the fixed effects when using mixed effect models
m	Mètre
mm	Millimètre
m^2	Mètre carré
min	Minute
n	Taille d’échantillon
Pseudo-R^2	Amount of explained variance when using generalised regression models
R^2	Amount of explained variance when using a simple linear regression
SE	Standard error
um	Micromètre
%	Pourcentage
α	Seuil alpha égal à 0.05 pour déterminer la significativité d’un test statistique

RÉSUMÉ

L'aménagement de zones réservées à la production ligneuse intensive permet d'augmenter la productivité forestière et peut, du même coup, aider à diminuer la pression de coupe sur la forêt naturelle tout en profitant aux industries transformant la ressource ligneuse.

Toutefois, la remise en production de territoire forestier récolté n'est pas garantie et peut mener à des échecs de régénération, ce qui compromet l'aménagement durable du territoire. Les échecs survenant après le reboisement se produisent lorsque les traitements sylvicoles ainsi que la préparation de terrain ne sont pas adaptés aux exigences physiologiques de l'espèce que l'on souhaite remettre en production. L'épinette blanche (*Picea glauca* [Moench] Voss) est l'une des principales espèces utilisées pour le reboisement, surtout en forêt boréale mixte, mais les échecs de régénération de cette espèce sont fréquents, notamment dans la ceinture d'argile du Québec. Pour comprendre les déterminants environnementaux et physiologiques menant à la stagnation de la croissance de cette espèce, le développement de quelques provenances d'épinette blanche, dont une locale de la forêt boréale mixte, a été comparé au développement d'une provenance d'épinette noire (*Picea mariana* [Mill.] B.S.P.) locale de la forêt boréale mixte, ainsi qu'au développement de quelques provenances d'épinette de Norvège (*Picea abies* [L.] Karst.), une espèce étrangère, mais qui possède un potentiel de croissance élevé.

L'hypothèse générale défendue dans cette thèse pour expliquer la stagnation de la croissance de l'épinette blanche sur la ceinture d'argile soutient que la présence des argiles humides ralentie le réchauffement du sol et accentue le phénomène d'inversion de la température de l'air, ce qui génère de fréquents évènements de gel printanier qui endommagerait les méristèmes (apicaux et latéraux) responsables de la croissance en hauteur et en diamètre, respectivement. Ces dommages ont respectivement comme conséquence de retarder la croissance en hauteur des arbres et de former des cernes de gel dans les cernes de croissance.

Dans cette thèse, déclinée en quatre chapitres, l'effet négatif du gel sur le développement des épinettes a été quantifié au niveau de l'arbre et au niveau du paysage régional de l'Abitibi-Ouest. Les études faisant l'objet des trois premiers chapitres ont été effectué au niveau de l'arbre dans deux plantations expérimentales établies en 2002 dans la forêt boréale mixte (Forêt d'enseignement et de recherche du lac Duparquet) et la forêt tempérée (Angliers). Le premier chapitre s'intéresse aux facteurs environnementaux (probabilité de gel, température et photopériode) déterminant la séquence de débourrement des bourgeons. Le deuxième chapitre quantifie à la sévérité des dommages aux cellules cambiales causés par le gel ainsi que

son impact sur la croissance en hauteur. Le troisième chapitre quantifie l'importance de la topographie et de la microtopographie sur la température minimale et la probabilité de gel survenant durant la saison de croissance. Le quatrième et dernier chapitre s'effectue au niveau du paysage régional de l'Abitibi-Ouest et s'intéresse aux facteurs topographiques et biotiques (espèces, âge) expliquant le mieux la croissance des arbres et leurs dommages causés par le gel.

Dans le premier chapitre, il a été démontré que la séquence de débourrement des bourgeons était d'abord déclenchée par la probabilité d'occurrence de gel et la photopériode, puis répondait à l'augmentation de la température de l'air. Spécifiquement, l'ouverture plus hâtive des bourgeons de l'épinette blanche comparativement à l'épinette noire et à l'épinette de Norvège était déclenchée par une plus grande sensibilité à la photopériode, surtout en forêt tempérée, ce qui augmente leur exposition aux gelées printanières. De plus, l'analyse intraspécifique a montré que, lorsque planté au nord, les provenances d'épinettes blanches du sud étaient plus sensibles à la photopériode que la provenance naturellement résidente à la forêt boréale mixte, ce qui déclenche l'ouverture plus hâtive de leurs bourgeons. Donc, dans les environnements où le dommage par le gel est rare, l'ouverture des bourgeons est contrôlée par la photopériode alors que dans les environnements où le dommage par le gel est plus fréquent, l'ouverture des bourgeons est contrôlée par la température.

Au deuxième chapitre, il a été établi que la croissance en hauteur des trois espèces d'épinettes étudiées était réduite plus la sévérité des dommages aux cellules cambiales était forte. De plus, l'épinette blanche est l'espèce qui présente la plus forte réduction en hauteur à la forêt boréale mixte. Au niveau intraspécifique, la hauteur des provenances d'épinettes blanches du sud était réduite comparativement à la hauteur de l'épinette blanche locale. Cependant, le gel printanier ne semble réduire la croissance en hauteur que sur les premiers deux mètres de hauteur, donc, planter des arbres plus grands et sur des buttes pourrait réduire la durée de la période de suppression de la croissance. Enfin, la croissance en hauteur des arbres était mieux prédite par la température minimale du mois de mai que par la température moyenne annuelle.

Au troisième chapitre, il est démontré que lors d'évènements de gel, le phénomène d'inversion de la température de l'air a permis la formation de pochettes de gel dans le bas des pentes où la température a atteint -2 °C, comparativement au haut des pentes où la température minimale a atteint 2 °C. L'importance de la microtopographie augmente aux endroits où le gel printanier est moins fréquent, comme en forêt tempérée. Cependant, dans les environnements où le gel printanier est fréquent, comme à la forêt boréale mixte, l'élévation est la variable la plus importante pour prédire l'intensité et la probabilité de gel survenant durant la saison de croissance. Cette forte variation de température sur un court gradient d'élévation peut probablement aussi expliquer la grande variation en hauteur intraspécifique observée à même une plantation.

Au dernier chapitre, il est montré que le phénomène de la stagnation de la croissance est important à l'échelle du paysage régional de l'Abitibi-Ouest, surtout pour l'épinette blanche, puisque même si l'arbre le plus haut de chaque parcelle suit le développement prédit par les courbes de croissance développées par le gouvernement, à l'intérieur d'une parcelle, il y a une forte variabilité en hauteur entre l'arbre le plus grand et l'arbre le plus petit (~2 mètres). Par surcroît, les arbres sont les plus petits lorsqu'ils sont plantés dans le bas des pentes de forme concave.

Les travaux de recherche présentés dans cette thèse ont montré que les évènements de gel survenant durant la saison de croissance se produisent fréquemment à l'écotone de la forêt tempérée et boréale et pourrait causer le phénomène de la stagnation de la croissance des plantations d'épinettes sur la ceinture d'argile. Puisque l'épinette blanche s'expose plus aux gelées printanières, cette espèce est plus sévèrement affectée par le gel que l'épinette noire. Suivant les résultats obtenus par l'analyse de tige nous avons élaborer des recommandations pratiques pour limiter la perte de productivité des plantations associée au gel printanier. Nos travaux ont aussi mené à des avancées théoriques qui remettent en question la mécanique des modèles écophysiologiques expliquant le débourrement des bourgeons en plus de discuter de l'effet des changements climatiques sur la future séquence de développement des bourgeons et de la productivité des plantations d'épinettes à l'avenir. Les connaissances acquises par les travaux de recherche menés dans le cadre de ma thèse montrent que les évènements climatiques extrêmes survenant lors de moments spécifiques du cycle de dormance-croissance ont des conséquences plus importantes sur la physiologie et la croissance des arbres que les variables climatiques agrégées et contribuent à l'aménagement durable de la forêt boréale mixte de l'ouest du Québec.

Mots-clés: Aménagement forestier durable, Cernes de gel, Gelées d'été, *Picea*, Productivité forestière

INTRODUCTION

La remise en production de territoire forestier récolté ou suivant le passage d’une perturbation majeure comporte plusieurs défis, surtout en forêt boréale mixte (Grossnickle, 2000). Les jeunes plants doivent surmonter la forte compétition pour l’espace, la lumière, les nutriments et l’impact des plantes compétitrices comme les espèces éricacée (Lieffers et Stadt, 1994; Thiffault, Titus et Munson, 2004). Les jeunes plants doivent aussi tolérer un environnement froid, mais qui, durant l’été, peut devenir chaud et sec (Hänninen, 2016). De plus, les fortes variations journalières de la température de l’air contribuent à augmenter le stress hydrique durant le jour ainsi qu’à augmenter la probabilité de subir un évènement de gel durant la nuit (Man et Lieffers, 1999). Lorsque la nouvelle pousse est endommagée par le gel, sa capacité photosynthétique diminue ce qui limite sa croissance (Örlander, 1993; Langvall, Nilsson et Örlander, 2001). Donc, l’incapacité des jeunes plants à surmonter ces défis peut mener au problème de stagnation de la croissance, une période où la croissance apicale peut être fortement réduite (Mullin, 1963; de Montigny et Weetman, 1990; Vyse, 1981) et entraîner des malformations similaires à celles observées à la limite des arbres telles que la présence d’une forme prostrée et la formation de tiges multiples (Dy et Payette, 2007; Pereg et Payette, 1998; Payette et al., 1996). Ce retard de croissance réduit la quantité, la qualité et la valeur du bois, en plus d’augmenter le temps nécessaire pour atteindre la maturité commerciale. Cela vient compromettre l’aménagement de la forêt boréale mixte, en plus de faire changer les caractéristiques écologiques du milieu, en faisant passer un ancien milieu productif à un milieu de faible productivité (Fenton et al., 2005; Simard et al., 2007). Ces problèmes se retrouvent dans l’ensemble de la forêt boréale mixte, mais, selon les caractéristiques propres aux différents milieux comme le type d’espèces, l’intensité de l’aménagement forestier et le type de sol, l’importance du phénomène de la stagnation de la croissance peut varier d’une région à l’autre (Groot et Carlson, 1996; Langvall et Löfvenius, 2002; Mullin, 1963; Vyse, 1981).

Ce retard de croissance pourrait s’expliquer par les évènements de gel qui surviennent durant la saison de croissance (Clements, Fraser et Yeatman, 1972). Le bourgeon apical des jeunes plants n’est pas assez haut pour sortir de la zone de gel au sol et pourrait régulièrement être endommagé, permettant donc la reprise de la croissance apicale par des bourgeons latéraux ce qui causerait la forme prostrée des arbres ainsi que le problème de tige multiple (Clements, Fraser et Yeatman, 1972; Dy et Payette, 2007; Langvall et Löfvenius, 2002). De plus, l’écorce mince des jeunes plants n’offre pas une capacité isolante suffisante pour protéger le cambium des évènements de gel printanier, ce qui peut endommager les cellules cambiales et former des séries de cellules déformées, appelé cerne de gel, à l’intérieur d’un cerne de croissance (Glerum et Farrar, 1966; Payette, Delwaide et Simard, 2010; Schweingruber, 2007). Le recensement des cernes de gel par l’utilisation de méthodes dendroécologiques permet de reconstruire les évènements de gel et permet donc de mieux comprendre la fréquence des évènements de gel passée ainsi que leur impact sur les arbres (Dy et Payette, 2010; Gurskaya et Shiyatov, 2002; LaMarche et Hirschboeck, 1984; Payette, Delwaide et Simard, 2010). Cette méthode dendroécologique est utile puisque les évènements de gel printanier sont difficiles à mesurer sur le terrain étant donné leur courte durée et parce qu’ils sont spatialement localisés (Chung et al. 2006; Laughlin et Kalma, 1987; Lindkvist et Lindqvist, 1997). La formation d’un évènement de gel printanier requiert la présence d’un ciel sans nuages, avec un minimum de vent, pour permettre la stratification des masses d’air selon leur densité (Oke, 1987). Comme l’air froid est plus dense que l’air chaud, les masses d’air froid restent près du sol et peuvent s’accumuler au creux des dépressions topographiques (Dugas, 1975; Dy et Payette, 2007; Laughlin et Kalma, 1987; Langvall, Nilsson et Örlander, 2001; Lindkvist et Lindqvist, 1997). Ce phénomène météorologique est aussi appelé une inversion de la température de l’air puisqu’au lieu de diminuer en fonction de l’élévation, la température de l'air augmente avec l'élévation (Wallace et Hobb, 2006). Les arbres subissant ces évènements d'inversion de la température de l'air peuvent, par irradiation, perdre plus de chaleur durant la nuit qu'il n'en avait accumulé durant le jour, ce qui peut mener à la formation de cristaux de glace à l'intérieur de leurs tissus et endommager leurs deux méristèmes (apical et latéral) (Dy et Payette, 2007; Langvall et Ottosson-Löfvenius, 2002). Cependant, les études qui s'intéressent à l'impact des inversions de la température de l'air sur le développement de la végétation sont surtout effectuées au nord de la forêt boréale ou à la limite altitudinale des arbres (Kollas, Körner et Randin, 2014; Körner et al., 2016; Lenz, et al., 2016; Plasse et Payette, 2015). À ces endroits, les évènements de gel peuvent survenir tous les deux à huit jours et être plus intenses dans les dépressions topographiques, empêchant ainsi l'établissement des arbres dans ces dépressions et inversant aussi la limite des arbres (Payette et Delwaide, 2018; Plasse et Payette, 2015). De plus, la limite de répartition latitudinale et altitudinale de plusieurs espèces d'arbres de la forêt décidues dans les Alpes suisses correspond mieux à l'occurrence d'évènements de gel se produisant durant la saison de croissance, comparativement à la température moyenne annuelle (Kollas, Körner et Randin, 2014). Les évènements de gel peuvent donc fortement affecter l'établissement, la croissance et la survie des arbres à leur limite de répartition (Inouye, 2008; Du et al., 2019). Toutefois, la fréquence et l'intensité des évènements de gel restent méconnues pour la forêt boréale mixte; l'endroit où le phénomène de stagnation de la croissance des plantations est observé.

Puisque l'occurrence des évènements de gel printanier semble dépendre des conditions locales du milieu physique, ce phénomène météorologique est difficile à anticiper et est, par le fait même, rarement considéré lors de l'établissement des plantations. Toutefois, certains pays d'Europe du nord comme la Suède et la Norvège utilisent le scarifiage par monticule pour planter les arbres sur des buttes artificiellement formées (Hjelm, Nilsson et Örlander, 2012; Langvall, Nilsson et Örlander, 2001; Tolvanen et Kubin, 1990). Cette position surélevée permettrait de maintenir le bourgeon apical hors de la zone de gel au sol et pourrait ainsi diminuer la durée de la stagnation de la croissance (Hjelm, Nilsson et Örlander, 2012; Langvall, Nilsson et Örlander, 2001).

Au Québec et en Ontario, le phénomène de stagnation de la croissance est surtout observé dans le cas des plantations d'épinettes établies dans la ceinture d'argile (Mullin, 1963). Le sol argileux étant compact, il ne permet pas un drainage rapide de l'eau vers les horizons plus profond du sol. Le réchauffement du sol au printemps pourrait être ralentie par la forte humidité à sa surface et accentuer le problème de stagnation de la croissance des plantations d'épinettes comparativement aux autres régions de la forêt boréale mixte (Dugas, 1975; Mullin, 1963). De plus, le relief vallonné de la ceinture d'argile favorise le drainage de l'air froid et de l'eau vers les dépressions topographiques, ce qui peut localement accentuer le problème de stagnation de la croissance au niveau de l'arbre (Chung et al. 2006; Dugas, 1975; Laamrani et al., 2014; Laughlin et Kalma, 1987; Lindkvist et Lindqvist, 1997). Cependant, le problème de stagnation de la croissance semble être plus important pour l'épinette blanche que pour l'épinette noire (Clements, Fraser et Yeatman, 1972), ce qui ne peut pas s'expliquer que par les attributs physiques permanents du milieu, donc, les mécanismes physiologiques expliquant cette différence de capacité à croître restent encore à élucider.

Suivant le réchauffement de la température de l'air causé par les changements climatiques, il est attendu que le débourrement des bourgeons s'effectuera plus hâtivement au printemps (Olsson, Olin, Lindström, et Jönsson, 2017; Parmesan et Yohe, 2003; Piao et al., 2007; Polgar et al., 2013), ce qui pourrait prolonger la saison de croissance (Bertin, 2008; Rossi, Girard et Morin, 2014), mais, du même coup, augmenterait aussi l'exposition des arbres aux gelées printanière (Ault et al., 2013; Cannell et Smith, 1986; Liu et al., 2018; Ma et al., 2018). De plus, dû aux variations intra-espèces dans la séquence de débourrement des bourgeons, les populations du sud ne devraient pas répondre de la même manière que les populations du nord à la future augmentation de la température de l'air, à la future l'intensité et à la future fréquence des évènements de gel printanier (Chen et al., 2019; Clark et al., 2014; Li et al., 1997; Olson et al., 2013; Villeneuve et al., 2016). Une mauvaise synchronicité entre le débourrement des bourgeons et le climat futur pourrait contrebalancer l'augmentation de la productivité qui est aussi attendu avec les changements climatiques (D'Orangeville et al., 2018; Lu et Man, 2011; Man et al., 2009).

Pour maintenir et même augmenter la productivité des futures plantations, effectuer de l'aménagement intensif en utilisant des provenances éloignées des sites de plantations (migration assistée) qui présenteraient de meilleures adaptations aux conditions climatiques futures que les provenances résidentes naturellement près des sites de plantation devient une pratique d'aménagement forestier phare (Beaulieu, 2009; Lu et al., 2014; Marris, 2009; McKenny, Pedlar et O'Neill, 2008). Puisque l'aire de répartition de l'épinette blanche et de l'épinette noire couvre une grande partie du nord-est de l'Amérique du Nord, ces deux espèces sont constituées de plusieurs populations qui vivent dans différents domaines bioclimatiques et qui se sont localement adaptées à leur environnement immédiat (Andalo et al., 2005; Li et al., 1997; Rossi, 2015; Villeneuve et al., 2016). On peut donc conclure que ces deux espèces représentent un bon modèle pour identifier les variations dans le développement des différentes provenances. De plus, l'utilisation d'espèces étrangères possédant un plus fort potentiel de croissance que les espèces natives doit aussi être envisagé (Pedlar et al., 2011). Par exemple, l'utilisation de l'épinette de Norvège, qui possède un meilleur potentiel de croissance que l'épinette blanche et que l'épinette noire pourrait aider à améliorer la croissance des plantations (Dehayes, Dickmann et Lemmien, 1980). Toutefois, la capacité de cette espèce étrangère à croître dans un nouvel environnement reste à déterminer. Ainsi, l'identification des espèces et des provenances les mieux adaptées aux conditions climatiques futures est un objectif important à réaliser pour l'aménagement durable de la forêt boréale mixte et passe par la compréhension des mécanismes physiologiques contrôlant le cycle de dormance-croissance des différentes espèces et provenances. Suivant cet objectif, l'identification des déterminant environnementaux de la stagnation de la croissance des plantations d'épinettes (blanches, noires et de Norvège) sur la ceinture d'argile de l'ouest du Québec a été entrepris dans cette thèse.

0.1 Caractéristique de la région d'étude

L'écotone de la forêt tempérée et boréale de l'ouest du Québec se retrouve enchâssé entre la forêt tempérée nordique au sud et la forêt boréale au nord (Saucier, Bergeron, Grondin et Robitaille, 1998; Saucier, Baldwin, Krestov et Jorgenson, 2015). Cette zone de transition, aussi appelé hémiboréale, forme la forêt boréale mixte, qui est constituée de peuplements forestiers d'espèces de feuillus et de conifères mélangés (Saucier, Baldwin, Krestov et Jorgenson, 2015). La partie sud de cette zone de transition forme le domaine bioclimatique de la sapinière à bouleau jaune et les peuplements forestiers qu'on y retrouvent sont constitués de feuillus atteignant la limite de leur aire de répartition tels que le bouleau jaune (*Betula alleghaniensis* Britt.), l'érable à sucre (*Acer saccharum* Marsh.) et l'érable rouge (*Acer rubrum* L.), ainsi que certains feuillus qui s'étendent jusque dans la zone boréale comme le peuplier faux-tremble (*Populus tremuloides* Michx.) et le bouleau blanc (*Betula papyrifera* Marsh.) qui sont mélangés au sapin baumier (*Abies balsamea* [L.] Mill.), à l'épinette blanche et, dans les plus vieux peuplements, au thuya occidental (*Thuja occidentalis* L.) (Saucier, Bergeron, Grondin et Robitaille, 1998; Saucier, Baldwin, Krestov et Jorgenson, 2015). Plus au nord, on atteint le domaine bioclimatique de la sapinière à bouleau blanc (Saucier, Bergeron, Grondin et Robitaille, 1998). Les peuplements forestiers y sont constitués de peuplements principalement résineux de sapin baumier mélangé à l'épinette blanche et à l'épinette noire, ainsi qu'au bouleau blanc et au peuplier faux-tremble (Saucier, Bergeron, Grondin et Robitaille, 1998; Saucier, Baldwin, Krestov et Jorgenson, 2015). À l'ouest du Québec, le sol de cette zone de transition de la végétation est formé de dépôts glacio-lacustres argileux issus du retrait de la calotte glaciaire des Laurentide et du drainage du lac pro-glaciaire Ojibway, qui, en se retirant, a mené à la formation de sol du type Gleysol et Luvisol, dans un paysage généralement plat intercalé de colline où l'élévation au-dessus du niveau de la mer varie entre 260 et 362 mètres (Laamrani *et al.*, 2014; Veillette, 1994).

À l'intérieur de cette région d'étude, trois sites ont été ciblés pour effectuer les travaux présentés dans cette thèse (Figure 0.1). Les deux premiers sites sont deux plantations de cinq hectares, établies en 2002, et situées dans un axe sud-nord, séparées par 115 km. La plantation située la plus au sud est établie dans le domaine bioclimatique de la sapinière à bouleau jaune (47.29° N; 79.12° O), la température moyenne annuelle y est de 3 °C, la température moyenne au mois de juillet et de janvier y est de 18 °C et de -15 °C respectivement, la saison de croissance dure en moyenne 165 jours, il s'y accumule 2660 degrés-jours de croissance (seuil de 0 °C) et le dernier jour de gel y est généralement vers la mi-juin (1981-2010 Normales climatiques, station climatique Barrage Angliers, située à 24 km de la plantation; Environnement Canada 2019a). La plantation située la plus au nord est établie dans le domaine bioclimatique de la sapinière à bouleau blanc (48.29° N; 79.26° O). La température moyenne annuelle y est de 1 °C, la température moyenne des mois de juillet et de janvier y est de 17 °C et de -18 °C, la saison de croissance dure environ 143 jours, il s'y accumule 2282 degrés-jours de croissance (seuil de 0 °C) et le dernier jour de gel peut survenir jusqu'en juillet (1981-2010 Normales climatiques, station climatique Mont Brun, située à 47 km de la plantation; Environnement Canada 2019b). La photopériode, durant l'été, est allongé de huit minutes au site le plus au nord comparativement au site le plus au sud (Calculatrice des levers et couchers du soleil, Environnement Canada, 2019c).

Projection : NAD 1983 MTM 10 | Source : MFFP, 2018 | Auteur : CEF, 2019

Figure 0.1 Emplacement des deux plantations dans la forêt tempérée nordique et boréale mixte du Québec (Canada).

À ces deux plantations (Figure 0.2), 20 provenances d’épinettes blanches de l’Ontario et du Québec incluant une provenance naturellement résidente de la forêt boréale mixte, 20 provenances d’épinettes de Norvège provenant de Bioélorussie, de Pologne et de Lettonie, ainsi qu’une provenance d’épinette noire résidente de la forêt boréale mixte issue de la banque de graine du Centre de foresterie des Laurentides ont été plantées. Les caractéristiques similaires en structure et en texture du sol argileux (Laamrani *et al.*, 2014; Veillette, 1994) ainsi que la différence négligeable de la durée de la photopériode entre les deux plantations, permettent d’analyser *in situ* l’effet de différentes variables climatiques relié à la température de l’air sur le développement des différentes espèces et provenances de graines testées tout en contrôlant pour la photopériode et le sol.

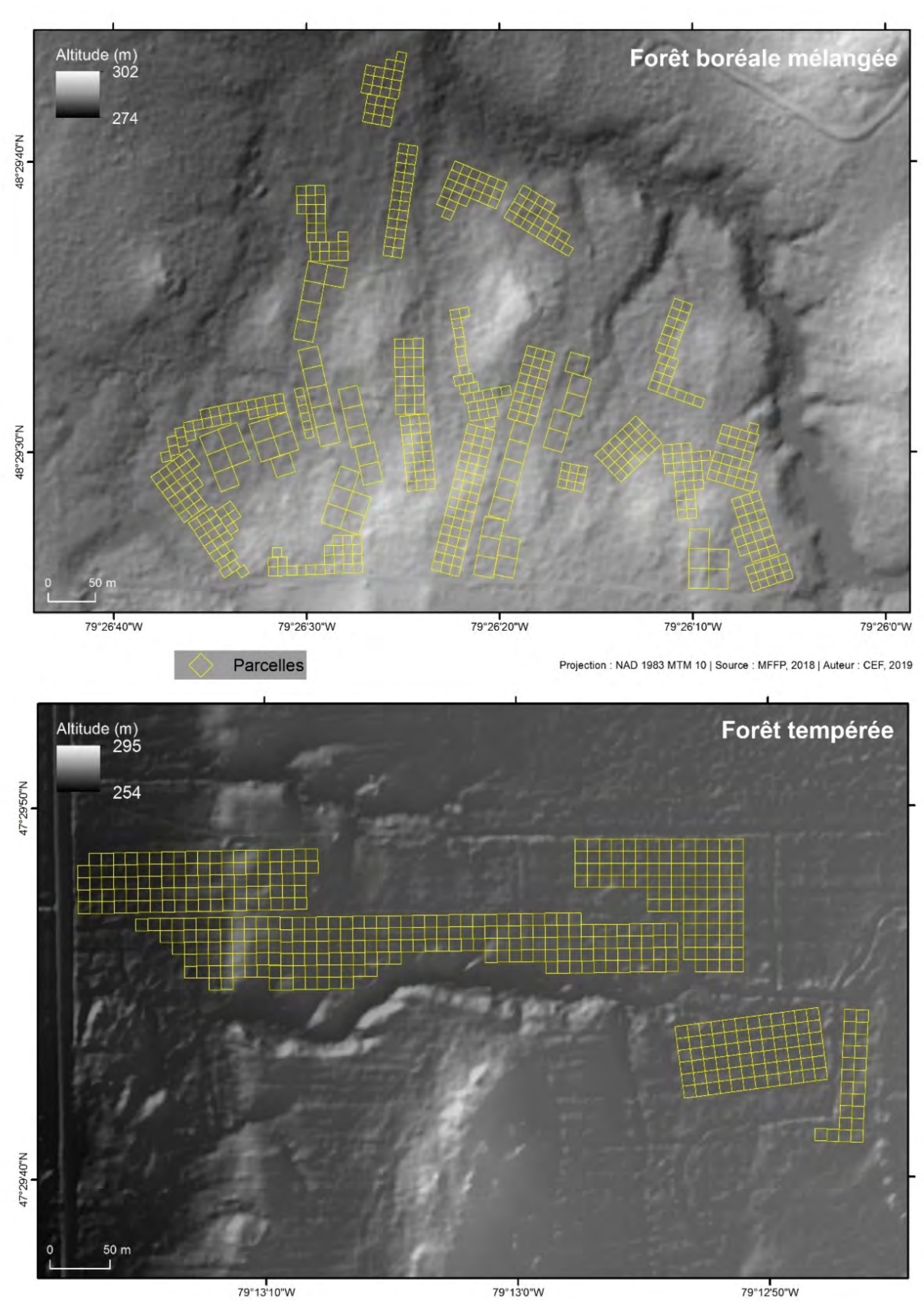

Projection : NAD 1983 MTM 10 | Source : MFFP, 2018 | Auteur : CEF, 2019

Figure 0.2 Le design expérimental montrant les parcelles où sont plantés les arbres, ainsi que le relief aux deux sites de plantations.

Le troisième site d’étude (Figure 0.3) est situé sur la ceinture d’argile, dans le domaine bioclimatique de la sapinière à bouleau blanc et a permis d’évaluer l’importance du phénomène de la stagnation de la croissance des épinettes à l’échelle régionale de l’Abitibi-Ouest. Nous avons mesuré la hauteur de tous les arbres mesurant plus d’un mètre se trouvant à l’intérieur de 428 parcelles de 3,57 mètres de rayon, échantillonnées dans un réseau de 66 jeunes plantations d’épinettes blanches et d’épinettes noires âgées entre 6 et 13 ans, couvrant au moins 1 hectare.

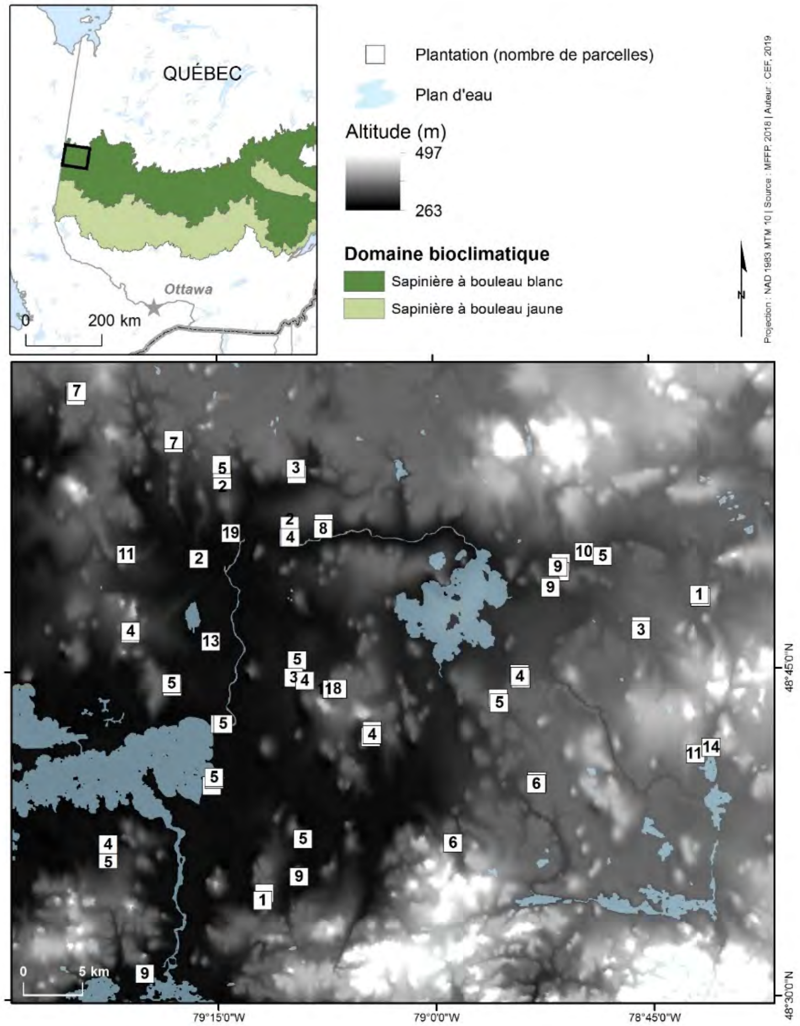

Figure 0.3 Réseau de plantations inventoriées en forêt boréale mixte du Québec (Canada) ainsi que le nombre de parcelles échantillonnées dans chaque plantation.

0.2 Objectifs et structure de la thèse

L’objectif principal de cette thèse est d’identifier les déterminants environnementaux de la stagnation de la croissance des plantations d’épinettes sur la ceinture d’argile de l’ouest du Québec. Pour expliquer cette faible croissance, nous avançons l’hypothèse que les évènements de gel survenant durant la saison de croissance endommagent les deux méristèmes (apical et latéral), ce qui ralentit la croissance en hauteur.

Cette thèse se divise en deux volets et quatre chapitres. Le premier volet vise à déterminer si la stagnation de la croissance de l’épinette blanche est due à une plus forte sensibilité ou à une exposition accrue aux gelées printanières, en comparant le développement de quelques provenances d’épinettes blanches, dont une locale de la forêt boréale mixte, au développement d’une provenance d’épinette noire locale de la forêt boréale mixte, ainsi qu’au développement de quelques provenances d’épinette de Norvège, une espèce étrangère, mais possédant un potentiel de croissance élevé. Pour se faire, des observations précises du développement des arbres, au niveau de l’individu, ont été récoltées, et ce, dans les deux plantations établies en 2002 de chacun des deux côtés de l’écotone de la forêt tempérée et boréale. Le premier chapitre analyse la séquence de débourrement des bourgeons. Le deuxième chapitre analyse la croissance en hauteur et la sévérité des dommages aux cellules cambiales causés par le gel et le troisième chapitre analyse l’importance des attributs physiques permanents du milieu ainsi que du microsite de plantation sur l’occurrence de gel printanier.

Les objectifs spécifiques du chapitre 1 sont : de comparer la synchronicité dans la séquence de débourrement des bourgeons de trois espèces d’épinettes ainsi que de différentes provenances de graines pour déterminer si la plus forte stagnation de la croissance observée sur l’épinette blanche comparativement à l’épinette noire pouvait être expliquée par un débourrement plus hâtif de ses bourgeons, ce qui augmenterait son exposition au gel printanier. Il vise aussi à déterminer l’importance de la variation intra-espèce dans la synchronicité de la séquence de débourrement des bourgeons et de déterminer le rôle des différentes variables environnementales dans le contrôle des différentes transitions de la séquence de débourrement des bourgeons. Ce chapitre s'appuie sur une solide base de données empiriques, qui sert à tester l'hypothèse que tant et aussi longtemps que les aiguilles seront protégées par les écailles du bourgeon, les transitions entre les premières étapes du débourrement des bourgeons seront principalement déterminées par la température minimale de l'air et la photopériode, alors qu'au moment où les aiguilles seront exposées à l'air, la sensibilité aux variables environnementales changera pour répondre principalement aux degrés-jours de croissance, et ce, jusqu'à l'ouverture complète du bourgeon. Au niveau inter-espèce, il est attendu que l'épinette noire sera moins sensible que l'épinette blanche aux différentes variables environnementales, ce qui retardera son débourrement et limitera son exposition aux gelées printanières. Au niveau intra-espèce, il est attendu que les provenances de graines du sud plantées au nord ouvriront leurs bourgeons plus hâtivement, puisqu'elles seront plus sensibles à la température de l'air que la provenance locale de la forêt boréale mixte, ce qui accroîtra leur exposition au gel printanier.

L'objectif principal du chapitre 2 est de déterminer si la sévérité des dommages observés aux cellules cambiales, sous forme de cerne de gel, peut être mise en relation avec la hauteur de l'arbre et ainsi expliquer les différences de hauteur inter- et intra-espèce observées aux deux sites de plantations situés à l'écotone de la forêt tempérée et boréale. Nous testons l'hypothèse que les espèces et les sources de graines qui sont plantées loin de leur site naturel de croissance seront moins bien adaptées aux conditions locales du site de plantation, que les espèces et provenances résidentes naturellement près des sites de plantations. Par conséquent, la sortie de la période de dormance des provenances non-résidentes ne sera pas aussi bien synchronisée avec l'augmentation de la température de l'air au printemps que dans le cas des provenances locales, ce qui augmentera la quantité de dommage au méristème (apical et latéral) causé par le gel et réduira la croissance des arbres. Au niveau inter-espèce il est attendu que 1) l’épinette de Norvège, l’espèce la plus éloignée des deux sites d’étude, devrait être la moins bien adaptée aux conditions locales des sites et présenter les dommages les plus importants aux cellules cambiales par le gel, ce qui réduirait de plus sa croissance en hauteur et 2) que les cellules cambiales de l’épinette blanche devraient être plus sévèrement endommagées par le gel que celles de l’épinette noire, puisque c’est l’épinette blanche qui présente le problème de stagnation de la croissance. Au niveau intra-espèce, 3) toutes les provenances d’épinettes de Norvège devraient être peu performantes, puisque le lieu de résidence naturel de chaque provenance est éloigné et non adapté aux conditions locales des sites de plantations et 4) la provenance d’épinette blanche qui réside naturellement le plus près de chaque plantation, devrait performer le mieux et être la moins endommagée par le gel. Nous avons aussi entrepris d’analyser comment la sévérité des dommages aux cellules cambiales causés par le gel varie à différentes hauteurs le long du tronc pour déterminer la hauteur à laquelle le gel arrête d’endommager le méristème apical. Notre dernier objectif est de déterminer si des variables climatiques représentant des évènements climatiques extrêmes, comme l’intensité des évènements de gel, mesurée par la température minimale par mois, et la fréquence de gel, mesurée comme étant la somme des évènements de gel durant un mois, permettrait de mieux expliquer les différences de croissance en hauteur aux niveaux inter- et intra-espèce comparativement à des variables climatiques plus couramment utilisées comme la température moyenne annuelle. Cette analyse pourrait révéler que, lorsque synchronisés avec certains moments clés du cycle physiologique de dormance-croissance des arbres, les évènements climatiques extrêmes sont plus importants que les variables climatiques agrégées sur de longues périodes pour expliquer les différences en hauteur des arbres. Si cela est le cas, les évènements extrêmes devraient être préférablement introduits dans les modèles prédisant la productivité présente et future des jeunes plantations d’épinettes à l’écotone de la forêt tempérée et boréale.

L’objectif spécifique du chapitre 3 est de montrer l’importance des attributs physiques et permanents du milieu comme l’élévation et la pente, qui peuvent, dans en environnement vallonnée comme la région de l’Abitibi-Ouest, mener à l’accumulation de masses d’air froid dans le creux des pentes et dans les micro-dépressions, et ce, même durant la saison de croissance. Dans ces zones où le gel au sol peut survenir fréquemment, la croissance des arbres en plantation peut être fortement compromise. Puisque l’analyse de l’effet des gelées printanières sur le développement de la végétation est surtout effectuée au nord de la forêt boréale ou à la limite altitudinale des plantes, la fréquence et l’intensité des évènements de gel reste peu connue à l’écotone de la forêt tempérée et boréale. En plus d’étudier l’impact de la position dans la topographie, notre étude se penche sur l’importance de la position du microsite de plantation dans la microtopographie. En effectuant cette étude dans deux plantations se trouvant dans deux régimes climatiques différents, il sera possible d’amener des recommandations pratiques pour déterminer les meilleurs microsites où planter les arbres afin d’éviter les zones de gel et de maximiser la croissance des arbres. Nous nous attendons à ce que la fréquence et l’intensité des évènements de gel sera moins forte à la forêt tempérée qu’à la forêt boréale mixte.

Le deuxième volet est constitué du quatrième et dernier chapitre formant cette thèse. Il vise à évaluer l’importance du phénomène de la stagnation de la croissance des épinettes au niveau du paysage régional de l’Abitibi-Ouest, en mettant en relation la hauteur des arbres mesurée dans 428 parcelles échantillonnées dans un réseau de 66 jeunes plantations d’épinettes noires et blanches âgées de 6 à 13 ans. Dans un deuxième temps, la hauteur du plus grand arbre par parcelle a été comparée à une courbe de croissance ainsi qu’à la hauteur du plus petit arbre de chaque parcelle, ce qui permet d’évaluer l’importance du phénomène de la stagnation de la croissance des épinettes. Puisque l’épinette blanche semble plus affectée par le phénomène de stagnation de la croissance que l’épinette noire, il est attendu que 1) pour un même âge de plantation, les épinettes blanches soient plus petites ou de même hauteur que les épinettes noires,

2) que la hauteur des arbres soit diminuée lorsque les arbres sont plantés dans des dépressions topographiques (creux ou bas de pente), comparativement à la hauteur des arbres plantés en mi-pente et en haut de pente et 3) que selon la qualité du microsite, l’arbre le plus grand de chaque parcelle suive la hauteur prédite par la courbe de croissance, mais que la différence de hauteur entre le plus grand arbre et le plus petit arbre soit forte. Ce résultat viendrait montrer une forte variabilité en hauteur, donc, que la productivité des plantations d’épinettes blanches serait probablement réduite par rapport à leur productivité attendue.

La conclusion de la thèse discute des caractéristiques physiologiques qui explique le phénomène accru de la stagnation de la croissance des plantations d’épinettes blanches comparativement aux plantations d’épinettes noires sur la ceinture d’argile de l’ouest du Québec. Une discussion sur l’apport théorique de cette thèse aux modèles écophysiologiques prédisant le débourrement et la croissance des arbres et sur l’impact attendu des changements climatiques sur la productivité future des plantations d’épinettes conclue la thèse.

CHAPITRE I

PROBABILITY OF SPRING FROSTS, NOT GROWING DEGREE-DAYS, DRIVES ONSET OF SPRUCE BUD BURST IN PLANTATIONS AT THE BOREAL-TEMPERATE FOREST ECOTONE

Benjamin Marquis, Yves Bergeron, Martin Simard et Francine Tremblay

Cet article est publié dans la revue scientifique

Frontiers in Plant Science

1.1 Résumé

Il est anticipé que le débourrement des bourgeons sera plus hâtif dans le futur à cause des changements climatiques qui font augmenter la température de l’air, ce qui pourrait faire augmenter la productivité forestière. Toutefois, cette ouverture plus hâtive des bourgeons augmente aussi leur exposition aux gelées printanières, ce qui pourrait réduire la productivité forestière. Nous avançons l’hypothèse que la probabilité reliée à l’occurrence des gels printaniers exerce un contrôle plus fort sur la séquence de débourrement des bourgeons que ne le fait les degrés-jours de croissance. Nous avons effectué un suivi hebdomadaire de la séquence de débourrement des bourgeons de trois provenances d’épinettes blanches (une provenance locale de la forêt boréale mixte et deux provenances de la forêt tempérée), une provenance d’épinette noire originaire de la forêt boréale mixte et quatre provenances d’épinette de Norvège durant les printemps 2016 et 2017 dans deux plantations établies de chaque côté de l’écotone entre la forêt tempérée et la forêt boréale mixte de l’est du Canada, (Québec). Notre objectif était de déterminer les variations inter et intra espèces dans la séquence de débourrement des bourgeons en plus de quantifier les différences en sensibilité à la température de l’air et à la photopériode. Il est attendu que l’ouverture des bourgeons des espèces et des provenances de la forêt boréale mixte sera mieux synchronisée avec la probabilité de gel comparativement aux espèces et aux provenances non locales. Nous avons utilisé des régressions binomiales mixtes et la sélection de modèle par AICc pour déterminer les variables environnementales qui prédisent le mieux chaque transition d’une étape à l’autre de la phénologie des bourgeons. Aux deux plantations, l’épinette blanche a commencé et a complété sa séquence de débourrement de ses bourgeons avant ceux de l’épinette noire et l’épinette de Norvège. Pour chaque espèce, les premières étapes du débourrement des bourgeons étaient sensibles à la probabilité d’occurrence d’un gel printanier, alors que les dernières étapes de la séquence de débourrement des bourgeons étaient sensibles aux degrés-jours de croissance. La sensibilité à la photopériode était plus élevée pour l’épinette blanche que pour l’épinette noire et l’épinette de Norvège; elle était maximale à la plantation en forêt tempérée. Au niveau intra-espèce, les deux provenances non locales d’épinette blanche étaient plus sensibles à la photopériode et ont ouvert leurs bourgeons plus hâtivement que ceux de la provenance locale de la forêt boréale mixte, ce qui a augmenté leur exposition au gel printanier. Pour les espèces et les provenances de la forêt boréale mixte, le début de la séquence de débourrement des bourgeons est synchronisé avec la probabilité d’occurrence de gel printanier et la photopériode, mais une fois entamé, le débourrement des bourgeons répond principalement à l’augmentation de la température de l’air. La forte sensibilité à la photopériode pourrait limiter le débourrement trop hâtif de l’épinette blanche, sous l’augmentation de la température causée par les changements climatiques, alors que la faible sensibilité de l’épinette noire à la photopériode pourrait permettre le devancement de la phénologie de ses bourgeons sous des températures plus chaudes. Nos résultats suggèrent d’adapter les hypothèses concernant le contrôle de la température sur la séquence de débourrement des bourgeons pour inclure la probabilité de l’occurrence des gels printanier.

1.2 Abstract

Climate warming-driven early leaf-out is expected to increase forest productivity but concurrently increases leaf exposure to spring frosts, which could reduce forests' net productivity. We hypothesized that due to their damaging effect on buds, spring frosts exert a stronger control on bud phenology than do growing degree-days. We monitored bud flush phenology of three white spruce seed sources (one local seed source from the boreal mixedwood forest and two seed sources from the temperate forest), one black spruce seed source originating from the boreal mixedwood forest and four nonlocal Norway spruce seed sources in 2016 and 2017 in two plantations located on both sides of the temperate-boreal mixedwood forest ecotone in eastern Canada (Quebec). We aimed to determine inter- and intraspecies variations in bud break timing and sensitivity to air temperature and photoperiod. We expected that bud break timing for boreal species and seed sources would be better synchronized with the decrease in frost probability than for nonlocal species and seed sources. We used mixed binomial regressions and AICc model selection to determine the best environmental variables predicting each transition from one stage of bud phenology to the next. At both plantation sites, white spruce bud flush began and ended earlier compared to black and Norway spruce. Buds of all spruce species were sensitive to frost probability for early phenological stages, whereas growing degree-days controlled the remaining stages. Photoperiod sensitivity was higher for white spruce compared to black and Norway spruce and reached its maximum in the temperate forest. At intraspecies level, the two southern white spruce seed sources opened their buds earlier than the local source and were more sensitive to photoperiod, which increased their exposure to spring frosts. Onset of spruce bud flush is driven by spring frosts and photoperiod, but once started, bud phenology responds to temperature. The high photoperiod sensitivity in white spruces could counterbalance climate warming and limit future premature leaf-out, whereas the low photoperiod sensitivity in black spruce should not restrain leaf-out advancement with climate warming. Our results call for adapting the temperature-driven hypotheses of ecophysiological models predicting leaf-out to include spring frost probability.

Keywords: bud phenology, growing degree-days, leaf-out, photoperiod, *Picea*, spring frost, temperature, thermal acclimation

1.3 Introduction

The observed 1°C increase in mean global air temperature above preindustrial levels (1850–2017; Allen et al., 2018) is desynchronising tree phenology from tracking the seasonal variation in air temperature by triggering earlier spring leaf-out (Parmesan and Yohe, 2003; Piao et al., 2007; Polgar et al., 2013) and later entrance into dormancy (Jeong et al., 2011; Liu et al., 2016; Fu et al., 2017). The earlier onset and the later ending of the growing season expose frost-sensitive plant organs (buds, leaves, flowers) to more frequent spring and autumn frost events (Cannell and Smith, 1986; Liu et al., 2018; Ma et al., 2018). In fact, 43% of the Northern Hemisphere has experienced an increase of more than one growing-season frost event per year over the period 1982–2012 (Liu et al., 2018). In addition, climate warming (both mean and extremes) is not equal across seasons and latitudes (Loarie et al., 2009; Brown, 2019). Winter and spring are warming faster than summer and autumn and the frequency and intensity of extreme climatic events such as heavy rainfall and droughts are rising (Easterling et al., 2000; Stott et al., 2015; Brown, 2019). Therefore, the response of trees to climate change will likely diverge across stands or populations of the same species (D'Orangeville et al., 2018; Marchand et al., 2019), increasing the need for population-specific response to climate change. However, these responses to climate change at the population level remain largely unknown, which stresses the importance of quantifying local adaptations to better forecast the fitness of forest tree species.

At the tree level, spring frosts damage both apical and cambial meristems, as well as the leaves, thereby reducing tree growth and altering tree architecture (Clements et al., 1972; Dy and Payette, 2007; Augspurger, 2009). In contrast, summer frosts can delay the formation of the following year's foliage by damaging the newly developed primordia of evergreen trees or by limiting nutrient resorption from damaged leaves in deciduous trees (Estiarte and Peñuelas, 2015). At the ecosystem level, frost damage to leaves can decrease net primary productivity of the forests (Hufkens et al., 2012).

The frequency and intensity of spring frosts are hard to predict, given their rare occurrence and dependency upon terrain complexity (Laughlin and Kalma, 1987; Lindkvist and Lindqvist, 1997; Chung et al., 2006), where cold air masses can be trapped in topographic depressions resulting in localized frost pockets across the landscape (Dy and Payette, 2007). The strong effects of spring frosts on the fitness of temperate and boreal plant species make them important drivers of species range limits (Inouye, 2008; Kollas et al., 2014; Körner et al., 2016; Du et al., 2019). Yet spring frost effects upon spring phenology have seldom been studied (Körner et al., 2016; Lenz et al., 2016). Furthermore, these later frosts have been excluded from ecophysiological models predicting leaf-out dates, thereby favoring the use of aggregated metrics such as growing degree-days (GDDs) and photoperiod (Fuchigami and Nee, 1987; Chuine, 2000; Hänninen, 2006; Linkosalo et al., 2006). Given the high daily variation that is observed for air temperature, the more predictable nature of night / day length would make photoperiod a more reliable environmental cue for preventing early dormancy release or late dormancy entrance (Partanen et al., 1998; Cooke et al., 2012; Soolanayakanahally et al., 2013; Lang et al., 2019). However, sensitivity to photoperiod varies between species and with successional status (Caffarra and Donnelly, 2011; Basler and Körner, 2012). Therefore, disentangling the relative effects that air temperature variables (growing degree-days *vs*. spring frosts) and photoperiod exert on the physiological processes driving tree growth is critical to better forecast climate change effects on the productivity of temperate and boreal species.

One of the best scientific records for analyzing environmental drivers of the dormancy-growth cycle of trees is the phenological observation of bud burst in spring and bud set in autumn, since these events determine the start and the end of the growing season (Aono and Kazui, 2008; Hänninen, 2016; Tang et al., 2016). Unfortunately, the performance of many ecophysiological models that have been implemented to predict the dates when buds are expected to break is under debate because: (1) no single model provides the best fit for all tree species and (2) different models using various combinations of climate and photoperiod variables lead to similar prediction of bud break dates (Basler, 2016). Therefore, the important environmental variables triggering the physiological mechanisms of bud burst cannot be identified. This discrepancy in model projections may be the results of methodological oversimplification in the input bud phenology data or the omission of significant air temperature variables, such as spring frost occurrence. In fact, the bud break sequence must be synchronized with the decrease in frost days during spring otherwise trees would recurrently be damaged by spring frosts. However, a late bursting of the buds would decrease the growing season length, potentially decreasing growth and losing competition for space, light and nutrients to trees bursting buds earlier. Thus, the bud break sequence first follows a frost avoidance trade-off followed by a rapid bud burst that maximizes the growing season length. Consequently, the various phenological stages of the bud break process might respond to different environmental cues. However, little is known about these ecological strategies driving the bud break sequence because bud phenology is traditionally analyzed using scattered discrete field observations of buds in spring, of which, only one phenological stage (the phenological stage where buds break) is analyzed, omitting the possibility that the sensitivity of buds to environmental cues may vary within the continuous process of bud break (Hannerz, 1999; Snyder et al., 1999; Polgar and Primack, 2011).

The objectives of our study were to identify the environmental drivers at each stage of the bud break process on three spruce species and various seed sources with different bud flushing dates in two plantations that were established in the northern temperate forest and in the boreal mixedwood forest of western Quebec (Canada). In each plantation, we expected that the white spruce (*Picea glauca* [Moench] Voss) would flush its buds earlier than both the black spruce (*Picea mariana* [Mill.] B.S.P.) and the Norway spruce (*Picea abies* [L.] Karst.). At the intraspecies level, we expected that in the boreal mixedwood plantation, the southern seed sources (from the temperate forest) would open their buds earlier than the local seed source (from the boreal mixedwood forest), which would increase their exposure to spring frosts and prove to be disadvantageous to early plantation productivity during years of these occurrences. For the environmental drivers of the bud break process, we expected that as long as needles are protected by the bud scales (phenological stages 0–3), the minimum air temperature and the day length would be the main environmental drivers of transition from one stage to the next. Once needles are exposed to variation in ambient air temperature (phenological stages 4–6), subsequent bud transitions would be driven by growing degreedays. We further expected that the seed source originating from the boreal mixedwood forest would better synchronize its bud break timing with frost probability compared to nonlocal seed sources.

1.4 Materials and Methods

1.4.1 Study site

Our study was conducted in two experimental plantations containing white spruces, black spruces, and Norway spruces. The two plantations were established in 2002; one in the northern temperate forest and one in the boreal mixedwood forest of the northern Clay Belt of Quebec (Figure 1.1). Mean annual temperature at the temperate forest plantation site (47.29° N; 79.12° W) is on average 2.1°C higher than at the boreal mixedwood forest plantation site (48.29° N; 79.26° W), with a mean annual temperature of 3.1°C and mean monthly temperatures of −15.0°C and 18.8°C in January and July, respectively (1981–2010 Normals, Barrage Angliers weather station located 24 km from the temperate forest plantation site, Environment Canada, 2019a) compared to a mean annual temperature of 1.0°C and mean monthly temperatures of −17.9°C and 16.7°C in the boreal mixedwood forest in January and July, respectively (1981–2010 Normals, Mont-Brun weather station located 47 km from the boreal mixedwood forest plantation site, Environment Canada, 2019b). At the temperate forest plantation site, the frost-free period is 46 days longer than at the boreal mixedwood forest plantation site, starting earlier by 21 days (May 24th, [DOY 144] *vs*. June 13th, [DOY 164]), and ending 25 days later (September 24th, [DOY 267] *vs*. August 31st, [DOY 243]). The last growing-season frost (0.10 probability that air temperature < 0°C) at the boreal mixedwood forest plantation site usually occurs 19 days later than in the temperate forest plantation site (June 15th, [DOY 166] *vs*. July 4th, [DOY 185]; 1981–2010 Normals, Barrage Angliers and Mont-Brun weather stations, Environment Canada, 2019a; Environment Canada, 2019b). These spring frosts mostly result from the temperature inversion phenomenon which generates nighttime near-ground frost events lasting few hours (Dugas, 1975; Laughlin and Kalma, 1987), which can damage both the buds and the cambium of small trees such as trees in young plantations (Dy and Payette, 2007). Precipitation is similar in the two plantation sites: the total rainfall is 709 mm *vs*. 705 mm and the total snowfall is 2580 *vs*. 2810 mm for the temperate forest and boreal mixedwood forest plantation sites, respectively. Day length in the temperate forest plantation site was eight minutes shorter during summer and eight minutes longer during winter compared to the boreal mixedwood forest plantation site (Sunset calculator, Environment Canada, 2019c).

1.4.2 Experimental design

The plantations consisted in 480 square plots of 64 m^2 and each plot was randomly assigned to a white spruce seed sources (20 seed sources tested), a Norway spruce seed source (20 seed sources tested) or a black spruce seed source (1 seed source tested). In each plot, 25 trees of the same seed source were planted with a 2 m by 2 m spacing in five rows of five. The 20 different white spruce seed sources were collected from a first-generation seed orchard established in Cap-Tourmente in 1981 (47.06°N, 70.45°W), the 20 Norway spruce seed sources were collected from a plantation established in 1969 in Valcartier Forest Experiment Station (46.56°N, 71.30°W) for an international project on Norway spruces coordinated by the International Union of

Forest Research Organizations (IUFRO) (Blouin et al., 1994; Matras, 2002). The two plantations were designed to compare the development of trees between local *vs*. nonlocal seed sources and to test for genetic-based adaptations and phenotypic plasticity by planting each seed sources in two contrasting climate regimes (the northern temperate forest and the boreal mixedwood forest) at the boreal-temperate forest ecotone of western Quebec (see Annexe A: Figure A1 for species range maps, location of the seed sources, location of the seed orchards and the location of the plantation sites). Both local black and white spruce seed sources from the boreal mixedwood forest were used as controls. To quantify inter- and intraspecies variation in the timing of bud break, the 20 seed sources for white and Norway spruce were split into four quartiles based upon tree heights that were previously measured in 2012; one seed source per quartile was randomly selected for bud observation. For the white spruce, most trees from the lower quartile were dead at the boreal mixedwood forest plantation site. Therefore, only three seed sources (quartiles 2 to 4) were selected (see Table 1.1 for the geographic locations of seed sources that were used in our study and see Table 1.2 for a description of the climate at their location of origin). Only one black spruce seed source was studied because the black spruce usually flushes its buds late compared to the white spruce and, therefore, the black spruce represents a reliable benchmark for determining the impact of spring frosts on bud phenology. We avoided plots where trees were infested by the white pine weevil (*Pissodes strobi*). For the remaining plots, stratified randomly sampling was performed to select 185 plots, which were distributed across species and seed sources.

Table 1.1 Number of trees monitored, bud observations and median day of year of budbreak (phenological stage 5) per species, seed source, tree height quartile, and plantation site.

Spruce species	**Seed source (height quartile)**	**Latitude**	**Longitude**	**Locality**	**Temperate forest plantation**		**Boreal mixedwood forest plantation**	
					Number of trees (buds)	Median day of budbreak	Number of trees (buds)	Median day of budbreak
Norway	K35 (Q4)	55.15° N	30.10° E	Glubokskii, Belarus	12 (601)	165	5 (190)	164
Norway	K39 (Q3)	49.33° N	18.52° E	Istebna, Poland	13 (619)	165	2 (68)	162
Norway	K50 (Q1)	55.30° N	30.00° E	Gorodokskii, Belarus,	15 (740)	158	4 (149)	164
Norway	K55 (Q2)	56.25 ° N	22.50 ° E	Auce, Latvia	13 (697)	155	6 (211)	155
	Total				53 (2657)		17 (618)	
White	J70 (Q4)	48.29° N	79,26° W	Duparquet, Québec	27 (1176)	155	27 (1026)	157
White	K20 (Q2)	45.36° N	74,28° W	Cushing, Québec	15 (727)	155	8 (320)	156
White	K24 (Q3)	45.54° N	77.20° W	Petawawa, Ontario	13 (557)	151	13 (247)	153
	Total				55 (2460)		48 (1593)	
Black	K32	48.29° N	79.26° W	Duparquet, Québec	51 (2357)	165	34 (1215)	164
	Grand total				159 (7474)		99 (3426)	

Table 1.2 Climate normals (1981-2010) at the location of origin of each nonlocal seed source.

Seed source (locality)	**Weather station (distance to locality)**	**Mean annual temp. in °C**	**Mean January temp. (min; max) in °C**	**Mean July temp. (min;max) in °C**	**Precipitation sum in mm**	**Growing degree-days (base temp. 0°C)**	**Date with 0.10 probability of frost in spring (DOY)**
K35[1] (Glubokskii)	Smolensk (130 km)	5.5	−6.2 (−33; 9)	17.8 (5; 35)	738	2713	May 11th (131)
K39[1] (Istebna)	Bielsko-Biala (33 km)	8.5	−1.3 (−27; 15)	18.0 (4; 34)	944	3365	May 5th (125)
K50[1] (Gorodokskii)	Velikie-Luki (98 km)	5.8	−5.5 (−37; 11)	18.0 (3; 35)	639	2774	May 19th (139)
K55[1] (Auce).	Siauliai (62 km)	6.8	−2.8 (−32;11)	17.8 (6; 35)	614	2904	May 17th (137)
K20[2] (Cushing)	Lachute (12 km)	6.0	−10.7 (−37; 11)	20.4 (4; 35)	1151	3177	May 27th (147)
K24[2] (Petawawa)	Sheenboro (10 km)	5.0	−12.1 (−39; 11)	19.3 (1; 40)	853	2972	June 10th (161)

[1] Climate data for European seed sources were retrieved from the KNMI Climate Explorer (European Climate Assessment and Data) https://climexp.knmi.nl/start.cgi.

[2] Climate data for Canadian seed sources were retrieved from Environment Canada (Climate normals) https://climate.weather.gc.ca/climate_normals

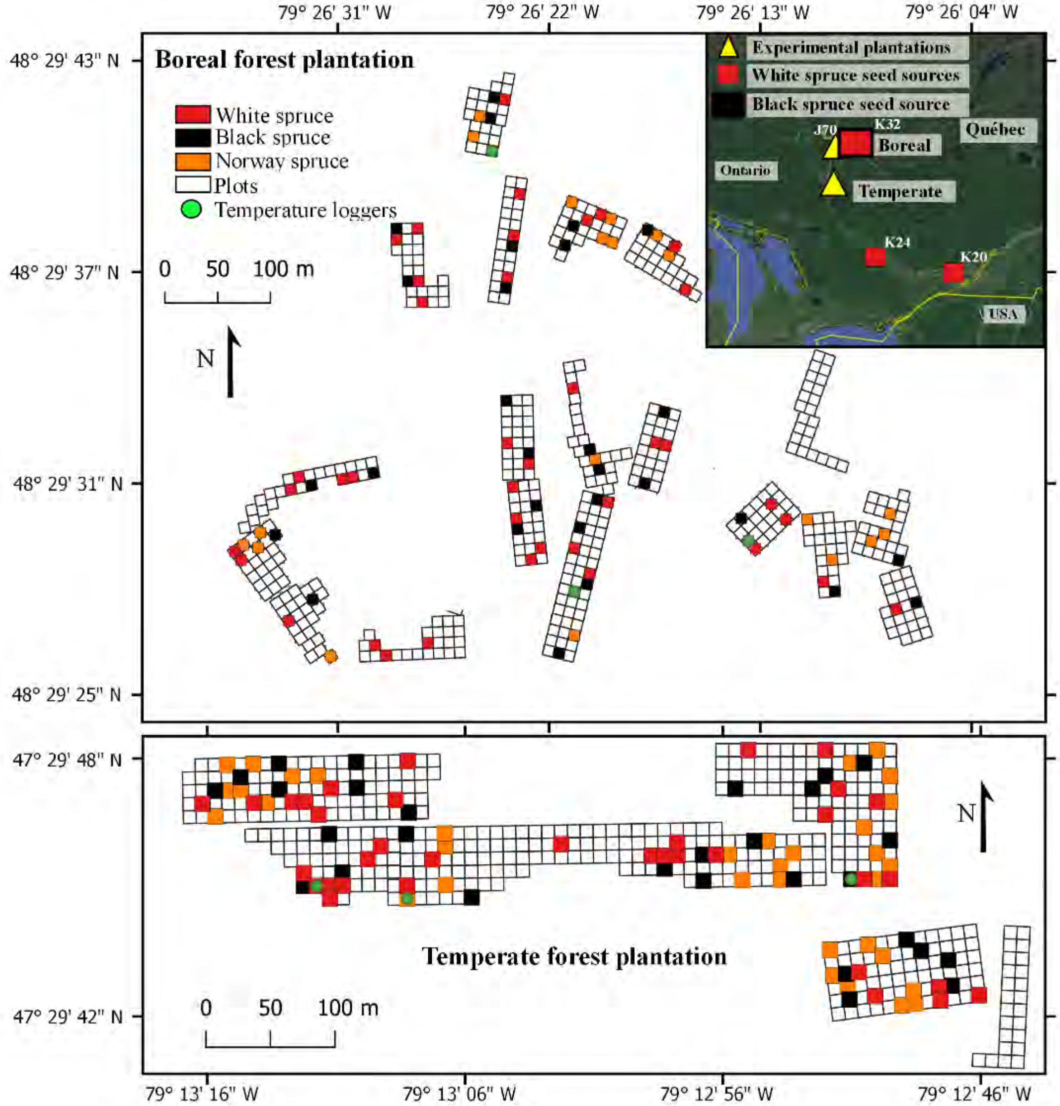

Figure 1.1 Experimental design of the plantations, the randomly sampled plots (colored squares) that were used for this study, and locations of air thermometer at the boreal mixedwood forest plantation (top) and at the temperate forest plantation (bottom). Inset shows the locations of the temperate forest and boreal mixedwood forest plantations, together with the North American seed sources.

1.4.3 Bud phenology observations

Each bud observation was classified into one of the seven bud break stages (0–6). The stages were described by Dhont et al. (2010) for white spruce buds, by Numainville and Desponts (2004) for black spruce buds, and by Sutinen et al. (2012) for Norway spruce buds. To maintain the same number of stages per species, we added one last stage to Norway spruce, i.e., needles elongating and expanding laterally (Table 1.3). Buds were observed weekly from May 10th until leaf-out (see Annexe A: Figure A2 for the precise sampling dates). This sampling time interval was based upon previous studies analyzing bud phenology (Clark et al., 2014a; Perrin et al., 2017) and because of logistical constraints (large distance between both plantation sites) that prevented observing bud phenology at a shorter time interval. The average time delay between bud observations at one plantation and bud observations at the other plantation was of only two to three days. Even if our sampling time interval could have led to missing observations for given phenology stages, the large amount of observations collected over 258 trees increases the robustness of our data and analyses compared to more frequent bud observations collected over a limited number of individuals. The apical bud could not be observed since trees were too tall. Therefore, the terminal buds of all branches belonging to the whorl at breast height (from two to six buds per tree) were followed for two consecutive years (2016–2017). In total, 10 900 buds were observed over 258 trees (Table 1.1). Since stages one and two closely resemble one another, they were difficult to identify in the field. Therefore, data were merged for these two stages.

Table 1.3 Development stages of the spring bud phenology of white spruce (Dhont et al., 2010, p. 9), black spruce (Numainville and Desponts, 2004, pp. 10–16, Figs 6B, 7B, 8B, 9B, 10B, 11A, 12A.) and Norway spruce (Sutinen et al., 2012, p. 990, Figure 2).

Stages	Description	White spruce	Black spruce	Norway spruce
0	Buds are closed and dormant.			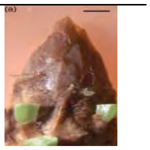
1	Bud scales are opening, and from an apical view, a white spot is visible at the top of the bud.			
2	Buds are elongating.		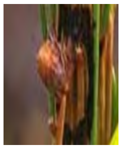	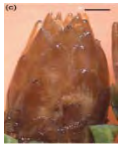
3	Buds are swelling.		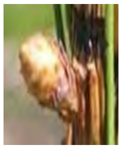	
4	Bud scales are translucent, and the needles are partly visible.			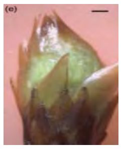
5	Bud scales are ripped at the base of the bud (white and black spruce) or open at the top (Norway spruce), and needles are tightly bundled.			
6	Needles are elongating and expanding laterally.			

No photograph showing buds of the Norway spruce in stage six was available.

1.4.4 Climate variables used to predict timing of bud break

To analyze the timing of bud break in relation to *in situ* air temperature, we installed three thermometers (iButton DS1922L, measurement accuracy of ± 0.5°C, Maxim Integrated, San Jose, CA, USA) per plantation site set to record air temperature every 30 min from snow melt in the spring to August for two consecutive years (2016–2017). We averaged the data from the three thermometers to create one daily temperature record per site. Due to the presence of snow on the ground at the time of the first bud observations, thermometers were set 13 days later, once snow had melted. The missing air temperature data from onsite measurements were supplemented using the following approach: we used the BioSIM 10 software that was developed by Natural Resources Canada (Régnière et al., 2014) to simulate daily air temperature by accounting for elevation and aspect at both plantation sites for the entire growing season. For each plantation and temperature logger, we then regressed the air temperature that was measured in the field against the simulated air temperature values. All linear regressions were significant (P-values < 0.05). The mean adjusted R^2 of all linear regressions was 0.86, being higher for mean temperature ($R^2 = 0.92$) and lower for minimum ($R^2 = 0.82$) and maximum temperature ($R^2 = 0.85$; Annexe A: Tables A1 and A2). Using the regression coefficients, we predicted the minimum, mean and maximum daily air temperature for the 13 missing days per data logger. We then averaged these predicted values per plantation and incorporated them into our observed air temperature dataset (Figure 1.2A). To determine which temperature variable best predicted each phase of the bud break process, we tested the minimum, mean and maximum daily air temperature, the sum of growing degree-days above 0°C, starting January 1st, which were calculated with the maximum daily air temperature (GDD max), and the mean daily air temperature (GDD mean; Figure 1.2B). We also analyzed the impact of photoperiod on bud phenology by retrieving the day length (hours of illumination during the day) from the sunset calculator (Environment Canada, 2019c) for both plantation sites (Figure 1.2C) and the daily probability of occurrence of a frost event, which was calculated from the binomial regression analysis of the frequency of frost events. Days where minimum daily air temperature was below 0°C were coded 1 and the others, 0 (Figure 1.2D).

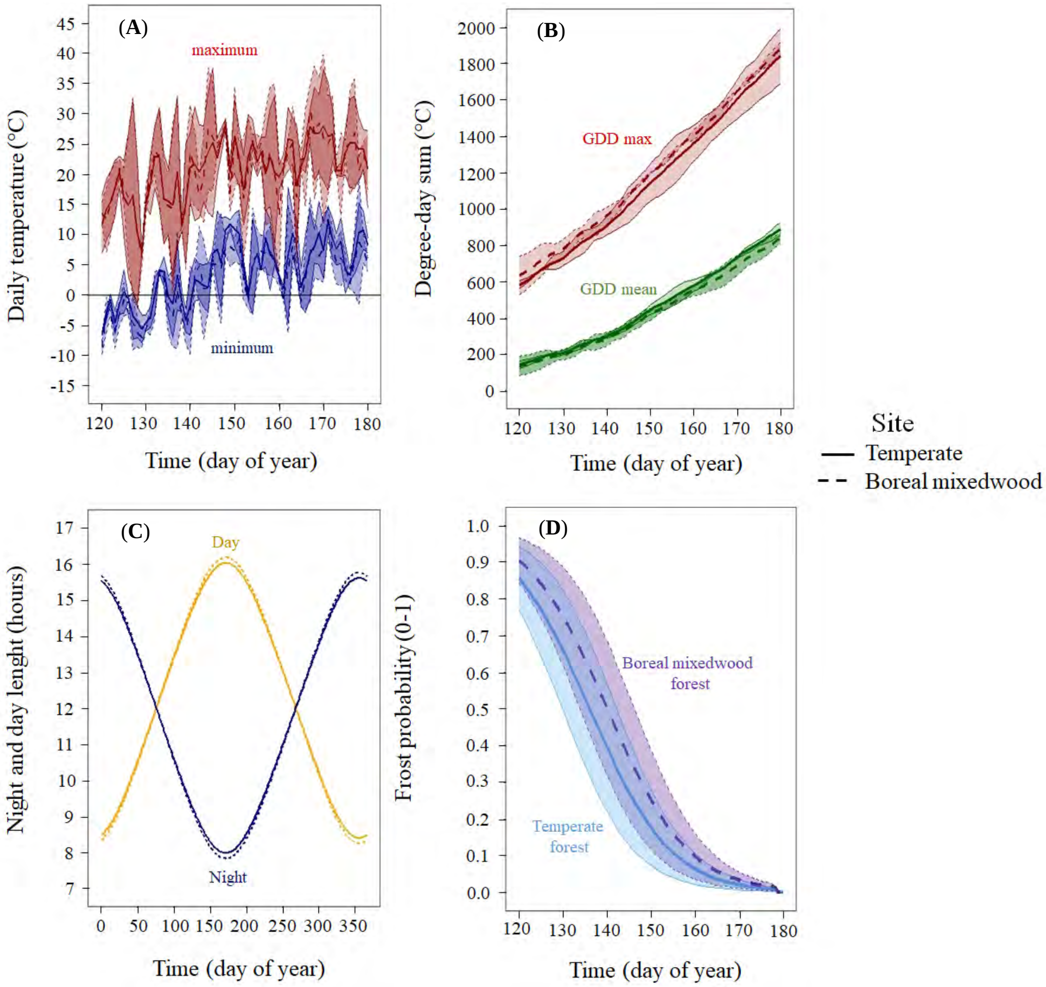

Figure 1.2 Mean (line) and standard error (shaded area) for the period 2016–2017 for air temperature and photoperiod variables that were tested: (A) mean daily minimum and mean daily maximum temperature; (B) sum of growing degree-days calculated with mean and maximum temperature; (C) night and day length in hours; and (D) probability of a frost event per site.

1.4.5 Statistical methods

Prior to all analyses, numerical variables were standardized to allow comparison of the strength of coefficients from different variables. Bud observations consist in a series of stages linked by time since buds can only transit from one stage to the next. Therefore, we separately analyzed the five transitions (0 –> 2; 2 –> 3; 3 –> 4; 4 –> 5; 5 –> 6) with a binomial model, using 0s for buds that remained in their current stage and 1s for buds that were transitioning to the next stage, a method also used by Perrin et al. (2017) (Figure 1.3). The site, species or seed sources, and their interactions were analyzed as fixed effect terms, whereas years and tree identity were incorporated into the random structure of the binomial regression model. We implemented these models in R using the `glmer` function with the bobiqa optimiser algorithm from the `lme4` package (Bates et al., 2015). We considered that a bud would transit to the next stage of bud phenology once the transition probability was 0.51. We quantified bud break duration by subtracting the day of year where the transition probability of reaching stage six in the bud phenology was 0.51 from the day of the year where the transition probability of reaching combined stages one and two was also 0.51. We acknowledge that by merging stages one and two, we had underestimated the duration of the bud break process.

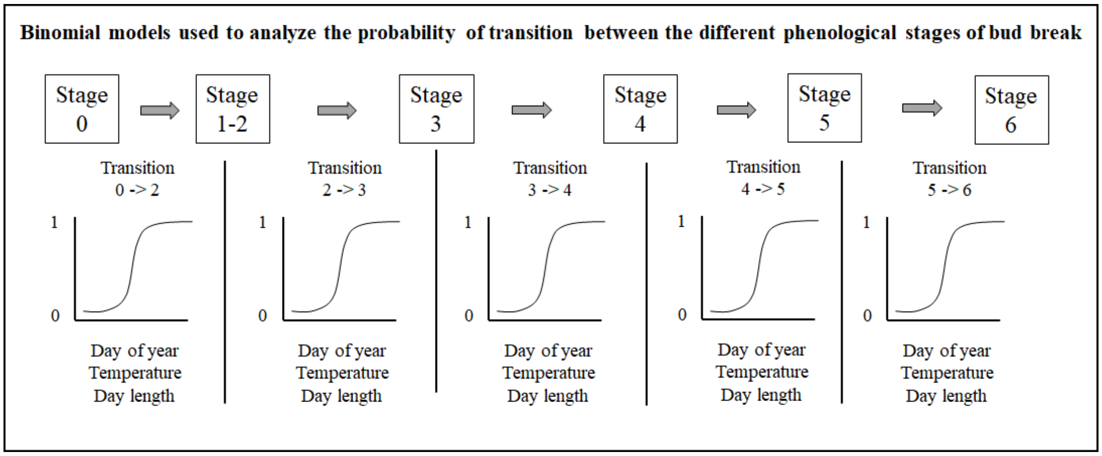

Figure 1.1 Mixed binomial regression models analyzing the probability of transition between the different phenological stages of bud break.

To determine which air temperature and photoperiod variables best predicted each phenological transition per species, we defined 31 air temperature models (Annexe A: Table A3) and six photoperiod models (Annexe A: Table A4), including a null model testing the occurrence of bud flush according to time only. This last model included day-of-year (DOY) as the predictor variable. We compared candidate models against the null using model selection, which evaluated model fit with the corrected Akaike's information criteria (AICc) (R package `AICcmodavg`; Mazerolle, 2017). If model selection failed to identify one best model, we used multi-model inference to average the coefficients in each probable model using the model.avg function from the R package `MuMIn` (Barton, 2018). To limit multicollinearity problems because of correlated climate variables and high (>10) variance inflation factors when two environmental variables co-occurred in a same model, we only tested models with single climate variables in various combinations with species, sites, and their two-way interactions. Since photoperiod and air temperature can interact to affect bud break timing (Rossi and Isabel, 2016), we first performed model selection to identify the best air temperature model per transition. We performed a second model selection to identify the best photoperiod model per transition. We then compared the best air temperature model to the best photoperiod model by analyzing the strength of their regression coefficients. Since statisticians still debate on how to properly calculate statistical significance of coefficients when regression analyses include a random structure, we considered a variable to be statistically significant if the error around the coefficient did not include zero. Once the best climate variables were identified per stage of bud phenology, we analyzed intraspecies variation in bud phenology by adding the seed source.

We restricted our analyses to the observed sequence of bud flush in spring only instead of using a dynamic model considering the interplay between spring warming and chilling requirement in autumn to model the dehardening process because 1) values for the chilling requirement were not available at the seed source level; 2) a previous study showed that the chilling requirement for spruce species were low (300– 500 chilling hours) compared to other boreal and temperate tree species (trembling aspen requires 1100 chilling hours) and were completed by the end of December (Man et al., 2017), therefore unlikely impacting bud break timing in spring; and 3) we gathered bud flush data for only two years. For the latter, the possibility that warmer autumn decreases the number of accumulated chilling units in autumn, thus postponing chilling completion to early spring and consequently delaying bud break is limited compared to long-term bud phenology studies using dynamic models. Hence, the importance of chilling temperatures in controlling bud flush phenology in the spring was less of a concern in our study.

To show how our bud phenology data compared with the more conventional bud phenology analyses, we compared the sum of growing degree-days above 0°C that was required for buds to open (phenological stage five; Table 1.3) per species and site with previously published results (Snyder et al., 1999; Man and Lu, 2010).

1.5 Results

1.5.1 Inter-and intraspecies variation in the timing of bud break

Results for the timing of bud break are based upon forecasts from the mixed binomial regression models predicting on which day-of-year (DOY) the transition probability was 0.51. For the white spruce, the black spruce and the Norway spruce, bud break in the temperate forest plantation was completed in 16, 23, and 15 days, respectively, compared to 19, 19, and 17 days in the boreal mixedwood forest plantation (Figures 1.4 and 1.5). The black spruce was the only species for which bud break phenology was faster in the boreal mixedwood forest than in the temperate forest. At both plantation sites, the white spruce reached each bud phenology stage the earliest. Also, at both plantation sites, interspecies variations were the highest for the bud swelling stage (stage three, see Table 1.3). For instance, the white spruce was the earliest species to swell buds (when the frost probability was of 0.31 and 0.33 at the temperate forest and at the boreal forest respectively) whereas both the black spruce and the Norway spruce swell buds when the frost probability was 20% and 23% lower at the temperate forest and the boreal forest respectively (Figure 1.5).

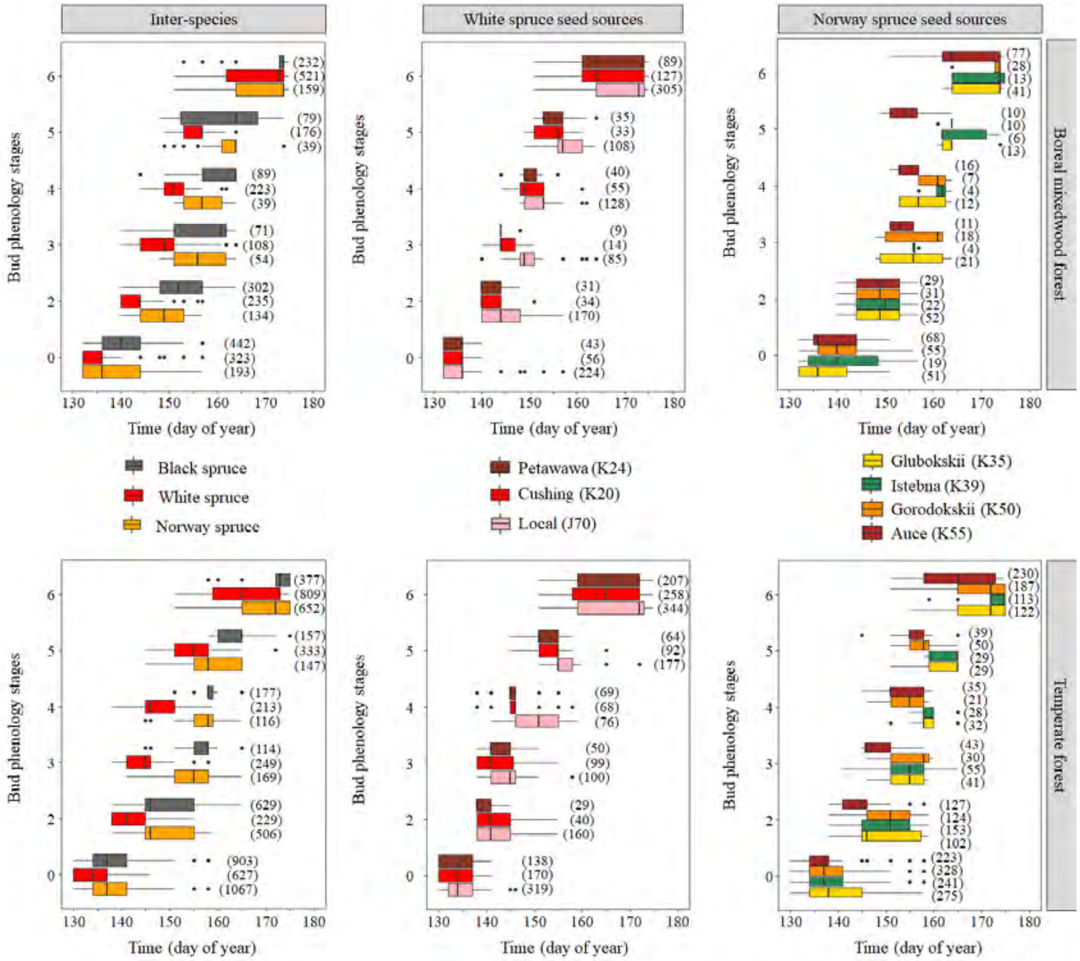

Figure 1.4 Observed distribution (box plots) of the phenological stages with time showing both inter- and intraspecies variations in the bud break process. The boxes show the 25th and 75th percentiles, and the line inside each box represent the median. The number in parenthesis shows the number of observations per phenological stage, species, and site.

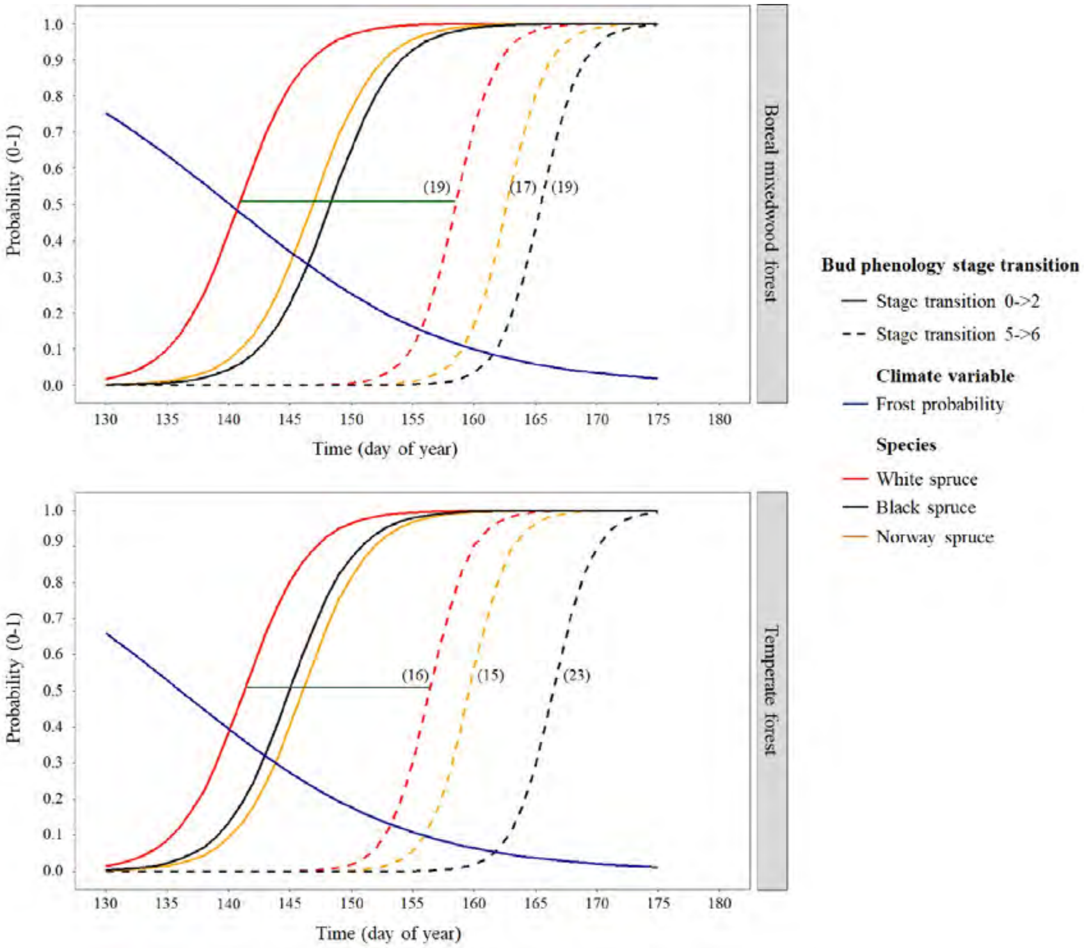

Figure 1.5 Interspecies variation in bud break timing showing the transition probabilities between the first and last transition stages of bud phenology per species, plantation site, and frost probability with time. The horizontal green line shows the duration of the bud break process for white spruce and the numbers in parentheses show the duration (in days) of the bud break process per species and site.

At the intraspecies level, the nonlocal southern white spruce seed sources K20 and K24 reached each phenological stage of the bud break process earlier than the local seed source J70 (Figures 1.4 and 1.6 and Table 1.5). In the temperate forest, white spruce intraspecies variations were the highest for the bud swelling stage (stage four). For instance, exposure to spring frost was 12% higher (from a probability of 0.41 to 0.29) for the southern seed sources compared to the local seed source originating from the boreal mixedwood forest. In the boreal mixedwood forest, white spruce intraspecies variations were highest for the translucent bud scales stage. For instance, exposure to spring frost was 10% higher (from a probability of 0.33 to 0.23) for the southern seed sources compared to the local seed source originating from the boreal mixedwood forest, which flushed its buds the latest (Table 1.5).

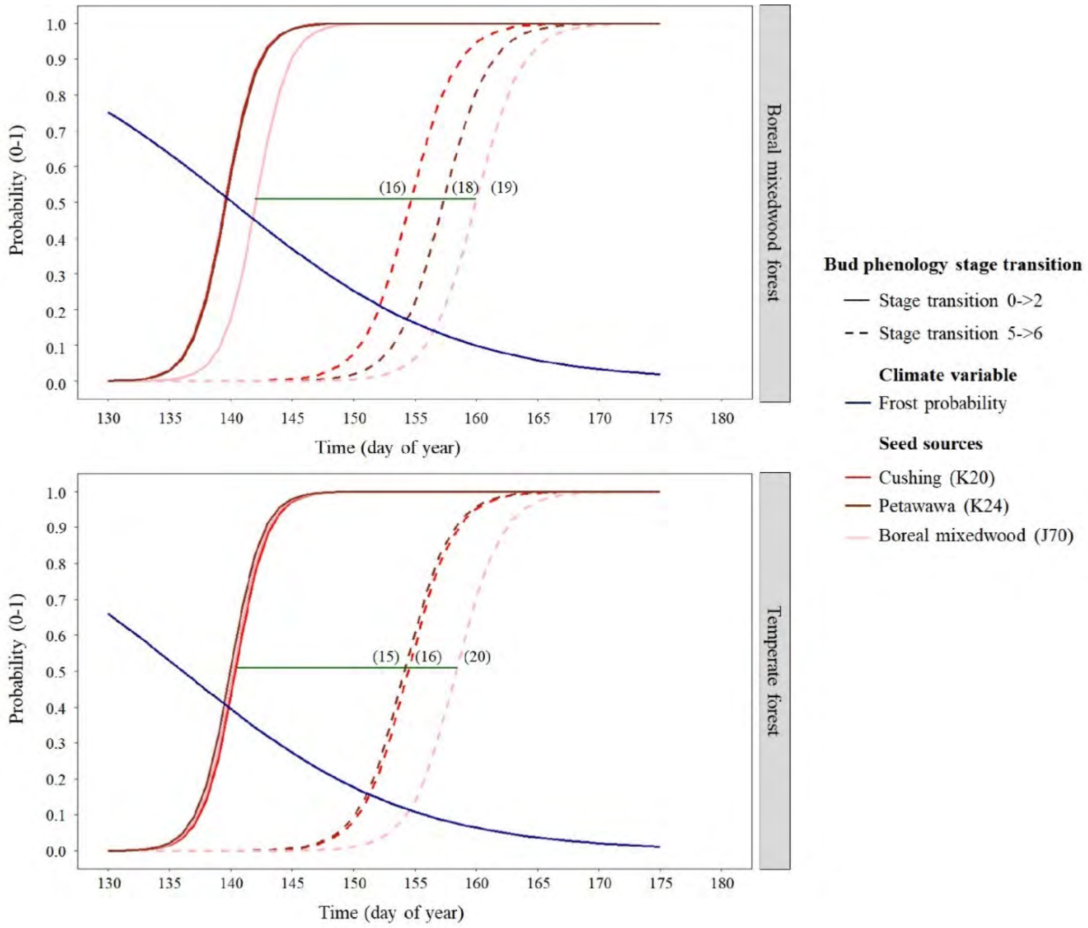

Figure 1.6 White spruce intraspecies variation in bud break timing showing the transition probabilities between the first and last transition stages of bud phenology per seed source, plantation site, and frost probability with time. The horizontal green line shows the duration of the bud break process for the local white spruce seed source naturally growing close to the boreal mixedwood forest plantation (J70) and the numbers in parenthesis show the duration (in days) of the bud break process per seed source and site.

For the Norway spruce, at both sites, the first and the last seed source to complete bud flush were the K55 and K39 respectively. Important differences in bud break timing were observed for intermediate bud phenology stages. Bud swelling occurred on average 7 days and 12 days earlier for the K55 seed source in the temperate forest and in the boreal mixedwood forest respectively when compared to the K39 seed source. These differences in timing of bud break increased exposure to spring frost by 7% (from a probability of 0.16 to 0.09) in the temperate forest and by 21% (from a probability of 0.33 to 0.12) in the boreal mixedwood forest (Figures 1.4 and 1.7 and Table 1.6).

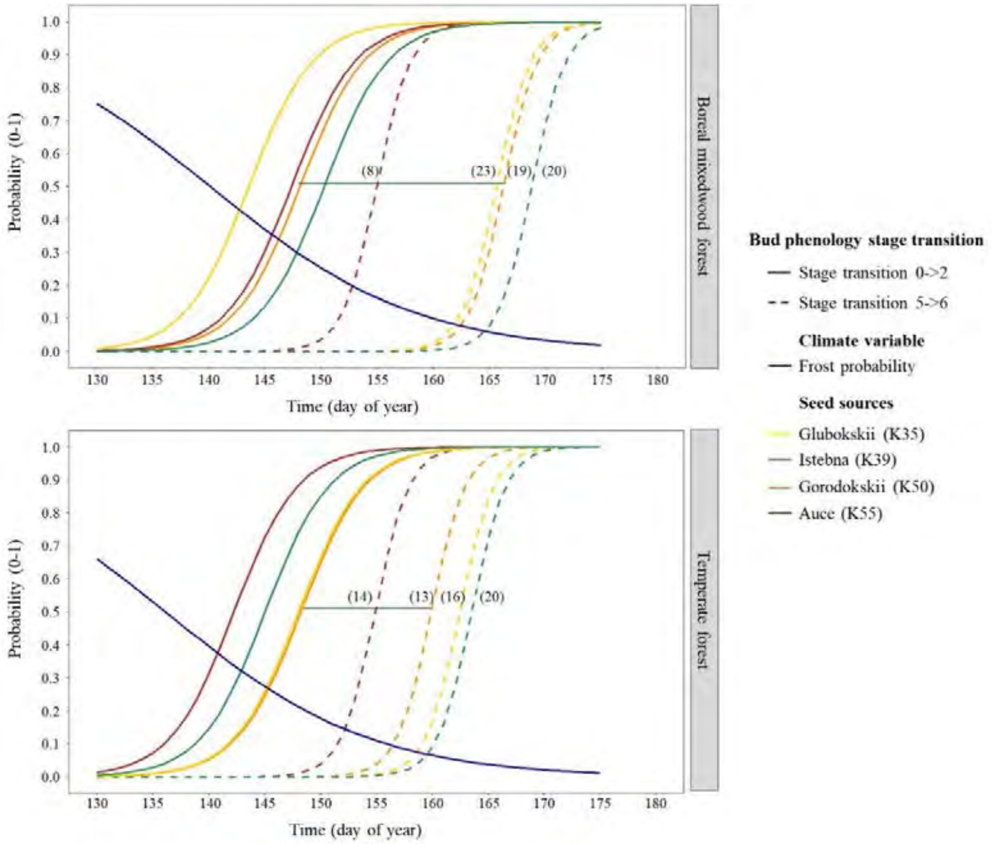

Figure 1.7 Norway spruce intraspecies variation in bud break timing showing the transition probabilities between the first and last transition stages of bud phenology per seed source, plantation site, and frost probability with time. The horizontal green line shows the duration of the bud break process for the K50 seed source naturally growing in Gorodokskii (Belarus) and the numbers in parenthesis show the duration (in days) of the bud break process per seed source and site.

1.5.2 Interspecies variation in the effect of air temperature and photoperiod for predicting bud break phenology

Model selection on the 31 air temperature candidate models produced from one to three statistically plausible models (5%) for each stage transition (Figure 1.8 and Annexe A: Tables A5–A9 for complete results of the AICc model selection per stage transition). The average marginal pseudo-R^2 was 0.47 ± 0.15 and the conditional pseudo-R^2 was 0.84 ± 0.06 for the selected models. Here, the marginal value of R^2 represents the variance that was explained by the fixed effects, while the conditional value represents the variance that was explained by both fixed and random effects (Barton, 2018). The null model for bud flush solely as a function of time was always rejected (Annexe A: Tables A5 to A9). Phenological stages where needles were still protected by the bud scales [bud elongation to bud swelling (stages two and three), see Table 1.3] were best predicted by the probability of spring frost occurrence whereas growing degree-days best predicted dates that buds reached phenological stages where needles were exposed to air temperature (stages four to six) (Figure 1.8).

Sensitivity to air temperature (both spring frost occurrence and GDDs) varied among species and sites (Table 1.4 and Annexe A: Tables A10–A14 for the coefficients of each climate variable per stage transition). Specifically, the white spruce was more sensitive to both the probability of spring frost occurrence and the growing degree-days compared to either the black spruce or the Norway spruce. The probability of spring frost occurrence was more important for predicting transition probabilities of buds in the boreal mixedwood compared to the temperate forest. In contrast, growing degree-days were more important for predicting transition probabilities of buds in the temperate forest plantation, particularly for the transition from phenological stage four to five (Table 1.4 and Annexe A: Tables A10–A14).

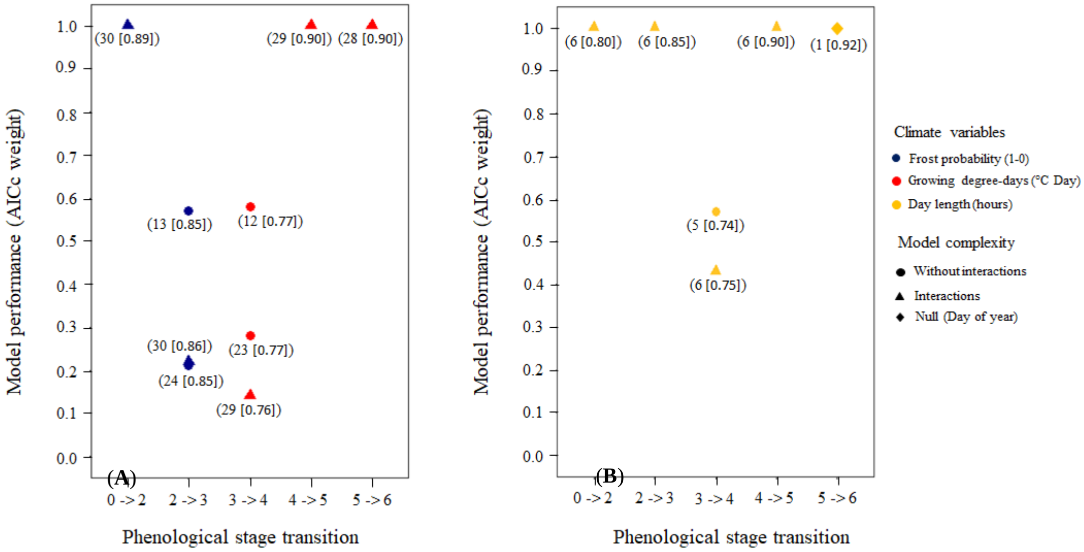

Figure 1.8 Best air temperature models (A) and best photoperiod models (B) predicting the transition of buds from a given stage to the next based upon corrected Akaike's information criteria (AICc) weights; only models with an AICc > 0.05 for each of the five bud phenology transitions are shown. Numbers in parentheses under each model refer to the candidate models prior to selection (Annexe A: Tables A3 and A4) and the numbers in brackets show the total amount of explained variance.

Table 1.4 Results of the generalized mixed binomial regressions for inter-species variation in the timing of the bud break process.

Bud break	Frost probability (0-1)						Growing degree-days (°C, base temperate = 0 °C)						Photoperiod (day length in hours)					
	Temperate forest			Boreal mixedwood forest			Temperate forest			Boreal mixedwood forest			Temperate forest			Boreal mixedwood forest		
	White spruce	Black spruce	Norway	White spruce	Black spruce	Norway	White spruce	Black spruce	Norway	White spruce	Black spruce	Norway	White spruce	Black spruce	Norway	White spruce	Black spruce	Norway
0 -> 2	**0.39** **(140)**	0.28 (144)	0.28 (144)	**0.46** **(141)**	0.35 (145)	0.34 (147)							**15.37** **(140)**	15.53 (145)	**15.55** **(145)**	**15.48** **(141)**	15.77 (148)	**15.77** **(148)**
2 -> 3	**0.31** **(144)**	**0.09** **(156)**	**0.13** **(152)**	**0.33** **(147)**	**0.08** **(161)**	**0.12** **(158)**	327 (143)	539 (157)	501 (155)	386 (149)	534 (160)	505 (157)	**15.40** **(141)**	**15.90** **(159)**	**15.81** **(154)**	**15.76** **(148)**	**16.04** **(159)**	**15.98** **(156)**
3 -> 4							**387** **(147)**	**530** **(157)**	**521** **(156)**	397 (149)	538 (160)	532 (160)	**15.59** **(147)**	**15.86** **(157)**	**15.84** **(156)**	**15.78** **(149)**	**16.02** **(158)**	**16.04** **(159)**
4 -> 5							**439** **(150)**	**589** **(160)**	**528** **(157)**	**461** **(154)**	**662** **(169)**	**616** **(166)**	**15.70** **(151)**	**15.93** **(160)**	**15.85** **(157)**	**15.93** **(154)**	**16.11** **(163)**	**16.10** **(162)**
5 -> 6							**525** **(156)**	**667** **(167)**	**569** **(160)**	523 (159)	662 (169)	565 (162)						

▨	Not better than the null model
☐	Better than the null model but not the best model from the AICc model selection
🟦	Best model from AICc model selection

The predicted value per environmental variable is shown at which the probability that a bud transitions to the next stage is 0.51 per species, while numbers in parentheses show day-of-year at which the transition is predicted to occur. Boldface type indicates coefficients that differ from zero, while colors indicate model performance evaluated based upon corrected Akaike's information criteria (AICc).

Model selection on the six candidate photoperiod models produced from one to two statistically plausible models (5%) for each stage transition (Figure 1.8 and Annexe A: Tables A15–A19 for complete results of the AICc model selection per transition stage). The average marginal pseudo-R^2 (i.e., fixed effects) was 0.50 ± 0.09, while the conditional pseudo-R^2 (i.e., fixed plus random effects) was 0.83 ± 0.08 for the selected models. The null model that tested the occurrence of bud flush solely as a function of time was rejected for the first four transitions but was the most probable model for predicting the last transition (Figure 1.8 and Annexe A: Tables A15–A19). Thus, sensitivity to photoperiod was important for the first and intermediate phenological stages only. Sensitivity to photoperiod was the highest for the white spruce, followed by the Norway spruce and by the black spruce, and was higher in the temperate plantation compared to the boreal mixedwood plantation (Table 1.4, Annexe A: Tables A10–A14).

The probability of spring frost occurrence was slightly more important in predicting bud elongation (stage 2) compared to photoperiod (Annexe A: Table A10). Growing degree-days and photoperiod had a similar importance in terms of predicting intermediate phenological stages (bud swelling and translucent bud scales), whereas growing degree-days were more important than photoperiod for predicting the completion of the bud break process (Annexe A: Tables A10 to A14). Overall, the white spruce required shorter day lengths, fewer growing degree-days, and opened its buds under higher frost probabilities than did either the black spruce or the Norway spruce (Table 1.4).

1.5.3 Intraspecies variations in the effect of air temperature and photoperiod for predicting bud break phenology

Buds of white spruce seed sources K20 and K24 from the temperate forest were more sensitive to photoperiod for phenological stages two (bud elongation, see Table 1.3) to five (bud scales ripped and needles exposed to air temperature), were more sensitive to spring frost occurrence for the phenological stages two (bud elongation) and three (bud swelling), and were more sensitive to growing degree-days for phenological stages four (translucent bud scales), five (bud scales ripped and needles exposed to air temperature), and six (complete bud flush) compared to the seed source J70 originating from the boreal mixedwood forest (Table 1.5 and Annexe A: Tables A20 to A24). Therefore, white spruce seed sources from the temperate forest required shorter day lengths, fewer growing degree-days, and opened their buds under a higher probability of spring frost occurrence than the seed source from the boreal mixedwood forest (Table 1.5).

Since coefficients for the photoperiod models were stronger than those of the frost probability models, seed sources from the temperate forest were more sensitive to photoperiod than the local seed source originating from the boreal mixedwood forest (Annexe A: Tables A20 and A21). This result is further supported since the frost probability model is incapable of predicting the observed earlier bud opening of seed sources from the temperate forest compared to the seed source from the boreal mixedwood forest whereas the photoperiod model more accurately predicts this difference in bud break timing (Table 1.5).

Table 1.5 Results of generalized mixed binomial regressions for white spruce intraspecies variation in the timing of the bud break process.

Bud break	Frost probability (0-1)						Growing degree-days (°C, base temperate = 0 °C)						Photoperiod (day length in hours)					
	Temperate forest			Boreal mixedwood forest			Temperate forest			Boreal mixedwood forest			Temperate forest			Boreal mixedwood forest		
	J70	K20	K24	J70	K20	K24	J70	K20	K24	J70	K20	K24	J70	K20	K24	J70	K20	K24
0 -> 2	🟦 **0.37** **(141)**	🟦 **0.40** **(140)**	🟦 **0.41** **(139)**	🟦 **0.47** **(141)**	🟦 **0.47** **(141)**	🟦 **0.48** **(141)**							🟦 **15.36** **(141)**	🟦 **15.34** **(140)**	🟦 **15.33** **(140)**	🟦 **15.57** **(143)**	🟦 **15.43** **(139)**	🟦 **15.43** **(139)**
2 -> 3	🟦 0.29 (143)	🟦 **0.44** **(138)**	🟦 **0.37** **(140)**	🟦 **0.25** **(149)**	🟦 **0.39** **(144)**	🟦 **0.33** **(147)**	366 (146)	247 (135)	305 (142)	417 (151)	364 (147)	351 (146)	🟦 **15.54** **(146)**	🟦 **15.21** **(137)**	🟦 **15.38** **(141)**	🟦 **15.81** **(150)**	🟦 **15.70** **(146)**	🟦 **15.66** **(145)**
3 -> 4							🟦 **426** **(150)**	🟦 **366** **(146)**	🟦 **344** **(144)**	🟦 424 (151)	🟦 369 (148)	🟦 351 (146)	🟦 15.67 (150)	🟦 **15.55** **(146)**	🟦 **15.48** **(144)**	🟦 **15.85** **(151)**	🟦 **15.70** **(146)**	🟦 **15.67** **(146)**
4 -> 5							🟦 **430** **(150)**	🟦 **406** **(148)**	🟦 **411** **(148)**	🟦 **492** **(156)**	🟦 **470** **(155)**	🟦 **452** **(153)**	🟦 15.72 (152)	🟦 **15.64** **(149)**	🟦 **15.66** **(149)**	🟦 **15.97** **(156)**	🟦 **15.95** **(154)**	🟦 **15.89** **(153)**
5 -> 6							**548** **(158)**	**470** **(153)**	**488** **(154)**	**554** **(162)**	**497** **(157)**	**505** **(157)**	▨	▨	▨	▨	▨	▨

▨	Not better than the null model
☐	Better than the null model but not the best model from the AICc model selection
🟦	Best model from AICc model selection

The predicted value per environmental variable is shown at which the probability that a bud transitions to the next stage is 0.51 per seed source, while numbers in parentheses show day-of-year at which the transition is predicted to occur. Boldface type indicates coefficients that differ from zero, while colors indicate model performance evaluated based upon corrected Akaike's information criteria (AICc).

For the Norway spruce, the early emerging seed source K55 was more sensitive to the probability of spring frost occurrence for the first two transitions (Table 1.6 and Annexe A: Tables A25 to A29), was more sensitive to photoperiod for phenological stages one to five (Table 1.6 and Annexe A: Tables A25 to A29), and was more sensitive to growing degree-days for phenological stages four to six compared to later emerging seed sources K35, K39, and K50 (Table 1.6 and Annexe A: Tables A25 to A29). Therefore, the seed source K55 required shorter day lengths, fewer growing degree-days, and opened its buds under a higher probability of spring frost occurrence than late-emerging seed sources (Table 1.6 and Annexe A: Tables A25 to A29).

Table 1.6 Results of generalized mixed binomial regressions showing Norway spruce intraspecies variation in the timing of the bud break process.

Bud break	Frost probability (0-1)								Growing degree-days (°C, base temperate = 0 °C)								Photoperiod (day length in hours)							
	Temperate forest				Boreal mixedwood forest				Temperate forest				Boreal mixedwood forest				Temperate forest				Boreal mixedwood forest			
	K35	K39	K50	K55	K35	K39	K50	K55	K35	K39	K50	K55	K35	K39	K50	K55	K35	K39	K50	K55	K35	K39	K50	K55
0 -> 2	0.27 (145)	0.28 (144)	0.24 (146)	0.32 (142)	**0.33** **(146)**	**0.33** **(146)**	**0.28** **(148)**	**0.37** **(145)**									**15.56** **(145)**	15.54 (145)	15.61 (147)	**15.47** **(144)**	**15.82** **(149)**	**15.70** **(146)**	**15.79** **(149)**	**15.64** **(145)**
2 -> 3	**0.11** **(154)**	0.09 (156)	0.10 (155)	0.16 (150)	**0.15** **(155)**	**0.12** **(157)**	**0.12** **(157)**	**0.33** **(146)**	503 (155)	534 (157)	516 (156)	448 (152)	506 (157)	528 (159)	516 (158)	468 (154)	**15.82** **(154)**	**15.86** **(156)**	**15.86** **(156)**	**15.71** **(150)**	**15.95** **(155)**	**15.97** **(155)**	**15.96** **(155)**	**15.90** **(153)**
3 -> 4									**567** **(159)**	**556** **(158)**	**594** **(161)**	**426** **(150)**	**541** **(161)**	**541** **(161)**	**543** **(161)**	**461** **(154)**	**15.89** **(159)**	**15.90** **(159)**	**15.90** **(159)**	**15.71** **(150)**	**16.04** **(159)**	**16.01** **(156)**	**16.15** **(166)**	**15.92** **(154)**
4 -> 5									**569** **(159)**	**591** **(161)**	**516** **(156)**	**505** **(155)**	607 (166)	614 (166)	547 (161)	538 (160)	**15.91** **(159)**	**15.94** **(161)**	**15.84** **(156)**	**15.79** **(154)**	**16.09** **(161)**	**16.07** **(160)**	**16.05** **(159)**	**16.12** **(164)**
5 -> 6									613 (163)	644 (165)	587 (161)	472 (153)	636 (168)	662 (169)	607 (163)	470 (155)	▨	▨	▨	▨	▨	▨	▨	▨

▨	Not better than the null model
☐	Better than the null model but not the best model from AICc model selection
🟦	Best model from AICc model selection

The predicted value per environmental variable is shown at which the probability that a bud transitions to the next stage is 0.51 per seed source, while numbers in parentheses show day-of-year at which the transition is predicted to occur. Boldface type indicates coefficients that differ from zero, while colors indicate model performance evaluated based upon corrected Akaike's information criteria (AICc).

1.5.4 Heating requirements for bud flush based upon a degree-day threshold

The stage where needles are exposed to air temperate (stage five, see Table 1.3) is the stage that is conventionally analyzed (Hunter and Lechowicz, 1992; Hannerz, 1999; Snyder et al., 1999). Therefore, we used our mixed binomial regression model to predict the number of growing degree-days that were required for buds to reach that stage of bud phenology (stage five, see Table 1.3). At both plantation sites, white spruce's buds required fewer heating units to break compared to buds of black spruce and Norway spruce (Table 1.4). At the temperate forest site, buds of all three spruce species required fewer heating units to break compared to those at the boreal mixedwood forest site (Table 1.4).

At the intraspecies level, all three white spruce seed sources required on average 56 more heating units at the boreal mixedwood plantation to break compared to the temperate forest site. In both plantation sites, buds of the nonlocal southern white spruce seed sources K20 and K24 required on average 26 fewer heating units to break compared to buds of the northern seed source J70 (Table 1.5).

All Norway spruce seed sources required more heating units in the boreal mixedwood forest than in the temperate forest to break their buds. At both sites, the Norway spruce seed source K55 required fewer heating units to break its buds compared to all remaining Norway spruce seed sources (Table 1.6).

1.6 Discussion

1.6.1 Inter-and intraspecies variation in the timing of bud break

Bud flush started first for white spruces, followed by black spruces, and lastly, by Norway spruces, while the termination of bud flush ended first in white spruces, then in Norway spruces, and finally in black spruces. O'Reilly and Parker (1982), and

Numainville and Desponts (2004) reported the same species ordering for the bud flush sequences. For each species, bud flush ended earlier in the temperate forest than in the boreal mixedwood forest plantation. The time required for buds to complete their leaf-out was within the 15–23 day range recorded for white spruces (16–19 days *vs*. 18 days reported by Rossi and Isabel, 2017), for black spruces (19–23 days *vs*. 15–23 days reported by Rossi and Bousquet, 2014; Sylvestro et al., 2019), and for Norway spruces (15–17 days *vs*. 18–23 days reported by Fløistad and Granhus, 2010). The shorter duration of black spruce bud flush in the boreal mixedwood relative to the temperate forest may result from an adaptation selected to maximize carbon gains during the shorter growing season of the north (Clark et al., 2014b; Sylvestro et al., 2019). Yet, the duration of bud flush of white spruce and Norway spruce was not faster in the boreal mixedwood forest compared to the temperate forest. Given that our study sites covered a small portion (47°– 48° N) of continent-wide species ranges likely contributed to the observed decrease in clinal trend in bud flush with latitude. Still, earlier bud flush of nonlocal white spruce seed sources, when compared to the local white spruce seed source in the boreal mixedwood plantation, increased their probability of exposure to spring frosts, a result that was also reported in a transplant study conducted on 23 white spruce seed sources in Ontario (Canada) by Lu and Man (2011).

At both sites, three Norway spruce seed sources followed a similar bud break sequence (K35, K39 and K50) whereas the K55 seed source from Latvia completed its bud break ~10 days earlier. Since the Norway spruce is widely distributed in Europe, different tree populations are probably adapted to their local conditions (Matras, 2009; Chmura et al., 2018), thus, the earlier bud break from the Latvia seed source probably reflects a local adaptation. The similar bud break sequence from three different Norway spruce seed sources could suggest weak local adaptations regarding the bud break sequence or that the eastern Canadian boreal forest is so stressful to these three Norway spruce seed sources that it masked their difference in bud break sequence. Effectively, Klisz et al. (2019) showed that when climate is the most important factor determining the development of trees such as at the margin of a species range, the importance of local adaptation is reduced.

1.6.2 Interspecies variation in the effect of air temperature and photoperiod for predicting bud break phenology

White spruces exhibited a clear change in sensitivity to air temperature variables, consistent with our hypothesis. Its first stages were driven by spring frost occurrence, whereas its intermediate and final stages were driven by growing degree-days. Therefore, the white spruce shifts its strategy from frost avoidance in the early stages to maximize the growing season length by flushing buds more rapidly with increasing air temperature for the intermediate and final stages. Specifically, spring frost occurrence was most important in controlling bud flush in the boreal forest, where this phenomenon was the most frequent. In contrast, sensitivity to photoperiod in the temperate forest could replace the lower spring frosts occurrence to trigger bud flush. In environments where spring frosts rarely damage trees severely, day length would be the environmental variable driving bud break timing. Both the black spruce and the Norway spruce, however, were less sensitive to spring frosts occurrence, but they were sensitive to growing degree-days for their intermediate and final stages of bud phenology. The black spruce was the least sensitive species to both growing degree-days and spring frost occurrence, but its late bud flush prevented damage to buds from spring frost events and its faster completion of the bud break process could maximize growing season length. Thus, late-emerging species may wait for a low frost frequency before opening their buds, but hasten their development, which maximizes the growing season length. In contrast, early-emerging species may develop their buds earlier, but more slowly to keep the leaf primordia protected by the bud scales while frost probability is high.

Since our study is only empirical, future experiments also aiming to disentangle the importance of frost, photoperiod and growing degree-days on the bud break sequence of spruces should be conducted and compared to our results. Still, frost probability in late spring represents a just simplification of the evolutionary trade-off imposed on boreal and temperate trees by the freezing temperatures. Even if laboratory studies suggest that frost events of low intensity have minimal impact on the bud break sequence of spruces since the dehardening threshold values preventing frost damage to buds decreased from −10°C at the swelling stage to −5°C at the bud break stage (Glerum, 1973; Repo, 1992; Bigras and Hé bert, 1996), it contradicts with the frost damage to buds or newly formed foliage we observed (gray-black buds or brown-white needles leaning downward, Annexe A: Figure A3) after a night frost of −2°C (data not shown), which was also reported by Cannell (1984). Frost damage to buds probably follows a dynamic process where frost damage occurs when the heat loss by trees during nighttime exceeds the heat accumulated during the day. Since laboratory studies likely grew seedlings to air temperatures above those observed in the field, field trees probably accumulated less heat during the day and could therefore be damaged by less intense frost events. Since the synchrony between spring frosts and the bud break was shown to be an important aspect of tree fitness (Vitra et al., 2017), the probability of spring frost could better represent the evolutionary pressure imposed by late-spring frosts on the survival of trees compared to growing degree-days.

1.6.3 Intraspecies variation in the effect of air temperature and photoperiod for predicting bud break phenology

We tried to quantify the capacity of nonlocal white and Norway spruce seed sources to adapt when transplanted to a new climate that was used as a proxy for climate change. We showed that nonlocal white spruce seed sources originating from the southern temperate forest opened their buds earlier than did the local seed source from the boreal mixedwood forest. Therefore, nonlocal southern seed sources could only partly adapt to their new climate, which is consistent with our hypothesis. Specifically, early stages of bud phenology of the nonlocal (southern) white spruce seed sources were more sensitive to photoperiod compared to the local seed source and were also more sensitive to growing degree-days for their intermediate stages of bud phenology. Our results for the black spruce seed source originating from the boreal forest, where spring frost probability is high, showed that bud flush was slightly more sensitive to air temperature than to photoperiod. We propose a general explanation driving the leaf-out process in spring. On one hand, tree populations that are growing in environments where spring frost is frequent and likely throughout the growing season, as is the case in the boreal forest, have adapted to the risk of frost damage. Accordingly, onset of bud flush is driven by frost probability. On the other hand, tree populations that are growing in environments where air temperature warms more rapidly, and where spring frost probability decreases quickly, have adapted to a photoperiod-triggered leaf-out, concomitant with the decrease in spring frost probability.

As in previous studies, we found a large within-tree variation in bud break timing (Rousi and Heinonen, 2007; Sylvestro et al., 2019) that probably results from an adaptation to limit the damage caused by spring frosts. The late bursting of some buds ensures that trees can still grow even if some buds were damaged by spring frosts. However, this large variation in bud break timing caused some problems when we predicted the average date buds transit from a phenological stage to the next because the predicted date at which buds reached late transitions could have been predicted prior to the dates at which buds reached earlier transitions (Figure 1.4). By analyzing each step separately instead of analyzing each step in a single model, we might have increased the overlap between stages (Clark et al., 2014a; Clark et al., 2014b). The overlap problem was mostly observed for Norway spruce seed sources (K50 and K55). Since the predictions were based upon the probability (0.51) that buds transited toward the next stage, the probability that buds did not transit was still of 0.49, which might have increased the overlap problem between successive stages. Had we chosen a different threshold value; the proportion of overlap would have also changed. We confirm that at the bud level no late stages were registered before earlier ones therefore, the overlap problem is likely due to the large variation in bud break timing between trees and to the smaller sample size at the seed source level. Still, errors were of fewer days than our sampling interval. Given the logistical constraints, it was not possible to sample at a shorter time interval. Since it is common for bud phenology data to show some overlap between successive stages (Clark et al., 2014a), these rare problems unlikely discredit the general conclusion of our study but call for increasing studies analyzing each stage of the bud break process, which for now are still scarce. We acknowledge that Clark et al. (2014a; 2014b) developed a continuous development model (CDM) consisting of a Multinomial Hidden Markov Chain within a Bayesian framework to analyze the bud break process, but the greater complexity of running this model compared to running separated binomial regressions informed our choice.

1.6.4 Heating requirements for bud flush based on growing degree-day thresholds

The bursting of buds is a phenotypic trait that is under the control of both genetic and phenotypic plasticity (Worrall and Mergen, 2006; Yakovlev et al., 2006; Pelgas et al., 2011; Rossi and Bousquet, 2014). However, the share of both components (genetics and phenotypic plasticity) is likely species- and population-dependent, thus, the capacity of different tree populations to vary their timing of bud break according to changes in climate will vary across tree populations and species. With heating requirement for bud flush varying between 77 and 1278 growing degree-days, the Norway spruce is a spruce species showing high variations in timing of bud break compared to the white spruce, which required between 233 and 360 degree-days (Man and Lu, 2010; Man et al., 2016; Man et al., 2017) and the black spruce, which required between 284 and 514 growing degree-days (Bronson et al., 2009; Antonucci et al., 2015; Man et al., 2016). In our study, the number of GDDs that were required for white (450 GDD) and black spruce, (626 GDD) bud flush was slightly above their previously reported upper range whereas the Norway spruce (572 GDD) was in the middle of its reported range.

Blum (1988) developed the hypothesis that populations of trees growing in colder sites (north) would require fewer heating units to flush their buds compared to southern populations. Similar results were reported by Sylvestro et al. (2019). In the present study, the heating requirement for all three spruce species were higher at the boreal mixedwood plantation site and contrast with Blum's (1988) hypothesis. However, our results are consistent with our hypothesis that frost probability outperformed degree-day sums to trigger onset of bud flush. We suggest that in sites where spring frost probability is high, onset of bud flush is postponed, which also increases their heating requirement whereas in sites where spring frost frequency is low, buds flush sooner, which decreases their heating requirement. Yet, complexity arises because air temperature increases more slowly in the boreal site. Even if bud flush is later in terms of calendar days, accumulated degree-days can still be lower compared to temperate sites where air temperature increases more rapidly. We suggest that the intraspecies variation in heating requirement found in previous studies probably represents the variation in spring frost probability that is experienced by the different tree populations. Even if traditional studies have used growing degree-days to predict bud flush, we have advanced the idea that spring frost occurrence is the main driver of spruce bud flush. In fact, Kollas et al. (2014) showed that the environmental driver common to both altitudinal and latitudinal species range limitation was frost risk during leaf-out. Frost probability was also shown to drive the leaf-out process of various tree species along an altitudinal gradient in Switzerland (Lenz et al., 2016) and on the Tibetan Plateau (Wang et al., 2019). Therefore, ecophysiological models of bud break should include spring frost variables.

1.6.5 Adaptation capacity to spring frosts in the context of climate change

Spring frosts are daily events that require a set of specific meteorological conditions, such as a night without wind and clouds, to occur (Laughlin and Kalma, 1987; Lindkvist and Lindqvist, 1997; Chung et al., 2006). These specific conditions are hardly modeled with accuracy by climate change models. Since climate change already increased the global mean annual temperature by 1°C (Allen et al., 2018) but that spring frosts still occur frequently in boreal mixedwood forests (see Study site section), climate warming over the next 50 years will unlikely decrease the future frequency and intensity of spring frosts enough to limit their impact on tree growth. Consistent with previous studies assessing the impact of climate change on bud phenology (Polgar et al., 2013; Olsson et al., 2017), our results suggest that bud flush of spruce species would hasten in the future because higher air temperatures will accelerate transitions of the temperature-sensitive stages of bud phenology. Yet, photoperiod-sensitive stages of bud phenology should limit premature leaf-out and become a more prominent safety mechanism preventing frost damage. Experimental temperature manipulations have shown that the bud break sequence of boreal tree species was completed earlier when they were artificially heated, but that faster bud break was restricted to the last stages of bud phenology, which are the stages we demonstrated to be less sensitive to photoperiod (Rossi, 2015; Rossi and Isabel, 2016; Rossi and Isabel, 2017). It was also shown that the first stages of bud phenology were under stronger genetic control compared to the last phenological stages (Perrin et al., 2017). Under a warmer climate, we would expect earlier bud flush in spruce species that are growing in boreal mixedwood forests, since they are more sensitive to air temperature compared to spruce species growing in southern temperate forests. We also expected that the black spruce, which is less photoperiod-sensitive than the white spruce, would advance its bud phenology more rapidly, which would increase its risk of frost damage. Overall, convergence of bud phenology across spruce species is to be expected, an observation that has also been reported over altitudinal gradients (Chen et al., 2018; Vitasse et al., 2018).

Our results can also guide climate-smart forestry practices aiming to manage the boreal-temperate forest ecotone in a sustainable way (Nagel et al., 2017; Verkerk et al., 2020). The long (60–100 years) rotation length of spruce plantations established in the boreal mixedwood forest paired with the fast rate of climate warming ensures that trees currently planted will be growing in a warmer climate than the current climate. However, planting for the future first requires the survival of the planted seedlings in their early years. Accordingly, photoperiod-sensitive seed sources such as the southern with spruce seed sources consist in a poor choice for establishing productive plantations in the boreal mixedwood forest since these seed sources will likely be frequently damaged by spring frosts. Local seed sources better adapted to prevent damage from spring frost consist in a better choice for establishing productive plantations. Since the black spruce is the spruce species that burst its buds the latest, it is the least likely species to be damaged by spring frosts, therefore, it currently represents the best species to plant in spring frost-prone environments. However, the warming of air temperature paired with the black spruce low photoperiod sensitivity should hasten its future bud burst and increase its exposure to spring frost, thus, probably reducing its future productivity. Interestingly, we showed that assisted migration and the use of foreign species might not always be a good option for increasing tree productivity, mostly when extreme events such as spring frosts can importantly damage trees.

1.7 Conclusion

Our novel approach allowed us to identify the probability of spring frost occurrence as the driver of bud break onset, while growing degree-days drove the intermediate and final phenological stages of bud break. Incorporating this change in sensitivity to climate along the bud break sequence should increase the realism of process-based models of bud burst in temperate and boreal tree species. Further, its inclusion should increase the accuracy of predicting the response of bud break phenology to climate change and help to plan forest management practices that could mitigate the negative effects of climate change on forest productivity.

1.8 Acknowledgements

We thank the Natural Sciences and Engineering Research Council of Canada (NSERC) for funding this research project. We acknowledge the valuable field assistance provided by L. Gervais and R. Mincheva. We are also grateful to F. Rousseau, who provided support and advice on the statistical analysis, together with the R codes that were used in this research project, and to P. Duval for his help in identifying the stages of bud phenology.

1.9 Conclusion

Cet article est novateur puisqu'il montre l'importance d'une variable climatique (probabilité d'occurrence de gel) qui a été jusqu'à présent peu considérée dans l'élaboration des modèles écophysiologiques. Étant érigé sur une base empirique solide, les fondements émis de l'avant dans cet article permettent de remettre en question la conception et la mécanique des modèles présentement utilisés pour représenter l'éveil de l'arbre au printemps, en plus d'ouvrir de nouvelles pistes de réflexion et de nouvelles hypothèses de recherche concernant l'impact des changements climatiques sur le débourrement des épinettes à l'écotone de la forêt boréale-tempérée de l'ouest du Québec. Effectivement, la faible sensibilité de l’épinette noire à la photopériode suggère que l’éveil de cette espèce au printemps sera plus fortement devancé par le réchauffement climatique que l’éveil printanier de l’épinette blanche et de l’épinette de Norvège, ce qui rapprochera le moment de leur éveil. Cette avancée probable du débourrement des bourgeons de l’épinette noire risque d’augmenter son exposition au gel printanier et possiblement de diminuer sa croissance future. Déterminer l’impact des dommages causés par le gel printanier sur les deux méristèmes (apical et latéral) devient donc primordial pour comprendre le développement des arbres et pour anticiper les effets des changements climatiques sur leur croissance future. Le deuxième chapitre de ma thèse vise donc cet objectif, en développant des séries dendroécologiques recensant les cernes de gels (séries de cellules endommagées par le gel printanier) le long du tronc, et en mettant en relation la sévérité des dommages aux cellules cambiales à la hauteur des arbres.

CHAPITRE II

GROWING-SEASON FROST IS A BETTER PREDICTOR OF TREE GROWTH THAN MEAN ANNUAL TEMPERATURE IN BOREAL MIXEDWOOD FOREST PLANTATIONS

Benjamin Marquis, Yves Bergeron, Martin Simard et Francine Tremblay

Cet article est publié à la revue scientifique

Global Change Biology

2.1 Graphical abstract

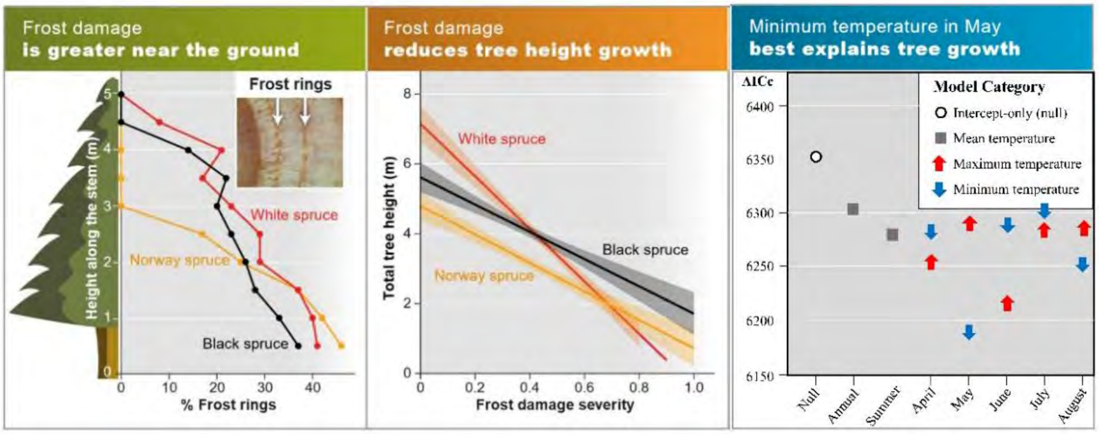

Figure 2.1 Impact of frost damage along the stem and on tree height in addition to the capacity (AICc units) of frost intensity to predict height growth compared to an intercept-only model (Null) and the mean and maximum air temperature for various periods (annual, summer [June-July-August], and monthly).

2.2 Résumé

Il est envisagé que l’éveil plus hâtif des arbres au printemps, qui est déclenché par le réchauffement climatique, pourrait augmenter la sévérité des dommages causés par le gel printanier et ainsi contrebalancer l’augmentation future de la productivité forestière. Nous avons quantifié l’impact des gelées survenant pendant la saison de croissance sur la performance de trois espèces d’épinettes (l’épinette blanche, l’épinette noire et l’épinette de Norvège) possédant une tolérance différente aux gelées d’été, et ce, dans deux plantations établies de chacun des côtés de l’écotone de la forêt tempérée-boréale de l’Est du Canada. Les objectifs de notre étude étaient de déterminer (1) si les espèces et les sources de graines plantées à des sites loin de leur résidence naturelle seraient moins bien adaptées aux conditions locales que la provenance résidente près du site de plantation, ce qui accroitrait les dommages causés par le gel et réduirait leur croissance; (2) à quelle hauteur les gelées d’été arrêtent d’endommager le méristème apical; (3) si

la croissance en hauteur était mieux prédite par l’intensité des gelées d’été ou bien par la température moyenne (annuelle ou d’été). À chaque site et pour chaque espèces et source de graine, des analyses de tige ont été effectuées. Les cernes de croissance ont été datés, identifiés et se sont vu attribuer une valeur de sévérité basée sur le niveau d’endommagement des cellules. Aux deux sites, la sévérité des dommages par le gel réduit la hauteur des arbres, et ce, pour chaque espèce et provenances. L’épinette de Norvège a été l’espèce qui a le plus gelé et qui était aussi la plus petite, et ce, aux deux sites. Cependant, à la plantation la plus au nord, c’est l’épinette blanche qui a été l’espèce subissant la plus forte réduction de croissance engendrée par le gel, ce qui suggère que cette espèce est hautement sensible aux évènements de gel printanier. À l’inverse, l’épinette noire a été l’espèce la moins affectée par le gel printanier, et ce, aux deux sites. Pour toutes les espèces, le méristème apical a été endommagé jusqu’à deux mètres de hauteur. La sélection de modèles par AICc a identifié que la température minimale du mois de mai était, et de loin, la meilleure variable climatique pour prédire la croissance en hauteur des arbres (poids d’Akaike=1), ce qui met en évidence l’importance de considérer les évènements climatiques extrêmes, surtout parce que ceux-ci devraient augmenter en intensité dans le futur.

2.3 Abstract

Increase in frost damage to trees due to earlier spring dehardening could outweigh the expected increase in forest productivity caused by climate warming. We quantified the impact of growing-season frosts on the performance of three spruce species (white, black, and Norway spruce) and various seed sources with different frost tolerance in two plantations, established on both sides of the eastern Canadian boreal-temperate forest ecotone. The objectives of this study were to determine (a) if spruce species and seed sources planted in sites far from their natural provenance would be less adapted to local site conditions, leading to increased frost damage and reduced height growth;

(b) at which height above the ground growing-season frosts ceased to damage apical meristems; and (c) if height growth was best predicted by extreme climatic events (growing-season frosts) or by mean annual or summer temperature. At each site and for all spruce species and seed sources, we cross-sectioned spruce trees at different heights above the ground. Tree rings were cross-dated and screened for frost rings, which were then given a severity score based on cellular damage. Frost severity reduced height growth of all spruce species and provenances at both sites. Height growth of the non-native Norway spruce was the most reduced by frost severity and was the smallest species at both sites. Frost caused the highest growth reduction in white spruce at the boreal mixedwood site and had the least effect on black spruce at both sites. For all spruce species, height growth was affected up to 2 m above the ground. Model selection based on corrected Akaike's information criteria (AICc) identified that minimum temperature in May was by far the best climate variable predicting tree growth (AICc weight = 1), highlighting the importance of considering extreme climatic events, which are likely to increase in the future.

Keywords: Boreal forest, Forest productivity, Frost rings, Growing-season frosts, *Picea*, Stem analysis, Sustainable forest management, Tree dormancy

2.4 Introduction

The fast rate at which climate change operates (Loarie et al., 2009), paired with the increase in frequency and intensity of extreme climatic events (Bonsal, Zhang, Vincent, and Hogg, 2000), can desynchronize the annual dormancy-growth cycle of trees with air temperature (Parmesan and Yohe, 2003). Climate warming-induced earlier dormancy release in spring and later autumn hardening of tree tissues could extend the growing season and increase forest productivity (Bertin, 2008; Rossi, Girard, and Morin, 2014). This could extend the growing season during the period where frost resistance of trees is at its lowest and could increase frost damage to trees (Ault et al., 2013; Cannell and Smith, 1986; Liu et al., 2018). Thus, extension of the growing season may result in decreased tree growth and potentially impede our capacity to reach sustainable forest management (Man, Kayahara, Dang, and Rice, 2009).

Several factors limit our ability to predict climate warming effects on frost damage to trees. First, dormancy release, autumn hardening, and frost resistance are physiological traits that vary both between and within species (Clark, Salk, Melillo, and Mohan, 2014; Li, Beaulieu, Daoust, and Plourde, 1997; Villeneuve et al., 2016). Determining the threshold values of the annual dormancy-growth cycle of trees requires long-term monitoring or extensive experiments (Olson et al., 2013), and thus even extensive studies are usually restricted to either the inter- or intra-species level, and tree physiological properties are most often based on model simulations parameterized on a limited number of species and locations (Chuine, 2000; Hänninen, 2016; Man and Lu, 2010; Morin et al., 2009). Second, frost effects on tree growth are most often modeled to occur below some specific temperature thresholds (Ma, Huang, Hänninen, and Berninger, 2018; Morin and Chuine, 2014) instead of being based on biological evidence such as damage to apical (bud mortality) or cambial (frost rings) meristems (Bigras and Hébert, 1996; Payette, Delwaide, and Simard, 2010; Sutinen, Roitto, and Repo, 2015). Not all freezing temperatures necessarily cause frost damage to trees (Dy and Payette, 2007) and it is unlikely that a given freezing temperature threshold equally impacts all tree species and populations. Third, most forest growth models like SORTIE and JABOWA are not built to include frost effects because they use aggregated temperature variables such as mean annual temperature or growing degree days (GDD) to predict tree growth (Bugmann, 2001; Pacala et al., 1996; Piao et al., 2019; Purves, Lichstein, Strigul, and Pacala, 2008). However, in boreal mixedwood forests, the mean annual temperature is not correlated with the occurrence of growing-season frosts (Hänninen, 2016). For instance, the last growing-season frosts could occur late in the season even if the mean annual temperature was generally warm and reversely, generally colder years do not imply a greater frequency of growing-season frosts (Hänninen, 2016). Therefore, during years of growing-season frosts, forest growth models can overestimate tree growth.

Growing-season frost damage to young trees is more important in young plantation forests than in semi-natural and natural forests since the reduced or lack of canopy cover in young plantations exposes trees to high daily variations in temperature, which can reduce tree performance since a frost event followed by high light intensity increases damage to photosynthetic organs (Langvall, Nilsson, and Örlander, 2001; Örlander, 1993). Moreover, the apical meristem of young trees can be within the zone of ground frost (approximately 0–2 m; Langvall and Löfvenius, 2002), which could cause it to freeze recurrently and delay height growth by decades (Clements, Fraser, and Yeatman, 1972). This frost-related growth reduction problem is mostly observed in plantations established in the boreal mixedwood forest like in Sweden and Canada (Groot and Carlson, 1996; Langvall et al., 2001; Man et al., 2009).

Transplant experiments offer the possibility to test inter- and intra- species variations in the annual dormancy-growth cycle of trees *in situ*. This type of study is specifically designed to determine the most adapted species and seed sources to a given site to increase forest productivity (Beaulieu, Perron, and Bousquet, 2004; Olson et al., 2013). In addition, transplant experiments can test the impact of climate warming on trees using the concept of space-for-time substitution to forecast future forest productivity of northern plantations based on observed forest productivity at southern plantations. This concept is the backbone theory supporting assisted migration, which is used to transplant faster-growing seed sources from southern populations to northern sites to increase forest productivity (Li et al., 1997; Nagel et al., 2017; Villeneuve et al., 2016). However, the higher frequency and intensity of frost events in the north could lead to reduced growth and increased tree mortality if ill-adapted seed sources were transplanted too far north. In addition, Liu et al. (2018) showed that climate warming can increase vegetation exposure to frost events, which could decrease productivity of the southern seed sources, in which case northern seed sources better acclimated to frost could be planted south to lessen the frost-induced reduction of forest productivity (Montwé, Isaac-Renton, Hamann, and Spiecker, 2018).

This study, carried out in the mixed boreal forest of eastern Canada, first aimed to determine the impact of growing-season frosts on the performance of three spruce species, white spruce (*Picea glauca* [Moench] Voss; three seed sources), black spruce (*Picea mariana* [Mill.] B.S.P.; one seed source), and Norway spruce (*Picea abies* [L.] Karst.; four seed sources), which have different frost tolerance and growth rates. Trees were sampled at two experimental plantations established in 2002 in the temperate and boreal mixedwood forests. Tree growth at the temperate forest plantation was also used as a proxy for the effect of climate warming on tree growth at the boreal mixedwood forest plantation. We hypothesized that species and seed sources planted in sites far from their natural provenance would be less adapted to local site conditions, causing greater asynchrony between dormancy release and air warming, in turn leading to increased frost damage and reduced tree growth. To test our hypothesis, we conducted three analyses: (a) we determined if species and seed sources showing severe frost damage to cambial cells would be smaller than species and seed sources showing undamaged cambial cells; (b) we determined the height along the stem at which growing-season frosts ceased damaging the apical meristem by analyzing cross-sections sampled at various heights along the stem; and (c) we determined whether climate variables measuring extreme climatic events like frost intensity and frost frequency better explained inter- and intra-species variations in height growth compared to conventional aggregated climate variables (mean annual temperature and summer temperature) that are less physiologically meaningful to the annual dormancy-growth cycle of trees. For our first analysis, we expected four outcomes: (a) Norway spruce, the most foreign and least-adapted species to local site conditions, should show the greatest frost damage (in the form of frost rings), causing it to have the lowest height growth even if it has the highest growth rate; (b) white spruce should show a higher frequency of frost rings and lower height growth than black spruce during years of growing-season frosts, even if it has a higher growth rate, because it exits dormancy earlier than black spruce, which increases its exposition to growing-season frosts (Marquis, Bergeron, Simard, and Tremblay, 2020); (c) all Norway spruce seed sources should perform poorly as all seed sources are foreign and are not adapted to local conditions; and (d) the closest white spruce seed source to each plantation site should perform the best and show less frost damage. For our second analysis, we expected that above 2 m from the ground, radiative frosts stop damaging the apical meristem and for our third and last analysis, we expected that tree height will be best explained by the minimum temperature in spring (frost intensity) and frost frequency (number of frost days). This last analysis should reveal that considering extreme climate events paired with the annual dormancy-growth cycle of trees is important and must be incorporated in models predicting current and future forest productivity of young plantations established in the boreal mixedwood forests.

2.5 Material and methods

2.5.1 Study site

The study was set in the Clay Belt of Quebec in the transition zone between the northern temperate forest and the boreal forest of eastern Canada (Saucier, Robitaille, and Grondin, 2009). One plantation was established in the Angliers township (47.29°N, 79.12°W), located in the balsam fir (*Abies balsamea* [L.] Mill.)-yellow birch (*Betula alleghaniensis* Britt.) bioclimatic domain (Saucier et al., 2009), which is at the northern edge of the temperate forest (see Annexe B: Figure B1). The mean annual temperature is 3.1°C (mean temperature in January and July is −15.0°C and 18.8°C, respectively), total annual precipitation is 967 mm, 27% of which falls as snow (1981–2010 normals, Barrage Angliers weather station, located 24 km from the plantation; Environment Canada, 2019a) the growing season lasts 165 days, with GDD above 0°C of 2,660, and the last growing-season frost usually occurs by the end of May (0.25 probability that air temperature drops below 0°C on May 30) but could occasionally occur by mid-June (0.10 probability that air temperature drops below 0°C on June 15). The other plantation was established in Lake Duparquet Research and Teaching Forest (48.29°N, 79.26°W), located in the balsam fir-white birch (*Betula papyrifera* Marsh.) bioclimatic domain which is at the southern edge of the boreal mixedwood forest (Saucier et al., 2009). The mean annual temperature is 1.0°C (mean temperature in January and July is −17.9°C and 16.7°C, respectively), and total annual precipitation is 985 mm, 28% of which falls as snow (1981–2010 normals, Mont Brun weather station, located 47 km from the plantation; Environment Canada, 2019b). The growing season lasts 143 days, with GDD above 0°C of 2,282, and the last growing-season frost usually occurs in mid-June (0.25 probability that air temperature drops below 0°C on June 23) but could occasionally occur by early July (0.10 probability that air temperature drops below 0°C on July 4). The poor drainage of the clay soils can limit soil warming and generate air temperature inversion causing nearground night frosts lasting few hours (Dugas, 1975). Since -5°C for 5 hr is enough to damage cambial cells, frost events of short duration can greatly impact the growth of young trees (Dy and Payette, 2007). The similar structure and texture of clay soils at both sites (Laamrani et al., 2014) and the negligible differences in photoperiod (less than 8 min; Environment Canada, 2019c) allowed us to test the effect of air temperature, growing-season frost intensity, and growing-season frequency on annual height increment while controlling for soil and photoperiod effects (Figure 2.2).

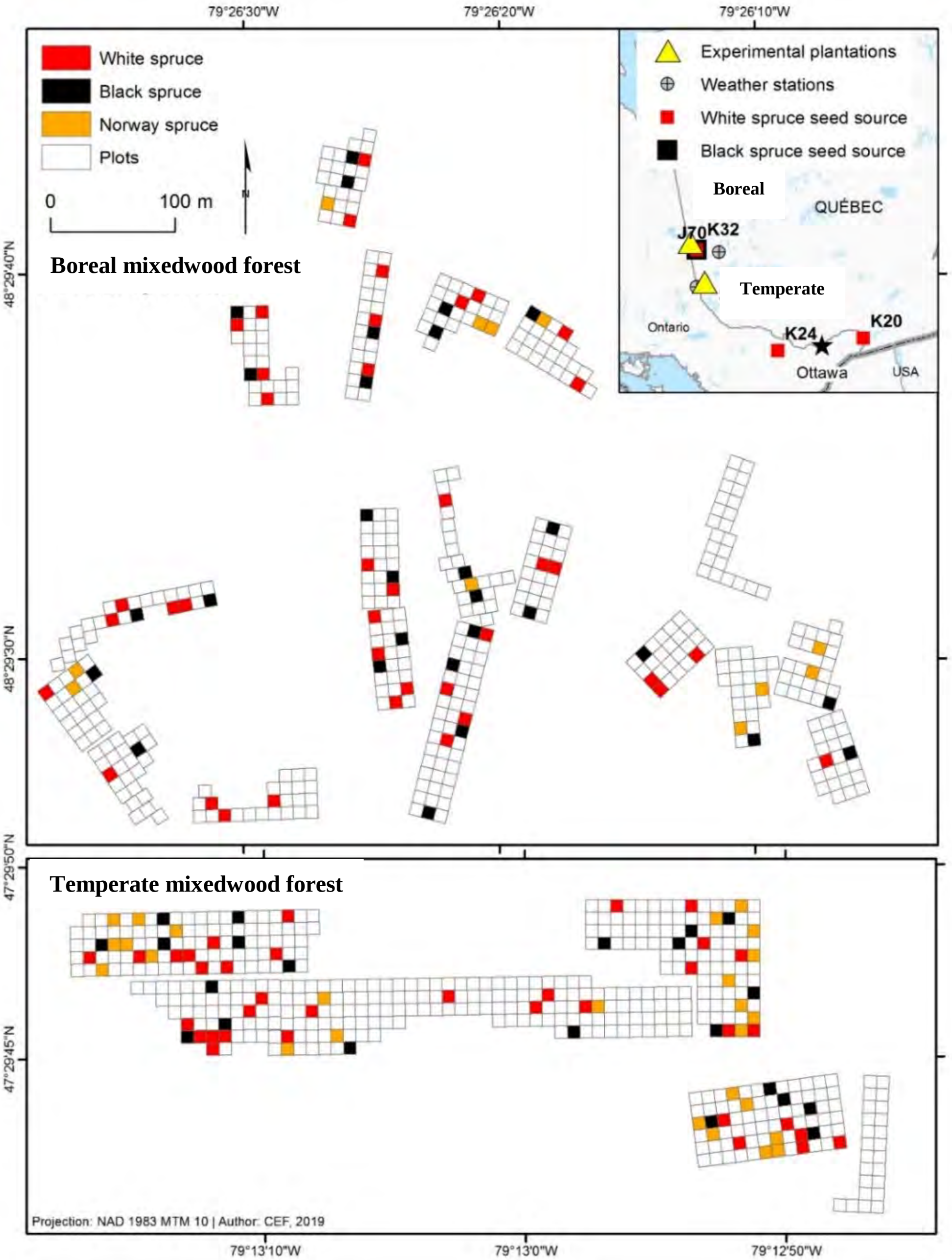

Figure 2.2 Map of the study sites showing the experimental design of the plantations and the randomly sampled plots used for this study at the boreal mixedwood forest (top) and at the temperate mixedwood forest (bottom) plantations. The inset shows the location of the temperate and boreal plantations (yellow triangles), of North American seed sources (black spruce = black square and white spruce = red square; see Table 2.1 for the description of the eight seed sources studied), and the location of the weather stations used in the analyses. The scale applies to both plantations.

2.5.2 Experimental design

In the two plantations established in 2002, 20 different Norway spruce seed sources, 20 different white spruce seed sources, and one black spruce seed source were planted with a density of 3,900 trees/ha (see Table B1 for the geographic location of the 41 seed sources). Therefore, in our study, all trees have the same age. Each plantation was divided in 480 square plots of 8 m × 8 m in which 25 seedlings of the same seed source were planted (Figure 2.2). The seed sources were randomly allocated to a plot. However, we restricted our analyses to eight seed sources (see Table 2.1 for a description of these eight seed sources). We selected the one black spruce seed source originating from the boreal mixedwood forest and we randomly selected four Norway spruce seed sources and three white spruce seed sources by grouping the 20 white spruce and the 20 Norway spruce seed sources in quartiles based on their average height (measured in 2012) and randomly selecting one seed source per quartile so that the studied sample covered the range of growth potential of both white and Norway spruce (Table 2.1; see Table B2 for a description of the climate at the location of origin of the non-local seed sources). The only quartile that was not randomly sampled was the one including the white spruce J70 seed source, which is naturally growing close to the boreal mixedwood plantation. This seed source was deliberately selected to compare local versus extra-local sources. Unfortunately, white spruce seed sources from the lower quartile (smallest trees) were dead in 2016 at the boreal mixedwood plantation so only three white spruce seed sources were used. Only one black spruce seed source originating from the boreal mixedwood plantation was tested since this seed source was expected to be the most tolerant to growing-season frosts, it thus proves a reliable control to test the impact of growing-season frost on tree performance. Also, black spruce is more tolerant of growing-season frosts than white spruce; however, the growth rate of white spruce is usually higher than black spruce; therefore, black spruce can be used as a benchmark control to disentangle productive versus unproductive white spruce seed sources (Poulin, 2013; Prégent, Bertrand, and Charrette, 1996;

Prégent, Picher, and Auger, 2010). All plots where the annual shoot was infested by the white pine weevil (*Pissodes strobi*) were discarded. From the remaining plots, a stratified sampling method was performed to randomly select 162 plots distributed across species and seed sources. In these selected plots, one tree was randomly sampled for a stem analysis (Figure 2.2; Table 2.1).

Table 2.1 Number of trees sampled for stem analysis, the quartile from which they were sampled (based on their average height in 2012), and the median height (measured in 2016) per species for the eight seed sources used in this study.

					Number of trees (median height in cm)	
Locality	**Latitude**	**Longitude**	**Spruce species**	**Seed source (quartile)**	**Temperate forest plantation**	**Boreal forest plantation**
Glubokskii, Belarus	55.15°N	30.10°E	Norway	K35 (Q4)	7 (323)	3 (192)
Istebna, Poland	49.33°N	18.52°E	Norway	K39 (Q3)	7 (300)	1 (218)
Gorodokskii, Belarus	55.30°N	30.00°E	Norway	K50 (Q1)	6 (347)	3 (208)
Auce, Latvia	56.25°N	22.50°E	Norway	K55 (Q2)	7 (346)	3 (163)
				Total	**27**	**10**
Duparquet, Québec	48.29°N	79.26°W	White	J70 (Q4)	20 (542)	26 (271)
Cushing, Québec	45.36°N	74.28°W	White	K20 (Q2)	7 (366)	7 (157)
Petawawa, Ontario	45.54°N	77.20°W	White	K24 (Q3)	7 (551)	6 (166)
				Total	**34**	**39**
Duparquet, Québec	48.29°N	79.26°W	Black	K32	23 (462)	29 (375)
				Grand total	**84**	**78**

2.5.3 Stem analyses and frost ring identification

To exclude abnormal growth due to tree planting, the year trees were planted was left out of the analysis, and only height increment data for the period 2003–2016 were used. Trees <1 m high were cross-sectioned every 2 cm, whereas trees taller than 1 m were cross-sectioned at 5 cm intervals in the first meter above the ground, at 10 cm intervals between 1 and 2 m high, and at 50 cm intervals thereafter. The finer sampling at the base of the trees ensured a precise measurement of the annual height increment when height growth is slower. Even with this thorough sampling procedure, we missed few internodes. In this case, we estimated height growth for the missing internodes using linear interpolation. Cross-sections were sanded to 400 grit, visually cross-dated under 40× magnification and observed for frost rings. Frost rings are a series of cambial cells within a tree ring showing damaged cell walls, bent radial rays and damaged tracheids caused either by the contraction and contortion of the frozen bark (Glerum and Farrar, 1966) or by a break in the water column induced by ice crystals and high vapor pressure due to the increased transpiration when frost days are followed by a sudden increase in temperature (Schweingruber, 2007). In cold environments subject to growing-season frosts like in the boreal mixedwood forest and at the alpine treeline, more than one frost ring can form within a tree ring and the cellular damage varies according to the intensity of the frost events, which can have various effect on the architecture and growth of the trees (Gurskaya and Shiyatov, 2002; Schweingruber, 2007). Thus, we analyzed the effects of frost ring severity on height growth by recording frost ring severity in three classes: class 1, slightly distorted cells, damage not present along the whole circumference of the annual ring; class 2, distorted cells present along the whole circumference of the annual ring; and class 3, heavily distorted cells present along the whole circumference of the annual ring (Figure 2.3).

Throughout this paper, minimum air temperature < 0°C is used to represent the intensity of a frost events which is a distinct concept from frost severity, which is instead used to represent the damageable effect growing-season frosts have on cambial cells and is represented by both the abundance (% rings showing a frost ring) and magnitude (the three classes cited above) of frost damage.

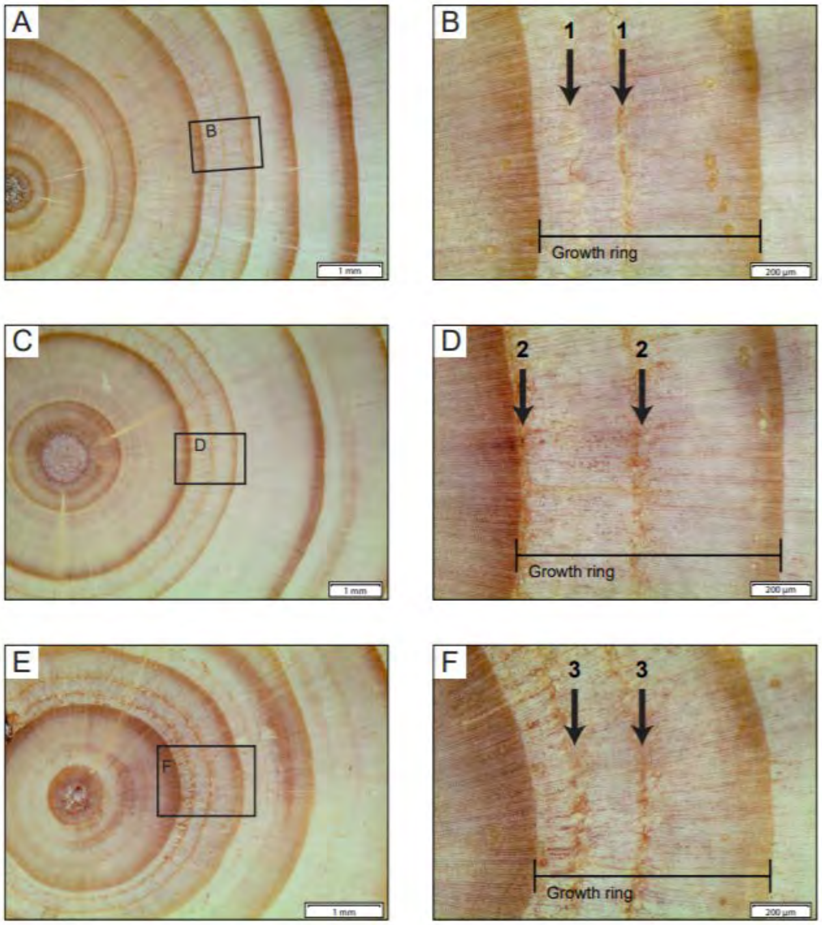

Figure 2.3 Multiple frost rings (arrows) can occur within an annual growth ring, as shown here. The three severity classes of frost rings (see text) are identified by the numbers above each arrow. Class 1: slightly distorted cells, damage not present along the whole circumference of the annual ring (A, B); class 2: distorted cells present along the whole circumference of the annual ring (C, D); class 3: heavily distorted cells present along the whole circumference of the annual ring (E, F). These pictures were taken at same magnification as observations (40×) were made, even if cellular details are difficult to see, the three different severity class of frost damage are quite distinct and are a just representation of the level of detail available to the observer.

2.5.4 Climate variables and frost measurements

The climate variables tested to predict annual height increment were as follows: mean annual temperature, mean summer temperature (June–July–August), maximum monthly temperature, minimum monthly temperature, and monthly freezing frequency, which is calculated as the sum of days for which absolute minimum temperature drops below 0°C. Recent daily climate data were obtained from weather stations that were farther from the plantation sites than the weather station used for determining climate normal (see Section 2.1) since the latter recently closed. The Earlton A weather station was located 57 km from the temperate plantation site (Environment Canada, 2019d), and the Rouyn station was located 80 km from the boreal mixedwood plantation site (Environment Canada, 2019e). To compare *in situ* temperature data with that of the weather stations, we installed three temperature loggers 30 cm above ground (iButtons DS1922L; Maxim Integrated) set to record air temperature every 30 min at both plantation sites from May to August 2016. The adjusted R^2 of the linear regression predicting the onsite mean daily air temperature to the mean daily air temperature registered by their corresponding weather station was .92, which shows that even if farther, the weather stations can still represent temperature at our site. However, we found five and nine more *in situ* frost events in the temperate forest and in the boreal mixedwood forest, respectively, compared to their corresponding weather stations. In both sites, the last day where the minimum temperature dropped below −1°C occurred the night of July 17, which is 61 days later than the last frost recorded by both weather stations (May 16 at both stations). This finding was consistent with the study conducted by Dugas (1975), who determined that growing-season frosts were recurrent in our study region. Since growing-season frosts require a set of specific meteorological conditions such as a clear sky without wind, these specific conditions limit the accuracy of their past prediction (Bootsma, 1976; Chung et al., 2006; Laughlin and Kalma, 1987; Oke, 1987). Moreover, climate models omit to consider the phenomenon of air temperature inversion, which generate growing-season frosts; therefore, we did not reconstruct the frequency and intensity of growing-season frosts for the past 16 years based upon our 1 year of onsite measurement. Instead, we assumed a constant temperature bias between onsite measurement and weather stations across time.

2.5.5 Statistical methods

To quantify the impact of growing-season frosts on total and annual tree height at both inter- and intra-species level and between plantation sites, we used linear (aims 1 and 2) and linear mixed regression models (aim 3). The analyses were first conducted at the inter-species level and once the best regression model was identified, this best model was used to analyze the intra-species variations, replacing the variable “species” by the variable “seed source.” All analyses were implemented in the statistical software R version 3.5.1 (R Development Core Team, 2018).

2.5.5.1 Growing-season frost effect on total tree height

To determine if trees showing increased severity of frost damage to their cambial cells, as observed in the form of frost rings, were also smaller, we regressed total tree height (response variable) to species, site and severity of frost damage (predictor variables). We also considered each two-way interaction between the predictor variables (Table 2.2). To identify which predictor variables best predict total tree height, 18 regression models were compared based upon the corrected Akaike's information criteria (AICc; Burnham, Anderson, and Huyvaert, 2011; Sanchez-Pinto, Venable, Fahrenbach, and Churpek, 2018). This analysis does not involve any climate data since the presence of frost damage to the cambial cells in the form of a frost ring already implies that a growing-season frosts occurred. Therefore, our first aim can be tested using only tree (total height and severity of frost damage to cambial cells) and site characteristics.

2.5.5.2 Varying effect of growing-season frosts on tree growth along the stem

To determine if increased frost damage to cambial cells did increase the time required to reach successive height intervals and at which height along the stem growing-season frost stopped damaging the apical meristem, we divided each tree in successive height intervals of 50 cm starting from the base of the tree up to 4 m. Then, we determined the number of years trees required to grow each 50 cm intervals. Then, we calculated the average severity of frost damage per height interval for each tree and we regressed the time (number of years) to reach a given height to the average severity of frost damage, also considering spruce species. Site was not added as an explanatory variable since there is no reason to believe that for the same spruce species, the same seed source, and the same damage, the trees would react differently at different locations (boreal mixedwood forest, temperate forest, or even in a lab).

Table 2.2 List of the linear regression models tested to identify the best set of variables (severity of frost damage to cambial cells [Sev_ Frost_Dam_Cells], species, and site) predicting total tree height.

Model	**Response variable**	**Predictor variables**	**Interactions**
1	Total height	1	NA
2	Total height	Site	NA
3	Total height	Species	NA
4	Total height	Sev_Frost_Dam_Cells	NA
5	Total height	Site, Species	NA
6	Total height	Site, Sev_Frost_Dam_Cells	NA
7	Total height	Species, Sev_Frost_Dam_Cells	NA
8	Total height	Sites, Species, Sev_Frost_Dam_Cells	NA
9	Total height	Site, Species	Site × Species
10	Total height	Site, Sev_Frost_Dam_Cells	Site × Sev_Frost_Dam_Cells
11	Total height	Species, Sev_Frost_Dam_Cells	Species × Sev_Frost_Dam_Cells
12	Total height	Sites, Species, Sev_Frost_Dam_Cells	Site × Sev_Frost_Dam_Cells
13	Total height	Sites, Species, Sev_Frost_Dam_Cells	Species × Sev_Frost_Dam_Cells
14	Total height	Sites, Species, Sev_Frost_Dam_Cells	Site × Species
15	Total height	Sites, Species, Sev_Frost_Dam_Cells	Site × Sev_Frost_Dam_Cells, Species × Sev_Frost_Dam_Cells
16	Total height	Sites, Species, Sev_Frost_Dam_Cells	Site × Sev_Frost_Dam_Cells, Site × Species
17	Total height	Sites, Species, Sev_Frost_Dam_Cells	Species × Sev_Frost_Dam_Cells, Site × Species
18	Total height	Sites, Species, Sev_Frost_Dam_Cells	Site × Sev_Frost_Dam_Cells, Species × Sev_Frost_Dam_Cells, Site × Species

2.5.5.3 Effect of growing-season frosts versus mean annual temperature on tree height

To determine if extreme climatic events such as growing-season frosts best predict annual height increment of young planted spruce species compared to the mean temperature aggregated over various periods, we performed a model selection based upon AICc (Burnham et al., 2011). For this purpose, 38 climate models were defined as such: 12 regression models, one per monthly maximum temperature, 12 regression models, one per monthly minimum temperature, 10 regression models, one per monthly frost frequency (number of frost event per month) except for July and August since no frost events occurred during that time, one regression model for mean annual temperature, one regression model for mean summer temperature, one regression model without any climate variables, and one intercept-only model. Even if some climate variables co-vary together, all climate variables were tested separately; therefore, co-variance did not impact the results of the regression analyses. To determine if spruce species were differently impacted by the climate variables and if climate variables had different impact on tree growth per site, we included the spruce species, the site, and their interaction with climate variables in the linear mixed regression model used to predict annual height increment from each climate variable (Bates, Maechler, Bolker, and Walker, 2015). The tree identification and the year were specified as random effects and all numerical variables were standardized to maximize comparison across predictors (Zuur, Ieno, Walker, Saveliev, and Smith, 2009). When needed, we performed a Box–Cox transformation of the response variable to reach homoscedasticity.

2.6 Results

2.6.1 Growing-season frost effect on total tree height

Tree height was best predicted by the linear regression model number 14 (Table 2.2), which included the interaction between site and species (Table 2.3). The AICc of this model was lower than that of competing models and its probability of being the best model (AICc weight = 0.54) was more than twice that of the second most probable regression model (model 16: AICc weight = 0.25). The third and following models had a negligible probability of being the best models (AICc weights < 0.1). Since the second most probable model also contained more interactions, we considered the simpler regression model 14 as the best regression model predicting total tree height. The adjusted R^2 of this best regression model was .47 and showed that irrespective of spruce species, severity of frost damage reduced total tree height (Figure 2.4; Table 2.4). Overall, Norway spruce grew the least at both plantation sites, whereas white and black spruce grew equally well at the temperate forest site, but black spruce grew taller than white spruce at the boreal mixedwood forest site (Figure 2.5; Table 2.4). Hence, compared to the other spruce species, white spruce is highly sensitive to growing-season frosts since its growth at the boreal mixedwood forest site was the most reduced by frost. On the contrary, black spruce's sensitivity to growing-season frost was low since its growth at the boreal mixedwood forest site was the least reduced when compared to the temperate forest site and that even if it freezes more at the boreal mixedwood forest site (Figure 2.5; Table 2.4).

Table 2.3 Results of the model selection based on AICc identifying the set of variables that best predict total tree height using linear regression models. Regression models are listed in order from the most (boldface) to the least probable using AICc weights (AICc. Wt.), which is a measure of the relative likelihood of the models calculated from the difference in AICc between the best model and each model (Delta AICc). The cumulative weight (Cum. Wt.) shows the cumulative sum of AICc weights from the most to least probable, which range from 0 to 1, and R^2 shows the amount of explained variance by the predictor variables. Numbers in parentheses refer to the candidate models prior to selection (Table 2.2).

Models	**AICc**	**Delta AICc**	**AICc Wt.**	**Cum. Wt.**	$\boldsymbol{R^2}$
(14) Sites, Species, Sev_Frost_Dam_Cells, Site × Species	**1,993.17**	**0.00**	**0.54**	**0.54**	**.47**
(16) Sites, Species, Sev_Frost_Dam_Cells, Site × Sev_Frost_Dam_Cells, Site × Species	1,994.74	1.56	0.25	0.79	.47
(17) Sites, Species, Sev_Frost_Dam_Cells, Species × Sev_Frost_Dam_Cells, Site × Species	1,996.64	3.47	0.10	0.89	.46
(18) Sites, Species, Sev_Frost_Dam_Cells, Site × Sev_Frost_Dam_Cells, Species × Sev_Frost_Dam_Cells, Site × Species	1,997.11	3.93	0.08	0.96	.47
(13) Sites, Species, Sev_Frost_Dam_Cells, Species × Sev_Frost_Dam_Cells	1,999.64	6.47	0.02	0.98	.45

Table 2.3 (suite)

Models	**AICc**	**Delta AICc**	**AICc Wt.**	**Cum. Wt.**	***R*^{2}**
(15) Sites, Species, Sev_Frost_Dam_Cells, Site × Sev_Frost_Dam_Cells, Species × Sev_Frost_Dam_Cells	2,001.59	8.41	0.01	0.99	.44
(8) Sites, Species, Sev_Frost_Dam_Cells	2,002.15	8.98	0.01	1.00	.43
(12) Sites, Species, Sev_Frost_Dam_Cells, Site × Sev_Frost_Dam_Cells	2,004.34	11.16	0.00	1.00	.43
(11) Species, Sev_Frost_Dam_Cells, Species × Sev_Frost_Dam_Cells	2,012.99	19.82	0.00	1.00	.39
(7) Species, Sev_Frost_Dam_Cells	2,016.80	23.63	0.00	1.00	.37
(9) Site, Species, Site × Species	2,019.66	26.49	0.00	1.00	.37
(6) Site, Sev_Frost_Dam_Cells	2,022.77	29.60	0.00	1.00	.34
(10) Site, Sev_Frost_Dam_Cells, Site × Sev_Frost_Dam_Cells	2,024.90	31.73	0.00	1.00	.34
(5) Site, Species	2,025.80	32.62	0.00	1.00	.34
(4) Sev_Frost_Dam_Cells	2,027.79	34.62	0.00	1.00	.32
(2) Site	2,051.42	58.24	0.00	1.00	.21
(3) Species	2,082.33	89.16	0.00	1.00	.05
(1) Intercept	2,089.04	95.86	0.00	1.00	.00

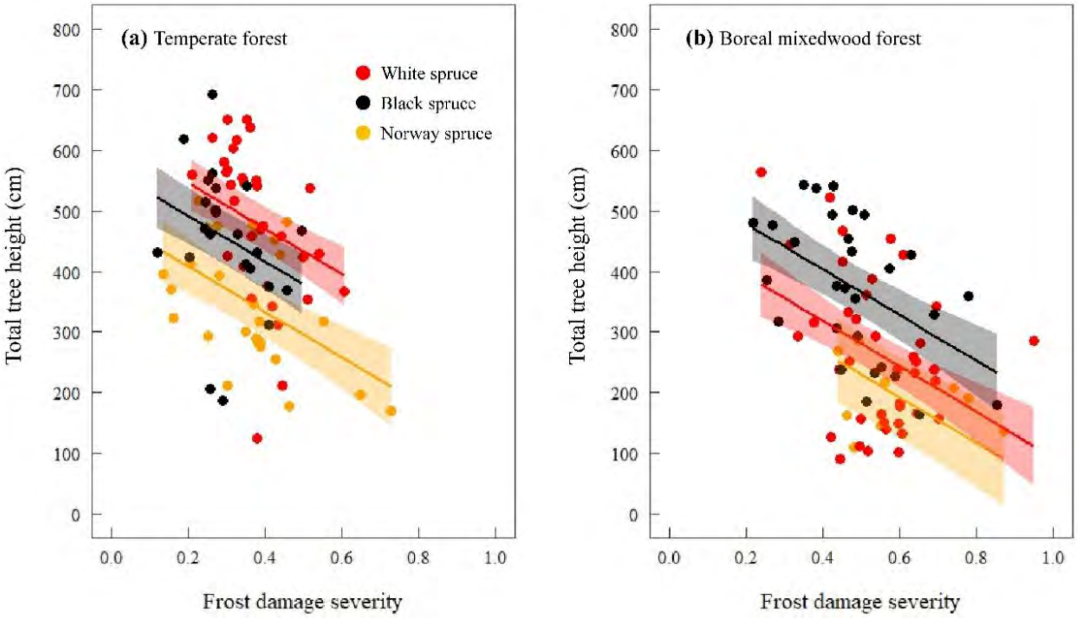

Figure 2.4 Modelled means (lines) and 95% confidence interval (shaded areas) predicting total tree height from frost damage severity per site (a, b) and species (colors).

Table 2.4 Summary table presenting coefficients, adjusted SEs, and p-values for each variable for the best model (model 14) predicting total tree height at the inter-species level. Boldface type indicates coefficients significantly different from 0 ($\alpha = 0.05$).

Variables	Coefficients (SE) in cm	P-value
Intercept (Norway spruce; Temperate forest site)	**483.68 (32.15)**	**$< 2.00 \times 10^{-16}$**
Boreal forest site	-66.04 (42.16)	0.12
White spruce	**137.30 (27.38)**	**1.43×10^{-6}**
Black spruce	**83.37 (30.41)**	**6.82×10^{-3}**
Frost severity	**-375.27 (68.47)**	**1.67×10^{-7}**
Boreal forest site × White spruce	-86.18 (46.59)	0.07
Boreal forest site × Black spruce	52.62 (49.32)	0.29

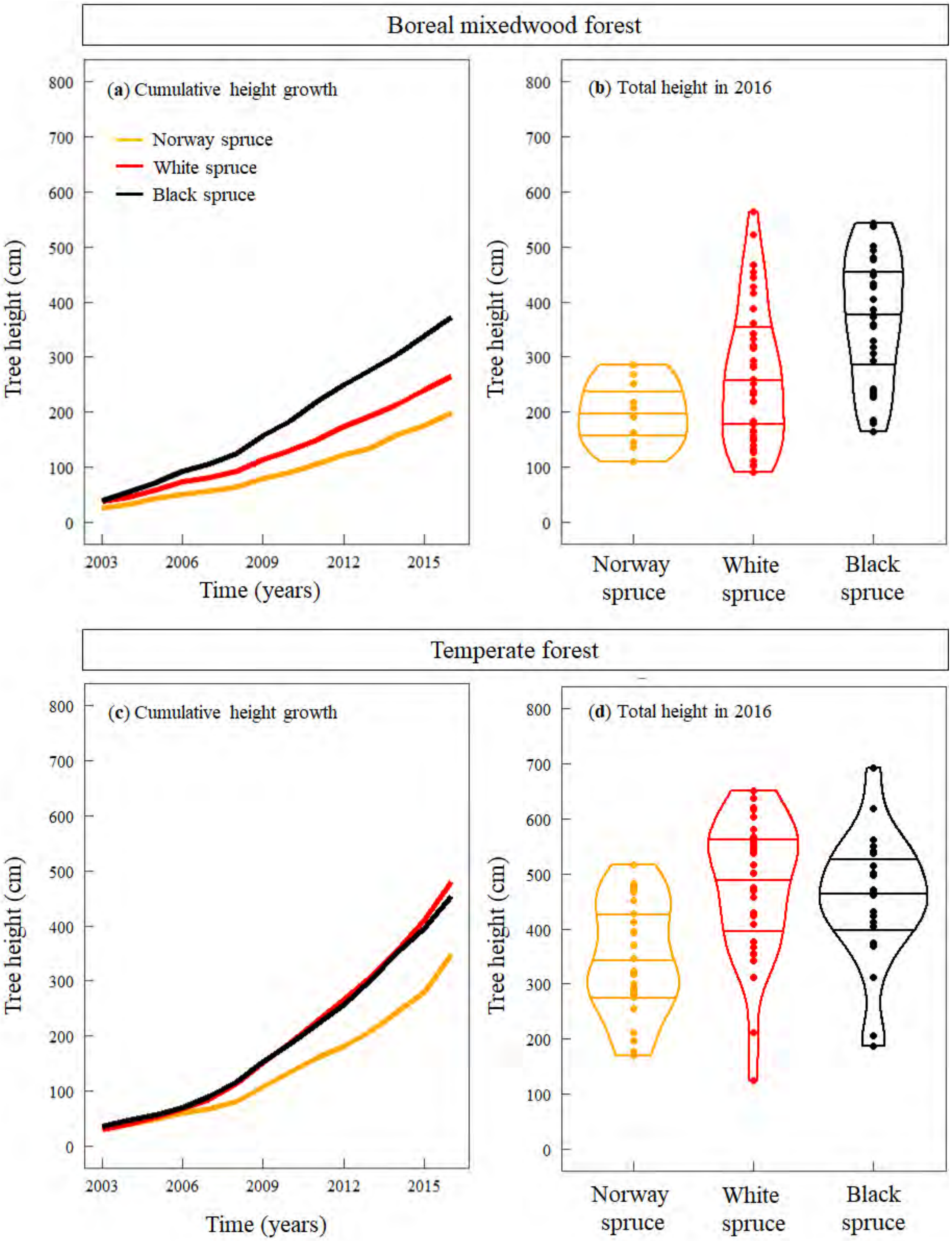

Figure 2.5 Mean cumulative height growth (lines) per species at both sites (a, c). Violin plots (b, d) show the distribution of total tree height per species and site. Horizontal lines within violins show quartiles and each dot represents a tree.

At the intra-species level, our analysis showed that none of the Norway spruce seed sources could grow as tall as white spruce and black spruce (Table 2.5; Annexe B: Figure B2). However, for white spruce, tree height from two seed sources, the J70 (the local seed source at the boreal mixedwood plantation) and the extra local seed source K24 from Petawawa Ontario were equal and taller than the southernmost seed source K20 at the temperate forest plantation (Annexe B: Figure B3). Yet, at the boreal mixedwood plantation, both extra local seed sources from the southern temperate forest K20 and K24 grew less than the local J70 seed source (Table 2.5; Annexe B: Figure B3).

Table 2.5 Summary table presenting coefficients, SEs, and p-values for the best model (model 14) predicting total tree height at the intra-species level. Boldface type indicates coefficients significantly different from 0 ($\alpha = 0.05$).

Variables	**Coefficient (SE) in cm**	**P-value**
Intercept (white spruce J70; Temperate forest site)	**645.93 (34.18)**	**$< 2.00 \times 10^{-16}$**
Boreal forest site	**-143.04 (34.09)**	**4.70×10^{-5}**
White spruce K20	**-106.48 (46.30)**	**0.02**
White spruce K24	20.59 (45.91)	0.65
Black spruce K32	**-73.02 (32.07)**	**0.02**
Norway spruce K35	**194.64 (46.38)**	**4.68×10^{-5}**
Norway spruce K39	**184.33 (45.83)**	**9.21×10^{-5}**
Norway spruce K50	**133.58 (49.25)**	**7.49×10^{-3}**
Norway spruce K55	**105.25 (46.03)**	**0.02**
Frost severity	**-394.65 (71.75)**	**1.65×10^{-7}**
Boreal forest site × White spruce K20	52.17 (64.28)	0.42
Boreal forest site × White spruce K24	-100.85 (63.84)	0.12
Boreal forest site × Black spruce K32	**133.11 (42.59)**	**2.14×10^{-3}**
Boreal forest site × Norway spruce K35	104.11 (78.98)	0.19
Boreal forest site × Norway spruce K39	121.73 (115.80)	0.29
Boreal forest site × Norway spruce K50	118.15 (80.11)	0.14
Boreal forest site × Norway spruce K55	-14.28 (78.89)	0.86

2.6.2 Varying effect of growing-season frosts on tree growth along the stem

As expected, frost damage severity and frost ring frequency were highest at the base of the trees for all species and sites (Figure 2.6). Compared to trees that were little affected by frost, highly impacted trees needed two additional years to grow from 0 to 50 cm high (Figure 2.7). Frost damage and its inhibitory effect on height growth gradually subsided (regression slopes gradually becoming flat; Figure 2.7; Table B3) higher up the stem until no effect was detectable above 2.0 m. In total, trees that were severely impacted by frost (frost severity = 1) took almost seven additional years to reach 2 m above the ground compared to trees that were not affected (frost severity = 0; Table B3). The strong relationship, in the frost-prone zone (near the ground), between frost severity estimated from frost rings and height growth indicate that frost events that damaged the cambial cells also damaged the apical meristems and, by extension, that frost rings are a good proxy for apical meristem damage.

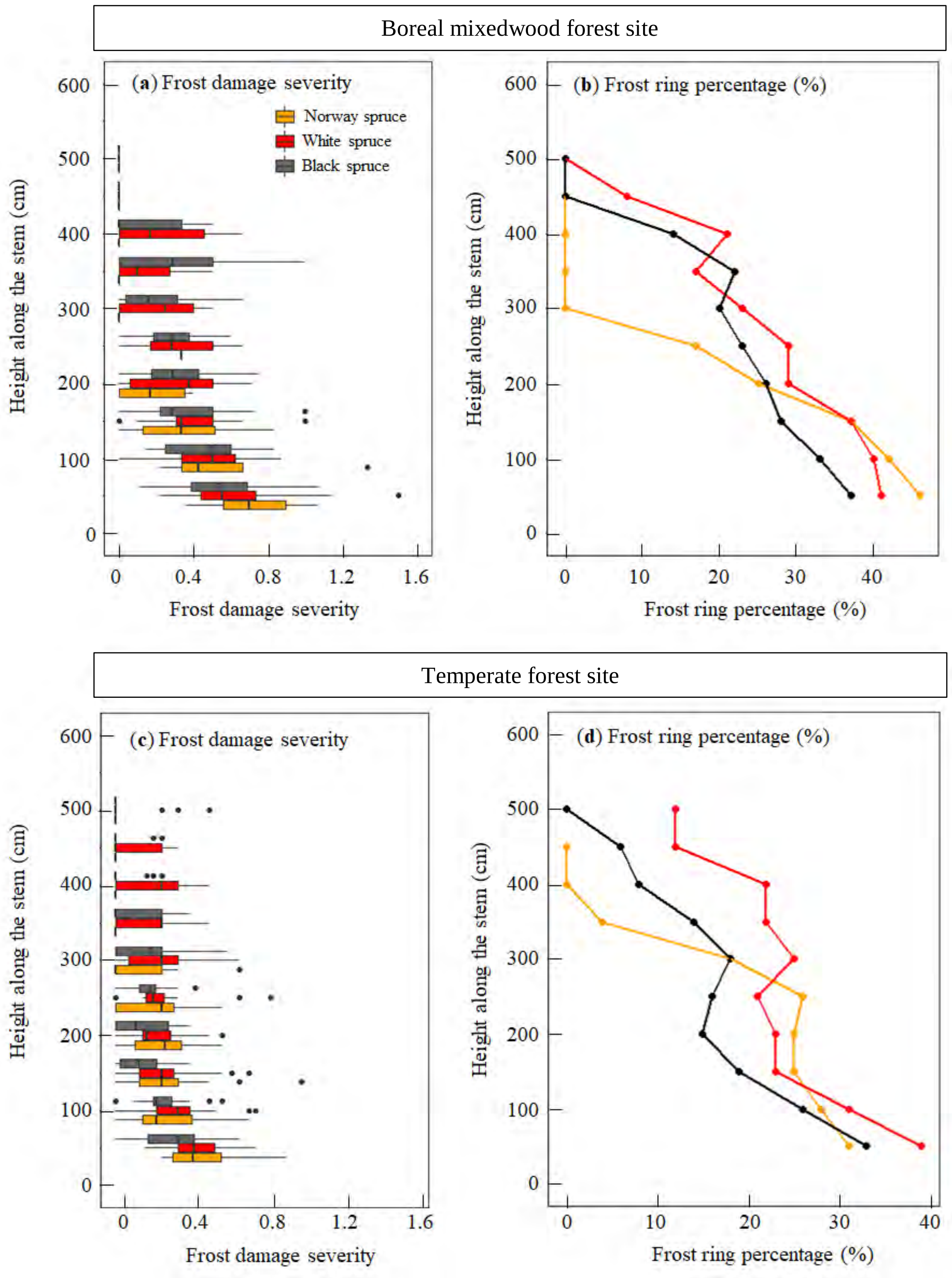

Figure 2.6 Frost damage severity (a, c) and frost ring frequency (b, d) along tree stems per species at both sites.

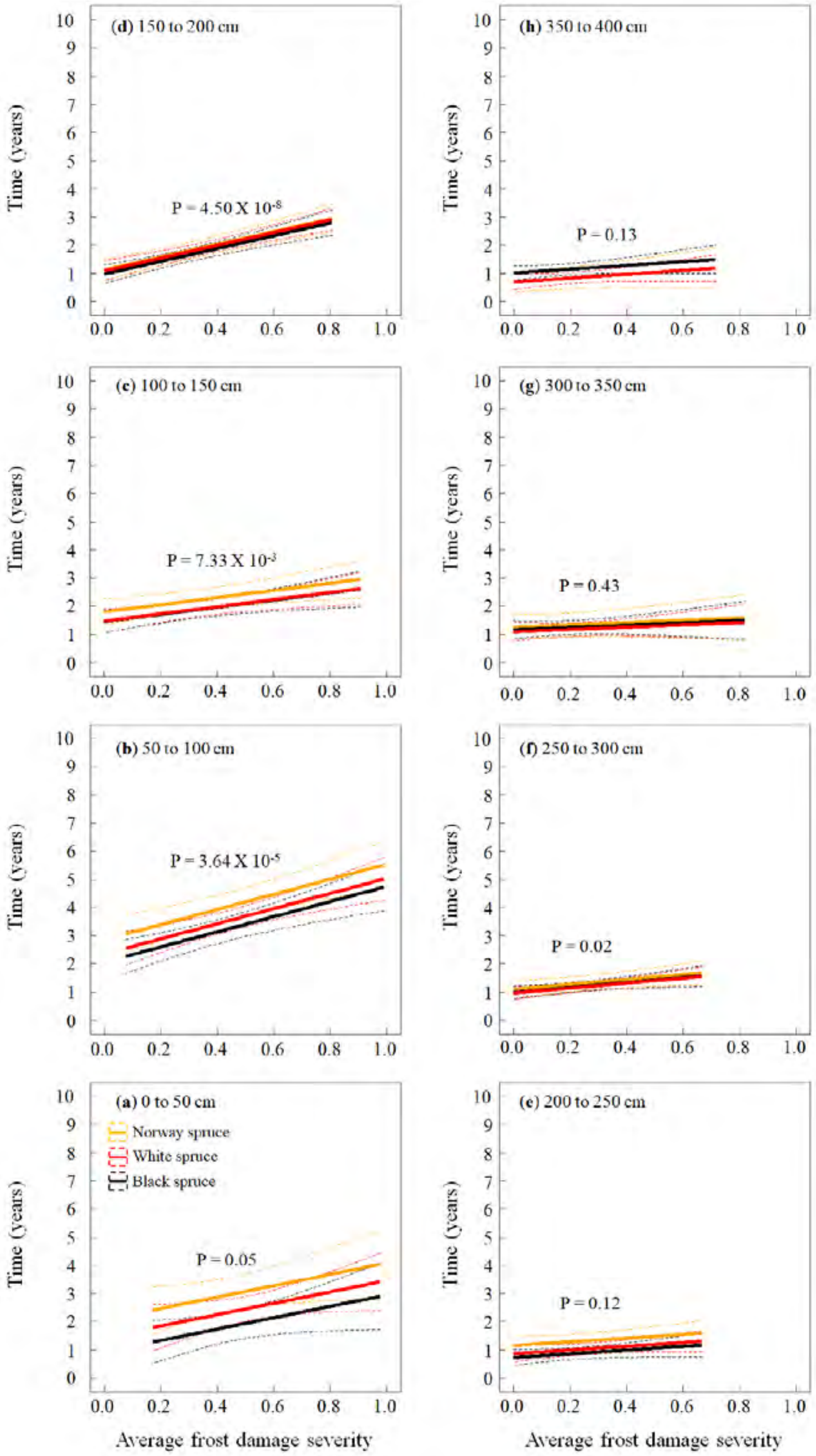

Figure 2.7 Effect of frost damage severity on the time needed to reach successive 50-cm intervals along the stem (a–h). Dash lines represent 95% confidence interval.

2.6.3 Effect of growing-season frosts versus mean annual temperature on tree height

All 36 models testing a climate variable outperformed (ΔAICc > 2 AICc units) the null (intercept only) model (Figure 2.8; Table B4). Moreover, 32 models testing a climate variable outperformed the regression model without climate variables (No climate) and 17 models testing a climate variable outperformed both the mean annual temperature and the mean summer temperature models (Figure 2.8). Out of these 17 climate regression models, 9 included either frost frequency or intensity. Model selection based on AICc identified one crucial model for predicting annual height increment: minimum temperature in May (n = 2,235; AICc = 6,192; and the amount of explained variance by the predictor variables for this mixed effect model [pseudo-R^2] is .57; see Table B4 for the complete results of the model selection analysis). This model was far superior to all other models, with an AICc weight of 1, that is, a 100% probability of being the best model tested (Table B4).

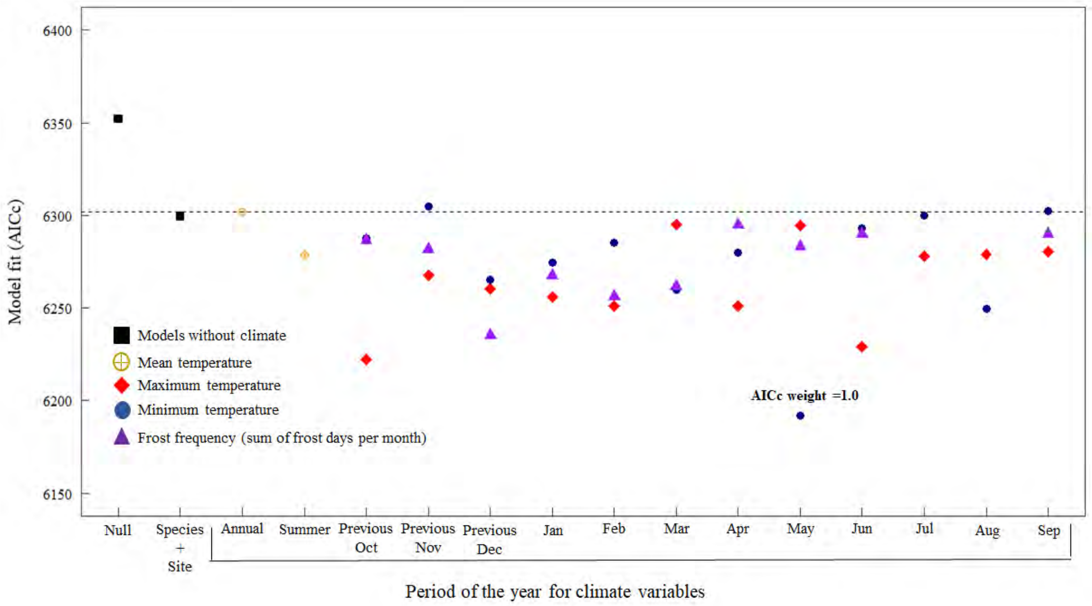

Figure 2.8 Performance (corrected Akaike's information criteria [AICc] units) of each regression model predicting annual height increment from different climate variables at various periods (annual, summer [June–July–August], and monthly), an intercept-only model (Null), and a model that does not include climate variables (No climate). All models except the null model include species and site as fixed effects. Monthly climate variables include maximum temperature, minimum temperature < 0°C (frost intensity), and frost frequency (number of days where minimum temperature is lower than 0°C); annual and summer climate variables only include mean temperature. The dotted line is aligned with the AICc of the mean annual temperature model as a reference.

The effect of minimum air temperature in May was similar at the inter- and intra-species level since the interaction terms between seed sources and minimum air temperature in May were not statistically significant (Annexe B: Tables B5 and B6). However, the positive effect of minimum air temperature in May on spruce's height growth at the temperate forest plantation decreased and even turned negative at the boreal mixedwood forest plantation (Figure 2.9; Annexe B: Tables B5 and B6).

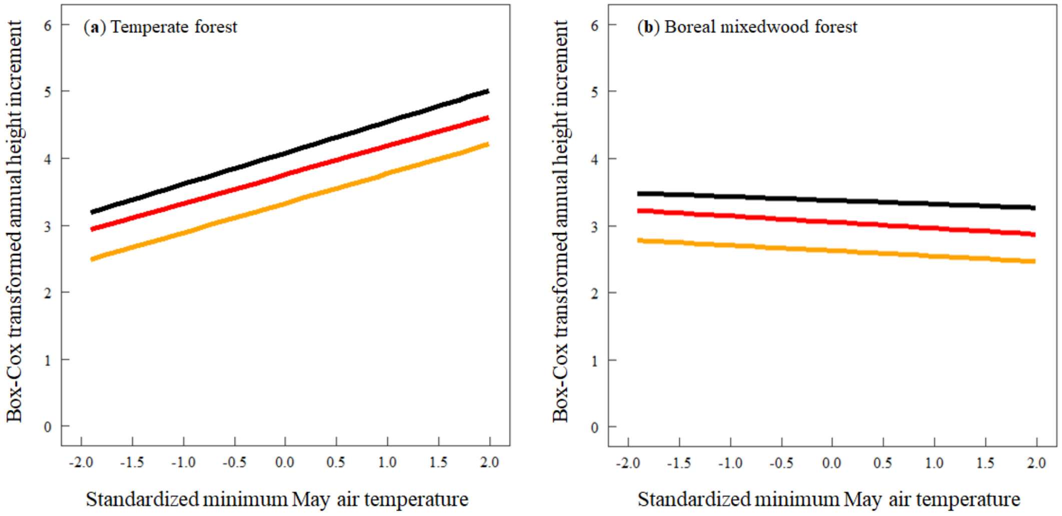

Figure 2.9 Mean effect of minimum air temperature in May (frost intensity) on annual height increment per species at each site (a, b).

2.7 Discussion

This study is one of the few to quantify the impact of extreme climatic events (frosts) on tree performance at the individual level and to link it to the annual dormancy-growth cycle of trees (Montwé et al., 2018). Our study, based on direct observation of frost damage and its impact on young tree performance, fills a gap in the scientific literature, which is dominated by studies inferring the effect of growing-season frosts on trees using phenological data and climate models (Liu et al., 2018; Ma et al., 2018). While global warming increased the mean annual temperature by 1°C over the 1850–2017 period (Allen et al., 2018), at our study sites, local growing-season frosts still occur frequently in June and occasionally in July. Accordingly, we believe that by triggering an earlier bursting of buds (Polgar, Gallinat, and Primack, 2013), the global increase in mean temperature might increase the exposition of frost-sensitive plant organs to growing-season frosts and increase frost damage to trees, an idea also supported by studies conducted by Liu et al. (2018) and Ma et al. (2018).

Near-ground radiative growing-season frosts have already been identified as important ecological and evolutional drivers of subalpine trees and of trees growing at the treeline (Li et al., 2017; Wang et al., 2019). Moreover, frost occurring during the opening of buds seems to better explain the altitudinal and latitudinal range limit of tree species compared to mean annual temperature (Du et al., 2019; Kollas, Körner, and Randin, 2014; Körner et al., 2016; Vitra, Lenz, and Vitasse, 2017). Even though growing-season frost was an important factor driving tree growth at northern latitudes and at high altitudes, growing-season frosts was seldom considered important in forestry and forest management disciplines where near-ground radiative growing-season frosts are less frequent.

However, we present striking results showing that growing-season frosts are indeed of major consideration for the successful growing of young planted spruce species in boreal mixedwood forests since growing-season frosts can damage both the apical and lateral meristems thus reducing tree growth, which then decrease net primary productivity of the young forest plantations (Augspurger, 2009; Clements et al., 1972; Dy and Payette, 2007; Hufkens et al., 2012)

2.7.1 Growing-season frost effect on total tree height

As expected, trees showing increased frost damage to their cambial cells also had smaller height increment, suggesting that frost also damaged their apical meristem. This result shows that growing-season frosts are decreasing tree productivity in the boreal mixedwood forest. Only black spruce could grow more than white and Norway spruce during years of high growing-season frost intensity at the boreal mixedwood forest plantation. Therefore, in environments prone to radiative frosts, black spruce is the best spruce species to plant, but in environments less likely to freeze, white spruce would be the best choice since it has a higher growth rate. Norway spruce should be avoided since it grew the least at both sites.

Consistent with our hypothesis at the intra-species level, the white spruce seed source closest to the boreal mixedwood forest plantation outperformed extra-local white spruce seed sources. This suggests that assisted migration may not be a good option in boreal environments, where growing-season frost intensity is high, probably because seed sources from southern temperate forests exit dormancy too early and are more damaged by frost (Lu and Man, 2011; Marquis et al., 2020). However, at the temperate forest site, both seed sources K24 and J70, growing, respectively, 350 km south and 150 km north, grew equally well and were taller than the K20 seed sources growing 600 km south. The southernmost seed source (K20, located 600 km south of the temperate forest plantation) was not adapted to the temperate forest plantation's climate regime, which is consistent with our hypothesis. Our results suggest that in environments where growing-season frost intensity is low, assisted migration could be used to increase forest productivity using seed sources not exceedingly far from the plantation site. Therefore, white spruce's high sensitivity to growing-season frosts will have consequence on the persistence of young productive plantations at the boreal-temperate forest ecotone if climate change (e.g., increased temperature average and variability) increases exposure of vulnerable tissues to frost events. Our results are consistent with those of Andalo, Beaulieu, and Bousquet (2005) who also showed that local seed sources of white spruce were optimally adapted to their site's thermal condition. However, these authors also pointed out that moisture played a key role on spruce growth and that the projected warmer temperature could decrease moisture availability at the local scale, which would have a greater impact on local seed sources than on extra-local seed sources. Due to the many uncertainties related to climate change (Park et al., 2014), it is critical to determine the physiological traits and thresholds affecting the dormancy-growth cycle of trees from different populations to be able to establish plantations with suitable seed sources. Interestingly, our results are not consistent with those of Otis Prud'homme et al. (2017), who found that non-local white spruce seed sources could grow more than the local ones. However, their study was conducted on sandy-loam soils, and not clay soils, which are soil types known to favor air temperature inversions (Dugas, 1975). Thus, growing-season frosts more importantly constrain tree growth in the Clay Belt of Quebec than they do elsewhere on sandy-loam soils (Dugas, 1975). Therefore, our results are new and important but need to be properly put in context since the importance of growing-season frosts at constraining the growth of young planted spruce occurs when a set of specific environmental conditions are met such as clay soils in the boreal mixedwood.

For Norway spruce, even if there was, on average, a one-meter difference in tree height between the tallest and the smallest seed sources, indicating local adaptations, the four Norway spruce seed sources tested grew poorly at the boreal mixedwood forest site, not reaching 3 m 16 years after planting. Therefore, the Clay Belt of Quebec may be too stressful for this species. This result is consistent with those of Klisz et al., (2019) who found that when extreme climatic events such as droughts, but in our case growing-season frosts, is the major environmental factor limiting tree growth, the importance of local adaptations in driving tree growth is reduced.

2.7.2 Effect of growing-season frost versus mean annual temperature on tree height

Consistent with our hypothesis, the lethal effect of growing-season frosts on young forest plantations is more important in forecasting annual height increment compared to all other temperature metrics, including mean annual or summer temperature. Therefore, extreme climatic events occurring at specific steps of the annual dormancygrowth cycle of young trees have greater physiological meaning and consequences on tree height than aggregated temperature metrics. High air temperature in May has a different effect on young planted spruce in the boreal mixedwood forest versus temperate forest plantations. In the temperate forest, where growing-season frost intensity is low, increased temperature in May is beneficial to growth of young planted spruce since the earlier dormancy release rarely increase exposure to growing-season frosts; however, when it occurs, the negative impacts on the growth of young planted spruce are analogous to those observed in the boreal forest (Ault et al., 2013; Gu et al., 2008; Lenz, Hoch, Körner, and Vitasse, 2016). Yet, in the boreal mixedwood forest, where frost intensity is higher, the earlier dormancy release triggered by higher air temperature in May increases the exposure of meristems to frost events, resulting in more tissue damage and decreased productivity of young planted spruce. If growing-season frost frequency or intensity increases with climate change, years with abnormally high air temperature in May should decrease productivity of young planted spruce in the boreal mixedwood forest site by increasing frost damage, whereas it could increase productivity of young planted spruce at the temperate forest site until growth is either altered by a moisture deficit (Andalo et al., 2005; D'Orangeville et al., 2018; Huang et al., 2010) or because dormancy release will occur too early and expose the meristems to frost events. We showed that growing-season frost was an important climate variable driving the growth of young planted spruce at the boreal mixedwood forest, a climate variable previously considered to be important in colder environments such as the boreal lichen woodland (Payette and Delwaide, 2018); therefore, we show a new important mechanism driving the growth dynamic of young planted spruce in the boreal mixedwood forests on clay soils.

2.7.3 Climate change and frost damage to boreal tree species

The earlier development of plant phenology triggered by warmer spring air temperature, which was observed in the last decades, is expected to continue in the future (Olsson, Olin, Lindström, and Jönsson, 2017; Parmesan and Yohe, 2003; Piao, Friedlingstein, Ciais, Viovy, and Demarty, 2007; Polgar et al., 2013). If climate variability also increases, future warmer springs may still have a high probability of frost events, which would increase exposure of meristems to frost (Bigler and Bugmann, 2018; Liu et al., 2018; Ma et al., 2018; Walther et al., 2002). Climate-change-induced increase in fall and winter air temperature affect another facet of the dormancygrowth cycle of trees, that is, the accumulation of chilling units, which are a metric of exposure to chilling temperature. In boreal and many temperate biomes, plants require a minimum period of cold weather (above 0°C) to enter dormancy and, later, emerge from that dormancy. Increased fall temperature could postpone dormancy release until these chilling units are accumulated in early spring (Cooke, Eriksson, and Junttila, 2012; Heide, 2003). Yet, the chilling requirements in hours are low for black (316 hr) and white (524 hr) spruce compared to other northern boreal mixedwood tree species (e.g., trembling aspen requires 1,246 chilling hours) and are likely completed before the end of December (Man, Lu, and Dang, 2017). It is therefore unlikely that the chilling requirement to complete rest break for spruce species will be delayed by future warmer fall temperature (Man et al., 2017). On the other hand, spruce species are highly sensitive to warmer air temperature in the spring since spruce buds are in the state of quiescence as soon as in January. When buds are quiescent, their development is only prevented by environmental conditions (sub-zero temperatures), and therefore, heating units are cumulating as soon as temperatures are adequate (Hänninen, 2016). However, the heating requirement in hours to start the bud break process for black and white spruce (9,204 and 6,831 hr, respectively) is high compared to other boreal species such as trembling aspen, which requires 4,816 heating units (Man et al., 2017). This high heating requirement of spruce species limits exposure to growing-season frost in the current climate but may not prevent earlier development caused by warmer air temperature, which could, in turn, increase exposure to frosts.

Simulations made by Morin and Chuine (2014) found no clear evidence of increased frost damage to trees with climate warming but the climate data that they used were forecasted by climate models. However, the chaotic component of climate models lowers the confidence and reliability of their daily projections and their extreme climatic events; thus, this question remains open. We call for great care when analyzing changes in frost events and their impact on tree growth when using climate models.

2.7.4 Implications for sustainable forest management

This study has regional- and local-scale implications for sustainable forest management. This study shows that at the regional scale, the different frost tolerance and growth potential of spruce species and seed sources need to be considered to maximize wood production of future plantations established in frostprone environments (Park et al., 2014). Black spruce buds flush later than white spruce, which reduces its exposure to spring frost, and increase growth during years of spring frost compared to white spruce (Man et al., 2017; Marquis et al., 2020). However, whereas black spruce grows more than white spruce during years of growing-season frosts, white spruce's greater growth rate makes it grow taller compared to black spruce during years without or with few growing-season frosts. Since the future frequency and intensity of frost events remain unknown, a conservative way to ensure wood production would be to establish mixed plantations of black and white spruce with a few different seed sources naturally growing within a close distance to ensure adequate thermal acclimation to site conditions. Even if black spruce and white spruce have different autecology, for instance, black spruce can tolerate wet environments, whereas white spruce does not, both spruce species grow better in moderately drained sites; therefore, both species can be planted in a same plantation (Wolken, Landhäusser, Lieffers, and Silins, 2011). Because both water and cold air can accumulate at the bottom of slopes (Laughlin and Kalma, 1987; Lindkvist and Lindqvist, 1997), it could be advantageous to plant black spruce in topographic depressions and to plant white spruce on hilltops.

At the local scale, this study showed that three measures could be taken to reduce growing-season frost damage in plantations. First, taller seedlings should be used for reforestation to rapidly reach 2 m since we determined that growing-season frosts greatly limit growth of young planted spruce in the first meter from the ground and that this effect dissipates as trees increase in height until no effect is detectable above 2 m from the ground. Second, because cold air can be trapped in microtopographic depressions or at the bottom of slopes, frost-sensitive tree species should be planted on mounds to raise the apical meristem above the zone of ground frost (2 m; Langvall et al., 2001). With the increased use of airborne LiDAR (airplanes or drones) that precisely measures microtopography, frost sensitivity maps could be created to help forest managers to better identify where to establish future plantations, and to identify planting microsites within the plantation, to minimize frost damage and help to manage the forest resource in a sustainable way (Côté, Fournier, Luther, and van Lier, 2018; Rowlandon et al., 2018; Wang et al., 2018). The third contribution of this study was to show that growing-season frosts are such a major determinant of spruce growth in young plantation that all measures should be taken to reduce the extreme daily temperature variations and radiative frosts experienced by young trees, such as keeping a canopy cover or at least a few mature trees in the plantation (Gärtner, Lieffers, and Macdonald, 2011; Groot and Carlson, 1996; Langvall and Löfvenius, 2002). Forest plantations play a key role in the sustainable management of the boreal forest because they can reduce harvesting pressure on natural forests (Messier et al., 2009). To preserve their productivity in a warming climate, it is essential to understand the mechanisms and consequences of growing-season frosts on tree growth.

2.8 Acknowledgements

We would like to thank the Natural Science and Engineering Research Council of Canada (NSERC) for the funding of this research project through a grant to F. Tremblay et al. We are also particularly grateful to L. Gervais, R. Mincheva, and P. Duval for their assistance in the field and in the laboratory. A special acknowledgement to Danielle Charron who helped coordinate the fieldwork. We are also thankful to Ann Delwaide for sharing her knowledge in frost ring identification and to François Rousseau and Stéphane Daigle for their help with statistical analyses and R codes.

2.9 Conclusion

Cet article s'appuie sur une base empirique solide pour conclure que les évènements climatiques extrêmes, comme les évènements de gel survenant durant la saison de croissance, sont de meilleurs déterminants de la croissance des épinettes que ne le sont les variables climatiques agrégées sur différentes périodes de temps, comme la température moyenne annuelle ou la température moyenne durant l'été. Cet article comporte un aspect pratique intéressant puisqu'en montrant que la sévérité des dommages aux cellules cambiales causés par le gel diminue avec la hauteur de l'arbre et s'arrête lorsque l'arbre atteint deux mètres de hauteur, planter de plus grands arbres et les planter sur des buttes permettraient de diminuer le phénomène de stagnation des épinettes, qui est plus fort pour l'épinette blanche que pour l'épinette noire. En ayant testé quelques sources de graines, nous avons montré que la provenance d'épinette blanche résidente à la forêt boréale mixte était mieux adaptée pour faire face aux évènements de gel printanier que les provenances qui croissent éloignées du site de plantation. En intégrant ces nouveaux résultats au contexte des changements climatiques, cette étude permet d'augmenter notre compréhension de la productivité future des plantations situées à l'écotone de la forêt boréale-tempérée et recommande fortement d'inclure des variables concernant les évènements de gel survenant durant la saison de croissance dans les modèles servant à prédire les trajectoires futures de la croissance des arbres. Puisque cette étude innove en mettant en relation une observation directe de dommages par le gel (cernes de gel) avec la capacité à croître, ce qui diffère des modélisations effectuées jusqu'à présent qui définissent un seuil de température en dessous duquel des dommages par le gel sont attendus mais qui ne sont pas calibrés sur de réelles observations, notre étude vient combler un vide dans la littérature et devrait servir d'étude de référence en ce qui concerne l'impact des évènements climatiques extrêmes sur la performance des arbres.

Toutefois, à même une plantation, il y avait une forte variation en hauteur intra-espèce, ce qui suggère que le microsite est important pour déterminer la croissance des arbres. L’importance du microsite a surtout été étudié en relation avec le drainage du sol. L’épinette blanche a une meilleure croissance dans des microsites bien drainés, tandis que l’épinette noire tolère des microsites plus humides (Andalo et al., 2005). Toutefois, l’importance du microsite sur l’intensité et la fréquence des évènements de gel survenant durant la période de croissance des arbres reste méconnue, mais pourrait avoir un impact non négligeable sur la fréquence et l’intensité des évènements de gel. Effectivement, lors d’un évènement de gel, le phénomène d’inversion de la température de l’air permet le développement d’une couche d’air froid qui reste près du sol et qui peut s’accumuler dans le bas des pentes et dans les dépressions microtopographiques, générant ainsi une forte variation de la température de l’air suivant un court gradient d’élévation. Ce phénomène d’inversion de la température a surtout été étudié au nord de la forêt boréale ou en montagne, mais peu à l’écotone de la forêt tempérée-boréale (Payette et Delwaide, 2018). Donc, l’importance de la variation de la température de l’air près du sol suivant la topographie et la microtopographie a été entreprise au troisième chapitre de ma thèse.

CHAPITRE III

DISENTANGLING THE EFFECT OF TOPOGRAPHY AND MICROTOPOGRAPHY ON NEAR-GROUND SUMMER FROSTS AT THE BOREAL-TEMPERATE FOREST ECOTONE (QUÉBEC, CANADA)

Benjamin Marquis, Yves Bergeron, Martin Simard et Francine Tremblay

Cet article est soumis à la revue scientifique
New Forests

3.1 Highlights

- Topographic variations caused temperature inversions in the boreal forest.
- A 15 meters change in elevation caused air temperature to vary by 4 °C.
- Sub-zero to above freezing temperatures were reached along the topographic gradient.
- Microtopographic variations were more important where frost events were less likely.
- LiDAR can help identify frost-free microsites prior plantation establishment.

3.2 Résumé

Les attributs permanents du paysage, tels que la topographie (élévation [m]) et la microtopographie (variation locale d'élévation par rapport au niveau du sol [cm]), peuvent entraîner le drainage des masses d'air froid vers les zones de basses élévations et dans les dépressions microtopographiques, générant des évènements de gel même durant l'été, et ce, sur de courtes distances autant verticales qu'horizontales. Puisque les études sur les gelées d'été sont surtout effectuées au nord de la forêt boréale, leurs conséquences sur la productivité des arbres à l'écotone de la forêt boréale-tempérée est peu connue. Donc, nous avons quantifié l'intensité et la probabilité des gelées d'été à l'écotone de la forêt tempérée-boréale, en lien avec les attributs permanents du paysage (l'élévation et la pente), lesquels ont été mesurés à partir d'un sondage effectué par LiDAR aéroporté. La température de l'air a été mesurée *in situ* par 252 capteurs de température qui ont été installés dans deux plantations établies en forêt tempérée et en forêt boréale mixte durant deux étés consécutif (2016-2017). La température de l'air a varié de 4 °C sur le gradient d'élévation de 15 mètres, atteignant des températures sous la barre de 0 °C dans les basses élévations et atteignant des valeurs au-dessus du point de congélation au sommet des buttes. Les gelées survenant l'été ont été plus intenses et probable à la forêt boréale mixte qu'à la forêt tempérée. Étant donné que les gelées d'été peuvent fortement réduire la productivité des arbres, les effets de la topographie et de la microtopographie sur la température de l'air devraient être mieux considérés pour identifier les microsites de plantations où le risque de subir des gelés d'été est faible.

3.3 Abstract

Permanent landscape attributes such as topography (elevation [m]) and microtopography (local variation in height above ground [cm]) can favor the drainage of cold air masses down-slopes and in microtopographic depressions, causing important temperature gradients that generate localized summer frosts over short vertical and horizontal distances. Since most studies on summer frosts are restricted to crops or to the northern parts of the boreal forest, their negative consequences on tree productivity at the boreal-temperate forest ecotone is often ignored. We quantified the intensity and probability of summer frosts at the boreal-temperate forest ecotone in regard to topographic (elevation and slope) and microtopographic (height above ground and micro-slope) landscape attributes, which were extracted from airborne LiDAR surveys. *In situ* air temperature was measured for two summers (2016 – 2017) with 252 temperature loggers installed in two plantations established in both temperate and a boreal mixedwood forests of Quebec (Canada). Summer frosts were more intense and probable at the boreal mixedwood forest site compared to the temperate forest site. Still, at both sites, when summer frost occurred, air temperature could vary by 4 °C along the elevation gradient of 15 m, often reaching sub-zero values at low elevation while reaching above-freezing values at high elevation. The importance of microtopography on frost hazard increased where frost events were less likely to occur such as at the temperate forest and at high elevation. Considering that summer frosts can importantly reduce tree productivity, the effects of both topography and planting microsite should be better assesed when determining where to establish plantations in the landscape and to determine the suitable frost-free microsites within plantation.

Keywords: Elevation, Frost pockets, Microenvironment, Microtopography, Summer frosts, Temperature inversions

3.4 Introduction

Air temperature variations at the local scale can have important effects on the establishment, growth and mortality of the vegetation (Dy and Payette, 2007; Payette and Delwaide, 2018; Inouye, 2008; Kollas et al., 2014; Körner et al., 2016). One of the meteorological phenomena that affects local air temperature is temperature inversion and is caused by drainage winds that transport dense cold air masses down-slope, thus inverting the usual temperature gradient existing between the warm surface and the cold troposphere (Wallace and Hobb, 2006). Temperature inversions are frequent in flat landscapes with small hills because the cold air masses can accumulate at the bottom of slopes, forming localized frost pockets (Laughlin and Kalma, 1987; Lindkvist and Lindqvist, 1997; Chung et al., 2006; Plasse and Payette, 2015; Payette and Delwaide, 2018). Temperature inversions occur most often on windless nights, which allows the stratification of air masses, and when skies are clear, which facilitates the radiation of heat from the ground to the atmosphere (Oke, 1987). Nighttime temperature inversion can cause a negative heat balance between heat accumulation during the day and heat loss during the night, which can severely damage plants (Dy and Payette, 2007; Langvall and Örlander, 2001; Langvall and Ottosson-Löfvenius, 2002). Temperature inversions are particularly damaging to plants growing in treeless or open forests, which lack a dense tree canopy that can buffer temperature fluctuations. For example, in open forests such as the lichen woodland, temperature inversions can cause frequent summer frosts every two to eight days that prevent the establishment of trees at the bottom of topographic depressions, forming an inverted tree line (Payette and Delwaide, 2018; Plasse and Payette, 2015). Similarly, young plantations and forests recently disturbed by logging or wildfires show a high frequency of near-ground frosts that affect seedling growth (Groot and Carlson, 1996; Langvall and Örlander, 2001; Langvall and Ottosson-Löfvenius, 2002; Mullin, 1963; Vyse, 1981).

Even if the number of frost days are expected to decrease worldwide because of the climate-change induced warmer air temperatures (IPCC, 2018), frost damage to trees is expected to increase because the earlier leaf-out triggered by the increase in mean air temperature (Parmesan and Yohe, 2003; Piao et al., 2007) simultaneously exposes frost sensitive plant organs to more frequent spring frosts (Bigler and Bugmann, 2018;

Liu et al., 2018; Ma et al., 2018), which could reduce tree productivity (Hufkens et al., 2012). Thus, determining the drivers of summer frost probability, intensity, and distribution in the landscape of different forest biomes is a necessary task to manage the forest resources in a sustainable way.

This study aimed to determine how topography, referred to as elevation over a 15-m gradient, microtopography, referred to as a variation from 10 to 80 cm in height above ground and slope angle (at two scales: 1 m and 20 m) can impact near-ground air temperature in two sites located in the Clay Belt of Québec, one in the western temperate and one in the boreal mixedwood forests of Québec, Canada. The small topographic variations of this region paired with the wet clay soils could limit soil warming in spring and enhance the phenomenon of temperature inversion (Dugas, 1975; Laamrani et al., 2014). Therefore, the Clay Belt represents an ideal *in situ* model to disentangle the importance of topography and microtopography on temperature inversions. We hypothesized that during nighttime, temperature inversions would favor the formation of frost pockets at low elevations and in microtopographic depressions and that the intensity of temperature inversions would be stronger at the boreal mixedwood forest compared to the temperate forest. We expected that the topographically-induced temperature gradient would be so important that at low elevation, air temperature could reach sub-zero values even though it is above the freezing point at high elevations. For the effect of microtopography, we expect that increasing height above ground would increase the minimum temperature.

3.5 Materials and methods

3.5.1 Study area

Our study was conducted in the northern Clay Belt of Quebec, a large geographic zone covering 180,000 km^2 where topography is generally flat (elevation between 260 and

362 m above sea level [a.s.l.]), with frequent small hills and depressions that were formed by the retreat of the Laurentide ice sheet and the subsequent formation of the pro-glacial lake Ojibway (Laamrani et al., 2014; Veillette, 1994). The wet clay soils in spring can limit soil warming which paired with the small topographic variations observed in the region, could cause frequent temperature inversions (Dugas, 1975). Therefore, the Clay Belt offers an ideal *in situ* model to test the effects of permanent landscape attributes on spring drainage of cold air masses toward low elevations and in microtopographic depressions. As part of a larger research program investigating the effects of growing-season frosts on tree growth and bud phenology, two 18-yr-old experimental plantations were selected at the boreal-temperate forest ecotone, one located in the temperate forest (47.29° N; 79.12° W) and one located in the boreal mixedwood forest (48.29° N; 79.26° W) of western Québec, Canada (Figure 3.1). At both sites, the topographic gradient is of 15 vertical meters, covering an elevation range of 260-275 meters a.s.l. at the temperate forest and of 278-293 (a.s.l.) at the boreal mixedwood forest (Figure 3.2). At both sites, slope angle (%) varies between 1 and 21 %.

Air temperature is on average 2.4 °C higher at the temperate forest site than at the boreal mixedwood forest site, with a mean annual temperature of 3.1 °C and a mean temperature of -15.0 °C and 18.8 °C for respectively January and July (1981-2010 Normals, Barrage Angliers weather station located 24 km from the study site, Environment Canada 2019a), compared to a mean annual temperature of 1.0 °C at the boreal mixedwood forest site with a mean temperature of -17.9 °C and 16.7 °C for respectively January and July (1981-2010 Normals, Mont-Brun weather station located 47 km from the study site, Environment Canada 2019b).

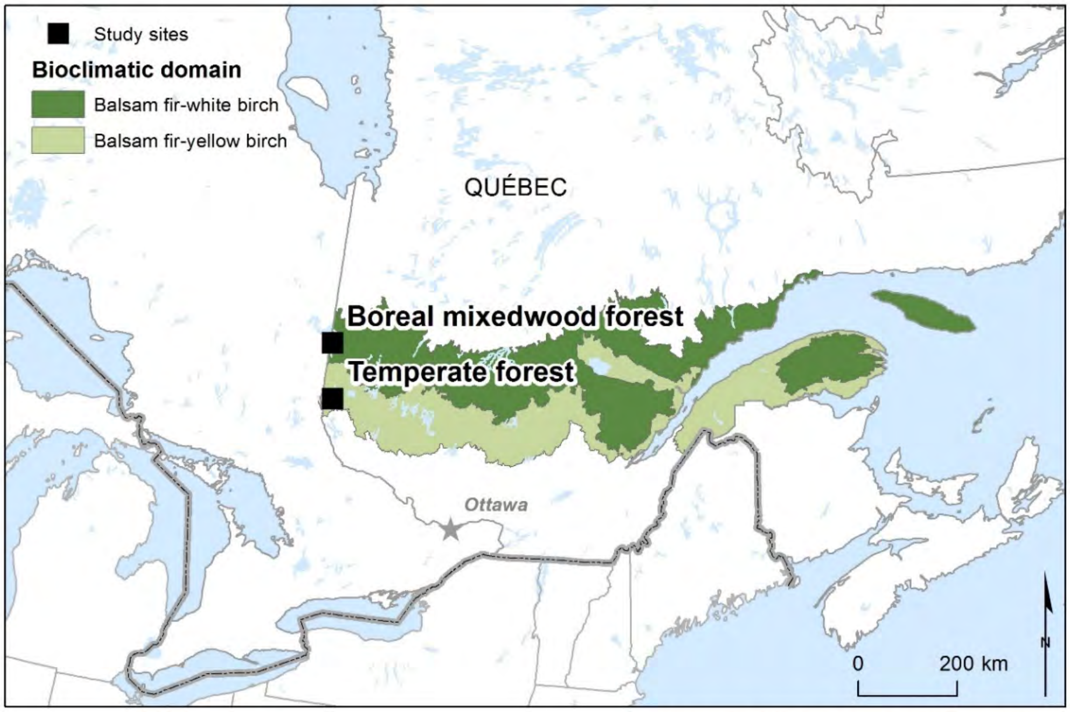

Projection: NAD 1983 MTM 10 | Source: MFFP, 2018 | Author : CEF, 2019

Figure 3.1 Location of the two study sites in the temperate and boreal mixedwood forest of Québec (Canada).

3.5.2 Near-ground measurement of air temperature

To measure *in situ* near-ground air temperature variations with the topographic variations, 204 air temperature loggers (iButtons DS1922L, Maxim Integrated, San Jose, California, USA) were installed at 30 cm above ground level and were set to record air temperature every half hour during two consecutive summers (2016-2017) from May to August. Since the study sites are experimental plantations, the temperature loggers were randomly assigned to plantation plots (Figure 3.2).

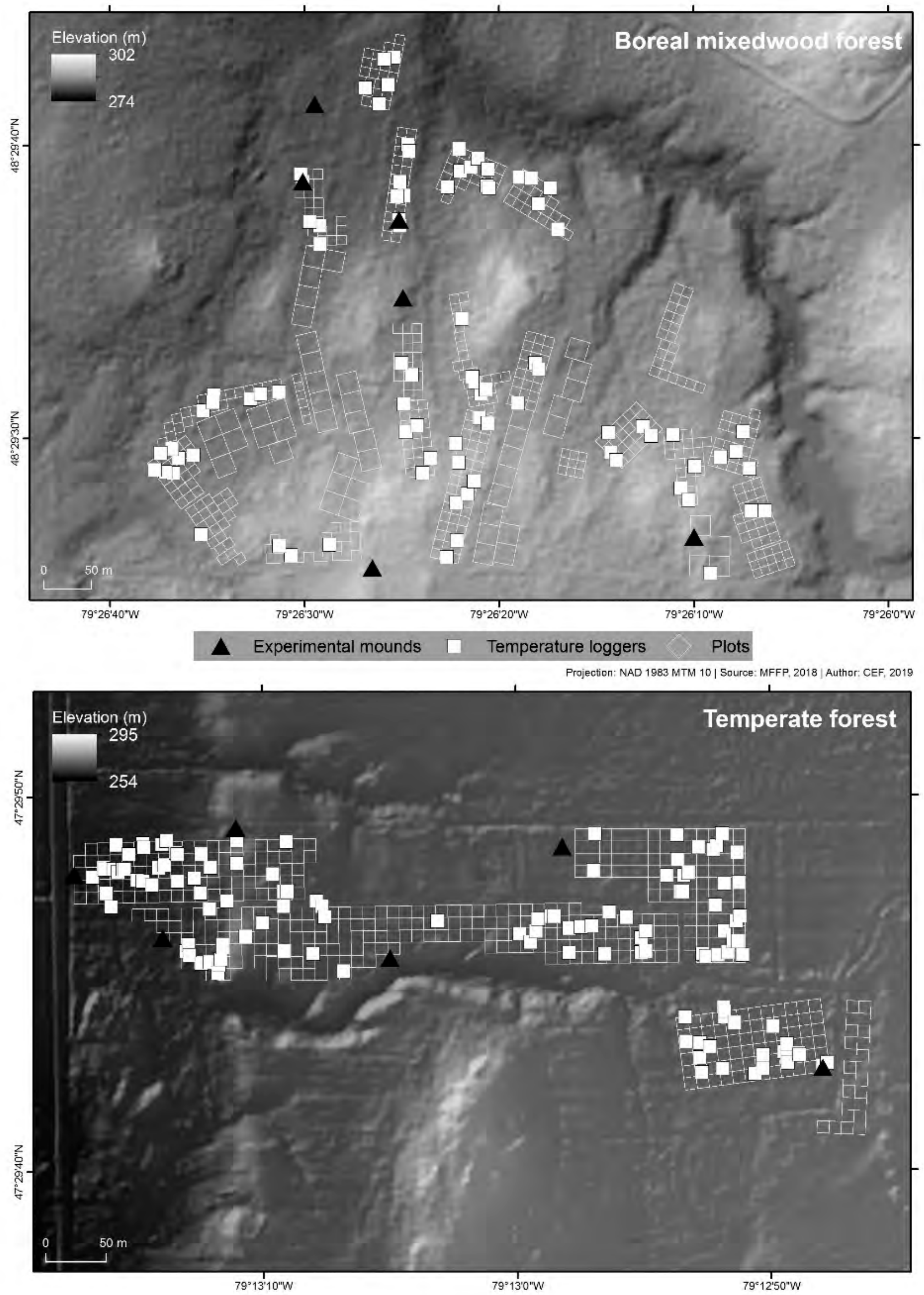

Projection: NAD 1983 MTM 10 | Source: MFFP, 2018 | Author: CEF, 2019

Figure 3.2 Experimental design and position of the artificial mounds at the two plantations.

3.5.3 Artificial mounds

To measure differences in air temperature caused by microtopography, we created six 50-cm tall by 50-cm wide artificial mounds at both sites in 2017. The mounds were set up at different elevations to cover the elevation gradient at both sites (Figure 3.2). At the temperate forest, the mounds were set at 260, 262, 269, 271, 273, and 276 m a.s.l. and at the boreal mixedwood forest, they were placed at 278, 279, 281, 287, 292, and 293 m a.s.l. Each mound was equipped with four loggers that recorded air temperature every half hour. The four loggers were arranged in two sets, each set consisting of a 30-cm post where one logger was fixed at 10 cm and another one at 30 cm. At each mound, one set of loggers was placed at ground level (bottom of the mound) and the other one was placed on top of the mound. Air temperature was therefore measured at 10 cm, 30 cm, 60 cm, and 80 cm from the ground.

3.5.4 Determination of landscape attributes from aerial LiDAR surveys

Airborne LiDAR survey data was acquired in 2003 at the boreal mixedwood forest site and in 2017 at the temperate forest site and were used to create a digital elevation model (DEM) at both sites. At the temperate forest, the aerial lidar survey was performed by the ministry of Forests, Wildlife and Parks at an altitude of 1200 m above ground and a spatial resolution of 1 m^2 with a return density of 4 hits per m^2 (Leboeuf et Pomerleau, 2016) whereas at the boreal mixedwood forest, the aerial lidar survey was performed at an altitude of 1000 m above ground and a spatial resolution of 20 cm with a return density of 0-6 hits per m^2 (Vepakomma et al., 2011). The DEM was used to extract the exact elevation of each temperature logger and to derive two different measures of slope angle. First, slope was calculated in a 1-m radius around the temperature logger (henceforth called the “1-m slope”) and was used to quantify the micro-slope near the logger location. Second, average slope was calculated over a 20-m radius around the temperature logger (henceforth called the “20-m slope”) to reflect the general aspect of the terrain. An abrupt 1-m slope at the temperature logger would indicate the presence of a microtopographic depression where cold air mass could potentially accumulate (a frost pocket) whereas an abrupt 20-m slope around the temperature logger would suggest that air temperature could be drained towards lower elevations. For both slope measurement, a flat terrain would indicate that air masses could either accumulate or be transported elsewhere by the wind.

3.5.5 Statistical methods

To limit the complexity of the analyses caused by the diurnal cycle of air temperature, we used the average temperature for the coldest hour, which was at 5:00 am (Annexe C: Table C1 and Figure C1). All analyses were conducted in the R software for statistical computing (R Development Core Team, 2018) and followed same procedure. Linear or generalized mixed binomial regression models were used to regress air temperature at 5:00 am (linear models) or frost probability (binomial models) to elevation, site and either the 1-m or the 20-m slope angle (candidate models are shown in Annexe C: Table C2). Temperature logger ID, year, month, and day of year were set as random effects. All models were implemented using the `lme4` R package (Bates et al., 2015) and compared to an intercept-only model. Model fit was evaluated according to the corrected Akaike’s information criteria (AICc) using the R package `AICcmodavg` (Mazerolle, 2017). If model selection failed to identify a single best model, we used multi-model inference to average the coefficients in each probable model using the `model.avg` function from the R package `MuMIn` (Barton, 2018). Since we aimed to quantify the effects of topography and microtopography on minimum air temperature and frost probability, we focused our analyses on the 41 days that experienced frosts over the 211-day monitoring period. For comparison however, we also performed the analyses on the frost-free days (170 days) and on the whole data set (211 days). These results are only reported in the supplementary material (Annexe C: Tables C5 to C7).

For the artificial mound experiment, eighteen linear or binomial mixed regression models were used to predict air temperature at 5:00 am (linear models) and frost probability (binomial models) from elevation, height above the ground (4 positions: 10, 30, 60, and 80 cm), and their interaction (candidate models are shown in Annexe C: Table C3). The experimental mound ID and the day of year were incorporated in the random structure of the model and model fit was evaluated using AICc. As this set up was only implemented in 2017, we performed the analyses on the 14 days that experienced frosts over the 103-day monitoring period. We also performed the analysis for the frost-free days (89) and on the whole data set (103 days). These results are only reported in the supplementary material (Annexe C: Tables C10 to C12).

3.6 Results

The coldest air temperature registered was at the boreal mixedwood forest site and was -8.2 °C (Figure 3.3). In 2016, 18 frost days were recorded, of which, 15 occurred at the temperature forest site and 14 occurred at the boreal mixedwood forest site (Figure 3.3a). In 2017, 23 frost days were recorded, of which 20 occurred at the boreal mixedwood forest site and 11 occurred at the temperature forest site (Figure 3.3b). During a frost event, temperature could vary by 4 °C along the elevation gradient (Figure 3.3c). From the experimental mounds, the averaged difference in air temperature between 80 and 10 cm above ground was -0.61 ± 1.96 °C. This small difference in air temperature could still reduce the risk of frost hazard since, on day of year 161, at high elevation, air temperature at 10 cm above ground was -0.5 while air temperature reached 0.1 at 80 cm above ground.

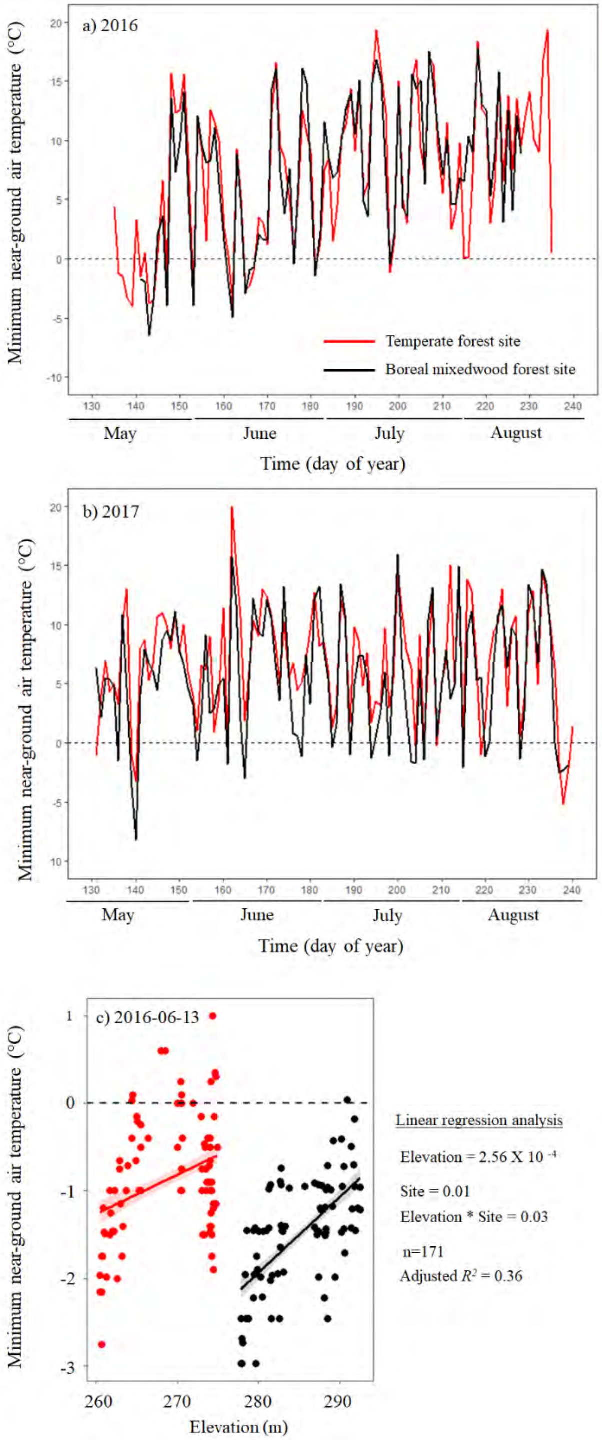

Figure 3.3 Lowest minimum temperature at 5h00 am registered from all temperature loggers per site for (a) 2016, (b) 2017 and (c) minimum air temperature per data logger for one frost day.

3.6.1 Effect of permanent landscape attributes on near-ground air temperature

Model selection for both the minimum temperature and frost probability produced one to two probable models (AICc weight > 0.60) (Table 3.1). The best model for both response variables were the most complex ones, containing all main effects and all two-way interactions. The only difference between the two sets of models was that the 1-m slope angle (measured at the temperature logger) was the best slope variable for predicting minimum temperature, whereas the 20-m slope was the best slope variable for predicting frost probability (Table 3.1). Minimum temperature increased and frost probability decreased from the boreal mixedwood forest to the temperate forest (Table 3.2). The importance of slope angle varied with increasing elevation (slope × elevation interaction; Table 3.2 and Figure 3.4). Specifically, at low elevation, minimum air temperature increased with increasing angular slope (Figure 3.4 (a) and (d)), whereas at high elevation, minimum air temperature decreased with increasing angular slope (Figure 3.4 (c). and (f)). The importance of slope angle to reduce frost hazard increases where cold air masses are less likely to accumulate such as at high elevations (Table 3.2).

The total amount of explained variance by the linear (minimum temperature) and binomial (frost probability) regression models was 80 and 85%, respectively, 12 and 16% of which were respectively explained by the fixed terms (Table 3.1).

Landscape attributes (elevation and slope), site, and their interactions had no effect on minimum air temperature and frost probability when only the frost-free days were considered (marginal pseudo-$R^2 = 0$; Annexe C: Tables C5 and C6), suggesting that the importance of the stratification of air masses is increased under night frost than when no frost event occurs.

Table 3.1 Best models predicting (**a**) minimum air temperature and (**b**) frost probability from landscape attributes (elevation [Elev] and slope) for days with night frosts in 2016-2017 (n = 41 days). Only models with AICc weights > 0.01 are shown (full table can be found in Annexe C: Tables C4 and C8). The most probable models are indicated with boldface type and numbers in parentheses before each model refer to the candidate models prior to selection (Annexe C: Tables C2).

Model	**AICc**	**Delta AICc**	**AICc Wt.**	**Cum. Wt.**	**Marginal pseudo-R^2 (conditional)**
(a) Temperature at 5:00 am best models					
(18) Site, Slope-1m, Elev; Site × Slope-1m; Site × Elev; Slope-1m × Elev	**21293.67**	**0.00**	**0.43**	**0.43**	**0.12 (0.80)**
(17) Site, Slope-1m, Elev; Site × Elev; Slope-1m × Elev	**21293.96**	**0.29**	**0.37**	**0.79**	**0.12 (0.80)**
(30) Site, Slope-20m, Elev; Site × Elev; Slope-20m × Elev	21296.75	3.08	0.09	0.88	0.12 (0.80)
(31) Site, Slope-20m, Elev; Site × Slope-20m; Site × Elev; Slope-20m × Elev	21297.10	3.43	0.08	0.96	0.12 (0.80)
(b) Frost probability best models					
(31) Site, Slope-20m, Elev; Site × Slope-20m; Site × Elev; Slope-20m × Elev	**3137.16**	**0.00**	**0.95**	**0.95**	**0.16 (0.85)**
(18) Site, Slope-1m, Elev; Site × Slope-1m; Site × Elev; Slope-1m × Elev	3144.01	6.85	0.03	0.98	0.15 (0.85)

Table 3.2 Standardized coefficients of the best models predicting (**a**) minimum temperature and (**b**) frost probability from landscape attributes (elevation [Elev] and slope) for days with night frosts (left column; n =41) and for frost-free nights (right column, for minimum temperature only; n = 170). Boldface type indicates coefficients that differ from zero.

Variable	**Standardized coefficients (SE)**	
	Days with frost	**Frost-free days**
(a) Temperature at 5:00 am best model		
Intercept: Temperate forest	**2.30 (0.97)**	**10.81 (2.47)**
Boreal mixedwood forest	**-3.49 (0.17)**	**-1.87 (0.10)**
Elev	**0.68 (0.10)**	**0.40 (0.06)**
Slope-1m	0.07 (0.12)	-0.04 (0.06)
Elev × Boreal mixedwood forest	**0.55 (0.17)**	**0.43 (0.10)**
Slope-1m × Elevation	**-0.26 (0.11)**	**-0.20 (0.06)**
Slope-1m × Boreal mixedwood forest	**0.32 (0.21)**	**0.29 (0.13)**
(b) Frost probability best model		
Intercept: Temperate forest	**-3.39 (1.49)**	NA
Boreal mixedwood forest	**6.20 (0.38)**	NA
Elev	**-1.13 (0.23)**	NA
Slope-20m	**0.64 (0.29)**	NA
Elev × Boreal mixedwood forest	**-1.88 (0.35)**	NA
Slope-20m × Elev	**1.08 (0.26)**	NA
Slope-20m × Boreal mixedwood forest	**-1.74 (0.52)**	NA

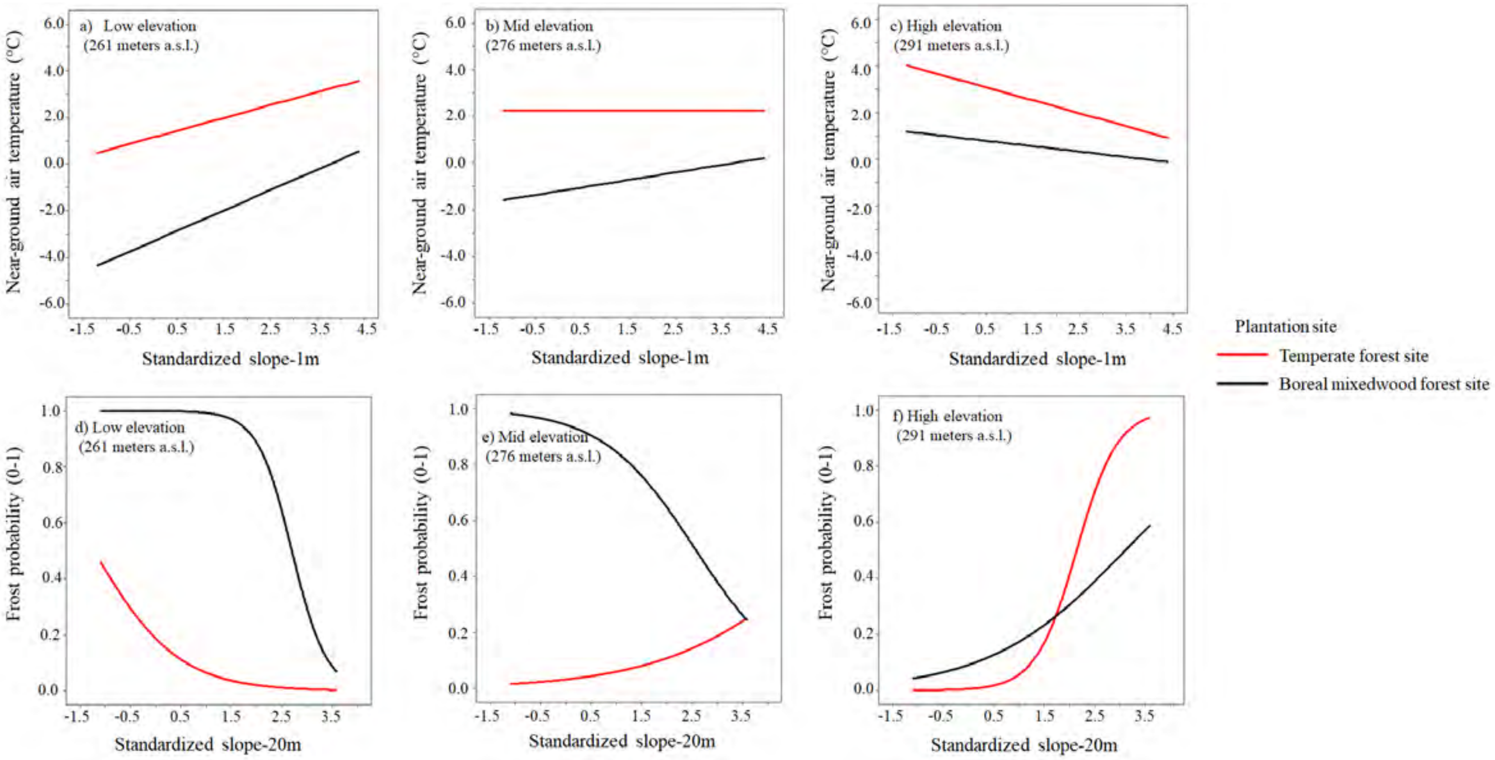

Figure 3.4 Modelled mean (line) showing the site-specific variations in near-ground minimum air temperature and frost probability along the angular slope gradient for (a and d) low elevation; (b and e) mid elevation and (c and f) high elevation.

3.6.2 Artificial mounds: effect of height above ground and elevation on near-ground air temperature

Model selection for minimum temperature and frost probability respectively identified one and two probable models (Table 3.3), which were the most complex among the candidate models (Annexe C: Table C3). Minimum temperature increased and frost probability decreased from the temperate forest site to the boreal mixedwood forest site (Figure 3.5). The importance of the height above ground varied per site (height above ground × Site interaction, Table 3.4) and along the elevation gradient (height above ground × elevation interaction, Table 3.4). Since air temperature rarely reached freezing values at the temperate forest site in 2017, frost probabilities are of zero whereas at the boreal mixedwood forest site frost probabilities only decreased with height above the ground at the highest elevation, otherwise, height above ground had little impact on frost probability at low and mid elevations which are subject to frequent freezing air temperature (Table 3.4 and Figure 3.5).

The total amount of explained variance by the linear (minimum temperature) and binomial (frost probability) regression models was 94 and 97%, respectively; of these explained variance values, respectively 31 and 61% were explained by the fixed terms (Table 3.3), which is significantly more than for the models using landscape attributes (12 and 16%; Table 3.1).

Site, height above the ground, elevation, and their interactions only explained 4% of the variation in minimum temperature when only frost-free days were analyzed (Annexe C: Tables C10 to C13).

Table 3.3 Best models predicting (**a**) minimum air temperature and (**b**) frost probability from height above the ground (Height_AG) and elevation (Elev) for days with night frosts in 2017 (n = 14 days). Only models with AICc weights > 0.01 are shown (full table can be found in Annexe C: Tables C9 and C13). The most probable models are indicated with boldface type and numbers in parentheses before each model refer to the candidate models prior to selection (Annexe C: Tables C3).

Model	**AICc**	**Delta AICc**	**AICc Wt.**	**Cum. Wt.**	**Marginal pseudo-R^2 (conditional)**
(a) Temperature at 5:00 am best models					
(18) Site, Height_AG, Elev; Site × Elev; Height_AG × Elev; Site × Height_AG	**1268.82**	**0.00**	**0.90**	**0.90**	**0.31 (0.94)**
(15) Site, Height_AG, Elev; Site × Height_AG; Site × Elev	1273.57	4.75	0.08	0.98	0.31 (0.94)
(b) Frost probability best models					
(17) Site, Height_AG, Elev; Site × Elev; Height_AG × Elev	**179.76**	**0.00**	**0.53**	**0.53**	**0.61 (0.97)**
(18) Site, Height_AG, Elev; Site × Elev; Height_AG × Elev Site × Height_AG	**180.57**	**0.80**	**0.35**	**0.88**	**0.55 (0.97)**

Table 3.4 Standardized coefficients of the best models predicting (**a**) minimum temperature and (**b**) frost probability from height above ground (Height_AG) and elevation (Elev) for days with night frosts (left column; n =14) and for frost-free nights (right column, for minimum temperature only; n = 89). Boldface type indicates coefficients that differ from zero.

Variable	**Standardized coefficients (SE)**	
	Days with frost	**Frost-free days**
(a) Temperature at 5:00 am best model		
Intercept: Temperate forest	**2.08 (0.95)**	**9.82 (0.58)**
Boreal mixedwood forest	**-3.06 (0.50)**	**-0.76 (0.35)**
Elev	**-1.14 (0.34)**	**-0.75 (0.24)**
Height_AG	**0.23 (0.09)**	**0.09 (0.05)**
Boreal mixedwood forest × Elev	**0.93 (0.17)**	**0.36 (0.12)**
Boreal mixedwood forest × Height_AG	**-0.60 (0.16)**	**-0.11 (0.08)**
Elev × Height_AG	**0.21 (0.08)**	**-0.01 (0.05)**
(b) Frost probability best model		
Intercept: Temperate forest	**-14.52 (4.55)**	NA
Boreal mixedwood forest	**22.52 (5.89)**	NA
Elev	**-4.99 (2.93)**	NA
Height_AG	**-2.38 (1.11)**	NA
Elevation × Boreal mixedwood forest	**-2.85 (2.40)**	NA
Height_AG × Boreal mixedwood forest	**4.23 (1.64)**	NA
Elev × Height_AG	**-1.71 (0.60)**	NA

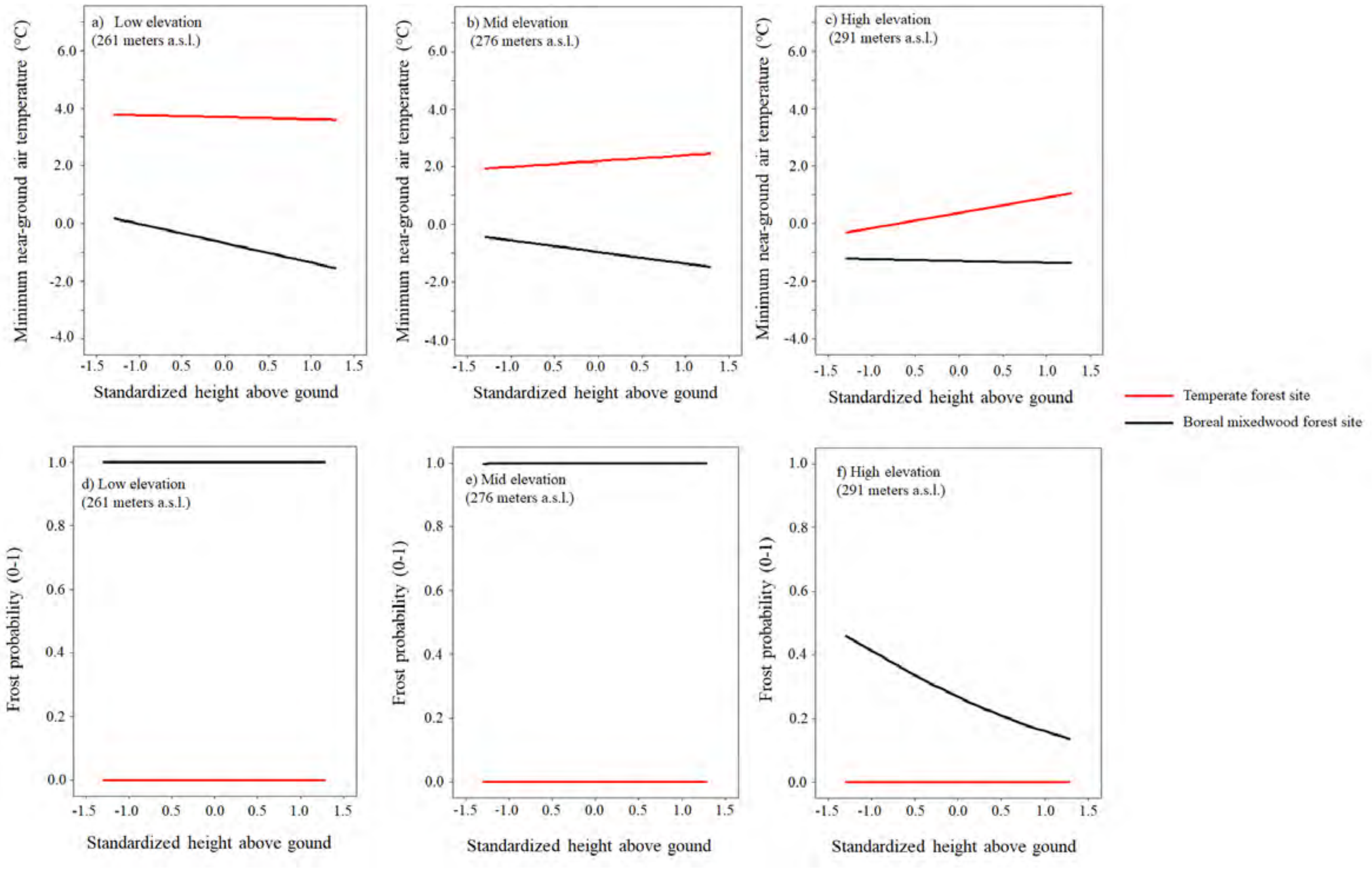

Figure 3.5 Modelled mean (line) showing the variations in near-ground minimum air temperature and frost probability per height above ground measured from the artificial mound experiment for (a) low elevation; (b) mid elevation and (c) high elevation.

3.7 Discussion

In line with our hypothesis, the drainage of cold air masses toward low elevations and at the bottom of microtopographic depression causing summer frosts occurred at both sites in the boreal-temperate forest ecotone and is therefore not restricted to northern parts of the boreal forest. As expected, temperature inversions were stronger and most frequent at the coldest site, still, below-freezing near-ground air temperature were also observed at the temperate forest throughout the summer. During the nights where frost occurred, the 4 °C difference in air temperature observed over the relatively small elevation gradient of 15 meters at our study sites was stronger than expected. This positive lapse rate (0.27 °C/m) was more than 50 times greater than the negative lapse rate that is usually found along a mountain slope, which is approximately 0.5 °C/100 m (Beckage et al., 2008). Despite that strong change in air temperature with topography, temperature inversions stay unaccounted for in climate models.

Our results showed that both topography (elevation and slope 20 m) and microtopography (height above ground and micro-slopes) were important for predicting minimum air temperature. Cold air accumulates where it cannot be drained elsewhere, therefore, incline terrain or micro-slopes can allow the drainage of cold air toward lower elevations or in microtopographic depressions. Specifically, at low elevation, flat microsite can accumulate more cold air than incline microsite. However, at high elevation, the cold air above flat microsite is drained toward lower elevations, which decreases the risk of spring frost compared to incline microsite where the cold air can be trapped at the bottom of micro-slopes. Micro-slopes are therefore important to consider mostly where cold air is less likely to accumulate such as at high elevation. This explanation is also supported by the results from the experimental mounds since the decrease risk in spring-frost associated with the height above ground could only be observed at high elevation. Surprisingly, at low elevation, air temperature at 80 cm above ground was colder than at 10 cm above ground, we think that the release of heat from the ground and the possible shelter made by the surrounding vegetation could have help increasing the air temperature close to the ground (10 cm). That warming was, however, insufficient to prevent frost from occurring. Therefore, a gradient of 80 cm above ground is not enough to prevent spring frost from occurring if other important variables at the landscape level like elevation are increasing the risk of spring frost. Still, that 80 cm variation in height above ground reduced the frost probability where frost events were less intense such as at high elevation.

Predicting where frost-induced lethal threshold value occurs could improve our ability to identify frost-free zones and establish productive plantations. Previous studies assessing frost hazard in complex terrain already identified the importance of elevation and slope shape (concave slopes trap cold air and convex slopes allow the movement of cold air) on the probability of summer frosts (Laughlin and Kalma, 1987; Lindkvist and Lindqvist, 1997; Chung et al., 2006). However, these studies were designed to understand the general impact of landform on frost hazard whereas our study brings out the importance of microsite-specific variations for predicting near-ground summer frosts. Elevation, slope angle and to a lesser extend, height above ground are required to properly identify frost-free zones because even if cold air masses tend to accumulate more at low elevations, microtopographic depressions at high elevations can still trap cold air and cause summer frosts. This effect prevailed at the temperate forest because the milder frost events restricted the accumulation of cold air masses above ground, rarely exceeding the microtopographic variations except at low elevations. On the other hand, at the boreal mixedwood forest, the more severe summer frosts favored the accumulation of cold air masses above the ground, exceeding microtopographic variations and potentially affecting larger portions of the landscape. Therefore, in frost-prone environments such as the boreal forest, elevation is a more important variable to consider than height above the ground, whereas in environment where summer frosts are rare such as in the temperate forest, microtopographic variations are more important to consider.

3.7.1 Implications for forest management

For forest management, the identification of local frost-free zones is crucial for establishing productive plantations. We suggest planting frost-tolerant species at low elevations and in microtopographic depressions to limit the reduction in tree productivity caused by summer frost and we suggest planting fast-growing species in frost-free zones (high elevation, incline terrain) to maximize wood production. Therefore, the decision of which species to plant at specific locations could be best achieved using LiDAR to precisely measure elevation and slope angle prior to the establishment of plantations to identify local frost-free zones.

With the increase in mean global air temperature above pre-industrial levels (IPCC, 2018), air temperature inversions at the boreal-temperate forest ecotone may decrease in importance. The decreased intensity of future summer frost should limit the accumulation of cold air masses above ground, restricting it to low elevations and at the bottom of topographic depressions. However, because climate change may also increase the frequency and intensity of extreme climatic events, more spring and summer frosts could occur at the boreal-temperate forest ecotone (Liu et al., 2018; Ma et al., 2018; Tebaldi et al., 2006). In this case, elevation will become a prominent factor determining tree productivity. Therefore, the various microclimates induced by the air temperature inversion at the boreal-temperate forest ecotone could potentially allow the establishment of southern species into the boreal forest. Since the future intensity and probability of summer frosts remain unknown, we put forward these recommendations to maintain or even increase future wood production in plantations:

1) Aerial LiDAR surveys should be used to determine local frost-prone and frost-free zones prior to plantation establishment;

2) In frost-prone zones, mound planting should be performed, and taller trees should be planted to ensure that the trees’ apical buds are out of the zone of ground frost;

3) Mixed plantations using frost-resistant species or seed sources should be planted in frost-prone zones and frost-sensitive species or seed sources should only be planted in frost-free zones;

4) Use of partial cutting and amount of tree retention should be increased to limit large open spaces where radiative cooling cause frost damage to newly-planted trees.

3.8 Conclusion

Frost damage can impede the regeneration of forest stands mostly if the area is exposed to large daily temperature variations. As frost events are more intense and probable in low elevation or in microtopographic depressions, greater attention should be given to the topography and microsite conditions to limit the occurrence of spring frosts in plantations established at the boreal-temperate forest ecotone.

3.9 Acknowledgments

We would like to thank L. Gervais and R. Mincheva for their important field assistance and to Mélanie Desrocher for her tremendous help on GIS, for manipulating lidar data and for producing the maps of our study sites.

3.10 Conclusion

Notre étude est l’une des premières à quantifier la fréquence et l’intensité des gelées d’été à l’écotone de la forêt tempérée-boréale et à mettre en évidence l’importance de la position dans la topographie et dans la microtopographie pour prédire l’intensité des gelées d’été. Lorsque les gelées d’été surviennent, il se forme un important gradient de température qui peut passer de -2 °C dans les basses élévations à 2 °C dans les hautes élévations, et ce, sur un faible gradient d’élévation de 15 mètres, qui varie aussi selon la distance verticale au-dessus du niveau du sol. Lorsque l’intensité des gelées d’été est forte, l’élévation est la variable la plus importante à considérer, alors que si l’intensité des gelées d’été est faible, la distance verticale au-dessus du niveau du sol devient plus importante. Même si les évènements de gel sont localisés, ils peuvent entraîner d’importantes conséquences sur le développement des jeunes arbres en plantation. Donc, identifier les zones sujettes aux gelées d’été pourrait améliorer la productivité des plantations d’épinettes. Toutefois, pour déterminer l’importance du phénomène de stagnation de la croissance des plantations d’épinettes en lien avec les gelées d’été, un suivi des plantations à l’échelle du paysage régional est requis. Cette tâche a d’ailleurs été entreprise au quatrième chapitre.

CHAPITRE IV

HEIGHT GROWTH STAGNATION OF PLANTED SPRUCE IN BOREAL MIXEDWOODS: IMPORTANCE OF LANDSCAPE, MICROSITE AND GROWING-SEASON FROSTS

Benjamin Marquis, Yves Bergeron, Nelson Thiffault, Philippe Duval, Martin Simard,
Francine Tremblay

Cet article est publié à la revue scientifique
Forest Ecology and Management

4.1 Highlights

- White spruce is more severely damaged by growing-season frosts than black spruce.
- Tree height was supressed even 13 years after planting.
- Microtopography impacted tree height, thus mound planting could favor growth.
- Mixed plantations of white and black spruce would increase plantation success.

4.2 Résumé

Le reboisement en forêt boréale s’effectue difficilement, puisque les arbres doivent survivre aux fortes variations journalières de la température de l’air et à l’environnement froid. Même si les espèces locales se sont adaptées à ces conditions environnementales extrêmes, les échecs de plantation d’épinettes après reboisement artificiel sont fréquents, ce qui a d’importantes répercussions sur l’aménagement durable de la forêt boréale. Nous émettons l’hypothèse que ce problème de régénération est causé par de fréquents évènements de gel survenant durant la saison de croissance, qui, en endommageant le bourgeon apical et les nouvelles pousses, limite la capacité photosynthétique et la croissance en hauteur des arbres plantés. L’objectif de ce chapitre était d’identifier les attributs permanents du paysage régional (élévation, forme de la pente et la pente %) et du microsite de plantation (élévation au-dessus du sol [dépression *vs.* butte]) qui prédisent le mieux la hauteur des arbres et les dommages aux pousses annuelles causés par le gel. Pendant l’été 2016 et l’été 2017, la hauteur de 2943 épinettes blanches et noires a été mesurée dans 66 plantations âgées de 6 et 13 ans, distribuées dans la ceinture d’argile du Québec, un environnement où les évènements de gel durant l’été sont fréquents. En utilisant des régressions linéaires et binomiales mixtes, nous avons analysé l’effet des attributs physiques du paysage régional et du microsite de plantation sur la hauteur des arbres (linéaire) et sur l’endommagement des nouvelles pousses par le gel (binomiale). La hauteur des arbres augmente lorsqu’ils sont plantés à de plus hautes élévations et lorsqu’ils sont plantés sur des buttes, comparativement à lorsqu’ils sont plantés à de plus basses élévations et lorsqu’ils sont plantés dans des dépressions microtopographiques. L’impact du microsite sur la hauteur des arbres augmente plus la plantation est âgée, alors que l’importance de l’élévation sur la hauteur des arbres diminue plus la plantation est âgée. La probabilité que les arbres soient endommagés par le gel augmente s’ils sont situés dans une dépression microtopographique et dans une pente concave. Ces relations sont surtout importantes pour les plus jeunes plantations. Toutefois, les arbres affectés par le problème de croissance restent plus petits que deux mètres même 13 ans après avoir été plantés. Nous avons aussi observé des différences entre les espèces, l'épinette blanche était significativement plus petite et plus endommagée par le gel que l'épinette noire. Donc, le gel printanier constitue un évènement climatique majeur causant le problème de suppression de la croissance des plantations d'épinettes établies en forêt boréale. Puisque le microsite joue un rôle déterminant dans le succès des plantations, les techniques de préparation de terrain ne devraient pas seulement viser à prévenir la compétition entre les arbres plantés et les plantes environnantes, mais devraient aussi chercher à limiter les dommages engendrés par le gel en plantant les arbres sur des microsites surélevés. Les résultats présentés dans cet article devraient pouvoir guider les pratiques forestières à utiliser à l'avenir pour limiter les échecs de plantation en forêt boréale.

4.3 Abstract

Reforestation in the boreal forest is challenging; trees must survive to large daily temperature variations and to the cold environment. Even if local tree species are adapted to withstand these harsh environmental conditions, spruce plantation failure after artificial regeneration occurs frequently, with important impacts on sustainable forest management. We hypothesized that this regeneration problem is caused by recurrent frost events occurring during the growing season. These events would freeze the terminal bud and the newly formed needles of the planted trees, thus limiting photosynthesis capacity and height growth. Our goal was to identify key permanent physical attributes of the landscape (elevation, slope shape and angular slope) and of microsite conditions (hole *vs*. mound) that best predict tree height and frost damage to foliage. In summer 2016 and 2017, we sampled tree height of 2,943 white spruce (*Picea glauca* [Moench] Voss) and black spruce (*Picea mariana* [Mill.] B.S.P.) trees in 66 monoculture plantations aged between 6 and 13 years distributed in the Clay Belt region of Quebec (Canada), an environment prone to frequent growing-season frosts. Using linear and binomial mixed regression models, we analyzed the effects of the physical attributes of the landscape and of microsite conditions on tree height (linear) and on frost damage (binomial). Tree height increased with increasing elevation and when seedlings were planted on mounds compared to planted in holes. The impact of microsite conditions on tree height increased as plantations aged, but the importance of elevation on tree height decreased with age. The probability of frost damage to foliage decreased for trees planted on mounds compared to trees planted in holes and from concave to convex slopes. These relations were most important in young plantations, but trees showing growth problems were still shorter by 2 m, even 13 years after planting. We also observed differences between species: white spruce was significantly more damaged by frost and was smaller compared to black spruce. Therefore, growing-season frosts can cause growth suppression problems in white spruce plantations established in the boreal mixedwood region. Since microsite conditions also play a key role in driving plantation success, mechanical site preparation techniques should not only focus on reducing the competition between the planted trees and the competing vegetation but should also focus on limiting frost damage by planting trees on elevated microsites. Our results will support forestry practices limiting plantation failure in boreal mixedwoods.

Keywords: Boreal mixedwoods, Forest productivity, Growing-season frosts, Microsite conditions, *Picea*, Spruce

4.4 Introduction

Successful regeneration after anthropogenic disturbances or wildfires faces many challenges in forest ecosystems (Grossnickle, 2000; Gärtner, Lieffers and Macdonald, 2011). Competing for space, light and nutrients with other plants, notably ericaceous species (Lieffers and Stadt, 1994; Thiffault, Hébert and Jobidon, 2012; Thiffault, Titus and Munson, 2004), and surviving to the cold environment (Hänninen, 2016) are critical in boreal biomes. Difficulties in overwhelming these challenges impact the time during which planted spruce seedlings experience stunted growth (also described as growth "check"), i.e. when height increment becomes < 2.5 cm y-1 (Mullin, 1963; de Montigny and Weetman, 1990; Vyse, 1981; Langvall, Nilsson and Örlander, 2001). During the growth check phase, planted seedlings can develop malformations analogous to those observed at the treeline, such as the emergence of multiple small stems (Dy and Payette, 2007; Pereg and Payette, 1998; Payette et al., 1996). Stunted growth and malformations reduce the quantity, the quality and the value of the wood for the industrial use and increase the rotation length, with significant impact on sustainable forest management.

Although being generalized, the extent of the growth stagnation period varies among species (Mullin, 1963; Vyse, 1981); for example, planted white spruce (*Picea glauca* [Moench] Voss) in the boreal regions of Canada seem to experience a longer check period than black spruce (*Picea mariana* [Mill.] B.S.P.) (Clements et al., 1972; Mullin, 1963). Even if causes of growth check in planted trees can be numerous (e.g. drought or wet soil conditions, competition, insect outbreaks), growing-season frosts stand out as one of the most probable drivers of the check period (Lu and Man, 2011; Lu et al., 2014; Man et al., 2009; Marquis et al., 2020). The removal of canopy trees by harvesting activities increases light intensity levels and near-ground temperature variations (Groot and Carlson, 1996; Langvall and Löfvenius, 2002), which increase the risk of photoinhibition during the day and of freezing during the night for planted trees (Hänninen, 2006; Hannerz, 1994; Man and Lieffers, 1999). Moreover, foliage submitted to growing-season frosts is more sensitive to damages by high radiation levels than intact foliage, which further reduces photosynthesis rates and limits height growth (Augspurger, 2009; Hufkens et al., 2012; Örlander, 1993; Langvall, Nilsson and Örlander, 2001). While the physiological mechanisms leading to the check problem remains unclear, white spruce's earlier budbreak compared to black spruce could increase its exposure to growing-season frosts and prolonged its check period (Clements et al., 1972; Man et al., 2009, 2017; Rossi and Isabel, 2017; Marquis et al., 2020).

Growing-season frosts in the boreal biome are frequent, occurring every two to eight days in open forests such as the lichen woodland (Payette and Delwaide, 2018). Even if the frequency of growing-season frost decreases toward the southern edge of the boreal biome, growing-season frosts still occur annually and when the intensity of the frost event exceeds the plant's frost hardiness, seedlings are damaged by ice crystals forming in their tissues (Hocevar and Martsolf, 1971; Groot and Carlson, 1996). A temperature of –5 °C for few hours is sufficient to damage cambial cells (Bigras and Hébert, 1996; Dy and Payette, 2007). Therefore, by damaging both the apical and the lateral meristems, respectively responsible for height and diameter growth, growing-season frosts can have important impact on plantation productivity. Radiative cooling of plants occurs by clear sky night without wind, a condition that allows the accumulation of dense cold air masses at the bottom of slopes or in of microtopographic depressions (Bootsma, 1976; Laughlin and Kalma, 1987; Lindkvist and Lindqvist, 1997; Oke, 1987). Concurrently, growth check also intensifies in concave and wet clay soils (Mullin, 1963, Dy and Payette, 2007). Although the frequency of frost events increases at low elevations and in concave slopes (Laughlin and Kalma, 1987), predicting the location of frost pockets is challenging since they are distributed across the landscape and affect trees at the microsite level (Langvall and Örlander, 2001). Climate change can further increase the severity of frost injuries and associated growth reductions by favouring earlier emergence from dormancy in spring, when frost events are frequent (Cannell and Smith, 1986; Liu et al., 2018; Ma et al., 2019). Knowledge of environmental factors favouring frost events at both the landscape and microsite scales and the ability to predict their impacts on tree growth is mandatory to ensure forest plantation success under a changing climate.

In this context, our aim was twofold; 1) to determine the extent at which young planted spruce plantations established in the Clay Belt region of northwestern Quebec (Canada) were affected by the check period and 2) to identify the permanent attributes of the landscape (elevation, angular slope, slope shape) and of the planting microsite (differences in height above ground [hole *vs.* mound]) that best predict tree height and frost damage to foliage. The wet clay soils and small topographic variations of the Clay Belt region can favor the formation of frequent growing-season frosts (Dugas, 1975; Laamrani et al., 2014; Veillette, 1994). Therefore, this region offers an ideal *in situ* model to analyze the possible differences in tree height between white and black spruce, in interaction with the growth reduction associated with frost events. We developed two hypotheses: 1) that spruce plantations in the Clay Belt would exhibit a check period and that check period would last longer for white spruce compared to black spruce (aim 1), and 2) tree height would decrease and the probability of frost damage to trees would increase at low elevations, concave slopes and in holes compared to high elevations, convex slopes and on mounds (aim 2). To test these two hypotheses, we collected field data in 66 spruce plantations and conducted four analyses: i) we compared observed tree heights to tree heights predicted by an height growth model developed by the provincial government of Quebec (hypothesis 1, aim 1) (Prégent et al., 2010); ii) we compared tree heights between species per plantation age (hypothesis 1, aim 1); iii) we analyzed the variation in tree height within plantations (both hypotheses and aims 1 and 2) and iiii) we modelled tree height (linear regression) and visible frost damage (binomial process) to newly formed needles using permanent attributes of the landscape and of the microsite (hypothesis 2, aim 2).

4.5 Materials and methods

4.5.1 Study site

We conducted our study in the northwestern clay belt region of Quebec, Canada (48.45°N, 79.10°W) (Figure 4.1). This area is part of the boreal mixedwood forest and stands in the balsam fir (*Abies balsamea* [L.] Mill.)–white birch (*Betula papyrifera* Marsh.) bioclimatic domain described by Saucier et al. (2009). Major soil types for the region are Luvisol and Gleysol (Soil Classification Working Group, 1998). The clay sediments where deposited after the retreat of the Laurentide ice sheet when the pro-glacial Lake Ojibway covered the region, 10,000 to 8,000 years ago (Veillette, 1994). The elevation ranges between 268 and 350 m a.s.l. (Laamrani et al., 2014). Topography is generally flat with frequent small hills and valleys (Laamrani et al., 2014), which paired with the wet clay soils in spring, makes this environment especially prone to the formation of frost pockets (Dugas, 1975). The region is characterized by a mean annual temperature of 1.0 °C with long winters (November to April) and short summers (May to August) (1981–2010 climate normals, Mont-Brun weather station located ~ 47 km from the study site, Environment Canada, 2019). Mean air temperature during the warmest month (July) is 17 °C with daily maximum reaching 35 °C, whereas the mean temperature during the coldest month (January) is –18 °C, with daily minimum reaching –49 °C. Frost events occur annually in May and June and occasionally in July (Annexe D: Figure D1). However, due to the distance between the plantation sites and the weather station, and to the sites' complex terrain, the frequency of *in situ* growing-season frost is likely superior to the frequency of the growing-season frost measured by the weather station (Bootsma, 1976; Laughlin and Kalma, 1987; Lindkvist and Lindqvist, 1997; Chung et al., 2006).

4.5.2 Sampling design and field methods

In summers 2016 and 2017, we surveyed 66 monoculture plantations of either white or black spruce aged between 6 and 13 years and covering at least 1 ha each (Figure 4.1). We randomly distributed 40 m^2 circular sampling plots in each plantation at a density of 1.5 plots/ha, for a total of 428 sampling plots. The x-y coordinates of each plot were determined with a hand-held GPS device and were used to extract elevation data based on a digital elevation model at a scale of 1:250,000, interpolated to a resolution of 20 m (Canada3D, Forest Canadian Center of Ontario). Plot level permanent landscape attributes such as angular slope (measured with a clinometer) and slope shape (categorized according to four levels: regular, irregular, convex, concave), were recorded. In each sampling plot, we measured the total height (cm) of all trees > 1 m, for a total of 2,943 trees (1,801 white spruce; 1,142 black spruce). Local variations in height above ground of the planting microsite was recorded according to three categories (hole, level or mound relative to the sampling plot). We also visually recorded frost damages to newly formed needles as a binary variable; trees with grey-brown needles leaning downward were considered damaged (1), whereas intact foliage was classified as undamaged (0).

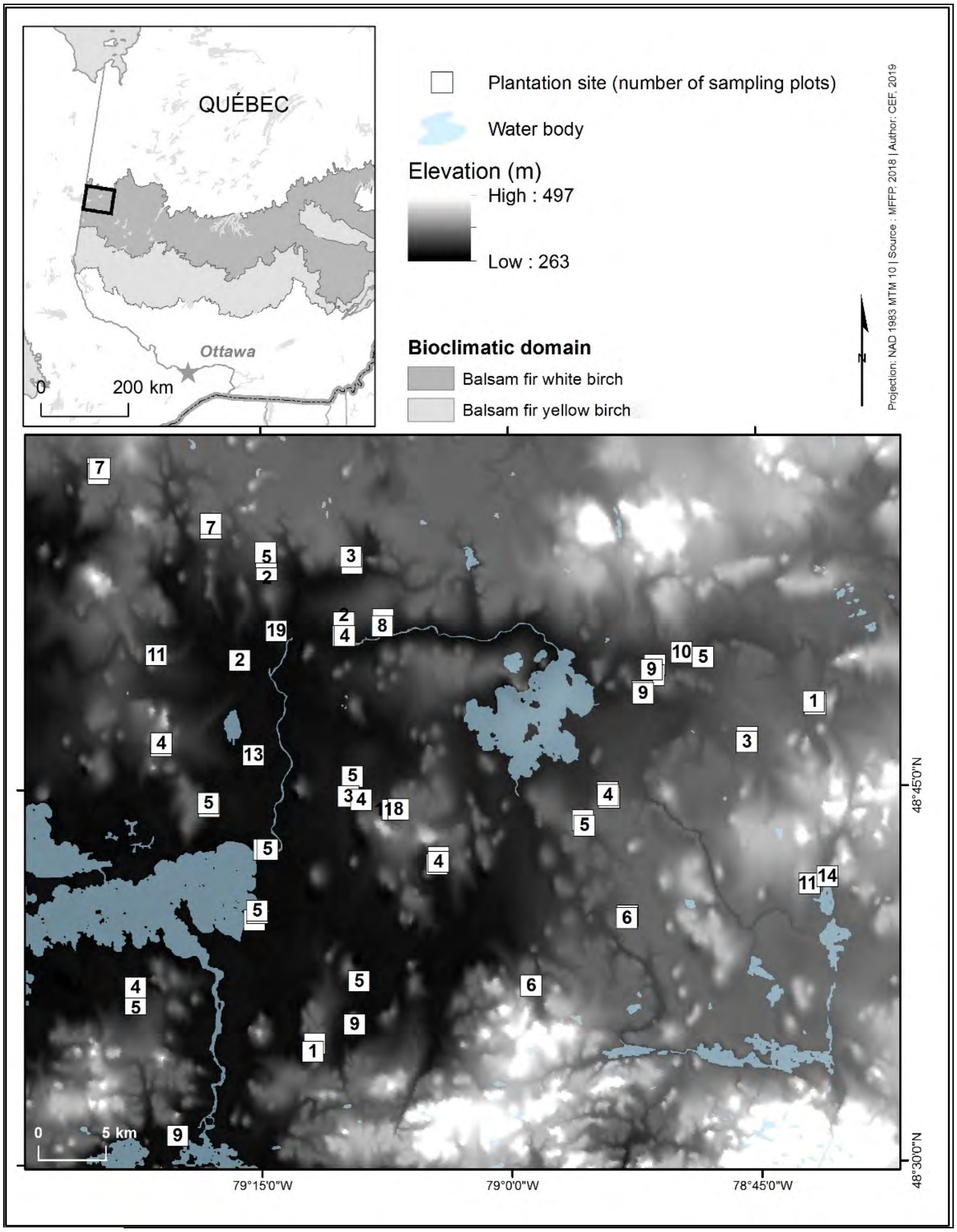

Figure 4.1 Inset shows the location of the study area in the boreal mixedwood forest of Quebec (Canada). The bottom panel shows the number of sampling plots per plantation site.

4.5.3 Statistical analyses

Numerical predictor variables were standardized using the `scale` function from R version 3.5.1 (R development core team, 2019), which subtract each value within a variable to its mean and then divide it by the standard error (Zuur et al., 2009). This procedure allows to maximize comparison between variables by putting them on the same scale (Zuur et al., 2009).

4.5.3.1 Determining the importance of the height growth stagnation problem

Since the check period is a concept that applies to plantations for which the main stems show the problem of stagnant growth (Mullin, 1963; Sutton, 1992), we compared the observed dominant tree height (tallest tree per plot) to the predicted dominant tree height produced by a governmental growth and yield model (Prégent et al., 2010) per plantation age using an unpaired, two-tailed, two sample student t-tests (analysis i).

The governmental growth model was calibrated based upon tree height measurements gathered from 334 sampling plots established in white spruce plantations of around 0.04 ha, of which, 87 plots were established throughout Québec's boreal mixedwood forests (Prégent et al., 2010). In this growth model, the dominant tree height represents the average height of the 100 tallest trees within 1 ha, which, for 0.04 ha plantations, represents the average height of the four tallest trees within a plantation (Prégent et al., 2010). Our plot density also averages to 4 plots per plantation, which increases the comparability between our field sampling and the field sampling performed to calibrate the growth model. Still, in the boreal mixedwood forest, tree productivity can vary importantly depending on the landscape and the microsite conditions, on the presence of competitive vegetation and because of the rigorous climate (Lieffers and Stadt, 1994; Grossnickle, 2000; Gärtner, Lieffers and Macdonald, 2011; Thiffault, Hébert and Jobidon, 2012). Therefore, this growth model was adjusted to predict 11 different growth trajectories that were defined according to the expected dominant tree height of the plantation 25 years after planting, which ranged between 4 and 14 m (Prégent et al., 2010). Since a plantation with a dominant tree height of four meters 25 years after planting is a plantation experiencing a check period, the growth model can predict plantation failures. Thus, even if the observed dominant tree height measurements are statistically in accordance with the mean growth trajectory, which consist in the average of the 11 growth trajectories, predicted by the growth model, it does not mean that the plantation is productive. Therefore, we considered that a plantation was experiencing a check period if > 75% of its sampling plots have their dominant tree height (tallest tree of the plot) following a growth trajectory leading to an expected dominant tree height reaching < 8 m 25 years after planting. This threshold was used since the governmental model predicts that the average expected dominant tree height should reach 10 m 25 years after planting in the boreal mixedwood forest (Prégent et al., 2010). Therefore, we considered that two meters below this average represents an important decrease in tree productivity showing that plantations are affected by the growth check period. This analysis was not conducted for black spruce, as the available height growth model for black spruce plantations only starts at age 10-y and most of our sampled plantations were younger than that.

Furthermore, we used the unpaired, two-tailed, two sample student t-tests to determine differences in observed tree height between species per plantation age (analysis ii). If, for a same plantation age, white spruce trees are smaller compared to black spruce trees, it would suggest that white spruce trees are experiencing the stagnant growth problem since white spruce's growth rate is usually higher than that of black spruce (Prégent, Bertrand, and Charrette, 1996; Prégent et al., 2010; Poulin, 2013). Finally, we analyzed the intra-sampling plot variation in tree height by calculating the difference in tree height between the smallest and tallest tree and the average tree height per sampling plot and plantation age (analysis iii). These analyzes allowed to determine how, on average, the growing stock planted (smallest and average tree height per sampling plot) performed compared to the tallest tree.

4.5.3.2 Environmental variables best predicting tree height and frost damage to foliage

To test hypothesis 2, we defined 31 linear (tree height) and binomial (frost damage to foliage) mixed regression models, using the `lme4` R library (Bates et al., 2015, R Development Core Team, 2019), to determine the set of environmental variables that best predict tree height and frost damage at the landscape and microsite level (hypothesis 2, analysis iiii). Regression models 1 to 16 included a null model and combinations of the environmental variables. Models 17 to 31 included two-way interaction terms between the predictor variables (Annexe D: Table D1). These interactions tested the varying effect frost events could have on the primary growth of trees per species (black spruce is less exposed to frost events than white spruce), at various elevations (cold air accumulates at low elevation), per slope shape (cold air accumulates more in concave *vs.* convex slopes) and following the height above ground of the planting microsite (cold air accumulates in microtopographic depressions). We also included interactions with plantation age, as trees from 13-y-old plantations likely have their apical meristem above the zone of ground frost (0–2 m; Langvall and Löfvenius, 2002), which likely decreases the limiting effect of growing-season frosts on height growth compared to trees from 6-y-old plantations. Since we only found damaged foliage on 22 black spruce trees, we restricted our analysis on frost damage to foliage to white spruce only. We included the sampling plot ID and plantation ID in the random structure of the mixed effect models to account for variations within sampling plot, within plantation and between plantations (Zuur et al., 2009). Models were evaluated according to the corrected Akaike's information criterion (AICc) using the `AICcmodAVG` library in R (Burnham, Anderson and Huyvaert, 2011; Mazerolle, 2019; R Development Core Team, 2019). If model selection produced few probable models, we used multimodel inference to average the coefficients from the different probable models using the `MuMIn` library (Barton, 2019; Grueber, et al., 2011). We chose AICc model selection over stepwise regression model because we preferred the Information-Theoretic paradigm and the concept of minimizing data loss compared to the frequentist statistics paradigm when identifying the best set of predictor variables (Mazerolle, 2006). Stepwise variable selection can also lead to bias parameter estimation, unreliable best model identification and has the tendency to include false positive variables (type 1 error) (Mazerolle, 2006; Whittingham et al., 2006). We used the corrected Akaike's information criteria (AICc) because it is a correction applied to AIC when the samples are small (Burnham and Anderson, 2002; Brewer, Butler and Cooksley, 2016). Even if we measured close to 3000 tree heights, when broken down per plantation age, plantations, elevation and categories such as slope shape and the local variation in height above ground of the planting microsite, the number of trees per category is low (Table 4.1).

4.6 Results

4.6.1 Comparison between observed tree heights and height growth curve and between species.

We found no significant difference in dominant tree height when we compared the tallest tree per plot per plantation age to the average dominant tree height predicted by the governmental height growth model (Figure 4.2 and Annexe D: Table D2) (aim 1, analysis i). However, 39% of plantation surveyed still showed stagnant growth of their main stems (Table 4.2) and on average, 70% of the planted trees were smaller than the dominant tree height following the growth trajectory leading to 8 m 25 years after planting, which represents plantation failure (Table 4.2 and Figure 4.2). White spruce was, on average, statistically smaller than black spruce at ages 6, 7, 8, 9 and 13 (Figure 4.3, Annexe D: Table D3) and for all other ages, white spruce and black spruce reached similar heights (aim 1, analysis ii). Moreover, we found large intra-plot and intra-plantation variations in tree height. These variations increased with plantation age. For example, the average intra-plot variation in tree height for white spruce increased from 16 cm for 6-y-old plantations to 178 cm for 13-y-old plantation; which indicates the importance of microsite conditions in driving seedling growth (aims 1 and 2, analysis iii)

Table 4.1 Summary statistics (mean tree height, standard deviation and number of trees shown in parentheses), per species and planting microsite condition.

Plantation age	**Average tree height in cm (number of trees)**					
	White spruce			**Black spruce**		
	hole	**level**	**mound**	**hole**	**level**	**mound**
6	114 ± 7 (5)	120 ± 13 (28)	119 ± 14 (11)	144 ± 25 (17)	151 ± 27 (92)	145 ± 19 (13)
7	141 ± 25 (40)	154 ± 35 (186)	157 ± 32 (38)	170 ± 49 (23)	185 ± 49 (135)	193 ± 51 (31)
8	144 ± 30 (37)	167 ± 46 (337)	159 ± 40 (35)	168 ± 35 (23)	174 ± 45 (135)	185 ± 53 (29)
9	175 ± 52 (24)	186 ± 57 (170)	179 ± 50 (37)	184 ± 52 (12)	218 ± 49 (96)	235 ± 58 (28)
10	188 ± 58 (44)	222 ± 78 (194)	239 ± 78 (20)	214 ± 70 (20)	236 ± 78 (94)	226 ± 69 (15)
11	121 ± 24 (8)	211 ± 76 (55)	213 ± 108 (6)	204 ± 36 (5)	225 ± 68 (48)	223 ± 57 (12)
12	218 ± 111 (14)	217 ± 82 (93)	215 ± 88 (8)	136 ± 25 (10)	220 ± 76 (60)	146 ± 23 (5)
13	267 ± 114 (60)	296 ± 124 (313)	327 ± 123 (38)	337 ± 102 (41)	312 ± 113 (167)	352 ± 114 (31)

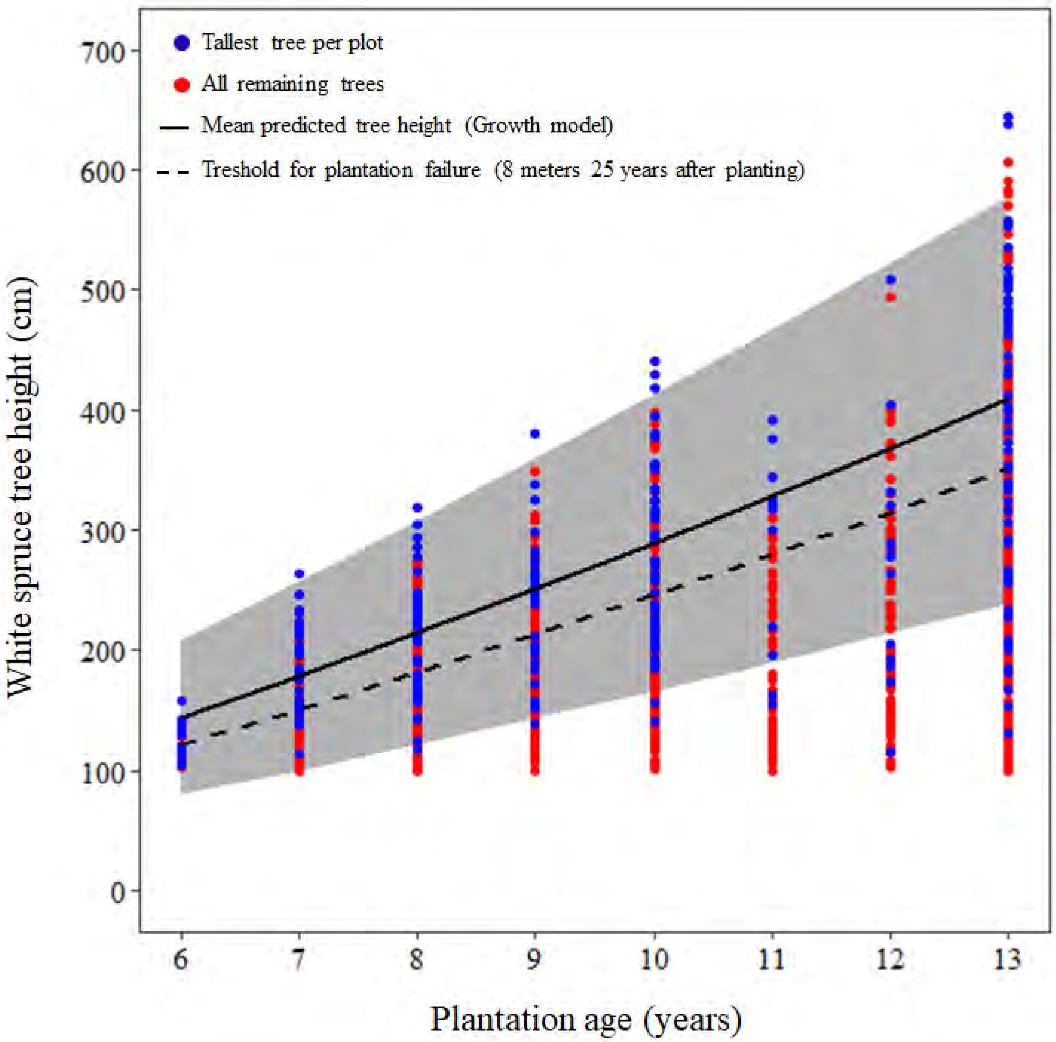

Figure 4.2 Comparison between observed tree heights and their corresponding expected tree height by the governmental growth model (mean [solid line], shaded area [SE], and a growth trajectory predicting a dominant tree height of 8 m 25 years after planting used as a threshold for plantation failure [dashed line]).

Table 4.2 Extent of the height growth stagnation problem of white spruce plantations established in the boreal mixedwood forest of northeastern Canada (Québec).

Plantation age	**Tree height threshold for plantation failure (cm)[1]**	**Tree level[2]**		**Plot level[3]**		**Plantation level[4]**	
		%	**proportion**	**%**	**proportion**	**%**	**proportion**
6	< 121	61	27/44	44	7/16	25	1/4
7	< 150	52	138/264	13	5/38	0	0/5
8	< 181	70	281/409	41	21/51	40	4/10
9	< 213	74	172/231	44	14/32	33	2/6
10	< 246	68	175/258	43	18/42	43	3/7
11	< 280	78	55/69	36	4/11	50	1/2
12	< 315	86	99/115	72	13/18	75	3/4
13	< 351	67	276/411	42	25/60	42	5/12

[1] Threshold representing the dominant tree height trajectory for trees expected to reach 8 meters tall 25 years after planting based on the governmental growth model.

[2] The percentage and the proportion of trees measured that grew less than expected by the height threshold.

[3] The percentage and the proportion of the tallest tree per plot that grew less than expected by the height threshold.

[4] The percentage and the proportion of plantation sampled that show the problem of stagnant height growth (> 75 % of plots with their tallest trees smaller than the tree height threshold).

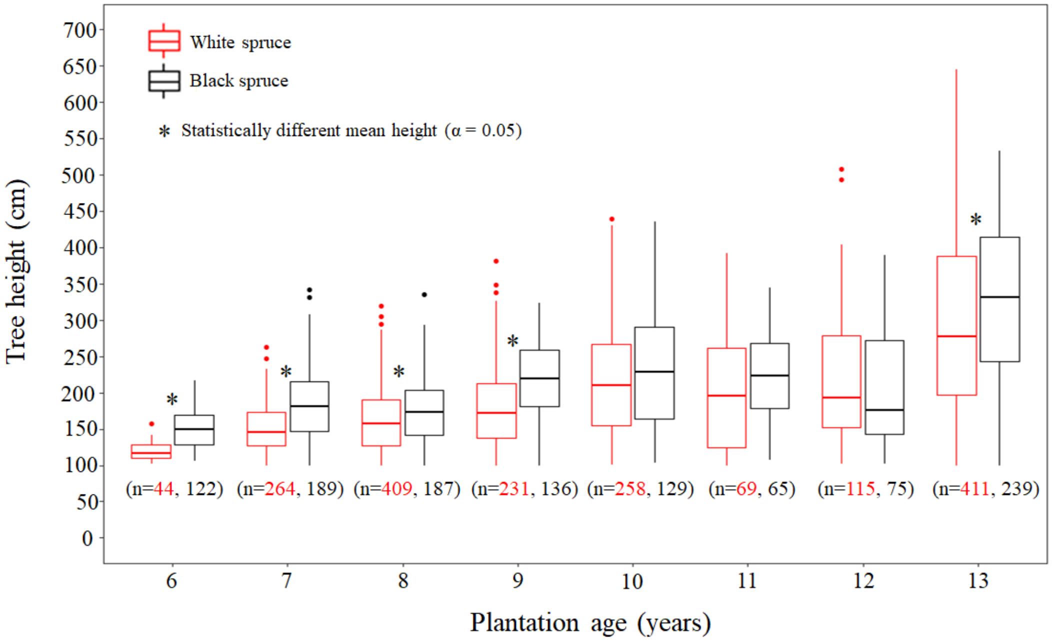

Figure 4.3 Box-plot comparison between white spruce and black spruce tree heights growing in plantations established in the boreal mixedwood forest of Quebec (Canada). The number of trees measured per species and plantation age is shown in brackets. The thick line in the middle of each box represents the median height of trees for that age, the lower and upper end of the box represents the 25th and 75th percentiles, respectively. Horizontal lines at both ends of the boxes show data inside 1.5 × interquartile range (IQR), the distance between the 1st and 3rd quartiles. Data points beyond the whiskers are outliers.

4.6.2 Effect of permanent physical attributes of the landscape and of the microsite on tree height and on frost damage to foliage.

Model selection based on the corrected Akaike information criterion produced one probable (AICc weight > 0.05) model (model 23, Table 4.3 and Annexe D: Table D4) for predicting tree height and six probable models (21, 23, 28, 18, 8, 5) for predicting frost damage to foliage (Table 4.4 and Annexe D: Table D5). These models respectively explained 69% and 86% of the variance in tree height and frost damage, of which 28% and 22% were explained by the fixed effects.

For both species, elevation and microsite condition (height above ground) had important effects on tree height (Table 4.5 and Figure 4.4). Trees were taller when planted at higher elevations compared to when planted in low elevations. Trees were also taller when planted on mounds than when planted in holes (Table 4.5 and Figure 4.4). The effect of microtopography (height above ground) on tree height also varied with elevation (height above ground × elevation interaction; Table 4.5). Trees planted on mounds at low elevations were on average 57 cm taller compared to trees planted in holes, however, at high elevations, tree height was only increased by 23 cm when planted on mounds compared to planted in holes (Figure 4.4). We also found differences in tree height between species and this difference increased for trees planted in holes and at high elevations (Figure 4.4). Specifically, at low elevation, both white spruce and black spruce planted in holes reached similar heights whereas, at high elevation, black spruce was 66 cm taller than white spruce. Moreover, the impact of elevation was more important in young plantations compared to older plantations (Figure 4.4). However, the impact of the microsite conditions increased in importance in older plantations (Figure 4.4).

Table 4.3. Best model predicting tree height from permanent physical attributes of the landscape.

Model	**AICc**	**Delta AICc**	**AICc Wt.**	**Cum. Wt.**	**Marginal pseudo-R^2 (conditional)**
(23) Elev; Height_AG; Species; Pl_Age; Elev×Height_AG; Elev×Species; Elev×Pl_Age; Height_AG×Species; Height_AG×Pl_Age; Species×Pl_Age	32175.08	0.00	0.95	0.95	0.28 (0.69)

Abbreviations: Elevation (Elev), height above ground (Height_AG), plantation age (Pl_Age). Only models with AICc weights > 0.05 are shown (complete analysis is shown in Annexe D: Table D4). The number in parenthesis before the model refers to the candidate model prior to selection (Annexe D: Table D1).

Table 4.4 Best models predicting probability of frost damage to foliage from permanent physical attributes of the landscape.

Model	**AICc**	**Delta AICc**	**AICc Wt.**	**Cum. Wt.**	**Marginal pseudo-R^2 (conditional)**
(21) Elev; Slope shape; Pl_Age; Elev×Slope shape; Elev×Pl_Age; Slope shape×Pl_Age	1434.28	0.00	0.23	0.23	0.22 (0.86)
(23) Elev; Height_AG; Pl_Age; Elev:Height_AG; Elev×Pl_Age; Height_AG×Pl_Age	1434.32	0.04	0.23	0.46	0.07 (0.84)
(28) Elev; Slope shape; Height_AG; Pl_Age; Elev:Slope shape; Elev×Height_AG; Elev×Pl_Age; Slope shape×Height_AG; Slope shape×Pl_Age; Height_AG×Pl_Age	1435.23	0.95	0.15	0.61	0.22 (0.86)
(18) Slope shape; Pl_Age; Slope shape×Pl_Age	1436.42	2.14	0.08	0.69	0.10 (0.84)
(8) Elev; Height_AG; Pl_Age	1437.08	2.80	0.06	0.74	0.06 (0.83)
(5) Height_AG; Pl_Age	1437.16	2.88	0.06	0.80	0.02 (0.83)

Abbreviations: Elevation (Elev), height above ground (Height_AG), plantation age (Pl_Age). Only models with AICc weights > 0.05 are shown (complete analysis is shown in Annexe D: Table D5). The number in parenthesis before each model refer to the candidate model prior to selection (Annexe D: Table D1).

Table 4.5 Results showing coefficients of the best model predicting tree height from permanent physical attributes of the landscape.

Variable	**Standardized coefficients (SE)**
Intercept: (Species [White spruce]; Height_AG [Mound])	**206.96 (7.59)**
Elev	-4.68 (7.39)
Height_AG [Hole]	**-46.68 (5.57)**
Height_AG [Level]	**-14.60 (4.48)**
Species [Black spruce]	**22.49 (7.16)**
Pl_Age	**52.78 (7.18)**
Elev × Species [Black spruce]	**14.80 (4.40)**
Elev × Height_AG [Hole]	**7.80 (4.48)**
Elev × Height_AG [Level]	-0.18 (3.80)
Species [Black spruce] × Height_AG [Hole]	**11.60 (8.27)**
Species [Black spruce] × Height_AG [Level]	0.79 (6.43)
Pl_Age × Elev	**-12.94 (6.83)**
Pl_Age × Height_AG [Hole]	**-14.04 (4.31)**
Pl_Age × Height_AG [Level]	**-5.63 (3.47)**
Pl_Age × Species [Black spruce]	2.39 (4.83)

Abbreviations: Elevation (Elev), height above ground (Height_AG), plantation age (Pl_Age). Boldface type indicates coefficients that differ from zero and brackets show the level of the categorical variable.

Table 4.6 Results showing coefficients (from the conditional averaging method) of the best models predicting probability of frost damage to foliage from permanent physical attributes of the landscape.

Variable	**Standardized coefficients (SE)**
Intercept: Slope shape [Concave]; Height_AG [Mound]	**1.83 (1.35)**
Elev	0.95 (1.18)
Slope shape [Convexe]	**-5.65 (5.31)**
Slope shape [Irregular]	**1.93 (1.91)**
Slope shape [Regular]	-0.62 (1.59)
Pl_Age	-1.37 (2.18)
Elev × Slope shape [Convexe]	-2.30 (2.93)
Elev × Slope shape [Irregular]	**2.84 (1.90)**
Elev × Slope shape [Regular]	-0.87 (1.37)
Pl_Age × Elev	**0.75 (0.70)**
Pl_Age × Slope shape [Convexe]	**8.65 (5.43)**
Pl_Age × Slope shape [Irregular]	**7.46 (2.63)**
Pl_Age × Slope shape [Regular]	**3.83 (1.43)**
Height_AG [Hole]	-0.37 (1.62)
Height_AG [Level]	-0.95 (1.28)
Elev × Height_AG [Hole]	**-1.18 (0.49)**
Elev × Height_AG [Level]	-0.20 (0.40)
Pl_Age × Height_AG [Hole]	-0.41 (0.43)
Pl_Age × Height_AG [Level]	0.03 (0.36)
Slope shape [Convexe] × Height_AG [Hole]	4.91 (6.44)
Slope shape [Irregular] × Height_AG [Hole]	**2.94 (2.27)**
Slope shape [Regular] × Height_AG [Hole]	**2.19 (2.16)**
Slope shape [Convexe] × Height_AG [Level]	2.04 (2.94)
Slope shape [Irregular] × Height_AG [Level]	1.31 (1.99)
Slope shape [Regular] × Height_AG [Level]	1.71 (1.90)

Abbreviations: Elevation (Elev), height above ground (Height_AG), plantation age (Pl_Age). Boldface type indicates coefficients that differ from zero and brackets show the level of the categorical variable.

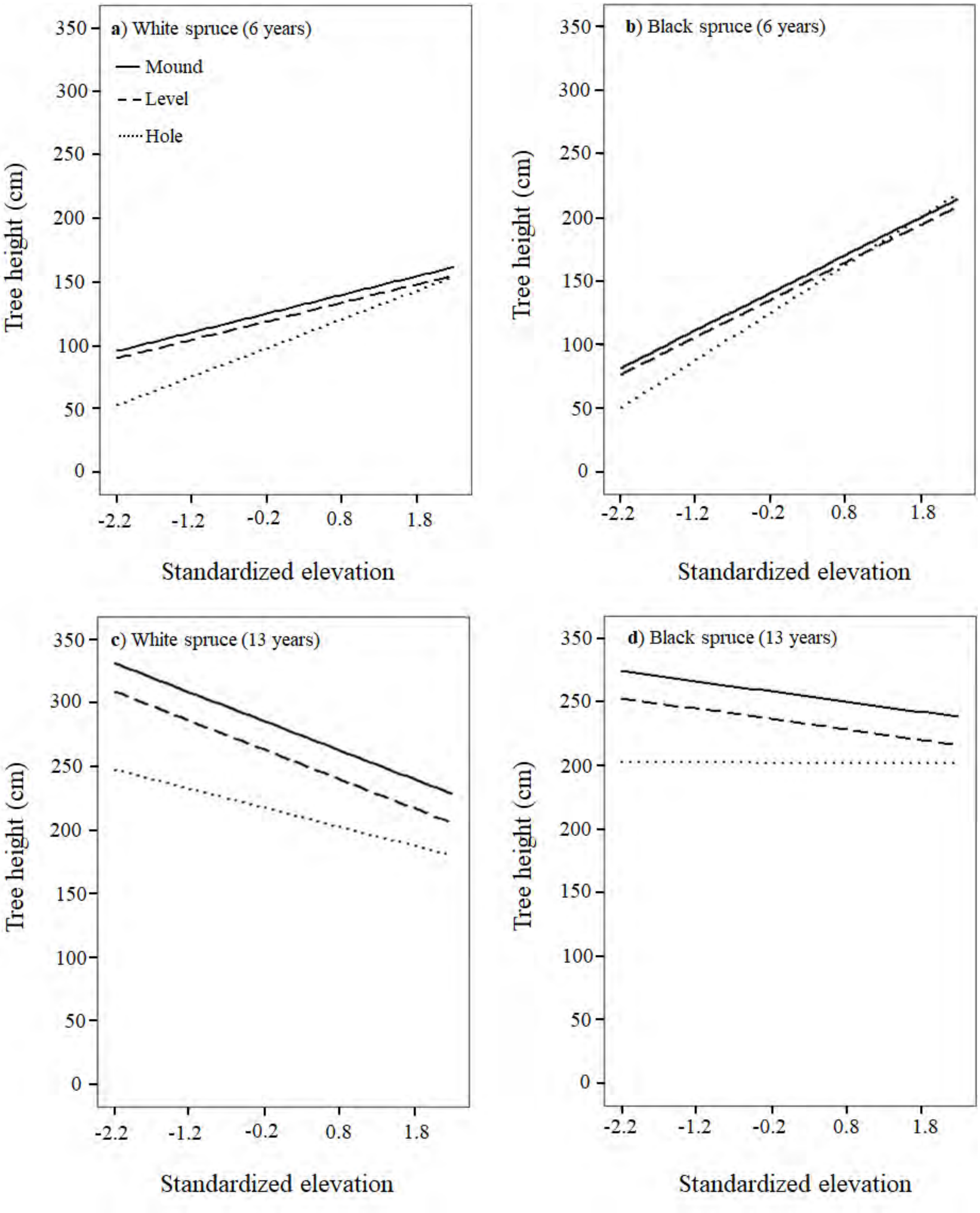

Figure 4.4 Mean effect of height above ground along the elevation gradient on tree height produced by the `predict` function for the best mixed linear regression model we identified for (a) 6-y-old white spruce plantations; (b) 6-y-old black spruce plantations; (c) 13-y-old white spruce plantation and (d) 13-y-old black spruce plantations in the boreal mixedwood forest of Quebec (Canada).

Black spruce foliage was almost not damaged by growing-season frosts (only 22 damaged trees out of 1,142 trees) whereas white spruce was frequently damaged (1,100 damaged trees out of 1,801 trees). As expected, the probability of frost damage to white spruce foliage increased for trees planted in holes compared to mounds (Table 4.6 and Figure 4.5). However, and unexpectedly, the probability of frost damage to foliage increased with elevation for trees planted on mounds but decreased for trees planted in holes (Figure 4.5). We observed a stronger difference in probability of frost damage with plantation age for trees planted in holes compared to planted on mounds or at level (Table 4.6 and Figure 4.5). Moreover, trees from 6-y-old plantations planted in concave slopes were subject to more freezing damage to foliage than when planted on other slope shapes (Figure 4.5). In contrast with our hypothesis, trees in 13-y-old plantations in convex slopes were more subject to freezing damage than when planted in concave slopes (Figure 4.6) (aim 2, analysis iiii).

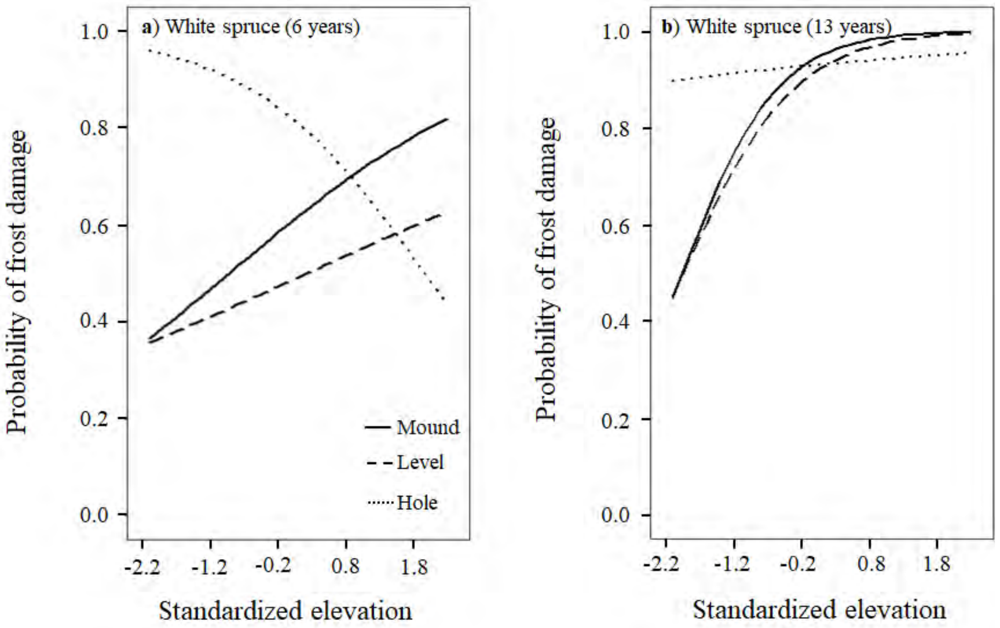

Figure 4.5 Mean probability of frost damage to foliage per height above ground categories along the elevation gradient produced by the `predict` function for the best generalized mixed binomial regression model we identified for (a) young white spruce plantations (6 years), and (b) older white spruce plantations (13 years) in the boreal mixedwood forest of Quebec (Canada).

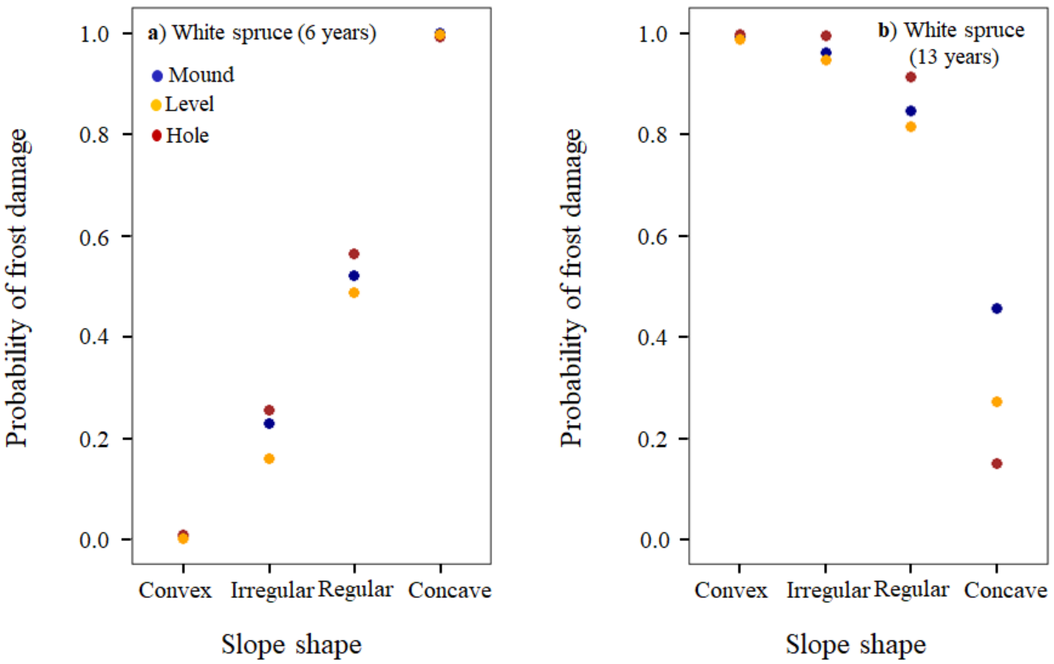

Figure 4.6 Mean probability of frost damage to foliage per slope shape categories produced by the `predict` function for the best generalized mixed binomial regression model we identified for (a) young white spruce plantations (6 years), and (b) older white spruce plantations (13 years) in the boreal mixedwood forest of Quebec (Canada). Each specific prediction for one variable is obtained by fixing to constant all other variables.

4.7 Discussion

4.7.1 Growth stagnation problem to spruce plantation in the boreal forest

The problem of stagnant growth for spruce plantations established in boreal mixedwood forests has important consequence on sustainable forest management since stagnant plantations can change the ecological characteristics of an environment by turning a productive forest to a paludified unproductive forest (Fenton et al., 2005; Simard et al., 2007). Moreover, productive plantations might help to reduce the harvesting pressure on natural forest, thus may help conserving biodiversity and the ecological integrity of natural forest ecosystems (Messier et al., 2009). Therefore, understanding the environmental drivers causing the growth stagnation problem of spruce plantations established in the boreal mixedwood forest is of primary concern to forest managers. Our first aim was to determine the extent to which spruce plantations were impacted by growth check. On average, the tallest tree per plot reached the mean expected dominant height predicted from the governmental growth model used in annual allowable cut calculations in Quebec (Prégent et al., 2010). However, the fact that 39% of plantations surveyed were classified as stagnant shows that plantations are affected by the check period and increasing our ability at evaluating the landscape conditions as well as the microsite conditions will likely help decreasing plantation failure. Even if the planting stock is not all expected to reach the dominant tree height predicted by the growth model, the fact that 70% of the planting stock is expected to grow < 8 m combined with the fact that the median tree height ≤ 2 m for plantations 6–12-y-old and that white spruce did not grow more than black spruce show a clear decrease in productivity of the plantations, even if some main stems are growing productively. Therefore, greater care should be put at selecting proper microsite when planting trees.

4.7.2 Effect of permanent physical attributes of the landscape and of the microsite on tree height and on frost damage to foliage.

Our second hypothesis was that tree height would be reduced and frost damage would increase at low elevation, in concave slopes and in holes compared to high elevation, convex slopes and on mounds. Our results supported this hypothesis, mostly for plantations in their early years since planting, as apical buds were likely within the zone of ground frost. In older plantations (13-y-old) with taller trees, apical buds were likely above the zone of ground frost, thus decreasing the importance of permanent landscape physical attributes as drivers of tree growth. However, trees affected by the check problem in their early years were still affected even seven years later. Consistent with results reported by Langvall and Örlander (2001), we showed that microsite conditions were important variables in predicting tree height. Therefore, selecting the appropriate planting sites (at both the landscape and microsite scales) can reduce the period of growth stagnation in boreal mixedwood regions.

Since frost damage to foliage was almost only observed on white spruce, we suggest that growing-season frosts cause the prolonged check period experienced by white spruce compared to black spruce. A large transplant experiment conducted in northern Ontario (Canada), using multiple white spruce seed sources, also showed that the growth of white spruce was importantly affected by growing-season frosts and that early emerging seed sources were more affected by frost compared to later emerging seed sources (Man et al., 2009; Lu and Man, 2011). Therefore, the late budbreak of black spruce might prevent damage from growing-season frost compared to the earlier budbreak of white spruce (Marquis et al., 2020). Our hypothesis regarding the importance of growing-season frosts on tree growth is also supported by the fact that both elevation and microsite conditions impacted the presence of frost damaged. As expected, low elevations and holes were the conditions most increasing the probability of frost damage, which also were the conditions most reducing tree height. These landscape features were also those where the check period was observed to be the most important (Mullin, 1963; Vyse, 1981).

However, for 13-y-old plantations, the probability of frost damage increased with elevation and increased in other slope shape types than concave slopes. This unexpected result was probably caused by increased exposure to wind on convex slopes and elevated positions (Brüchert, and Gardiner, 2006). We recorded frost events as a binary variable based on presence or absence of symptoms and did not note the position of the frost damages on the trees. Then, we can only speculate that frost damages to trees in older plantations were restricted to the lower parts of the tree only, not affecting the terminal bud, thus, allowing trees to grow tall even if trees were recorded as damaged. Still, frost damages to lower branches can cause architectural problems (Dy and Payette, 2007); plantation silviculture should thus aim at limiting these as well.

Elevation was a prominent variable surpassing slope shape and slope angle as a predictor of tree height. The precise elevation measure we used outperformed the variables previously used to analyze the impact of the general landform such as slope shape on tree height and frost damage (Chung et al., 2006; Lindkvist and Lindqvist, 1997; Laughlin and Kalma, 1987; Oke, 1987). Therefore, the use of airborne LiDAR to derive precise digital elevation models will enable selecting microsite conditions that favor tree growth and limit frost damages (Côté, Fournier, Luther, and van Lier, 2018; Rowlandon et al., 2018; Wang et al., 2019).

Our results will support the development of adaptive silviculture to climate change (Nagel et al, 2017). Three measures could be done to increase plantation productivity in east-Canadian boreal mixedwood forests. First, site preparation methods creating elevated planting microsite such as mound planting should be performed (Hjelm, Nilsson and Örlander, 2012; Löf et al., 2012; Sutton, 1993; Tolvanen and Kubin, 1990; Thiffault and Hébert, 2017). Second, mixed-species plantations where black spruce would be planted in frost-prone sites like at low elevations and in topographic depression whereas white spruce would be planted at higher elevations and on mounds could replace monoculture plantations. Third, planting trees from different genotypes previously selected from tree populations naturally growing within close range of the planting sites would ensure adaptation to the current growing-season frost frequency and intensity.

Even if the three measures we suggest to improve plantation productivity would imply allocating more time in the field for the mechanical site preparation and to select the proper planting microsites consequently increasing the cost for establishing spruce plantations, we have no doubt that it will prove economically and ecologically profitable. Effectively, establishing productive spruce plantations at a higher cost seem a better idea than establishing unproductive spruce plantations providing poor-quality wood not meeting industrial standards, but at a lower cost. These mixed-species plantations would also be beneficial to sustainable forest management as well, since productive plantations might help to reduce the harvesting pressure on natural forest (Messier et al., 2009).

Our study is based upon local field data, still, our results likely apply to the whole boreal mixedwood environment since the growth check problem is common throughout this biome. Therefore, when considering the establishment of a plantation in the boreal mixedwood forest, frost events should be of a primary concern to limit plantation failures. Still, growth check and frost damage to trees is more likely to occur at low elevations and in topographic depressions. These latter conditions are also accumulating water at the soil’s surface, which also contributes to growth check since white spruce grows better in moderately drained sites (Wolken et al., 2011). Deficiency in soil nutrient was also reported by to reduce spruce growth (MacAlister and Timmer, 1998). Since the boreal mixedwood forest encompasses many different soil types and topographic characteristics, white spruce plantations established in well drained loam soils will likely be more productive compared to spruce plantations established on wet clay soils (Otis Prud'homme et al., 2018; Mullin, 1963; Vyse, 1981). Therefore, growth check is an important problem to asses but is not affecting all plantations established in the boreal mixedwoods. Growth stagnation is more likely to occur under specific conditions we were able to identify. Therefore, improving site selection and field preparation methods to meet spruce’s physiological requirement will increase spruce plantation productivity throughout the boreal mixedwood forest.

4.8 Acknowledgements

We thank the Natural Science and Engineering Research Council of Canada as well as the Canadian Wood Fibre Centre of Natural Resources Canada for funding. We are grateful to R. Mincheva and to S. Robert for their assistance in the field work.

4.9 Conclusion

Dans ce chapitre, l’approche empirique a été utilisée pour montrer l’importance de la stagnation de la croissance des plantations d’épinettes établies en forêt boréale mixtes de l’ouest du Québec. L’impressionnante quantité d’information récoltée sur la hauteur des arbres, sur les dommages aux nouvelles pousses et sur les caractéristiques physiques du milieu montrent que l’épinette blanche était à la fois plus affectée par le retard de croissance et plus endommagée par le gel que ne l’était l’épinette noire. Le risque de gel était aussi supérieur dans les pentes concaves ainsi que pour les microsites de plantation situés dans les dépressions microtopographiques. Ces résultats permettent d’identifier le gel printanier comme cause principale du retard de croissance et confirment les spéculations émises par les études, de moindre envergure, traitant du phénomène de la stagnation de la croissance des plantations d’épinettes (Vyse 1981, Mullin, 1963, Clements, Fraser et Yeatman, 1972). Il est maintenant possible d’améliorer le succès des plantations en forêt boréale mixte en favorisant l’établissement des plantations sur : 1) des sites qui occupent des positions élevées dans le paysage régional et 2) planter les épinettes sur des microsites surélevés par rapport au niveau du sol. De plus, la productivité des plantations serait maximisée en développant des plantations mixtes où l’épinette blanche serait plantée dans les zones les moins susceptibles aux gelées printanières (zones surélevées comme le haut des pentes) alors que l’épinette noire pourrait être plantée dans les zones les plus sujettes aux gelées printanières comme le bas des pentes et dans les dépressions microtopographiques. Ces résultats revêtent une importance locale puisqu’ils sont d’intérêt pour les acteurs du milieu forestier œuvrant dans les groupements forestiers, les agences régionales de la mise en valeur des forêts privées et dans les instances gouvernementales telles que le Bureau du forestier en chef, qui doit prévoir la possibilité forestière. Ces résultats ont aussi une portée internationale puisque la stagnation de la croissance des plantations d’épinettes s’observe aussi dans plusieurs régions du monde (Langvall, Nilsson et Örlander, 2001; Langvall et Örlander, 2001;

Langvall et Ottosson-Löfvenius, 2002; Man et al., 2009; Mullin, 1963; Vyse, 1981). Les recommandations émises dans ce chapitre sont donc applicables partout où le retard de croissance des plantations est observé. Même si les espèces diffèrent d'une région à l'autre, il faudrait planter les espèces, qui ouvrent leurs bourgeons plus hâtivement, dans les zones les moins à risque de gelées au printemps, et planter les espèces présentant une ouverture tardive de leurs bourgeons dans les endroits les plus à risque de gelées au printemps.

CONCLUSION

Depuis 2010, la loi provinciale A-18.1 sur l'aménagement durable du territoire forestier vise à effectuer un aménagement du territoire qui contribue non seulement à la productivité des forêts mais aussi à :

> La conservation de la diversité biologique; […] à la conservation des sols et de l'eau; au maintien de l'apport des écosystèmes forestiers aux grands cycles écologiques; au maintien des avantages socioéconomiques multiples que les forêts procurent à la société; à la prise en compte, dans les choix de développement, des valeurs et des besoins exprimés par les populations concernées (Gouvernement du Québec, article 2 de la loi provinciale A-18.1, 2010).

Dans cette optique, l'aménagement du territoire doit maintenant suivre les fondements et les pratiques de l'aménagement écosystémique (Gauthier *et al.*, 2008). Cette pratique vise à réduire les écarts entre la forêt naturelle et la forêt aménagée, en adaptant les pratiques sylvicoles pour reproduire, quoiqu'imparfaitement, les effets des perturbations naturelles sur la structure et la composition de la forêt (Bergeron, Drapeau, Gauthier et Lecomte, 2007; Gauthier *et al.*, 2008). Toutefois, cette pratique d'aménagement du territoire forestier entre régulièrement en conflit avec l'enjeu économique et l'ancien paradigme de gestion de la ressource ligneuse suivant un rendement soutenu (Groupe de travail sur la définition du rendement durable, 2015; Messier et Kneeshaw, 1999). Augmenter la productivité des forêts en instaurant des zones d'aménagement intensif permettrait, d'une part, de solidifier le volet économique relié au secteur forestier, et d'autre part, de réduire la coupe forestière en forêt naturelle, ce qui apparait impératif pour préserver la résilience des écosystèmes forestiers

(Bergeron *et al.*, 1999; Bergeron *et al.*, 2007; Bergeron *et al.*, 2017; Franklin, 1993; Messier et Kneeshaw, 1999).

Toutefois, l'augmentation de la productivité des plantations basée sur l'intensification des pratiques sylvicoles à l'échelle du peuplement est loin d'être garantie. Il incombe d'abord de comprendre les déterminants environnementaux contrôlant le cycle physiologique de dormance-croissance des arbres au niveau de l'espèce et au niveau des provenances pour ensuite déterminer les pratiques sylvicoles qui favorisent leur croissance. Les expériences de transplantations sont spécifiquement conçues pour déterminer ces différences physiologiques entre les espèces et entre les provenances. Cette approche a donc été utilisée lors des trois premiers chapitres pour identifier les causes environnementales du retard de croissance des épinettes plantées dans la ceinture d'argile de l'ouest du Québec. L'approche utilisée dans le quatrième chapitre a, quant à elle, permis d'identifier l'importance de la stagnation de la croissance des plantations d'épinettes à l'échelle régionale de l'Abitibi-Ouest, située dans la forêt boréale mixte de l'ouest du Québec.

Pour atteindre ces objectifs, l'approche empirique effectuée au niveau de l'arbre a permis d'identifier les déterminants environnementaux contrôlant les différentes étapes de la séquence de débourrement des bourgeons (chapitre I) ainsi que la croissance en hauteur (chapitre II). Les résultats obtenus soutiennent l'hypothèse que la stagnation de la croissance, qui est plus forte pour l'épinette blanche comparativement à l'épinette noire, serait induite par un débourrement plus hâtif de ses bourgeons, ce qui accroîtrait son exposition aux évènements de gel printanier et endommagerait ses méristèmes apicaux et latéraux, respectivement responsable de la croissance en hauteur et en diamètre. Le troisième chapitre met en évidence l'importance des attributs du milieu physique du paysage et du microsite de plantation sur la hauteur des arbres et la probabilité de gel durant la saison de croissance. Finalement, le dernier chapitre de cette thèse permet de mieux comprendre l'importance des attributs physiques du paysage régional (l'élévation et la pente) et du microsite de plantation (butte *vs.*

dépression microtopographique) sur le succès ou l'échec de la régénération artificielle des plantations d'épinettes établies sur la ceinture d'argile en forêt boréale mixte. Ces résultats, mis ensemble, suggèrent que pour améliorer la productivité forestière des plantations, il est préférable d'améliorer le choix des sites et des microsites de plantation avant d'utiliser des espèces ou des provenances étrangères, et ce, particulièrement dans la forêt boréale mixte de la ceinture d'argile de l'ouest du Québec. Effectivement, le sol argileux de cette zone ne permet pas un bon drainage de l'eau, qui en s'accumulant près de la surface peut ralentir le réchauffement du sol au printemps et générer de fréquents phénomènes d'inversion de la température de l'air qui causent des évènements de gel au sol durant la saison de croissance (Dugas, 1975).

5.1 Effet du gel printanier sur la séquence de débourrement des bourgeons des épinettes à l'écotone de la forêt tempérée et boréale

Les espèces d'arbres de la forêt tempérée et boréale ont développé une période de dormance pendant laquelle leurs fonctions physiologiques deviennent limitées et des adaptations physiologiques telles que l'envoi de l'eau préalablement contenue dans les cellules vers l'espace extracellulaire permettent de survivre aux températures en dessous du point de congélation durant l'hiver (Körner, 2016). Cette adaptation permet à l'eau de geler autour de la cellule conséquemment, les cristaux de glaces n'endommagent pas les organelles ni la paroi cellulaire (Körner, 2016). La synchronicité entre la période de dormance et la période de croissance est donc sous forte pression évolutive puisqu'une mauvaise synchronicité entre ses deux évènements entraîne des dommages aux arbres. Lorsque les dommages sont récurrents, ils diminuent fortement la valeur adaptative de l'arbre et peuvent même entraîner la mort (Hänninen, 2016).

Au niveau inter-espèces, nos résultats montrent que la sortie hâtive de l'épinette blanche semblait être causée par une sensibilité accrue à la photopériode et à la probabilité de gel, comparativement à l’épinette noire et à l’épinette de Norvège, qui, elles, répondaient plus aux degrés-jours de croissance. Cette sortie hâtive de la période de dormance augmente l’exposition au gel printanier, ce qui semble pouvoir expliquer pourquoi l’épinette blanche montre une plus forte stagnation de la croissance que l’épinette noire, et ce, particulièrement au site où la probabilité de gel printanier était la plus forte.

Au niveau intra-espèces, les provenances d’épinettes blanches du sud, lorsque plantées au nord ont débourré avant la provenance locale de la forêt boréale mixte. Ce devancement de la phénologie des bourgeons semble être induit par une sensibilité accrue à la photopériode. De plus, au site de la forêt boréale mixte, la probabilité d’occurrence de gel était une variable plus importante pour déterminer le déclenchement de la séquence de débourrement des bourgeons que ne l’était la photopériode, donc, la température de l’air a un effet plus important dans les environnements plus froids. Les espèces locales (l’épinette blanche et l’épinette noire) et les provenances locales de la forêt boréale mixte semblent donc mieux adaptées à la forte pression causée par le gel printanier que ne le sont les espèces non locale (l’épinette de Norvège) ou les provenances du sud qui n’ont pas évolué sous ce contexte climatique particulier. Il est donc possible de spéculer qu’au sud, l’augmentation de la photopériode est synchronisée avec la diminution de l’occurrence de gel et constitue donc un bon signal environnemental pour déterminer la sortie de la période de dormance. En revanche, au nord, la photopériode n’est pas nécessairement synchronisée avec la diminution de la probabilité d’occurrence de gel (Hänninen, 2016) et devient donc un moins bon signal environnemental que l’augmentation de la température de l’air.

Ces différentes réponses physiologiques du débourrement des bourgeons à la photopériode, à la probabilité de gel printanier et à l’augmentation de la température de l’air ont le potentiel d’affecter la croissance des arbres des différentes espèces et des différentes provenances. Effectivement, l’étude effectuée par Antonucci et al., (2015) montrent une forte synchronisation entre la première étape de la séquence de développement des bourgeons et la formation de la première cellule mature par le xylème, donc, lorsque les bourgeons s'ouvrent, la croissance radiale commence. Si les évènements de gel printanier peuvent endommager les bourgeons nouvellement ouverts, les évènements de gel peuvent tout autant endommager les cellules cambiales nouvellement formées. Donc, comprendre les liens entre le méristème apical et le méristème latéral est important pour prévoir la productivité forestière. Toutefois, cette étude était restreinte à deux espèces uniquement, donc il faudrait étendre les connaissances à plusieurs espèces pour être plus en mesure de prévoir la productivité forestière.

5.2 Effet du gel printanier sur la croissance en hauteur des épinettes à l'écotone de la forêt tempérée et boréale

Les résultats présentés au chapitre II ont d'abord montré que plus un arbre subissait des dommages par le gel, plus il était petit. Cette relation était plus forte lorsque l'arbre était petit (< 1 mètre), diminuait en importance à mesure que l'arbre grandissait et n'était plus importante lorsque l'arbre dépassait les deux mètres de hauteur. Ces résultats sont novateurs puisqu'ils mettent en relation une observation directe de dommages aux arbres par le gel, sous forme de cernes de gel, à la performance des arbres (hauteur). En se basant sur des observations et non sur des résultats de modélisation, notre approche permet une meilleure estimation de l'impact du gel printanier sur la croissance en hauteur.

Selon les résultats présentés au chapitre I, les espèces et les provenances qui s'exposaient plus au gel printanier en ouvrant leurs bourgeons plus hâtivement que les autres étaient aussi les plus sévèrement endommagées (sous forme de cernes de gel) par le gel et étaient également de plus petite taille. Conséquemment, l'exposition accrue au gel printanier semble pouvoir expliquer les variations de hauteur inter- et intra-espèces, ce qui vient contrecarrer l’hypothèse que les différences de hauteurs inter- et intra- espèces seraient plutôt induite par une différence de tolérance au gel printanier. L’interprétation de nos résultats concorde aussi avec l’étude de Vitasse et al. (2014), qui a montré que les jeunes arbres, qui poussent à l’ombre dans le sous-bois, ouvraient leurs bourgeons plus hâtivement que les plus vieux arbres pour pouvoir profiter de la lumière. Mais, en contrepartie, ceux-ci s’exposaient plus au gel printanier et risquaient donc d’être plus sévèrement endommagés par le gel que les plus gros arbres.

Au site où la probabilité et l’intensité des gelées printanières étaient plus faibles, les arbres étaient plus grands qu’au site où la probabilité et l’intensité des gelées printanières étaient fortes. L’espèce introduite, l’épinette de Norvège, a été, aux deux sites, l’espèce la plus endommagée par le gel et la plus petite. Toutefois, à la forêt tempérée nordique, l’épinette blanche et l’épinette noire ont eu une croissance similaire, même si l’épinette blanche a ouvert ses bourgeons en moyenne 6 jours plus tôt que l’épinette noire. À la plantation au nord, où la fréquence de gel est élevée, l’épinette blanche avait une croissance plus faible que celle de l’épinette noire. Le débourrement plus hâtif de ses bourgeons par rapport à ceux de l’épinette noire a donc augmenté son exposition au gel printanier, ce qui a retardé sa croissance. Puisqu’en forêt tempérée nordique, la faible augmentation de la longueur de la saison de croissance n’a pas permis d’augmenter suffisamment la croissance en hauteur de l’épinette blanche pour supplanter l’épinette noire et, qu’à la forêt boréale mixte, la croissance de l’épinette blanche était nettement inférieure à celle de l’épinette noire, le compromis entre la durée de la saison de croissance et l’exposition au gel printanier semble pencher en faveur de limiter l’exposition au gel.

Aux deux sites, la forte variabilité en hauteur intra-espèce montre que les caractéristiques du microsite sont importantes à considérer pour établir des plantations productives. Les résultats du chapitre III montrent que les microsites sur terrains plats ou au bas des pentes, ainsi que les dépressions microtopographiques, sont des endroits favorables à l’accumulation d’air froid. Les résultats du chapitre IV indiquent que la hauteur des arbres était diminuée lorsque ceux-ci étaient plantés au bas des pentes et dans des dépressions microtopographiques. Donc, le méristème apical des arbres plantés dans les zones fortement à risque de geler au printemps a pu être endommagé, limitant leur croissance en hauteur. Cependant, la plus faible probabilité et la plus faible intensité de gel printanier à la forêt tempérée nordique font en sorte que les différences reliées à la microtopographie du sol sont plus importantes à considérer qu'à la forêt boréale mixte. Effectivement, la forte intensité de gel à la forêt boréale mixte permet l'accumulation d'air froid au-dessus des variations microtopographiques affectant ainsi une plus grande portion du paysage. L'élévation est donc une variable clé à considérer au moment d'établir une plantation en forêt boréale mixte.

5.3 Incohérence entre la pression évolutive et les modèles écophysiologiques régissant le débourrement des bourgeons au printemps

Le chapitre I qui démontre que la sensibilité aux différentes variables environnementales change au long de la séquence de débourrement des bourgeons fait une contribution théorique importante sur la conception des modèles écophysiologique servant à prédire le débourrement des bourgeons. Puisque ces modèles écophysiologiques sont principalement basés sur les degrés-jours de croissance (Chuine, 2000; Fuchigami et Nee, 1987; Hänninen, 2006; Linkosalo *et al.*, 2006; Morin et al, 2009), ils n'arrivent pas à bien représenter la pression évolutive induite par le gel printanier sur le débourrement des bourgeons. Plusieurs modèles avec différents agencements de variables environnementales (température, photopériode, degrés de refroidissement) performent de façon similaire pour prédire la date à laquelle les bourgeons débourrent, ce qui prévient l'identification des phénomènes environnementaux réellement en cause (Basler, 2016; Linkosalo *et al.*, 2006). De plus, la marge d'erreur des modèles écophysiologiques est d'environ 5-7 jours, ce qui, pour un évènement qui dure entre 15-30 jours, est élevé (Basler, 2016). Dès lors, un modèle peut prédire qu'un bourgeon est dans un stade phénologique avancé alors que la séquence de débourrement n’est en réalité qu’entamée. Plus un modèle écophysiologique est complexe et plus grande est sa marge d’erreur (Basler, 2016). Ce résultat vient appuyer l’idée que la mécanique de ces modèles n’est pas adéquate et pourrait potentiellement être améliorée en ajoutant la pression évolutive induite par le gel printanier sur le cycle de dormance-croissance des arbres (Körner et al., 2016; Lenz et al., 2016).

En décortiquant la séquence de débourrement des bourgeons en plusieurs étapes, ce chapitre identifie de nouveaux mécanismes déterminant la phénologie des bourgeons. Cette décortication de la séquence de débourrement des bourgeons a déjà été effectuée dans les études de Rossi (2015) et de Clark et al., (2014), mais notre étude innove en identifiant les variables environnementales déterminantes à chaque étape de cette séquence. Donc, des études empiriques, comme celle entreprise dans ce chapitre, sont requises pour mieux calibrer et mieux construire les relations entre les différentes variables environnementales importantes à considérer par les modèles écophysiologiques du débourrement des bourgeons.

Pour soutenir les nouvelles idées exposées dans ce chapitre, il serait important, dans de futurs travaux de recherche, de tester de manière expérimentale l’importance du gel printanier sur le déclenchement de la séquence de débourrement des bourgeons au printemps et d’étendre notre étude à plusieurs espèces et provenances évoluant dans différents régimes climatiques.

5.4 Changements climatiques

Il est anticipé par le groupe d’experts sur l’évolution du climat que la température moyenne annuelle augmentera (IPCC, 2018). De plus, la température de l’air se réchauffe inégalement entre les saisons (Brown, 2019) et la fréquence des évènements climatiques extrêmes tend à augmenter (Tebaldi et al., 2006). Suivant l’augmentation moyenne de la température de l’air, le débourrement des bourgeons pourrait être devancé (Parmesan et Yohe, 2003; Piao *et al.*, 2007; Polgar *et al.*, 2013). Cependant, l’augmentation de la variabilité du climat pourrait faire augmenter l’exposition des bourgeons au gel printanier et accroître le problème de stagnation de la croissance (Cannell et Smith, 1986; Liu *et al.*, 2018; Ma *et al.*, 2018). La plupart de ces études n’ont pas analysé l’importance des différents contrôles environnementaux du débourrement des bourgeons sur toute sa séquence. Si les variables environnementales déterminant les différentes transitions de la séquence de débourrement des bourgeons changent sous l’effet des changements climatiques, et ce, de manière inégale, le processus de débourrement des bourgeons pourrait être ralenti ou accéléré. Présentement, les modèles écophysiologiques déterminant la séquence de débourrement des bourgeons ne peuvent que difficilement considérer cette possibilité.

Puisque la photopériode n’est pas affectée par les changements climatiques, les transitions sensibles à la photopériode devraient se comporter de façon similaire dans le futur, mais les étapes affectées par la température de l’air ont le potentiel de faire avancer le débourrement des bourgeons. Comme la photopériode a un effet plus important sur le déclenchement des premières transitions de la séquence de débourrement des bourgeons, elle devrait limiter l’avancement du débourrement des bourgeons dans le futur. Ce résultat concorde avec l’étude de Körner et Basler, (2010) qui prévoit que la séquence de débourrement des bourgeons des espèces de fin de succession sera de moins en moins bien synchronisé avec la température de l’air, puisque les espèces de fin de succession semble être plus affectées par la photopériode que les espèces de début de succession. Toutefois, l’augmentation de la température de l’air pourrait faire compléter le débourrement des bourgeons plus rapidement puisque les dernières étapes étaient fortement sensibles à l’augmentation de la température.

L’épinette noire répond plus fortement à la température de l’air que l’épinette blanche. Donc, nous spéculons que, dans le futur, l’augmentation de la température de l’air pourrait faire devancer le débourrement des bourgeons de l’épinette noire plus rapidement que ceux de l’épinette blanche. Ce résultat concorde aussi avec l’étude de Vitasse et al., (2018) qui montre que la séquence de débourrement des bourgeons tend à s’uniformiser entre les espèces. Dès lors, l’avancée du débourrement de l’épinette noire pourrait augmenter son exposition au gel printanier et causer un retard de croissance similaire à celui observé chez l’épinette blanche. Même si, présentement, cette espèce semble un bon choix pour limiter la stagnation de la croissance des plantations d’épinettes, ce pourrait ne plus être le cas dans le futur.

5.5 Effet du gel printanier sur l’aménagement forestier en forêt boréale mixte

Selon les résultats présentés aux chapitres III et IV, il est primordial de considérer les attributs physiques du paysage au moment d’établir une plantation. Les plantations devraient être principalement établies à de hautes élévations et les arbres devraient être plantés sur des buttes. De plus, les résultats du chapitre II suggèrent de planter des arbres de plus grandes tailles. Ces recommandations sont surtout importantes à la forêt boréale mixte où la fréquence et l’intensité des gelées printanières sont élevées et où la stagnation de la croissance est régulièrement observée.

Les espèces ou les provenances utilisées pour le reboisement doivent être adaptées aux conditions climatiques présentes et futures (Marris, 2009; O’Neill et al., 2008). Par contre, si les arbres plantés ne réussissent pas à croître adéquatement pendant leur jeune âge, ces arbres ne devraient pas être économiquement rentables au moment de leur récolte. Donc, les pratiques d’aménagement forestier en forêt boréale devraient d’abord se préoccuper d’améliorer le choix des sites où établir des plantations et améliorer le choix du microsite de plantation avant d’effectuer des plantations suivant les principes de la migration assistée. Seulement lorsque la probabilité d’occurrence de gel printanier aura diminué, l’utilisation d’espèces ou de provenances non locales sera envisageable.

Cependant, à la forêt tempérée nordique, la plus faible probabilité et la plus faible intensité de gel printanier semblent permettre l'utilisation de provenances du sud pour améliorer la productivité forestière. Puisque les provenances du sud seraient aussi mieux adaptées à la sécheresse et que la sécheresse devrait augmenter dans le futur (Andalo, Beaulieu, et Bousquet, 2005; D'Orangeville et al., 2018), ce choix apparait important. L'aménagement forestier devrait donc viser l'établissement de plantations mixtes utilisant plusieurs provenances d'épinettes blanches et plusieurs provenances d'épinettes noires qui ne résideraient pas très loin des sites de plantation.

Finalement, voici quelques recommandations pour limiter le problème de stagnation de la croissance des plantations d'épinettes en forêt boréale mixte.

5.6 Recommandations

- Avant l'établissement des plantations, utiliser le lidar aéroporté (par avion ou drone) pour établir des cartes montrant la susceptibilité au gel printanier en fonction de la position dans la topographie et dans la microtopographie.

- Dans les zones sujettes aux gelées printanières comme les dépressions topographiques et le bas des pentes, il serait préférable de planter des arbres de plus grande taille sur des buttes, pour élever le bourgeon apical au-dessus de la zone de gel.

- Développer des plantations mixtes où des espèces ou des provenances tolérantes aux gelées printanières seraient plantées dans les zones de basse élévation sujettes aux gelées printanières et planter des espèces ou des provenances non locales à croissance rapide seulement dans les zones rarement sujettes aux gelées printanières comme les hautes élévations sur des buttes.

- Augmenter l’utilisation des coupes partielles et augmenter la rétention des arbres à l’intérieur d’une coupe forestière pour limiter les grandes aires ouvertes où les évènements de gel printanier sont intensifiés.

ANNEXE A

SUPPORTING INFORMATION AND RESULTS FOR CHAPITRE I

PROBABILITY OF SPRING FROSTS, NOT GROWING DEGREE-DAYS, DRIVES ONSET OF SPRUCE BUD BURST IN PLANTATIONS AT THE BOREAL-TEMPERATE FOREST ECOTONE

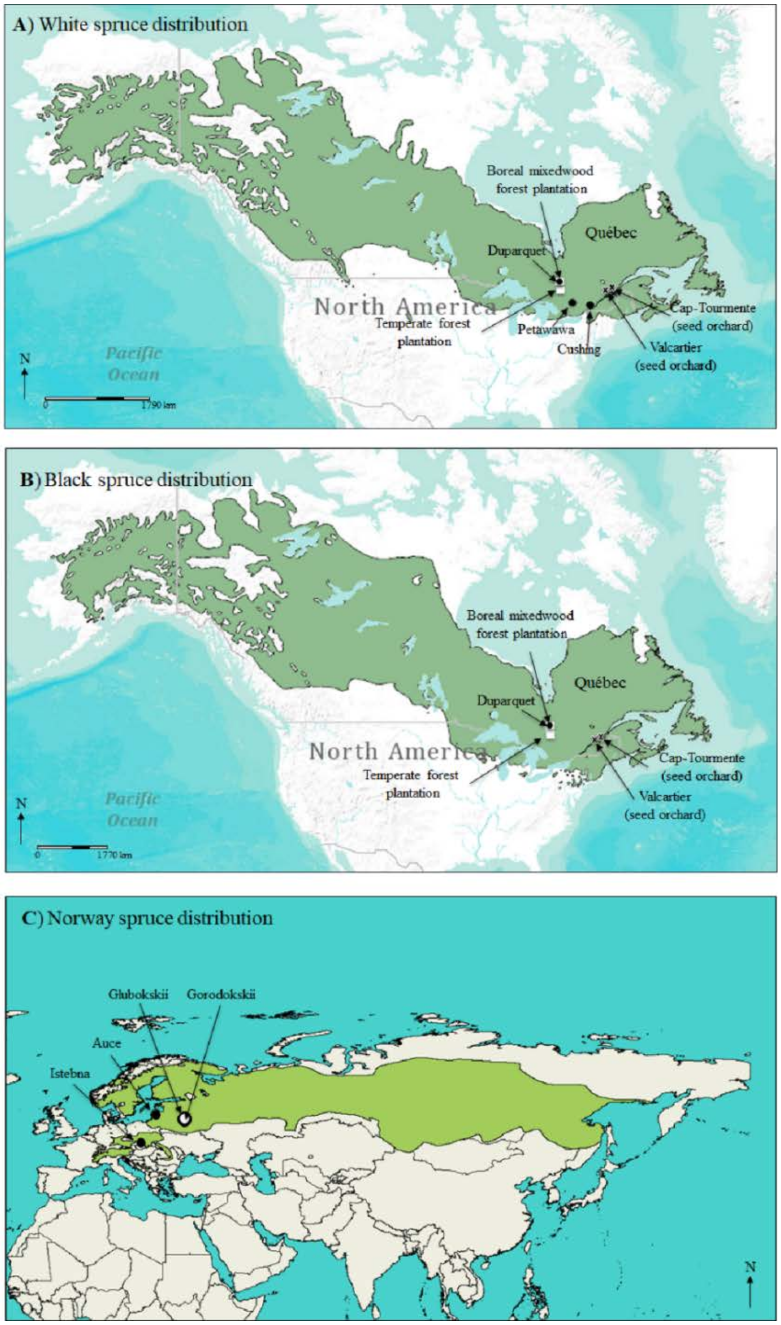

Figure A1 Maps showing the locations of the seed sources within each species range. Species distribution data were retrieved from data basin https://databasin.org/datasets/0dd88c1ae391403698fbc9d457154bdc for white spruce and black spruce and from the European Forest Genetic Resources Programme (EUFORGEN) http://www.euforgen.org/species/picea-abies/ for Norway spruce.

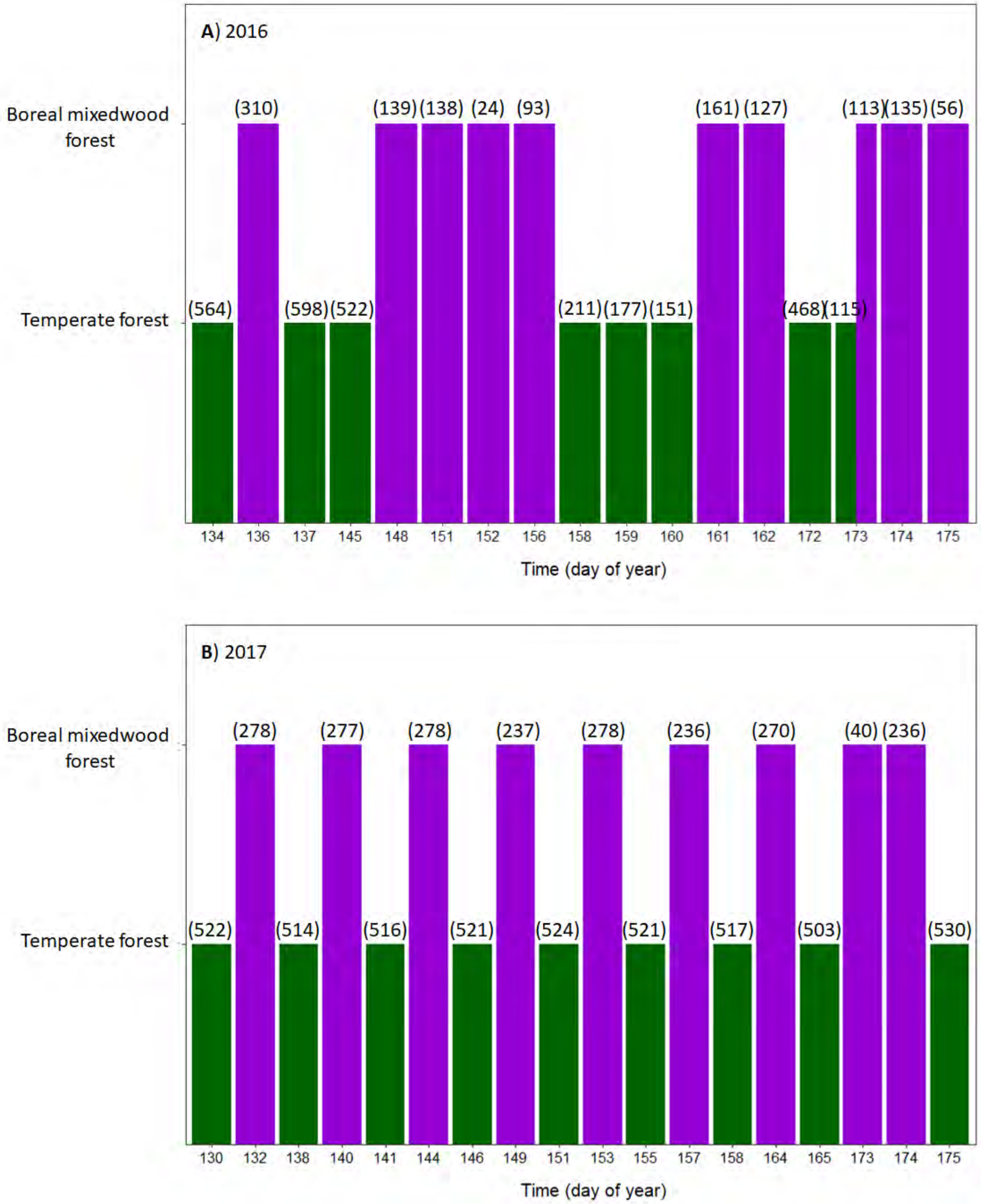

Figure A2 Timeline showing the dates (in day of year) and the number of bud observations (in parentheses) at which buds were observed at each plantation sites (green represent temperate forest plantation and violet represents the boreal.

Figure A3 Spring frost damage on newly formed needles (brown-grey needles leaning downward).

Table A1 Results of the linear regression between daily minimum, mean and maximum air temperature measured with the temperature loggers (iButtons) and the temperature simulated with the software Biosim 10 at the plantation in temperate forest. The P-value for each regression is below the significance level of 0.05.

Site	**iButtons**	**# Days (period)**	**Years**	**Climate Variables**	**Adjusted R^2**	**# Missing dates (period)**
Temperate	1	99 (137-235)	2016	Minimum temp	0.81	7 (130-136)
Temperate	1	95 (146-240)	2017	Minimum temp	0.81	16 (130-145)
Temperate	1	99 (137-235)	2016	Mean temp	0.91	7 (130-136)
Temperate	1	95 (146-240)	2017	Mean temp	0.91	16 (130-145)
Temperate	1	99 (137-235)	2016	Maximum temp	0.85	7 (130-136)
Temperate	1	95 (146-240)	2017	Maximum temp	0.85	16 (130-145)
Temperate	2	99 (137-235)	2016	Minimum temp	0.81	7 (130-136)
Temperate	2	95 (146-240)	2017	Minimum temp	0.81	16 (130-145)
Temperate	2	99 (137-235)	2016	Mean temp	0.91	7 (130-136)
Temperate	2	95 (146-240)	2017	Mean temp	0.91	16 (130-145)
Temperate	2	99 (137-235)	2016	Maximum temp	0.89	7 (130-136)
Temperate	2	95 (146-240)	2017	Maximum temp	0.89	16 (130-145)
Temperate	3	96 (145-240)	2016	Minimum temp	0.83	15 (130-144)
Temperate	3	95 (146-240)	2017	Minimum temp	0.83	16 (130-145)
Temperate	3	96 (145-240)	2016	Mean temp	0.91	15 (130-144)
Temperate	3	95 (146-240)	2017	Mean temp	0.91	16 (130-145)
Temperate	3	96 (145-240)	2016	Maximum temp	0.82	15 (130-144)
Temperate	3	95 (146-240)	2017	Maximum temp	0.82	16 (130-145)

Table A2 Results of the linear regression between daily minimum, mean and maximum air temperature measured with the temperature loggers (iButtons) and the temperature simulated with the software Biosim 10 at the plantation in boreal mixedwood forest. The P-value for each regression is below the significance level of 0.05.

Site	**iButtons**	**# of days (period)**	**Years**	**Climate variables**	**Adjusted *R^2***	**Missing dates (period)**
Boreal	1	80 (143-222)	2016	Minimum temp	0.86	13 (130-142)
Boreal	1	97 (143-239)	2017	Minimum temp	0.86	13 (130-142)
Boreal	1	80 (143-222)	2016	Mean temp	0.93	13 (130-142)
Boreal	1	97 (143-239)	2017	Mean temp	0.93	13 (130-142)
Boreal	1	80 (143-222)	2016	Maximum temp	0.92	13 (130-142)
Boreal	1	97 (143-239)	2017	Maximum temp	0.92	13 (130-142)
Boreal	2	82 (141-222)	2016	Minimum temp	0.77	11 (130-140)
Boreal	2	97 (143-239)	2017	Minimum temp	0.77	13 (130-142)
Boreal	2	82 (141-222)	2016	Mean temp	0.92	11 (130-140)
Boreal	2	97 (143-239)	2017	Mean temp	0.92	13 (130-142)
Boreal	2	82 (141-222)	2016	Maximum temp	0.74	11 (130-140)
Boreal	2	97 (143-239)	2017	Maximum temp	0.74	13 (130-142)
Boreal	3	89 (140-228)	2016	Minimum temp	0.85	10 (130-139)
Boreal	3	97 (143-239)	2017	Minimum temp	0.85	13 (130-142)
Boreal	3	89 (140-228)	2016	Mean temp	0.94	10 (130-139)
Boreal	3	97 (143-239)	2017	Mean temp	0.94	13 (130-142)
Boreal	3	89 (140-228)	2016	Maximum temp	0.86	10 (130-139)
Boreal	3	97 (143-239)	2017	Maximum temp	0.86	13 (130-142)

Table A3 List of the 31 candidate models tested to determine the best air temperature predictors of the transition between phenological stages.

Model ID	**Predictor variables**	**Interactions**
1	DOY (Null)	NA
2	Daily max temp.	NA
3	Daily mean temp.	NA
4	Daily min temp.	NA
5	GDD (max)	NA
6	GDD (mean)	NA
7	Frost prob.	NA
8	Daily max temp.; Species	NA
9	Daily mean temp.; Species	NA
10	Daily min temp.; Species	NA
11	GDD (max); Species	NA
12	GDD (mean); Species	NA
13	Frost prob; Species	NA
14	Daily max temp.; Site	NA
15	Daily mean temp.; Site	NA
16	Daily min temp.; Site	NA
17	GDD (max); Site	NA
18	GDD (mean); Site	NA
19	Frost prob; Site	NA
20	Daily max temp.; Species; Site	NA
21	Daily mean temp.; Species; Site	NA
22	Daily min temp.; Species; Site	NA
23	GDD (max); Species; Site	NA
24	GDD (mean); Species; Site	NA

(Table A3 suite)

Model ID	**Predictor variables**	**Interactions**
25	Frost prob; Species; Site	NA
26	Daily max temp.; Species; Site	Daily max temp. × Species; Daily max temp. × Site
27	Daily mean temp.; Species; Site	Daily mean temp × Species; Daily mean temp × Site
28	Daily min temp.; Species; Site	Daily min temp. × Species; Daily min temp. × Site
29	GDD (max); Species; Site	GDD (max) × Species; GDD (max) × Site
30	GDD (mean); Species; Site	GDD (mean) × Species; GDD (mean) × Site
31	Frost prob; Species; Site	Frost prob × Species; Frost prob × Site

Table A4 List of the six candidate models that were tested to determine the best photoperiod predictors of transitions between phenological stages.

Model ID	**Predictor variables**	**Interactions**
1	DOY (Null)	NA
2	Photoperiod	NA
3	Photoperiod; Species	NA
4	Photoperiod; Site	NA
5	Photoperiod; Species; Site	NA
6	Photoperiod; Species; Site	Photoperiod × Species; Photoperiod × Site

Table A5 Results of the AICc model selection to determine the best combination of air temperature variables for predicting the transition from stage zero to stage two of spruce bud phenology, bold indicated the selected models and numbers in parentheses before each model refer to the candidate models before selection (Table A3).

Models	**AICc**	**Delta AICc**	**AICc weight**	**AICc cum. weight**
(31) Frost prob.; Species; Site, Interactions	**3342.35**	**0.00**	**1.00**	**1.00**
(25) Frost prob.; Species; Site	3510.61	168.26	0.00	1.00
(13) Frost prob.; Species	3525.47	183.11	0.00	1.00
(19) Frost prob.; Site	3582.67	240.32	0.00	1.00
(7) Frost prob.	3603.42	261.07	0.00	1.00
(1) Day of year	3861.83	519.48	0.00	1.00
(29) GDD max; Species; Site, Interactions	3862.54	520.19	0.00	1.00
(30) GDD mean; Species; Site, Interactions	3933.03	590.68	0.00	1.00
(17) GDD max; Site	3980.74	638.39	0.00	1.00
(11) GDD max; Species	3995.71	653.35	0.00	1.00
(5) GDD max	4020.06	677.71	0.00	1.00
(24) GDD mean; Species; Site	4076.76	734.41	0.00	1.00
(12) GDD mean; Species	4077.00	734.65	0.00	1.00
(6) GDD mean	4117.77	775.42	0.00	1.00
(18) GDD mean; Site	4119.66	777.31	0.00	1.00
(27) Mean daily T. °C; Species; Site; Interactions	5706.09	2363.73	0.00	1.00
(21) Mean daily T. °C; Species	5747.40	2405.04	0.00	1.00
(15) Mean daily T. °C; Site	5751.30	2408.95	0.00	1.00
(9) Mean daily T. °C; Species	5751.80	2409.45	0.00	1.00
(3) Mean daily T. °C	5758.77	2416.42	0.00	1.00

(Table A5 suite)

Models	**AICc**	**Delta AICc**	**AICc weight**	**AICc cum. weight**
(28) Min daily T. °C; Species; Site; Interactions	5826.21	2483.86	0.00	1.00
(26) Max daily T. °C; Species; Site; Interactions	5940.38	2598.02	0.00	1.00
(8) Max daily T. °C; Species	5951.48	2609.13	0.00	1.00
(2) Max daily T. °C	5952.15	2609.80	0.00	1.00
(14) Max daily T. °C; Site	5953.01	2610.66	0.00	1.00
(20) Max daily T. °C; Species; Site	5953.02	2610.67	0.00	1.00
(22) Min daily T. °C; Species; Site	5997.91	2655.56	0.00	1.00
(16) Min daily T. °C; Site	6001.03	2658.68	0.00	1.00
(10) Min daily T. °C; Species	6021.29	2678.94	0.00	1.00
(4) Min daily T. °C	6029.29	2686.94	0.00	1.00
(23) GDD max; Species; Site	NA	NA	NA	NA

Table A6 Results of the AICc model selection to determine the best combination of air temperature variables for predicting the transition from stage two to stage three of spruce bud phenology, bold indicated the selected models and numbers in parentheses before each model refer to the candidate models before selection (Table A3).

Models	**AICc**	**Delta AICc**	**AICc weight**	**AICc cum. weight**
(13) Frost prob.; Species	**2244.30**	**0.00**	**0.57**	**0.57**
(31) Frost prob.; Species; Site; Interactions	**2246.16**	**1.86**	**0.22**	**0.79**
(25) Frost prob.; Species; Site	**2246.31**	**2.01**	**0.21**	**1.00**
(29) GDD max; Species; Site; Interactions	2260.66	16.36	0.00	1.00
(30) GDD mean; Species; Site; Interactions	2268.96	24.67	0.00	1.00
(24) GDD mean; Species; Site	2282.31	38.01	0.00	1.00
(12) GDD mean; Species	2286.54	42.25	0.00	1.00
(23) GDD max; Species; Site	2305.66	61.37	0.00	1.00
(11) GDD max; Species	2348.35	104.05	0.00	1.00
(1) Day of year	2366.18	121.88	0.00	1.00
(7) Frost prob.	2390.25	145.95	0.00	1.00
(19) Frost prob.; Site	2392.06	147.76	0.00	1.00
(6) GDD mean	2420.85	176.56	0.00	1.00
(18) GDD mean; Site	2421.12	176.83	0.00	1.00
(28) Min daily T °C; Species; Site; Interactions	2807.79	563.49	0.00	1.00
(27) Mean daily T °C; Species; Site; Interactions	2876.97	632.68	0.00	1.00
(22) Min daily T °C; Species; Site	2887.51	643.21	0.00	1.00
(10) Min daily T °C; Species	2887.80	643.50	0.00	1.00

(Table A6 suite)

Models	**AICc**	**Delta AICc**	**AICc weight**	**AICc cum. weight**
(26) Max daily T °C; Species; Site; Interactions	2897.44	653.14	0.00	1.00
(21) Mean daily T °C; Species; Site	2899.96	655.67	0.00	1.00
(20) Max daily T °C; Species; Site	2900.11	655.81	0.00	1.00
(9) Mean daily T °C; Species	2903.15	658.86	0.00	1.00
(8) Max daily T °C; Species	2903.79	659.50	0.00	1.00
(4) Min daily T °C	2948.31	704.01	0.00	1.00
(16) Min daily T °C; Site	2949.44	705.14	0.00	1.00
(15) Mean daily T °C; Site	2960.00	715.71	0.00	1.00
(14) Max daily T °C; Site	2960.21	715.91	0.00	1.00
(3) Mean daily T °C	2960.43	716.13	0.00	1.00
(2) Max daily T °C	2960.93	716.63	0.00	1.00
(17) GDD max; Site	NA	NA	NA	NA
(5) GDD max	NA	NA	NA	NA

Table A7 Results of the AICc model selection to determine the best combination of air temperature variables for predicting the transition from stage three to stage four of spruce bud phenology, bold indicated the selected models and numbers in parentheses before each model refer to the candidate models before selection (Table A3).

Models	AICc	Delta AICc	AICc weight	AICc cum. weight
(12) GDD mean; Species	**1766.43**	**0.00**	**0.56**	**0.56**
(24) GDD mean; Species; Site	**1767.87**	**1.45**	**0.27**	**0.83**
(30) GDD mean; Species; Site; Interactions	**1769.28**	**2.85**	**0.13**	**0.97**
(23) GDD max; Species; Site	1772.67	6.24	0.02	0.99
(29) GDD max; Species; Site; Interactions	1775.56	9.14	0.01	1.00
(11) GDD max; Species	1803.13	36.70	0.00	1.00
(31) Frost prob.; Species; Site; Interactions	1853.69	87.26	0.00	1.00
(6) GDD mean	1873.76	107.34	0.00	1.00
(18) GDD mean; Site	1875.45	109.03	0.00	1.00
(17) GDD max; Site	1878.87	112.44	0.00	1.00
(5) GDD max	1886.48	120.05	0.00	1.00
(25) Frost prob.; Species; Site	1899.68	133.25	0.00	1.00
(13) Frost prob.; Species	1905.39	138.96	0.00	1.00
(1) Day of year	1905.80	139.38	0.00	1.00
(19) Frost prob.; Site	1974.29	207.87	0.00	1.00
(7) Frost prob.	1983.20	216.77	0.00	1.00
(26) Max daily T °C; Species; Site; Interactions	2120.31	353.88	0.00	1.00
(27) Mean daily T °C; Species; Site; Interactions	2122.52	356.10	0.00	1.00

(Table A7 suite)

Models	AICc	Delta AICc	AICc weight	AICc cum. weight
(28) Min daily T °C; Species; Site; Interactions	2124.11	357.69	0.00	1.00
(22) Min daily T °C; Species; Site	2136.55	370.13	0.00	1.00
(21) Mean daily T °C; Species; Site	2142.08	375.65	0.00	1.00
(10) Min daily T °C; Species	2143.70	377.28	0.00	1.00
(20) Max daily T °C; Species; Site	2143.90	377.48	0.00	1.00
(16) Min daily T °C; Site	2145.15	378.72	0.00	1.00
(9) Mean daily T °C; Species	2147.04	380.61	0.00	1.00
(8) Max daily T °C; Species	2148.12	381.69	0.00	1.00
(15) Mean daily T °C; Site	2149.31	382.88	0.00	1.00
(14) Max daily T °C; Site	2151.04	384.61	0.00	1.00
(4) Min daily T °C	2153.78	387.36	0.00	1.00
(3) Mean daily T °C	2156.02	389.59	0.00	1.00
(2) Max daily T °C	2157.00	390.57	0.00	1.00

Table A8 Results of the AICc model selection to determine the best combination of air temperature variables for predicting the transition from stage four to stage five of spruce bud phenology, bold indicated the selected models and numbers in parentheses before each model refer to the candidate models before selection (Table A3).

Models	**AICc**	**Delta AICc**	**AICc weight**	**AICc cum. weight**
(30) GDD mean; Species; Site; Interactions	**1622.99**	**0.00**	**1.00**	**1.00**
(24) GDD mean; Species; Site	1653.11	30.12	0.00	1.00
(12) GDD mean; Species	1667.49	44.51	0.00	1.00
(29) GDD max; Species; Site; Interactions	1673.58	50.59	0.00	1.00
(23) GDD max; Species; Site	1695.36	72.37	0.00	1.00
(1) Day of year	1724.92	101.93	0.00	1.00
(11) GDD max; Species	1784.42	161.44	0.00	1.00
(18) GDD mean; Site	1809.84	186.86	0.00	1.00
(6) GDD mean	1812.91	189.92	0.00	1.00
(17) GDD max; Site	1850.01	227.02	0.00	1.00
(5) GDD max	1890.37	267.38	0.00	1.00
(31) Frost prob.; Species; Site; Interactions	2002.32	379.33	0.00	1.00
(13) Frost prob.; Species	2060.68	437.70	0.00	1.00
(25) Frost prob.; Species; Site	2062.66	439.67	0.00	1.00
(7) Frost prob.	2139.35	516.36	0.00	1.00
(19) Frost prob.; Site	2141.31	518.32	0.00	1.00
(26) Max daily T °C; Species; Site; Interactions	2366.40	743.41	0.00	1.00
(20) Max daily T °C; Species; Site	2422.06	799.07	0.00	1.00

(Table A8 suite)

Models	**AICc**	**Delta AICc**	**AICc weight**	**AICc cum. weight**
(14) Max daily T °C; Site	2424.40	801.41	0.00	1.00
(8) Max daily T °C; Species	2434.30	811.31	0.00	1.00
(2) Max daily T °C	2435.98	812.99	0.00	1.00
(21) Mean daily T °C; Species; Site	2436.75	813.76	0.00	1.00
(15) Mean daily T °C; Site	2439.26	816.28	0.00	1.00
(9) Mean daily T °C; Species	2447.76	824.77	0.00	1.00
(3) Mean daily T °C	2449.49	826.50	0.00	1.00
(4) Min daily T °C	NA	NA	NA	NA
(10) Min daily T °C; Species	NA	NA	NA	NA
(16) Min daily T °C; Site	NA	NA	NA	NA
(22) Min daily T °C; Species; Site	NA	NA	NA	NA
(27) Mean daily T °C; Species; Site; Interactions	NA	NA	NA	NA
(28) Min daily T °C; Species; Site; Interactions	NA	NA	NA	NA

Table A9 Results of the AICc model selection to determine the best combination of air temperature variables for predicting the transition from stage five to stage six of spruce bud phenology, bold indicated the selected models and numbers in parentheses before each model refer to the candidate models before selection (Table A3).

Models	**AICc**	**Delta AICc**	**AICc weight**	**AICc cum. weight**
(29) GDD max; Species; Site; Interactions	**2003.92**	**0.00**	**1.00**	**1.00**
(23) GDD max; Species; Site	2018.47	14.55	0.00	1.00
(30) GDD mean; Species; Site; Interactions	2023.61	19.68	0.00	1.00
(12) GDD mean; Species	2024.32	20.40	0.00	1.00
(24) GDD mean; Species; Site	2026.25	22.32	0.00	1.00
(11) GDD max; Species	2052.07	48.14	0.00	1.00
(1) Day of year	2085.67	81.75	0.00	1.00
(17) GDD max; Site	2116.96	113.04	0.00	1.00
(6) GDD mean	2123.60	119.68	0.00	1.00
(18) GDD mean; Site	2125.06	121.14	0.00	1.00
(5) GDD max	2133.21	129.28	0.00	1.00
(31) Frost prob.; Species; Site; Interactions	2398.94	395.01	0.00	1.00
(25) Frost prob.; Species; Site	2488.35	484.43	0.00	1.00
(13) Frost prob.; Species	2508.16	504.24	0.00	1.00
(19) Frost prob.; Site	2540.27	536.34	0.00	1.00
(7) Frost prob.	2558.11	554.19	0.00	1.00
(28) Min daily T °C; Species; Site; Interactions	3750.38	1746.46	0.00	1.00
(22) Min daily T °C; Species; Site	3829.88	1825.96	0.00	1.00

(Table A9 suite)

Models	AICc	Delta AICc	AICc weight	AICc cum. weight
(10) Min daily T °C; Species	3836.79	1832.86	0.00	1.00
(16) Min daily T °C; Site	3851.59	1847.67	0.00	1.00
(27) Mean daily T °C; Species; Site; Interactions	3852.39	1848.47	0.00	1.00
(4) Min daily T °C	3854.57	1850.65	0.00	1.00
(9) Mean daily T °C; Species	3861.40	1857.48	0.00	1.00
(21) Mean daily T °C; Species; Site	3863.17	1859.25	0.00	1.00
(3) Mean daily T °C	3876.91	1872.99	0.00	1.00
(15) Mean daily T °C; Site	3878.89	1874.97	0.00	1.00
(26) Max daily T °C; Species; Site; Interactions	3923.80	1919.88	0.00	1.00
(8) Max daily T °C; Species	3955.41	1951.48	0.00	1.00
(20) Max daily T °C; Species; Site	3957.14	1953.22	0.00	1.00
(2) Max daily T °C	3973.27	1969.35	0.00	1.00
(14) Max daily T °C; Site	3975.24	1971.32	0.00	1.00

Table A10 Results of the mixed binomial regression model for transition stage zero to two showing the coefficients and standard errors for the best air temperature and photoperiod variables per species and sites; boldface type indicates coefficients that differ from zero.

Variable	**Frost probability**	**Photoperiod (hours)**
	Standardised coefficients (SE)	**Standardised coefficients (SE)**
Intercept: Norway spruce in the temperate forest	0.79 (0.99)	**1.37 (0.47)**
Frost prob. or Photoperiod	**-4.69 (0.20)**	**3.83 (0.19)**
White spruce	**4.36 (0.41)**	**4.46 (0.44)**
Black spruce	0.05 (0.32)	0.11 (0.31)
Boreal mixedwood forest	**0.56 (0.28)**	**-2.32 (0.28)**
White spruce × Frost prob. or Photoperiod	**-2.86 (0.35)**	**2.92 (0.39)**
Black spruce × Frost prob. or Photoperiod	0.12 (0.20)	-0.19 (0.22)
Boreal mixedwood forest × Frost prob. or Photoperiod	**1.66 (0.19)**	**-0.47 (0.22)**

Table A11 Results of the mixed binomial regression model for transition stage two to three showing the coefficients and standard errors for the best air temperature and photoperiod variables per species and sites; boldface type indicates coefficients that differ from zero.

Variable	**Frost probability**	**Photoperiod (hours)**
	Standardised coefficients (SE)	**Standardised coefficients (SE)**
Intercept: Norway spruce in the temperate forest	**-2.71 (1.65)**	**-2.16 (0.59)**
Frost prob. or Photoperiod	**-5.43 (0.34)**	**5.59 (0.49)**
White spruce	**4.54 (0.49)**	**4.79 (0.54)**
Black spruce	**-1.22 (0.52)**	**-1.61 (0.59)**
Boreal mixedwood forest	0.07 (0.38)	**-3.72 (0.48)**
White spruce × Frost prob. or Photoperiod	0.04 (0.43)	**-2.17 (0.56)**
Black spruce × Frost prob. or Photoperiod	**-0.98 (0.56)**	0.29 (0.67)
Boreal mixedwood forest × Frost prob. or Photoperiod	**0.56 (0.39)**	**1.31 (0.49)**

Table A12 Results of the mixed binomial regression model for transition stage three to four showing the coefficients and standard errors for the best air temperature and photoperiod variables per species and sites; boldface type indicates coefficients that differ from zero.

Variable	**GDD (° C-days)**	**Photoperiod (hours)**
	Standardised coefficients (SE)	**Standardised coefficients (SE)**
Intercept: Norway spruce in temperate forest	**-1.92 (0.57)**	**-2.74 (0.50)**
GDD mean or Photoperiod	**5.77 (0.62)**	**5.83 (0.66)**
White spruce	**4.15 (0.52)**	**4.10 (0.56)**
Black spruce	-0.42 (0.49)	-0.55 (0.92)
Boreal mixedwood forest	-0.28 (0.36)	**-3.05 (0.50)**
White spruce × GDD mean or Photoperiod	**1.32 (0.71)**	-0.15 (0.76)
Black spruce × GDD mean or Photoperiod	**1.48 (0.78)**	**1.84 (1.02)**
Boreal mixedwood forest × GDD mean or Photoperiod	0.05 (0.58)	-0.36 (0.62)

Table A13 Results of the mixed binomial regression model for transition stage four to five showing the coefficients and standard errors for the best air temperature and photoperiod variables per species and sites; boldface type indicates coefficients that differ from zero.

Variable	**GDD (° C-days)**	**Photoperiod (hours)**
	Standardised coefficients (SE)	**Standardised coefficients (SE)**
Intercept: Norway spruce in temperate forest	**-2.74 (0.65)**	**-6.62 (1.09)**
GDD mean or Photoperiod	**7.21 (0.93)**	**13.19 (1.40)**
White spruce	**4.10 (0.75)**	**5.76 (1.12)**
Black spruce	**-4.47 (0.94)**	**-7.87 (1.56)**
Boreal mixedwood forest	**-1.47 (0.56)**	**-6.33 (1.00)**
White spruce × GDD mean or Photoperiod	**5.31 (0.99)**	-1.07 (1.24)
Black spruce × GDD mean or Photoperiod	**2.90 (1.01)**	**6.30 (1.66)**
Boreal mixedwood forest × GDD mean or Photoperiod	**-2.29 (0.77)**	**-2.35 (1.00)**

Table A14 Results of the mixed binomial regression model for transition stage five to six showing the coefficients and standard errors for the best air temperature and photoperiod variables per species and sites; boldface type indicates coefficients that differ from zero.

Variable	**GDD (° C-days)**	**Photoperiod (hours)**
	Standardised coefficients (SE)	**Standardised coefficients (SE)**
Intercept: Norway spruce in temperate forest	**-2.87 (0.52)**	NA
GDD max	**5.98 (0.49)**	NA
White spruce	**0.97 (0.60)**	NA
Black spruce	**-5.91 (0.94)**	NA
Boreal mixedwood forest	**-3.49 (0.68)**	NA
White spruce × GDD max	**1.38 (0.58)**	NA
Black spruce × GDD max	**2.55 (0.71)**	NA
Boreal mixedwood forest × GDD max	**1.01 (0.55)**	NA

Table A15 Results of the AICc model selection to determine the best combination of photoperiod variables for predicting the transition from stage zero to stage two of spruce bud phenology, bold indicated the selected models and numbers in parentheses before each model refer to the candidate models before selection (Table A4).

Models	AICc	Delta AICc	AICc weight	AICc cum. weight
(6) Photoperiod; Species; Site; Interactions	**3607.81**	**0.00**	**1.00**	**1.00**
(5) Photoperiod; Species; Site	3699.05	91.23	0.00	1.00
(3) Photoperiod; Species	3748.94	141.13	0.00	1.00
(4) Photoperiod; Site	3758.72	150.90	0.00	1.00
(2) Photoperiod	3785.84	178.03	0.00	1.00
(1) Day of year	3861.83	254.02	0.00	1.00

Table A16 Results of the AICc model selection to determine the best combination of photoperiod variables for predicting the transition from stage two to stage three of spruce bud phenology, bold indicated the selected models and numbers in parentheses before each model refer to the candidate models before selection (Table A4).

Models	AICc	Delta AICc	AICc weight	AICc cum. weight
(6) Photoperiod; Species; Site; Interactions	**2210.37**	**0.00**	**1.00**	**1.00**
(5) Photoperiod; Species; Site	2239.27	28.90	0.00	1.00
(3) Photoperiod; Species	2302.05	91.68	0.00	1.00
(1) Day of year	2366.18	155.81	0.00	1.00
(4) Photoperiod; Site	2386.22	175.84	0.00	1.00
(2) Photoperiod	2412.99	202.62	0.00	1.00

Table A17 Results of the AICc model selection to determine the best combination of photoperiod variables for predicting transition from stage three to stage four of spruce bud phenology, bold indicated the selected models and numbers in parentheses before each model refer to the candidate models before selection (Table A4).

Models	**AICc**	**Delta AICc**	**AICc weight**	**AICc cum. weight**
(5) Photoperiod; Species; Site	**1790.18**	**0.00**	**0.57**	**0.57**
(6) Photoperiod; Species; Site; Interactions	**1790.77**	**0.59**	**0.43**	**1.00**
(3) Photoperiod; Species	1854.18	64.00	0.00	1.00
(4) Photoperiod; Site	1895.12	104.94	0.00	1.00
(1) Day of year	1905.80	115.62	0.00	1.00
(2) Photoperiod	1917.85	127.66	0.00	1.00

Table A18 Results of the AICc model selection to determine the best combination of photoperiod variables for predicting the transition from stage four to stage five of spruce bud phenology, bold indicated the selected models and numbers in parentheses before each model refer to the candidate models before selection (Table A4).

Models	**AICc**	**Delta AICc**	**AICc weight**	**AICc cum. weight**
(6) Photoperiod; Species; Site; Interactions	**1643.40**	**0.00**	**1.00**	**1.00**
(5) Photoperiod; Species; Site	1670.69	27.29	0.00	1.00
(1) Day of year	1724.92	81.52	0.00	1.00
(4) Photoperiod; Site	1808.03	164.63	0.00	1.00
(3) Photoperiod; Species	1839.24	195.84	0.00	1.00
(2) Photoperiod	1902.71	259.31	0.00	1.00

Table A19 Results of the AICc model selection to determine the best combination of photoperiod variables for predicting transition from stage five to stage six of spruce bud phenology, bold indicated the selected models and numbers in parentheses before each model refer to the candidate models before selection (Table A4).

Models	**AICc**	**Delta AICc**	**AICc weight**	**AICc cum. weight**
(1) Day of year	**2085.67**	**0.00**	**1.00**	**1.00**
(6) Photoperiod; Species; Site; Interactions	2322.73	237.05	0.00	1.00
(5) Photoperiod; Species; Site	2375.84	290.16	0.00	1.00
(4) Photoperiod; Site	2433.20	347.52	0.00	1.00
(3) Photoperiod; Species	2569.36	483.69	0.00	1.00
(2) Photoperiod	2586.51	500.83	0.00	1.00

Table A20 Results of the mixed binomial regression model for transition stage zero to two showing the coefficients and standard errors for the best intra-species air temperature and photoperiod variables per seed source and sites for white spruce; boldface type indicates coefficients that differ from zero.

Variable	**Frost probability**	**Photoperiod (hours)**
	Standardised coefficients (SE)	**Standardised coefficients (SE)**
Intercept: White spruce J70 in temperate forest	**3.78 (1.10)**	**6.79 (1.52)**
Frost prob. or Photoperiod	**-6.64 (0.67)**	**7.79 (0.80)**
White spruce K20	**2.75 (1.09)**	**6.64 (2.17)**
White spruce K24	**3.01 (1.16)**	**4.92 (1.92)**
Boreal mixedwood forest	**2.08 (0.73)**	**-5.23 (0.88)**
White spruce K20 × Frost prob. or Photoperiod	**-2.73 (1.33)**	**6.62 (2.26)**
White spruce K24 × Frost prob. or Photoperiod	**-2.74 (1.34)**	**4.39 (1.92)**
Boreal mixedwood forest × Frost prob. or Photoperiod	**0.89 (0.70)**	**-2.57 (0.83)**

Table A21 Results of the mixed binomial regression model for transition stage two to three showing the coefficients and standard errors for the best intra-species air temperature and photoperiod variables per seed source and sites for white spruce; boldface type indicates coefficients that differ from zero.

Variable	**Frost probability**	**Photoperiod (hours)**
	Standardised coefficients (SE)	**Standardised coefficients (SE)**
Intercept: White spruce J70 in temperate forest	0.90 (1.41)	**1.20 (0.44)**
Frost prob. or Photoperiod	**-4.55 (0.50)**	**3.07 (0.52)**
White spruce K20	**2.18 (0.58)**	**2.01 (0.66)**
White spruce K24	**1.76 (0.61)**	**2.67 (0.80)**
Boreal mixedwood forest	**-0.76 (0.45)**	**-3.56 (0.57)**
White spruce K20 × Frost prob. or Photoperiod	**1.46 (0.74)**	-0.65 (0.74)
White spruce K24 × Frost prob. or Photoperiod	-0.46 (1.06)	**1.63 (1.02)**
Boreal mixedwood forest × Frost prob. or Photoperiod	0.02 (0.61)	**2.93 (0.77)**

Table A22 Results of the mixed binomial regression model for transition stage three to four showing the coefficients and standard errors for the best intra-species air temperature and photoperiod variables per seed source and sites for white spruce; boldface type indicates coefficients that differ from zero.

Variable	**GDD (° C-days)**	**Photoperiod (hours)**
	Standardised coefficients (SE)	**Standardised coefficients (SE)**
Intercept: White spruce J70 in temperate forest	**0.83 (0.60)**	0.02 (0.51)
GDD mean or Photoperiod	**4.46 (0.87)**	**5.59 (0.88)**
White spruce K20	**3.48 (0.98)**	**2.29 (0.64)**
White spruce K24	**3.70 (0.97)**	**3.13 (0.69)**
Boreal mixedwood forest	0.23 (0.57)	**-3.00 (0.64)**
White spruce K20 × GDD mean or Photoperiod	**4.25 (1.31)**	**2.07 (1.00)**
White spruce K24 × GDD mean or Photoperiod	**2.92 (1.37)**	0.97 (1.05)
Boreal mixedwood forest × GDD mean or Photoperiod	0.93 (1.04)	**1.53 (1.02)**

Table A23 Results of the mixed binomial regression model for transition stage four to five showing the coefficients and standard errors for the best intra-species air temperature and photoperiod variables per seed source and sites for white spruce; boldface type indicates coefficients that differ from zero.

Variable	**GDD (° C-days)**	**Photoperiod (hours)**
	Standardised coefficients (SE)	**Standardised coefficients (SE)**
Intercept: White spruce J70 in temperate forest	**1.77 (1.64)**	-1.33 (1.68)
GDD mean or Photoperiod	**11.41 (1.33)**	**10.11 (1.10)**
White spruce K20	**1.21 (0.59)**	**2.16 (0.72)**
White spruce K24	**2.25 (0.69)**	**1.64 (0.75)**
Boreal mixedwood forest	**-3.51 (0.55)**	**-7.73 (0.96)**
White spruce K20 × GDD mean or Photoperiod	-1.08 (1.36)	**-1.89 (1.05)**
White spruce K24 × GDD mean or Photoperiod	**4.03 (1.88)**	**1.27 (1.24)**
Boreal mixedwood forest × GDD mean or Photoperiod	**-1.70 (1.30)**	0.61 (1.19)

Table A24 Results of the mixed binomial regression model for transition stage five to six showing the coefficients and standard errors for the best intra-species air temperature and photoperiod variables per seed source and sites for white spruce; boldface type indicates coefficients that differ from zero.

Variable	**GDD (°C days)**	**Photoperiod (hours)**
	Standardized coeffiicents (SE)	**Standardised coefficients (SE)**
Intercept: White spruce J70 in temperate forest	**-2.20 (0.43)**	NA
GDD max	**5.33 (0.49)**	NA
White spruce K20	**2.03 (0.62)**	NA
White spruce K24	**1.15 (0.67)**	NA
Boreal mixedwood forest	**-4.75 (0.77)**	NA
White spruce K20 × GDD max	**1.96 (0.90)**	NA
White spruce K24 × GDD max	**3.63 (1.19)**	NA
Boreal mixedwood forest × GDD max	**3.63 (0.95)**	NA

Table A25 Results of the mixed binomial regression model for transition stage zero to two showing the coefficients and standard errors for the best intra-species air temperature and photoperiod variables per seed source and sites for Norway spruce; boldface type indicates coefficients that differ from zero.

Variable	**Frost probability**	**Photoperiod (hours)**
	Standardised coefficients (SE)	**Standardised coefficients (SE)**
Intercept: Norway spruce K35 in temperate forest	0.58 (1.07)	**1.05 (0.62)**
Frost prob. or Photoperiod	**-3.78 (0.33)**	**3.38 (0.33)**
Norway spruce K39	0.27 (0.69)	0.68 (0.74)
Norway spruce K50	-0.56 (0.65)	-0.23 (0.68)
Norway spruce K55	**1.24 (0.66)**	**1.26 (0.70)**
Boreal mixedwood forest	**0.70 (0.56)**	**-2.01 (0.59)**
Norway spruce K39 × Frost prob. or Photoperiod	**-0.93 (0.44)**	**1.13 (0.51)**
Norway spruce K50 × Frost prob. or Photoperiod	**-0.82 (0.41)**	**1.45 (0.51)**
Norway spruce K55 × Frost prob. or Photoperiod	**-1.09 (0.44)**	**0.62 (0.46)**
Boreal mixedwood forest × Frost prob. or Photoperiod	**0.66 (0.38)**	**-1.03 (0.39)**

Table A26 Results of the mixed binomial regression model for transition stage two to three showing the coefficients and standard errors for the best intra-species air temperature and photoperiod variables per seed source and sites for Norway spruce; boldface type indicates coefficients that differ from zero.

Variable	**Frost probability**	**Photoperiod (hours)**
	Standardised coefficients (SE)	**Standardised coefficients (SE)**
Intercept: Norway spruce K35 in temperate forest	**-4.39 (2.01)**	**-2.19 (1.03)**
Frost prob. or Photoperiod	**-8.02 (1.18)**	**5.42 (1.01)**
Norway spruce K39	-0.75 (1.20)	-1.03 (1.16)
Norway spruce K50	-0.85 (1.09)	**-1.38 (1.17)**
Norway spruce K55	**2.77 (1.02)**	**1.74 (1.03)**
Boreal mixedwood forest	**2.46 (0.87)**	**-3.80 (1.26)**
Norway spruce K39 × Frost prob. or Photoperiod	-0.04 (1.29)	0.64 (1.34)
Norway spruce K50 × Frost prob. or Photoperiod	-0.25 (1.20)	**1.52 (1.49)**
Norway spruce K55 × Frost prob. or Photoperiod	1.07 (1.07)	-0.86 (1.19)
Boreal mixedwood forest × Frost prob. or Photoperiod	0.89 (0.89)	**2.20 (1.39)**

Table A27 Results of the mixed binomial regression model for transition stage three to four showing the coefficients and standard errors for the best intra-species air temperature and photoperiod variables per seed source and sites for Norway spruce; boldface type indicates coefficients that differ from zero.

Variable	**GDD (° C-days)**	**Photoperiod (hours)**
	Standardised coefficients (SE)	**Standardised coefficients (SE)**
Intercept: Norway spruce K35 in temperate forest	**-2.35 (1.07)**	**-3.95 (0.49)**
GDD mean or Photoperiod	**4.12 (1.57)**	**6.54 (0.71)**
Norway spruce K39	-1.09 (1.42)	**-1.81 (0.95)**
Norway spruce K50	0.49 (1.16)	**1.86 (0.96)**
Norway spruce K55	**3.75 (1.19)**	**3.39 (0.52)**
Boreal mixedwood forest	**-1.61 (1.11)**	**-5.62 (0.99)**
Norway spruce K39 × GDD mean or Photoperiod	**2.88 (1.94)**	**3.17 (0.00)**
Norway spruce K50 × GDD mean or Photoperiod	-1.41 (1.71)	**-3.80 (0.00)**
Norway spruce K55 × GDD mean or Photoperiod	**5.04 (2.22)**	**0.06 (0.00)**
Boreal mixedwood forest × GDD mean or Photoperiod	**4.91 (2.10)**	**3.15 (0.00)**

Table A28 Results of the mixed binomial regression model for transition stage four to five showing the coefficients and standard errors for the best intra-species air temperature and photoperiod variables per seed source and sites for Norway spruce; boldface type indicates coefficients that differ from zero.

Variable	**GDD (° C-days)**	**Photoperiod (hours)**
	Standardised coefficients (SE)	**Standardised coefficients (SE)**
Intercept: Norway spruce K35 in temperate forest	**-3.57 (1.42)**	**-10.59 (3.22)**
GDD mean or Photoperiod	**5.99 (1.72)**	**16.03 (4.18)**
Norway spruce K39	**-3.64 (2.34)**	**-6.67 (4.08)**
Norway spruce K50	1.52 (1.62)	**3.72 (3.07)**
Norway spruce K55	**2.13 (1.45)**	**7.54 (3.22)**
Boreal mixedwood forest	-0.80 (1.27)	**-6.87 (3.64)**
Norway spruce K39 × GDD mean or Photoperiod	**3.99 (2.67)**	**6.91 (4.62)**
Norway spruce K50 × GDD mean or Photoperiod	0.55 (1.96)	-1.67 (3.41)
Norway spruce K55 × GDD mean or Photoperiod	-0.23 (1.95)	**-6.84 (3.65)**
Boreal mixedwood forest × GDD mean or Photoperiod	-0.57 (1.59)	-1.36 (3.28)

Table A29 Results of the mixed binomial regression model for transition stage five to six showing the coefficients and standard errors for the best intra-species air temperature and photoperiod variables per seed source and sites for Norway spruce; boldface type indicates coefficients that differ from zero.

Variable	**GDD (° C-days)**	**Photoperiod (hours)**
	Standardised coefficients (SE)	**Standardised coefficients (SE)**
Intercept: Norway spruce K35 in temperate forest	**-6.50 (1.60)**	NA
GDD max or Photoperiod	**8.71 (1.46)**	NA
Norway spruce K39	-2.21 (2.38)	NA
Norway spruce K50	**2.09 (1.71)**	NA
Norway spruce K55	**6.77 (1.79)**	NA
Boreal mixedwood forest	**-3.84 (1.68)**	NA
Norway spruce K39 × GDD max or Photoperiod	1.23 (2.10)	NA
Norway spruce K50 × GDD max or Photoperiod	-1.27 (1.47)	NA
Norway spruce K55 × GDD max or Photoperiod	**-2.52 (1.57)**	NA
Boreal mixedwood forest × GDD max or Photoperiod	0.12 (1.27)	NA

ANNEXE B

SUPPORTING INFORMATION AND RESULTS FOR CHAPITRE II

GROWING-SEASON FROST IS A BETTER PREDICTOR OF TREE GROWTH THAN MEAN ANNUAL TEMPERATURE IN BOREAL MIXEDWOOD FOREST PLANTATIONS

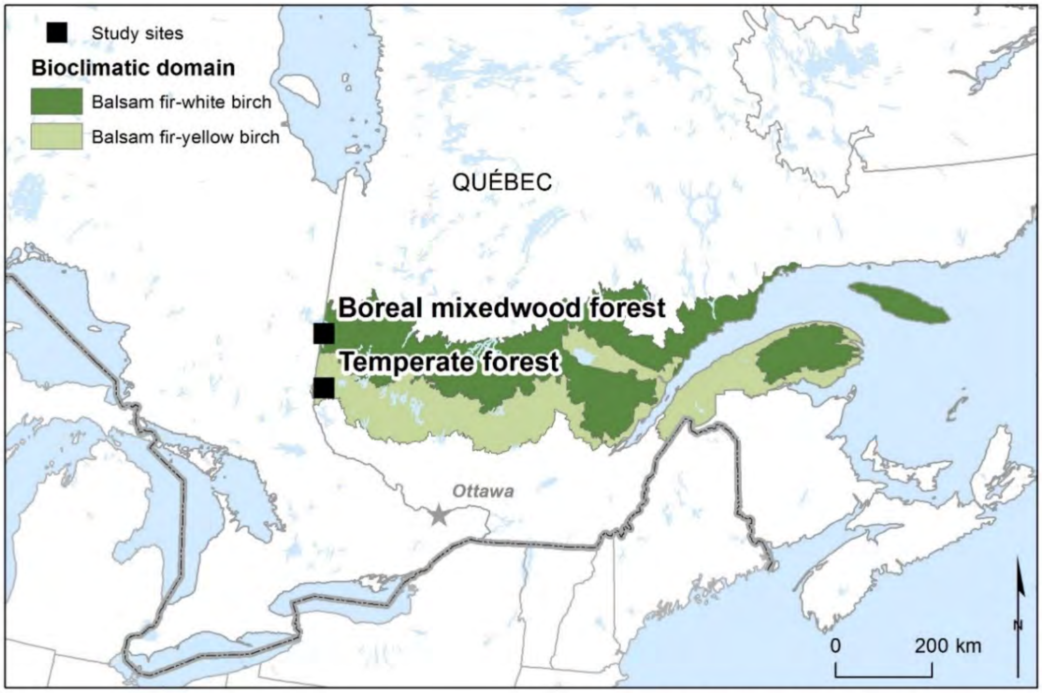

Projection: NAD 1983 MTM 10 | Source: MFFP, 2018 | Author : CEF, 2019

Figure B1 Location of the two study sites in the temperate and boreal mixedwood forest of Québec (Canada).

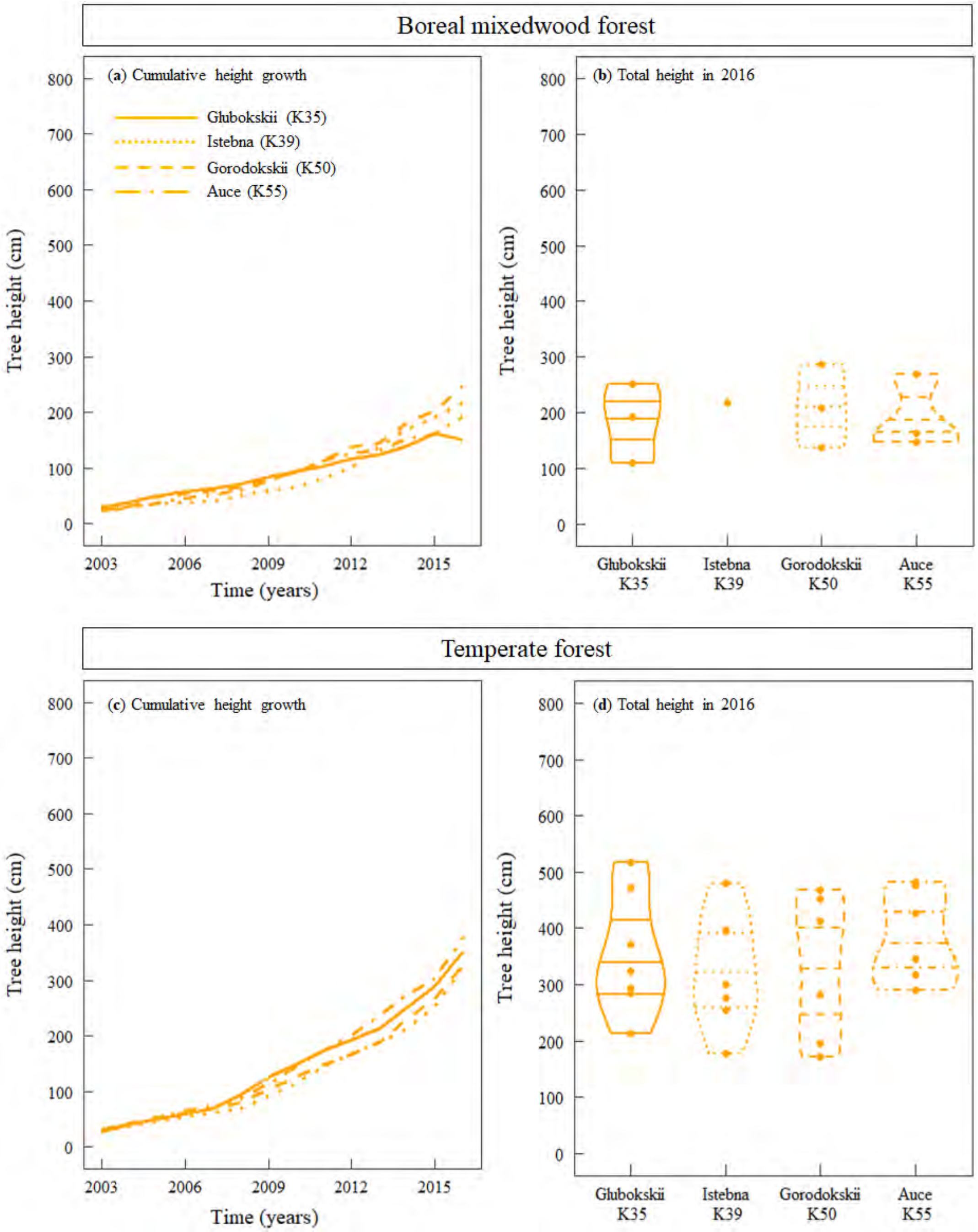

Figure B2 Cumulative height growth (lines) per Norway spruce seed sources at both sites (a and c). Violin plots (b and d) show the distribution of total tree height per seed sources and site. Each dot represents a tree.

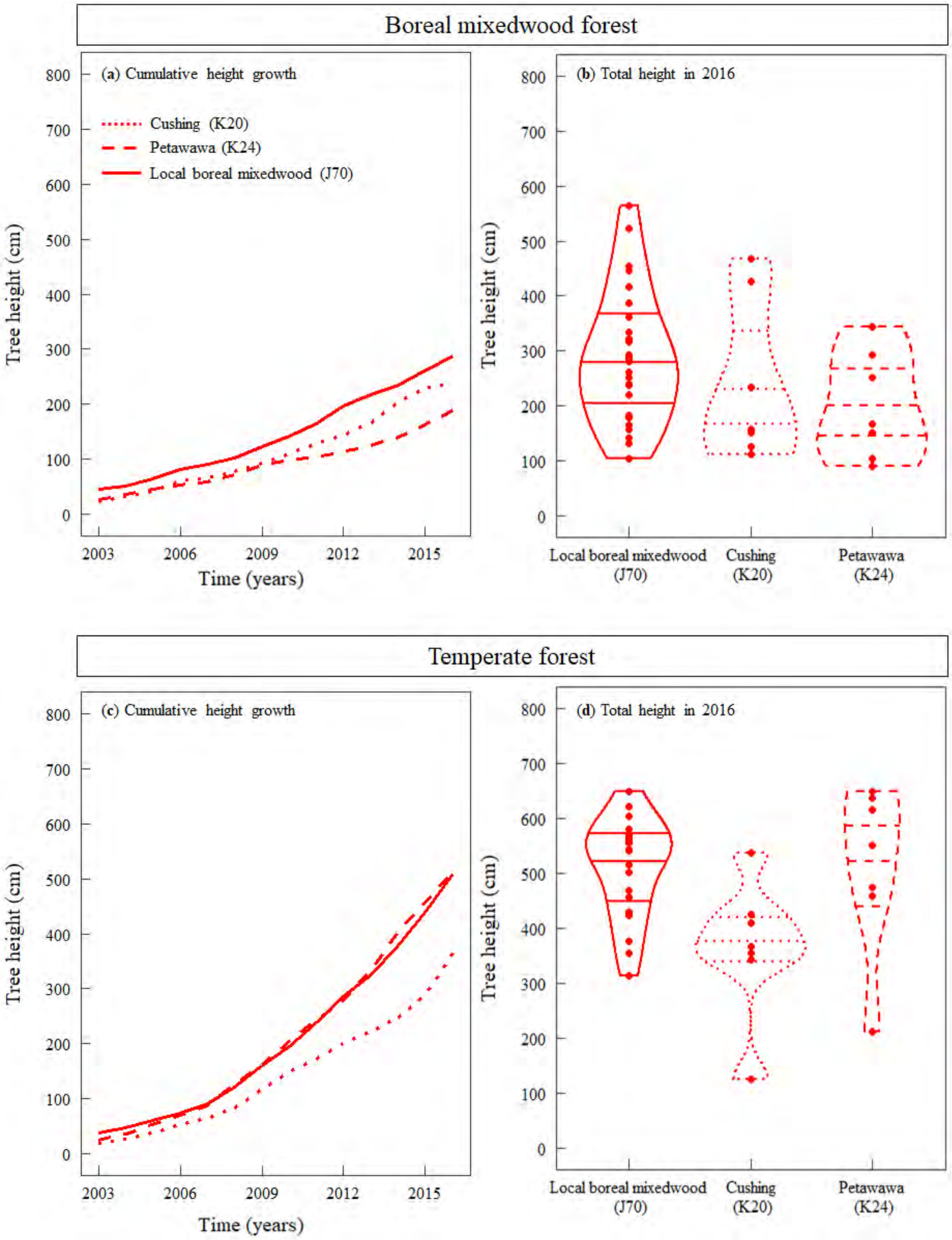

Figure B3 Cumulative height growth (lines) per white spruce seed sources at both sites (a and c). Violin plots (b and d) show the distribution of total tree height per seed sources and site. Each dot represents a tree.

Table B1 Description (locality and the geographic location) of the 41 seed sources present in both plantation sites. Boldface type indicates the eight seed sources that were selected in our specific study.

Species	Seed source	Locality	Latitude (°N)	Longitude (°E or °W)
Norway spruce	5397 (K34)	Auce, Latvia	56.25	22.50
Norway spruce	**5405 (K35)**	**Glubokskii, Belarus**	**55.15**	**30.10**
Norway spruce	5406 (K36)	Minskii, Belarus	53.50	27.35
Norway spruce	5411 (K37)	Istebna, Poland	49.33	48.55
Norway spruce	**5411 (K39)**	**Istebna, Poland**	**49.33**	**48.55**
Norway spruce	5411 (K40)	Istebna, Poland	49.33	48.55
Norway spruce	5423 (K41)	Borki, Poland	54.10	22.08
Norway spruce	5428 (K42)	Bialowieza, Poland	52.67	23.78
Norway spruce	5428 (K43)	Bialowieza, Poland	52.67	23.78
Norway spruce	5397 (K44)	Auce, Latvia	56.25	22.50
Norway spruce	5397 (K45)	Auce, Latvia	56.25	22.50
Norway spruce	5397 (K46)	Auce, Latvia	56.25	22.50
Norway spruce	5404 (K48)	Gorodokskii, Belarus	55.30	30.00
Norway spruce	5404 (K49)	Gorodokskii, Belarus	55.30	30.00
Norway spruce	**5404 (K50)**	**Gorodokskii, Belarus**	**55.30**	**30.00**
Norway spruce	5404 (K51)	Gorodokskii, Belarus	55.30	30.00
Norway spruce	5405 (K52)	Glubokskii, Belarus	55.15	30.10
Norway spruce	5405 (K53)	Glubokskii, Belarus	55.15	30.10
Norway spruce	5406 (K54)	Minskii, Belarus	53.50	27.35
Norway spruce	**5397 (K55)**	**Auce, Latvia**	**56.25**	**22.50**
White spruce	K04	Parc Algonquin, Ontario	45.50	78.30
White spruce	K05	Canton Franchère,	46.51	75.02
White spruce	K09	Cormac, Ontario	45.28	77.18
White spruce	K10	Beloil, Québec	45.34	73.12
White spruce	K11	Sunridge, Ontario	45.46	79.20

Table B1 (suite)

Species	**Seed source**	**Locality**	**Latitude (°N)**	**Longitude (°E or °W)**
White spruce	K12	Canton Bromley, Ontario	45.35	76.58
White spruce	K13	Parc Algonquin, Ontario	45.50	78.30
White spruce	K14	Petawawa, Ontario	45.54	77.20
White spruce	K16	Hungerford, Ontario	44.28	77.15
White spruce	K17	Hungerford, Ontario	44.28	77.15
White spruce	K18	Petawawa, Ontario	45.54	77.20
White spruce	K19	Canton Franchère, Québec	46.51	75.02
White spruce	**K20**	**Cushing, Québec**	**45.36**	**74.28**
White spruce	K21	Peterborough, Ontario	44.33	78.15
White spruce	K22	Carnavon, Ontario	45.04	78.42
White spruce	K23	Sunridge, Ontario	45.46	79.20
White spruce	**K24**	**Petawawa, Ontario**	**45.54**	**77.20**
White spruce	K25	St-Maurice, Québec	46.55	72.56
White spruce	K26	Lac des Quinze, Québec	47.06	70.45
White spruce	**J70**	**Duparquet, Quebec**	**48.29**	**79.26**
Black spruce	K32	Duparquet, Quebec	48.29	79.26

Table B2 Description of the climate at the location of origin of the six non-local seed sources used in this study for the 30 years period of 1981-2010.

Seed source (locality)	**Weather station (distance to locality)**	**Mean annual temp. in °C**	**Mean January temp. (min; max) in °C**	**Mean July temp. (min; max) in °C**	**Precipitation sum in mm**	**Growing degree-days (base temp. 0 °C)**	**Date with 0.10 probability of frost in spring (DOY)**
K35[1] (Glubokskii)	Smolensk (130 km)	5.5	-6.2 (-33; 9)	17.8 (5; 35)	738	2713	May 11th (131)
K39[1] (Istebna)	Bielsko-Biala (33 km)	8.5	-1.3 (-27; 15)	18.0 (4; 34)	944	3365	May 5th (125)
K50[1] (Gorodokskii)	Velikie-Luki (98 km)	5.8	-5.5 (-37; 11)	18.0 (3; 35)	639	2774	May 19th (139)
K55[1] (Auce)	Siauliai (62 km)	6.8	-2.8 (-32;11)	17.8 (6 ; 35)	614	2904	May 17th (137)
K20[2] (Cushing)	Lachute (12 km)	6.0	-10.7 (-37; 11)	20.4 (4; 35)	1151	3177	May 27th (147)
K24[2] (Petawawa)	Sheenboro (10 km)	5.0	-12.1 (-39; 11)	19.3 (1; 40)	853	2972	June 10th (161)

[1] Climate data for European seed sources were retrieved from the KNMI Climate Explorer (European Climate Assessment and Data) https://climexp.knmi.nl/start.cgi

[2] Climate data for Canadian seed sources were retrieved from Environment Canada (Climate normals) https://climate.weather.gc.ca/climate_normals/

Table B3 Results of linear regressions predicting the number of years needed to grow successive 50-cm intervals. Boldface type indicates statistically significant variables (alpha = 5%).

Height intervals	**Explanatory variables**	**Coefficients (SE)**	**P-value**
0-50	**Intercept: Norway spruce**	**2.07 (0.55)**	**2.63 X10^{-4}**
	Frost severity	**2.02 (1.02)**	**0.05**
	White spruce	-0.62 (0.39)	0.11
	Black spruce	**-1.14 (0.41)**	**6.12 X 10^{-3}**
50-100	**Intercept: Norway spruce**	**2.86 (0.38)**	**4.17 X 10^{-12}**
	Frost severity	**2.69 (0.63)**	**3.64 X 10^{-5}**
	White spruce	-0.51 (0.32)	0.11
	Black spruce	**-0.79 (0.34)**	**0.02**
100-150	**Intercept: Norway spruce**	**1.80 (0.23)**	**2.01 X 10^{-12}**
	Frost severity	**1.27 (0.47)**	**7.33 X 10^{-3}**
	White spruce	-0.33 (0.23)	0.16
	Black spruce	-0.34 (0.24)	0.15
151-200	**Intercept: Norway spruce**	**1.13 (0.19)**	**2.29 X 10^{-8}**
	Frost severity	**2.27 (0.39)**	**4.50 X 10^{-8}**
	White spruce	-0.04 (0.19)	0.84
	Black spruce	-0.16 (0.19)	0.42
201-250	**Intercept: Norway spruce**	**1.15 (0.17)**	**3.13 X 10^{-10}**
	Frost severity	0.66 (0.42)	0.12
	White spruce	-0.29 (0.17)	0.08
	Black spruce	**-0.42 (0.17)**	**0.01**

Table B3 (suite)

Height intervals	Explanatory variables	Coefficients (SE)	P-value
251-300	**Intercept: Norway spruce**	**1.10 (0.15)**	**1.89×10^{-10}**
	Frost severity	0.87 (0.37)	0.02
	White spruce	-0.13 (0.15)	0.39
	Black spruce	-0.11 (0.16)	0.48
301-350	**Intercept: Norway spruce**	**1.26 (0.22)**	**1.20×10^{-7}**
	Frost severity	0.41 (0.51)	0.43
	White spruce	-0.16 (0.25)	0.50
	Black spruce	-0.09 (0.24)	0.70
351-400	**Intercept: Norway spruce**	**0.70 (0.18)**	**1.71×10^{-4}**
	Frost severity	0.68 (0.44)	0.13
	White spruce	5.67×10^{-5} (0.22)	0.99
	Black spruce	0.31 (0.22)	0.15

Table B4 Result of the model selection based on AICc and AICc weights to determine the best climate variable predicting annual height increment of spruce trees. The best climate model is shown in bold.

Climate models	**Parameters**	**AICc**	**Delta AICc**	**AICc Wt.**	**Cum. Wt.**
Min. Temp. May	**11**	**6191.96**	**0.00**	**1.00**	**1.00**
Max. Temp. Oct.	11	6222.00	30.04	0.00	1.00
Max. Temp. Jun.	11	6229.07	37.12	0.00	1.00
Frost Freq. Dec.	11	6235.36	43.41	0.00	1.00
Min. Temp. Aug.	11	6249.36	57.40	0.00	1.00
Max. Temp. Feb.	11	6251.03	59.07	0.00	1.00
Max. Temp. Apr.	11	6251.13	59.18	0.00	1.00
Max. Temp. Jan.	9	6256.08	64.12	0.00	1.00
Frost Freq. Feb.	11	6256.31	64.35	0.00	1.00
Min. Temp. Mar.	11	6260.03	68.08	0.00	1.00
Max. Temp. Dec.	11	6260.29	68.33	0.00	1.00
Frost. Freq. Mar.	11	6261.79	69.84	0.00	1.00
Min. Temp. Dec.	11	6265.28	73.33	0.00	1.00
Frost. Freq. Jan.	11	6267.28	75.33	0.00	1.00
Max. Temp. Nov.	11	6267.45	75.49	0.00	1.00
Min. Temp. Jan.	11	6274.46	82.50	0.00	1.00
Max. Temp. Jul.	11	6277.88	85.93	0.00	1.00
Mean summer temp.	11	6278.31	86.35	0.00	1.00
Max. Temp. Aug.	11	6278.97	87.01	0.00	1.00

(Table B4 suite)

Climate models	**Parameters**	**AICc**	**Delta AICc**	**AICc Wt.**	**Cum. Wt.**
Min. Temp. Apr.	11	6280.07	88.11	0.00	1.00
Max. Temp. Sep.	11	6280.58	88.63	0.00	1.00
Frost Freq. Nov.	11	6281.63	89.68	0.00	1.00
Frost Freq. May	11	6283.03	91.08	0.00	1.00
Min. Temp. Feb.	11	6285.34	93.39	0.00	1.00
Frost Freq. Oct.	11	6286.40	94.44	0.00	1.00
Min. Temp. Oct.	11	6287.93	95.97	0.00	1.00
Frost Freq. Jun.	11	6290.11	98.15	0.00	1.00
Frost Freq. Sep.	11	6290.21	98.26	0.00	1.00
Min. Temp. Jun.	11	6293.12	101.16	0.00	1.00
Max. Temp. May	11	6294.52	102.56	0.00	1.00
Max. Temp. Mar.	11	6295.01	103.05	0.00	1.00
Frost Freq. Apr.	11	6295.04	103.09	0.00	1.00
Species and site	7	6299.44	107.49	0.00	1.00
Min. Temp. Jul.	11	6300.16	108.20	0.00	1.00
Mean annual temp.	11	6301.71	109.75	0.00	1.00
Min. Temp. Sep.	11	6302.55	110.60	0.00	1.00
Min. Temp. Nov.	11	6305.04	113.08	0.00	1.00
Intercept only	4	6351.94	159.98	0.00	1.00

Table B5 Summary statistics (coefficients and standard error) for the mixed effect model predicting annual height increment of spruce trees from minimum May temperature at the inter-species level. Coefficients whose standard error does not include zero are shown in bold. (n= 2235, pseudo R^2 = 0.57, AICc = 6192).

Variables	**Box-cox transformed coefficients (SE)**
Intercept (Temperate site; Norway spruce)	**3.33 (0.21)**
Minimum May temperature	**0.44 (0.07)**
Boreal site	**-0.70 (0.10)**
White spruce	**0.43 (0.13)**
Black spruce	**0.75 (0.14)**
Minimum May temperature × Boreal site	**-0.52 (0.05)**
Minimum May temperature × White spruce	-0.01 (0.05)
Minimum May temperature × Black spruce	0.03 (0.06)

Table B6 Summary statistics (coefficients and standard error) for the mixed effect model predicting annual height increment of spruce trees from minimum May temperature at the intra-species level. Coefficients whose standard error does not include zero are shown in bold. (n= 2235, pseudo $R^2 = 0.57$, AICc = 6204).

Variables	**Box-cox transformed coefficients (SE)**
Intercept (temperate site, white spruce J70)	**3.89 (0.21)**
Minimum May temperature	**0.43 (0.07)**
Boreal site	**-0.72 (0.10)**
White spruce (K20)	**-0.41 (0.19)**
White spruce (K24)	-0.28 (0.19)
Black spruce (K32)	0.20 (0.12)
Norway spruce (K35)	**-0.57 (0.21)**
Norway spruce (K39)	**-0.65 (0.24)**
Norway spruce (K50)	**-0.59 (0.22)**
Norway spruce (K55)	**-0.45 (0.21)**
Minimum May temperature × Boreal site	**-0.52 (0.05)**
Minimum May temperature × White spruce (K20)	0.01 (0.07)
Minimum May temperature × White spruce (K24)	0.01 (0.08)
Minimum May temperature × Black spruce (K32)	0.04 (0.05)
Minimum May temperature × Norway spruce (K35)	-0.02 (0.09)
Minimum May temperature × Norway spruce (K39)	0.07 (0.11)
Minimum May temperature × Norway spruce (K50)	-0.05 (0.10)
Minimum May temperature × Norway spruce (K55)	0.06 (0.09)

ANNEXE C

SUPPORTING INFORMATION AND RESULTS FOR
CHAPITRE III

DISENTANGLING THE EFFECT OF TOPOGRAPHY AND MICROTOPOGRAPHY ON NEAR-GROUND SUMMER FROSTS AT THE BOREAL-TEMPERATE FOREST ECOTONE (QUÉBEC, CANADA)

Table C1 Regression coefficient and standard error showing the near-ground air temperature variations per hour. Boldface type indicate coefficients that differ from zero.

Variable	**Coefficient (SE)**
Intercept: midnight hour 0	**10.30 (1.26)**
Hour 1	**-0.50 (0.03)**
Hour 2	**-0.89 (0.03)**
Hour 3	**-1.24 (0.03)**
Hour 4	**-1.49 (0.03)**
Hour 5	**-1.69 (0.03)**
Hour 6	**-1.17 (0.03)**
Hour 7	**0.97 (0.03)**
Hour 8	**3.67 (0.03)**
Hour 9	**5.68 (0.03)**
Hour 10	**7.46 (0.03)**
Hour 11	**8.94 (0.03)**
Hour 12	**10.05 (0.03)**
Hour 13	**10.90 (0.03)**
Hour 14	**11.33 (0.03)**
Hour 15	**11.33 (0.03)**
Hour 16	**10.92 (0.03)**
Hour 17	**10.20 (0.03)**
Hour 18	**9.05 (0.03)**
Hour 19	**7.30 (0.03)**
Hour 20	**4.88 (0.03)**
Hour 21	**2.64 (0.03)**
Hour 22	**1.37 (0.03)**
Hour 23	**0.63 (0.03)**

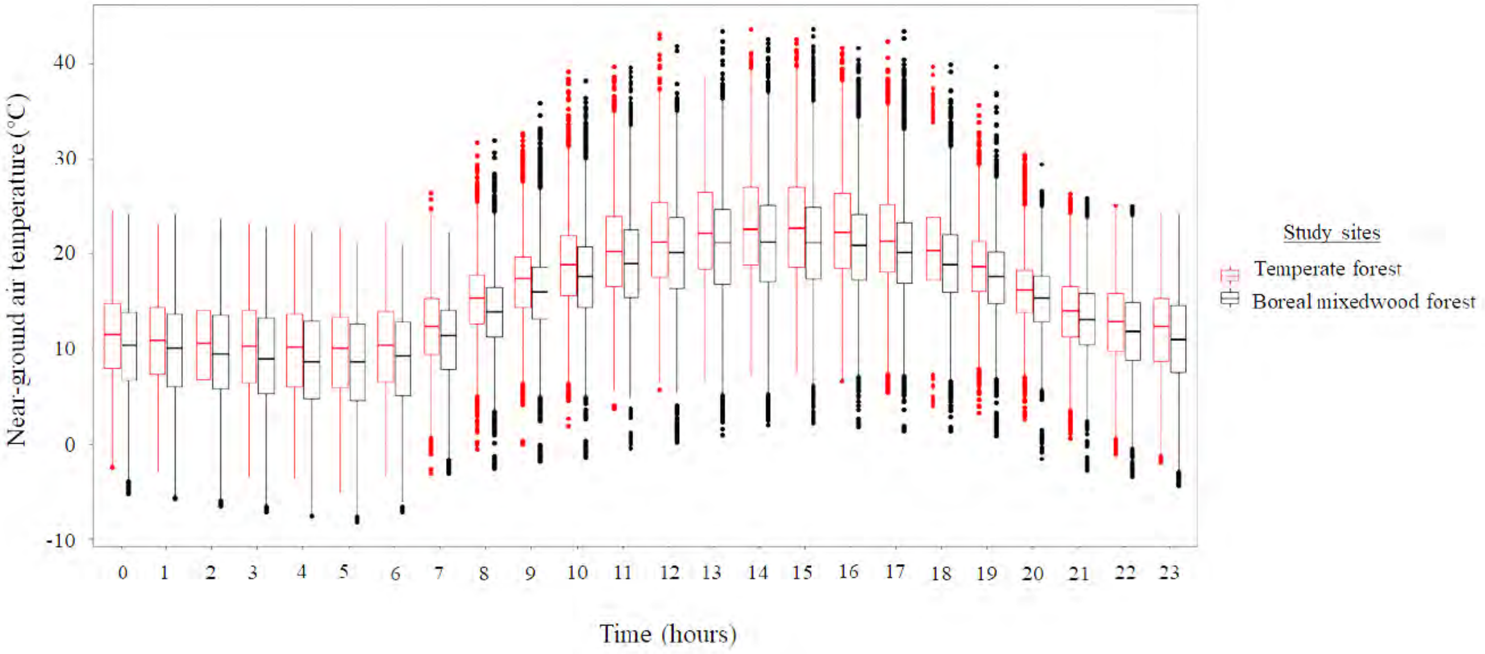

Figure C1 Observed distributions (boxplots) showing the diurnal cycle of near-ground air temperature at both sites. The boxes show the 25th and 75th percentiles, and the dashed lines represent the medians.

Table C2 List of the 31 candidate models used to determine the best permanent landscape attributes (elevation [Elev] and slope angle) predicting the daily minimum near-ground air temperature and frost probability at 5:00 am.

Model	**Variables**	**Interactions**
1	1	NA
2	Site	NA
3	Slope-1m	NA
4	Elev	NA
5	Site; Slope-1m	NA
6	Site; Elev	NA
7	Slope-1m; Elev	NA
8	Site, Slope-1m, Elev	NA
9	Site; Slope-1m	Site × Slope-1m
10	Site; Elev	Site × Elev
11	Slope-1m; Elev	Slope-1m × Elev
12	Site, Slope-1m, Elev	Site × Slope-1m
13	Site, Slope-1m, Elev	Site × Elev
14	Site, Slope-1m, Elev	Slope-1m × Elev
15	Site, Slope-1m, Elev	Site × Slope-1m; Site × Elev
16	Site, Slope-1m, Elev	Site × Slope-1m; Slope-1m × Elev
17	Site, Slope-1m, Elev	Site × Elev; Slope-1m × Elev
18	Site, Slope-1m, Elev	Site × Slope-1m; Site × Elev; Slope-1m × Elev
19	Slope-20m	NA
20	Site; Slope-20m	NA

(Table C2 suite)

Model	**Variables**	**Interactions**
21	Slope-20m; Elev	NA
22	Site, Slope-20m, Elev	NA
23	Site; Slope-20m	Site × Slope-20m
24	Slope-20m; Elev	Slope-20m × Elev
25	Site, Slope-20m, Elev	Site × Slope-20m
26	Site, Slope-20m, Elev	Site × Elev
27	Site, Slope-20m, Elev	Slope-20m × Elev
28	Site, Slope-20m, Elev	Site × Slope-20m; Site × Elev
29	Site, Slope-20m, Elev	Site × Slope-20m; Slope-20m × Elev
30	Site, Slope-20m, Elev	Site × Elev; Slope-20m × Elev
31	Site, Slope-20m, Elev	Site × Slope-20m; Site × Elev; Slope-20m × Elev

Table C3 List of the 18 candidate models used to experimentally determine the importance of height above the ground (Height_AG) and elevation (Elev) on the daily minimum near-ground air temperature and on frost probability at 5:00 am.

Model	Variables	Interactions
1	1	NA
2	Site	NA
3	Height_AG	NA
4	Elev	NA
5	Site; Height_AG	NA
6	Site; Elev	NA
7	Height_AG; Elev	NA
8	Site, Height_AG, Elev	NA
9	Site; Height_AG	Site × Elev
10	Site; Elev	Site × Elevation
11	Height_AG; Elev	Height_AG × Elev
12	Site, Height_AG, Elev	Site × Height_AG
13	Site, Height_AG, Elev	Site × Elev
14	Site, Height_AG, Elev	Height_AG × Elev
15	Site, Height_AG, Elev	Site × Height_AG; Site × Elev
16	Site, Height_AG, Elev	Site × Height_AG; Height_AG × Elev
17	Site, Height_AG, Elev	Site × Elev; Height_AG × Elev
18	Site, Height_AG, Elev	Site × Height_AG; Site × Elev; Height_AG × Elev

Table C4 Importance of landscape attributes at predicting minimum near-ground air temperature on the 41 frost days upon AICc and cumulative AICc weights; boldface type indicates the selected models and numbers in parentheses before each model refer to the candidate models prior to selection (Table C2).

Model	**AICc**	**Delta AICc**	**AICc Wt.**	**Cum. Wt.**	**Marginal pseudo-R^2 (conditional)**
(18) Site, Slope-1m, Elev; Site × Slope-1m; Site × Elev; Slope-1m × Elev	**21293.67**	**0.00**	**0.43**	**0.43**	**0.12 (0.80)**
(17) Site, Slope-1m, Elev; Site × Elev; Slope-1m × Elev	**21293.96**	**0.29**	**0.37**	**0.79**	**0.12 (0.80)**
(30) Site, Slope-20m, Elev; Site × Elev; Slope-20m × Elev	21296.75	3.08	0.09	0.88	0.12 (0.80)
(31) Site, Slope-20m, Elev; Site × Slope-20m; Site × Elev; Slope-20m × Elev	21297.10	3.43	0.08	0.96	0.12 (0.80)
(28) Site, Slope-20m, Elev Site × Slope-20m; Site × Elev	21300.82	7.15	0.01	0.97	0.12 (0.80)
(15) Site, Slope-1m, Elev; Site × Slope-1m; Site × Elev	21301.24	7.57	0.01	0.98	0.12 (0.80)
(14) Site, Slope-1m, Elev; Slope-1m × Elev	21302.24	8.57	0.01	0.99	0.12 (0.80)

Table C4 (suite)

Model	**AICc**	**Delta AICc**	**AICc Wt.**	**Cum. Wt.**	**Marginal pseudo-*R*^{2} (conditional)**
(27) Site, Slope-20m, Elev; Slope-20m × Elev	21303.61	9.94	0.00	0.99	0.12 (0.80)
(26) Site, Slope-20m, Elev; Site × Elev	21304.03	10.36	0.00	0.99	0.12 (0.80)
(16) Site, Slope-1m, Elev; Site × Slope-1m; Slope-1m × Elev	21304.10	10.43	0.00	1.00	0.12 (0.80)
(25) Site, Slope-20m, Elev; Site × Slope-20m	21304.56	10.89	0.00	1.00	0.12 (0.80)
(29) Site, Slope-20m, Elev; Site × Slope-20m; Slope-20m × Elev	21305.60	11.93	0.00	1.00	0.12 (0.80)
(12) Site, Slope-1m, Elev; Site × Slope-1m	21306.18	12.52	0.00	1.00	0.12 (0.80)
(22) Site, Slope-20m, Elev	21307.70	14.03	0.00	1.00	0.12 (0.80)
(13) Site, Slope-1m, Elev; Site × Elev	21308.15	14.48	0.00	1.00	0.12 (0.80)
(8) Site, Slope-1m, Elev	21314.00	20.33	0.00	1.00	0.11 (0.80)
(10) Site; Elev; Site × Elev	21325.49	31.82	0.00	1.00	0.11 (0.80)
(6) Site; Elev	21337.25	43.58	0.00	1.00	0.11 (0.80)
(20) Site; Slope-20m	21408.15	114.48	0.00	1.00	0.09 (0.80)
(5) Site; Slope-1m	21408.85	115.19	0.00	1.00	0.09 (0.80)

(Table C4 suite)

Model	**AICc**	**Delta AICc**	**AICc Wt.**	**Cum. Wt.**	**Marginal pseudo-R^2 (conditional)**
(23) Site; Slope-20m; Site × Slope-20m	21409.78	116.11	0.00	1.00	0.08 (0.80)
(9) Site; Slope-1m; Site × Slope-1m	21410.66	116.99	0.00	1.00	0.09 (0.80)
(2) Site	21411.96	118.29	0.00	1.00	0.08 (0.80)
(24) Slope-20m; Elev Slope-20m × Elev	21533.95	240.28	0.00	1.00	0.03 (0.80)
(11) Slope-1m; Elev; Slope-1m × Elev	21536.03	242.36	0.00	1.00	0.03 (0.80)
(4) Elev	21541.23	247.56	0.00	1.00	0.02 (0.80)
(7) Slope-1m; Elev	21542.90	249.23	0.00	1.00	0.03 (0.80)
(21) Slope-20m; Elev	21542.99	249.32	0.00	1.00	0.02 (0.80)
(1) 1	21574.29	280.62	0.00	1.00	0.00 (0.80)
(3) Slope-1m	21575.49	281.82	0.00	1.00	0.00 (0.80)
(19) Slope-20m	21575.84	282.18	0.00	1.00	0.00 (0.80)

Table C5 Importance of landscape attributes at predicting minimum near-ground air temperature on the 170 days where night frost did not occur upon AICc and cumulative AICc weights; boldface type indicates the selected models and numbers in parentheses before each model refer to the candidate models prior to selection (Table C2).

Model	**AICc**	**Delta AICc**	**AICc Wt.**	**Cum. Wt.**	**Marginal pseudo-R^2 (conditional)**
(18) Site, Slope-1m, Elev; Site × Slope-1m; Site × Elev; Slope-1m × Elev	**134703.90**	**0.00**	**0.50**	**0.50**	**0.00 (0.87)**
(31) Site, Slope-20m, Elev; Site × Slope-20m; Site × Elev; Slope-20m × Elev	134705.20	1.31	0.12	0.76	0.00 (0.87)
(17) Site, Slope-1m, Elev; Site × Elev; Slope-1m × Elev	134706.80	2.86	0.09	0.88	0.00 (0.87)
(30) Site, Slope-20m, Elev; Site × Elev; Slope-20m × Elev	134707.40	3.46	0.01	0.97	0.00 (0.87)
(28) Site, Slope-20m, Elev Site × Slope-20m; Site × Elev	134711.80	7.82	0.01	0.98	0.00 (0.87)
(15) Site, Slope-1m, Elev; Site × Slope-1m; Site × Elev	134712.20	8.27	0.01	0.99	0.00 (0.87)
(26) Site, Slope-20m, Elev; Site × Elev	134712.50	8.51	0.01	0.99	0.00 (0.87)
(13) Site, Slope-1m, Elev; Site × Elev	134712.90	8.98	0.01	1.00	0.00 (0.87)

(Table C5 suite)

Model	**AICc**	**Delta AICc**	**AICc Wt.**	**Cum. Wt.**	**Marginal pseudo-*R*^{2} (conditional)**
(27) Site, Slope-20m, Elev; Slope-20m × Elev	134719.20	15.22	0.00	1.00	0.00 (0.87)
(14) Site, Slope-1m, Elev; Slope-1m × Elev	134719.20	15.29	0.00	1.00	0.00 (0.87)
(25) Site, Slope-20m, Elev; Site × Slope-20m	134720.20	16.27	0.00	1.00	0.00 (0.87)
(16) Site, Slope-1m, Elev; Site × Slope-1m; Slope-1m × Elev	134720.50	16.61	0.00	1.00	0.00 (0.87)
(22) Site, Slope-20m, Elev	134720.90	16.93	0.00	1.00	0.00 (0.87)
(29) Site, Slope-20m, Elev; Site × Slope-20m; Slope-20m × Elev	134721.10	17.17	0.00	1.00	0.00 (0.87)
(12) Site, Slope-1m, Elev; Site × Slope-1m	134722.00	18.07	0.00	1.00	0.00 (0.87)
(8) Site, Slope-1m, Elev	134723.50	19.57	0.00	1.00	0.00 (0.87)
(10) Site; Elev; Site × Elev	134728.00	24.10	0.00	1.00	0.00 (0.87)
(6) Site; Elev	134745.40	41.51	0.00	1.00	0.00 (0.87)
(5) Site; Slope-1m	134835.20	131.31	0.00	1.00	0.00 (0.87)
(20) Site; Slope-20m	134835.50	131.58	0.00	1.00	0.00 (0.87)
(23) Site; Slope-20m; Site × Slope-20m	134836.00	132.07	0.00	1.00	0.00 (0.87)
(2) Site	134836.50	132.55	0.00	1.00	0.00 (0.87)
(9) Site; Slope-1m; Site × Slope-1m	134836.70	132.81	0.00	1.00	0.00 (0.87)

(Table C5 suite)

Model	**AICc**	**Delta AICc**	**AICc Wt.**	**Cum. Wt.**	**Marginal pseudo-R^2 (conditional)**
(24) Slope-20m; Elev Slope-20m × Elev	134914.80	210.87	0.00	1.00	0.00 (0.87)
(11) Slope-1m; Elev; Slope-1m × Elev	134918.60	214.67	0.00	1.00	0.00 (0.87)
(4) Elev	134920.40	216.45	0.00	1.00	0.00 (0.87)
(21) Slope-20m; Elev	134922.20	218.31	0.00	1.00	0.00 (0.87)
(7) Slope-1m; Elev	134922.30	218.33	0.00	1.00	0.00 (0.87)
(1) 1	134928.90	224.93	0.00	1.00	0.00 (0.87)
(3) Slope-1m	134930.60	226.65	0.00	1.00	0.00 (0.87)
(19) Slope-20m	134930.60	226.71	0.00	1.00	0.00 (0.87)

Table C6 Importance of landscape attributes at predicting minimum near-ground air temperature on the 211 days the study lasted upon AICc and cumulative AICc weights; boldface type indicates the selected models and numbers in parentheses before each model refer to the candidate models prior to selection (Table C2).

Model	**AICc**	**Delta AICc**	**AICc Wt.**	**Cum. Wt.**	**Marginal pseudo-R^2 (conditional)**
(18) Site, Slope-1m, Elev; Site × Slope-1m; Site × Elev; Slope-1m × Elev	**183714.80**	**0.00**	**0.58**	**0.58**	**0.01 (0.80)**
(31) Site, Slope-20m, Elev; Site × Slope-20m; Site × Elev; Slope-20m × Elev	183716.20	1.35	0.29	0.87	0.00 (0.80)
(17) Site, Slope-1m, Elev; Site × Elev; Slope-1m × Elev	183719.60	4.76	0.05	0.92	0.00 (0.80)
(30) Site, Slope-20m, Elev; Site × Elev; Slope-20m × Elev	183720.60	5.76	0.03	0.96	0.00 (0.80)
(16) Site, Slope-1m, Elev; Site × Slope-1m; Slope-1m × Elev	183723.00	8.20	0.01	0.97	0.00 (0.80)
(13) Site, Slope-1m, Elev; Site × Elev	183723.60	8.80	0.01	0.97	0.00 (0.80)
(14) Site, Slope-1m, Elev; Slope-1m × Elev	183723.70	8.88	0.01	0.98	0.00 (0.80)
(15) Site, Slope-1m, Elev; Site × Slope-1m; Site × Elev	183724.40	9.53	0.00	0.99	0.00 (0.80)

(Table C6 suite)

Model	**AICc**	**Delta AICc**	**AICc Wt.**	**Cum. Wt.**	**Marginal pseudo-R^2 (conditional)**
(27) Site, Slope-20m, Elev; Slope-20m × Elev	183725.20	10.41	0.00	0.99	0.00 (0.80)
(28) Site, Slope-20m, Elev Site × Slope-20m; Site × Elev	183725.70	10.90	0.00	0.99	0.00 (0.80)
(29) Site, Slope-20m, Elev; Site × Slope-20m; Slope-20m × Elev	183725.90	11.07	0.00	0.99	0.00 (0.80)
(26) Site, Slope-20m, Elev; Site × Elev	183726.00	11.17	0.00	1.00	0.00 (0.80)
(8) Site, Slope-1m, Elev	183726.80	11.96	0.00	1.00	0.00 (0.80)
(12) Site, Slope-1m, Elev; Site × Slope-1m	183727.10	12.31	0.00	1.00	0.00 (0.80)
(25) Site, Slope-20m, Elev; Site × Slope-20m	183728.00	13.15	0.00	1.00	0.00 (0.80)
(22) Site, Slope-20m, Elev	183728.30	13.44	0.00	1.00	0.00 (0.80)
(10) Site; Elev; Site × Elev	183737.30	22.45	0.00	1.00	0.00 (0.80)
(6) Site; Elev	183745.10	30.28	0.00	1.00	0.00 (0.80)
(5) Site; Slope-1m	183824.70	109.84	0.00	1.00	0.00 (0.80)
(9) Site; Slope-1m; Site × Slope-1m	183825.60	110.80	0.00	1.00	0.00 (0.80)
(2) Site	183825.60	110.80	0.00	1.00	0.00 (0.80)
(20) Site; Slope-20m	183825.90	111.04	0.00	1.00	0.00 (0.80)
(23) Site; Slope-20m; Site × Slope-20m	183826.60	111.73	0.00	1.00	0.00 (0.80)

(Table C6 suite)

Model	**AICc**	**Delta AICc**	**AICc Wt.**	**Cum. Wt.**	**Marginal pseudo-R^2 (conditional)**
(24) Slope-20m; Elev Slope-20m × Elev	183899.10	184.27	0.00	1.00	0.00 (0.80)
(11) Slope-1m; Elev; Slope-1m × Elev	183905.00	190.13	0.00	1.00	0.00 (0.80)
(4) Elev	183906.20	191.37	0.00	1.00	0.00 (0.80)
(21) Slope-20m; Elev	183907.80	192.95	0.00	1.00	0.00 (0.80)
(7) Slope-1m; Elev	183908.10	193.23	0.00	1.00	0.00 (0.80)
(1) 1	183915.20	200.36	0.00	1.00	0.00 (0.80)
(19) Slope-20m	183916.60	201.81	0.00	1.00	0.00 (0.80)
(3) Slope-1m	183916.90	202.05	0.00	1.00	0.00 (0.80)

Table C7 Results of the linear mixed regression models showing the coefficients and standard errors for the best landscape attributes predicting minimum near-ground air temperature using all 211 dates; boldface type indicates coefficients that differ from zero.

Variable	**All days (n= 33 880) standardized coefficients (SE)**
Intercept: Temperate forest	**8.89 (2.49)**
Boreal mixedwood forest	**-2.10 (0.13)**
Elevation	**0.48 (0.08)**
Slope1m	**0.09 (0.08)**
Elevation × Boreal mixedwood forest	**0.41 (0.13)**
Slope1m × Elevation	**-0.27 (0.08)**
Slope1m × Boreal mixedwood forest	**0.43 (0.16)**

Table C8 Importance of landscape attributes at predicting near-ground probability of frost occurrence on the 41 days where night frost did occur upon AICc and cumulative AICc weights; boldface type indicates the selected models and numbers in parentheses before each model refer to the candidate models prior to selection (Table C2).

Model	**AICc**	**Delta AICc**	**AICc Wt.**	**Cum. Wt.**	**Marginal pseudo-R^2 (conditional)**
(31) Site, Slope-20m, Elev; Site × Slope-20m; Site × Elev; Slope-20m × Elev	**3137.16**	**0.00**	**0.95**	**0.95**	**0.16 (0.85)**
(18) Site, Slope-1m, Elev; Site × Slope-1m; Site × Elev; Slope-1m × Elev	3144.01	6.85	0.03	0.98	0.15 (0.85)
(30) Site, Slope-20m, Elev; Site × Elev; Slope-20m × Elev	3146.06	8.90	0.01	0.99	0.15 (0.85)
(17) Site, Slope-1m, Elev; Site × Elev; Slope-1m × Elev	3147.40	10.24	0.01	1.00	0.15 (0.85)
(28) Site, Slope-20m, Elev; Site × Slope-20m; Site × Elev	3152.43	15.27	0.00	1.00	0.15 (0.85)
(26) Site, Slope-20m, Elev; Site × Elev	3152.50	15.34	0.00	1.00	0.15 (0.85)
(15) Site, Slope-1m, Elev; Site × Slope-1m; Site × Elev	3154.96	17.79	0.00	1.00	0.15 (0.85)
(13) Site, Slope-1m, Elev; Site × Elev	3158.01	20.85	0.00	1.00	0.15 (0.85)
(27) Site, Slope-20m, Elev; Slope-20m × Elev	3161.84	24.68	0.00	1.00	0.15 (0.85)

(Table C8 suite)

Model	**AICc**	**Delta AICc**	**AICc Wt.**	**Cum. Wt.**	**Marginal pseudo-R^2 (conditional)**
(29) Site, Slope-20m, Elev; Site × Slope-20m; Slope-20m × Elev	3162.94	25.78	0.00	1.00	0.15 (0.85)
(25) Site, Slope-20m, Elev; Site × Slope-20m	3164.02	26.86	0.00	1.00	0.15 (0.85)
(22) Site, Slope-20m, Elev	3164.22	27.05	0.00	1.00	0.15 (0.85)
(14) Site, Slope-1m, Elev; Slope-1m × Elev	3164.84	27.68	0.00	1.00	0.15 (0.85)
(16) Site, Slope-1m, Elev; Site × Slope-1m; Slope-1m × Elev	3166.51	29.35	0.00	1.00	0.15 (0.85)
(12) Site, Slope-1m, Elev; Site × Slope-1m	3168.21	31.05	0.00	1.00	0.15 (0.85)
(10) Site; Elev; Site × Elev	3169.73	32.57	0.00	1.00	0.14 (0.85)
(8) Site, Slope-1m, Elev	3172.66	35.49	0.00	1.00	0.15 (0.85)
(6) Site; Elev	3190.81	53.65	0.00	1.00	0.14 (0.85)
(23) Site; Slope-20m; Site × Slope-20m	3294.14	156.97	0.00	1.00	0.09 (0.85)
(20) Site; Slope-20m	3294.67	157.50	0.00	1.00	0.09 (0.85)
(5) Site; Slope-1m	3295.81	158.65	0.00	1.00	0.09 (0.85)
(2) Site	3296.01	158.84	0.00	1.00	0.09 (0.85)
(9) Site; Slope-1m; Site × Slope-1m	3297.65	160.49	0.00	1.00	0.09 (0.85)
(24) Slope-20m; Elev; Slope-20m × Elev	3382.81	245.65	0.00	1.00	0.02 (0.85)

(Table C8 suite)

Model	**AICc**	**Delta AICc**	**AICc Wt.**	**Cum. Wt.**	**Marginal pseudo-R^2 (conditional)**
(11) Slope-1m; Elev; Slope-1m × Elev	3384.82	247.66	0.00	1.00	0.02 (0.85)
(4) Elev	3387.88	250.72	0.00	1.00	0.02 (0.85)
(7) Slope-1m; Elev	3389.39	252.23	0.00	1.00	0.00 (0.85)
(21) Slope-20m; Elev	3389.71	252.55	0.00	1.00	0.01 (0.85)
(1) 1	3398.15	260.99	0.00	1.00	0.01 (0.85)
(3) Slope-1m	3399.31	262.15	0.00	1.00	0.00 (0.85)
(19) Slope-20m	3399.85	262.68	0.00	1.00	0.01 (0.85)

Table C9 Importance of the height above ground at predicting minimum near-ground air temperature on the 14 days where night frost did occur in 2017 upon AICc and cumulative AICc weights; boldface type indicates the selected models and numbers in parentheses before each model refer to the candidate models prior to selection (Table C3).

Model	**AICc**	**Delta AICc**	**AICc Wt.**	**Cum. Wt.**	**Marginal pseudo-R^2 (conditional)**
(18) Site, Height_AG, Elev; Site × Elev; Height_AG × Elev	**1268.82**	**0.00**	**0.90**	**0.90**	**0.31 (0.94)**
(15) Site, Height_AG, Elev; Site × Height_AG; Site × Elev	1273.57	4.75	0.08	0.99	0.31 (0.94)
(9) Site; Height_AG; Site × Height_AG	1278.88	10.06	0.01	0.99	0.32 (0.94)
(12) Site, Height_AG, Elev; Site × Height_AG	1279.03	10.20	0.01	1.00	0.31 (0.94)
(16) Site, Height_AG, Elev; Site × Height_AG; Height_AG × Elev	1280.52	11.70	0.00	1.00	0.31 (0.94)
(17) Site, Height_AG, Elev; Site × Elev; Height_AG × Elev	1295.40	26.58	0.00	1.00	0.33 (0.93)
(10) Site; Elev; Site × Elev	1297.72	28.90	0.00	1.00	0.33 (0.93)
(13) Site, Height_AG, Elev; Site × Elev	1299.42	30.60	0.00	1.00	0.33 (0.93)
(2) Site	1300.98	32.16	0.00	1.00	0.33 (0.92)
(6) Site; Elev	1301.66	32.84	0.00	1.00	0.33 (0.93)
(5) Site; Height_AG	1302.98	34.15	0.00	1.00	0.33 (0.93)
(8) Site, Height_AG, Elev	1303.60	34.78	0.00	1.00	0.33 (0.93)

(Table C9 suite)

Model	**AICc**	**Delta AICc**	**AICc Wt.**	**Cum. Wt.**	**Marginal pseudo-R^2 (conditional)**
(14) Site, Height_AG, Elev; Height_AG × Elev	1305.26	36.44	0.00	1.00	0.33 (0.93)
(7) Height_AG; Elev	1348.36	79.54	0.00	1.00	0.33 (0.95)
(3) Height_AG	1349.50	80.68	0.00	1.00	0.33 (0.95)
(11) Height_AG; Elev; Height_AG × Elev	1349.73	80.91	0.00	1.00	0.33 (0.95)
(1) 1	1978.35	709.53	0.00	1.00	0.00 (0.69)
(4) Elev	1978.39	709.57	0.00	1.00	0.00 (0.69)

Table C10 Importance of the height above ground at predicting minimum near-ground air temperature on the 89 days where night frost did not occur in 2017 upon AICc and cumulative AICc weights; boldface type indicates the selected models and numbers in parentheses before each model refer to the candidate models prior to selection (Table C3).

Model	**AICc**	**Delta AICc**	**AICc Wt.**	**Cum. Wt.**	**Marginal pseudo-R^2 (conditional)**
(15) Site, Height_AG, Elev; Site × Height_AG; Site × Elev	**8961.61**	**0.00**	**0.31**	**0.31**	**0.04 (0.88)**
(12) Site, Height_AG, Elev; Site × Height_AG	**8962.05**	**0.44**	**0.25**	**0.55**	**0.04 (0.88)**
(16) Site, Height_AG, Elev; Site × Height_AG; Height_AG × Elev	**8962.81**	**1.20**	**0.17**	**0.72**	**0.04 (0.88)**
(9) Site; Height_AG; Site × Height_AG	**8963.48**	**1.87**	**0.12**	**0.84**	**0.04 (0.88)**
(18) Site, Height_AG, Elev; Site × Elev; Height_AG × Elev	**8963.54**	**1.93**	**0.12**	**0.96**	**0.04 (0.88)**
(13) Site, Height_AG, Elev; Site × Elev	8968.69	7.08	0.01	0.97	0.04 (0.88)
(8) Site, Height_AG, Elev	8969.01	7.39	0.01	0.98	0.04 (0.88)
(14) Site, Height_AG, Elev; Height_AG × Elev	8969.81	8.20	0.01	0.98	0.04 (0.88)
(6) Site; Elev	8969.90	8.29	0.00	0.99	0.04 (0.88)
(10) Site; Elev; Site × Elev	8970.05	8.44	0.00	0.99	0.04 (0.88)
(5) Site; Height_AG	8970.56	8.95	0.00	0.99	0.04 (0.88)

(Table C10 suite)

Model	**AICc**	**Delta AICc**	**AICc Wt.**	**Cum. Wt.**	**Marginal pseudo-*R*^{2} (conditional)**
(17) Site, Height_AG, Elev; Site × Elev; Height_AG × Elev	8970.63	9.02	0.00	1.00	0.04 (0.88)
(2) Site	8972.08	10.47	0.00	1.00	0.04 (0.88)
(7) Height_AG; Elev	8974.25	12.63	0.00	1.00	0.06 (0.89)
(11) Height_AG; Elev; Height_AG × Elev	8974.87	13.26	0.00	1.00	0.06 (0.89)
(3) Height_AG	8974.97	13.36	0.00	1.00	0.05 (0.88)
(1) 1	9491.41	529.80	0.00	1.00	0.00 (0.85)
(4) Elev	9492.17	530.56	0.00	1.00	0.00 (0.85)

Table C11 Importance of the height above ground and elevation at predicting minimum near-ground air temperature on the 103 days in 2017 upon AICc and cumulative AICc weights; boldface type indicates the selected models and numbers in parentheses before each model refer to the candidate models prior to selection (Table C3).

Model	**AICc**	**Delta AICc**	**AICc Wt.**	**Cum. Wt.**
(15) Site, Height_AG, Elev; Site × Height_AG; Site × Elev	**10834.14**	**0.00**	**0.44**	**0.44**
(18) Site, Height_AG, Elev; Site × Elev; Height_AG × Elev	**10835.09**	**0.95**	**0.27**	**0.71**
(9) Site; Height_AG; Site × Height_AG	**10836.75**	**2.62**	**0.12**	**0.83**
(12) Site, Height_AG, Elev; Site × Height_AG	10837.29	3.16	0.09	0.92
(16) Site, Height_AG, Elev; Site × Height_AG; Height_AG × Elev	10837.63	3.49	0.08	1.00
(13) Site, Height_AG, Elev; Site × Elev	10850.64	16.51	0.00	1.00
(17) Site, Height_AG, Elev; Site × Elev; Height_AG × Elev	10851.68	17.55	0.00	1.00
(5) Site; Height_AG	10853.08	18.94	0.00	1.00
(8) Site, Height_AG, Elev	10853.46	19.32	0.00	1.00

(Table C11 suite)

Model	**AICc**	**Delta AICc**	**AICc Wt.**	**Cum. Wt.**
(14) Site, Height_AG, Elev; Height_AG × Elev	10853.89	19.76	0.00	1.00
(10) Site; Elev; Site × Elev	10854.61	20.47	0.00	1.00
(6) Site; Elev	10856.61	22.48	0.00	1.00
(2) Site	10856.75	22.61	0.00	1.00
(3) Height_AG	10865.90	31.76	0.00	1.00
(7) Height_AG; Elev	10867.01	32.88	0.00	1.00
(11) Height_AG; Elev; Height_AG × Elev	10867.16	33.03	0.00	1.00
(1) 1	11785.53	951.39	0.00	1.00
(4) Elev	11787.47	953.34	0.00	1.00

Table C12 Results of the multi-model conditional averaging of linear mixed regression models 15, 18 and 9 showing the coefficients and standard errors for the position in the microtopography and elevation predicting near-ground minimum air temperature using all 103 dates in 2017; boldface type indicates coefficients that differ from zero.

Variable	**All days (n= 2793)** standardized coefficients (SE)
Intercept: Temperate forest	**9.02 (0.66)**
Boreal mixedwood forest	**-0.96 (0.32)**
Elevation	**-0.94 (0.22)**
Microtopography	**0.12 (0.05)**
Elevation × Boreal mixedwood forest	**0.47 (0.11)**
Microtopography × Elevation	0.05 (0.05)
Microtopography × Boreal mixedwood forest	**-0.16 (0.09)**

Table C13 Importance of the height above ground at predicting near-ground probability of frost occurrence on the 14 days where night frost did occur in 2017 upon AICc and cumulative AICc weights; boldface type indicates the selected models and numbers in parentheses before each model refer to the candidate models prior to selection (Table C3).

Model	**AICc**	**Delta AICc**	**AICc Wt.**	**Cum. Wt.**	**Marginal pseudo-R^2 (conditional)**
(17) Site, Height_AG, Elev; Site × Elev; Height_AG × Elev	**179.76**	**0.00**	**0.53**	**0.53**	**0.61 (0.97)**
(18) Site, Height_AG, Elev; Site × Elev; Height_AG × Elev	**180.57**	**0.80**	**0.35**	**0.88**	**0.55 (0.97)**
(5) Site; Height_AG	185.51	5.75	0.03	0.91	0.60 (0.95)
(14) Site, Height_AG, Elev; Height_AG × Elev	186.18	6.42	0.02	0.94	0.62 (0.96)
(8) Site, Height_AG, Elev	186.82	7.06	0.02	0.95	0.60 (0.95)
(9) Site; Height_AG; Site × Height_AG	186.82	7.06	0.02	0.97	0.55 (0.95)
(16) Site, Height_AG, Elev; Site × Height_AG; Height_AG × Elev	187.46	7.70	0.01	0.98	0.56 (0.95)
(12) Site, Height_AG, Elev; Site × Height_AG	188.09	8.33	0.01	0.99	0.55 (0.95)
(13) Site, Height_AG, Elev; Site × Elev	188.78	9.02	0.01	0.99	0.60 (0.95)
(15) Site, Height_AG, Elev; Site × Height_AG;	190.04	10.28	0.00	0.99	0.55 (0.95)
(2) Site	190.16	10.40	0.00	1.00	0.48 (0.95)

(Table C13 suite)

Model	**AICc**	**Delta AICc**	**AICc Wt.**	**Cum. Wt.**	**Marginal pseudo-R^2 (conditional)**
(6) Site; Elev	191.36	11.60	0.00	1.00	0.48 (0.95)
(10) Site; Elev; Site × Elev	193.30	13.54	0.00	1.00	0.47 (0.95)
(3) Height_AG	202.77	23.00	0.00	1.00	0.38 (0.97)
(11) Height_AG; Elev; Height_AG × Elev	203.45	23.69	0.00	1.00	0.39 (0.97)
(7) Height_AG; Elev	203.80	24.04	0.00	1.00	0.38 (0.97)
(1) 1	449.70	269.94	0.00	1.00	0.00 (0.63)
(4) Elev	451.29	271.52	0.00	1.00	0.00 (0.64)

ANNEXE D

SUPPORTING INFORMATION AND RESULTS FOR CHAPITRE IV

HEIGHT GROWTH STAGNATION OF PLANTED SPRUCE IN BOREAL MIXEDWOODS: IMPORTANCE OF LANDSCAPE, MICROSITE AND GROWING-SEASON FROSTS

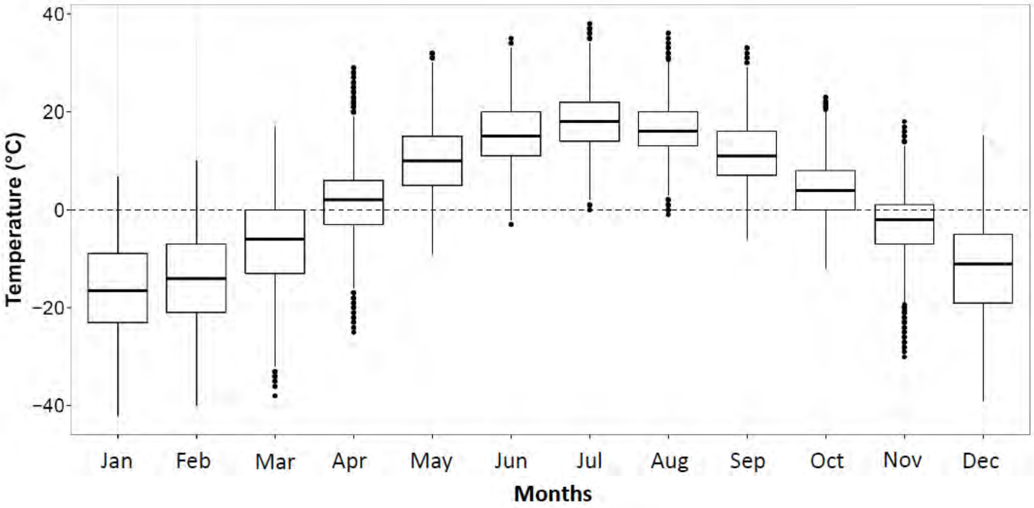

Figure D1 Average monthly temperatures for the period 1973-2016 (Environment Canada, weather station CYUY). The thick line in each box represents the median temperature; the lower and upper ends of the box represent the 25th and 75th percentiles, respectively. The vertical lines illustrate the 1.5×interquartile range (IQR). Data points beyond whiskers are outliers.

Table D1 Set of candidate models used to determine the permanent attributes at the landscape (elevation [Elev], slope shape and angular slope [A-slope]) and microsite (height above ground [Height_AG]) level along with the biotic (plantation age [Pl_Age] and species) variables best predicting tree height and frost damage to foliage.

Model	**Predictor variables**	**Interactions**
1	Intercept-only (null model)	None
2	Elev; Species; Pl_Age	None
3	Slope shape; Species; Pl_Age	None
4	A-slope; Species; Pl_Age	None
5	Height_AG; Species; Pl_Age	None
6	Elev; Slope shape; Species; Pl_Age	None
7	Elev; A-slope; Species; Pl_Age	None
8	Elev; Height_AG; Species; Pl_Age	None
9	Slope shape; A-slope; Species; Pl_Age	None
10	Slope shape; Height_AG; Species; Pl_Age	None
11	A-slope; Height_AG; Species; Pl_Age	None
12	Elev; Slope shape; A-slope; Species; Pl_Age	None
13	Elev; Slope shape; Height_AG; Species; Pl_Age	None
14	Elev; Height_AG; A-slope; Species; Pl_Age	None
15	Slope shape; A-slope; Height_AG; Species; Pl_Age	None
16	Elev; Slope shape; A-slope; Height_AG; Species; Pl_Age	None
17	Elev; Species; Pl_Age	Elev × Species; Elev×Pl_Age; Species×Pl_Age
18	Slope shape; Species; Pl_Age	Slope shape×Species Slope shape×Pl_Age Species × Pl_Age

(Table D1 suite)

Model	Predictor variables	Interactions
19	Height_AG; Species; Pl_Age	Height_AG × Species; Height_AG ×Pl_Age; Species×Pl_Age
20	A-slope; Species; Pl_Age	A-slope × Species; A-slope × Pl_Age; Species × Pl_Age
21	Elev; Slope shape; Species; Pl_Age	Elev × Slope shape; Elev × Species; Elev × Pl_Age; Slope shape × Species; Slope shape × Pl_Age; Species × Pl_Age
22	Elev; A-slope; Species; Pl_Age	Elev × A-slope; Elev × Species; Elev × Pl_Age; A-slope × Species; A-slope × Pl_Age; Species × Pl_Age
23	Elev; Height_AG; Species; Pl_Age	Elev × Height_AG; Elev × Species; Elev × Pl_Age; Height_AG × Species; Height_AG × Pl_Age; Species × Pl_Age

(Table D1 suite)

Model	Predictor variables	Interactions
24	Slope shape; A-slope; Species; Pl_Age	Slope shape × A-slope; Slope shape × Species; Slope shape × Pl_Age; A-slope × Species; A-slope × Pl_Age; Species × Pl_Age
25	Slope shape; Height_AG; Species; Pl_Age	Slope shape × Height_AG; Slope shape × Species; Slope shape × Pl_Age; Height_AG × Species; Height_AG × Pl_Age; Species×Pl_Age
26	A-slope; Height_AG; Species; Pl_Age	A-slope × Height_AG; A-slope × Species; A-slope × Pl_Age; Height_AG × Species; Height_AG × Pl_Age; Species × Pl_Age
27	Elev; Slope shape; A-slope; Species; Pl_Age	Elev × Slope shape; Elev × A-slope; Elev × Species; Elev × Pl_Age; Slope shape × A-slope; Slope shape × Species; Slope shape × Pl_Age; A-slope × Species; A-slope × Pl_Age; Species × Pl_Ag

(Table D1 suite)

Model	Predictor variables	Interactions
28	Elev; Slope shape; Height_AG; Species; Pl_Age	Elev × Slope shape; Elev × Height_AG; Elev × Species; Elev × Pl_Age; Slope shape × Height_AG; Slope shape × Species; Slope shape × Pl_Age; Height_AG × Species; Height_AG × Pl_Age; Species×Pl_Age
29	Elev; Height_AG; A-slope; Species; Pl_Age	Elev × Height_AG; Elev × A-slope; Elev × Species; Elev × Pl_Age; Height_AG × A-slope; Height_AG × Species; Height_AG × Pl_Age; A-slope; Species; A-slope; Pl_Age; Species×Pl_Age

(Table D1 suite)

Model	Predictor variables	Interactions
30	Slope shape; A-slope; Height_AG; Species; Pl_Age	Slope shape × A-slope; Slope shape × Height_AG; Slope shape × Species; Slope shape × Pl_Age; A-slope × Height_AG; A-slope × Species; A-slope × Pl_Age; Height_AG × Species; Height_AG × Pl_Age; Species×Pl_Age
31	Elev; Slope shape; A-slope; Height_AG; Species; Pl_Age	Elev × Slope shape; Elev × A-slope; Elev × Height_AG; Elev × Species; Elev × Pl_Age; Slope shape × A-slope; Slope shape × Height_AG; Slope shape × Species; Slope shape × Pl_Age; A-slope × Height_AG; A-slope × Species; A-slope × Pl_Age; Height_AG × Species; Height_AG × Pl_Age; Species×Pl_Age

Table D2 Results of student t-test comparing observed to predicted dominant white spruce tree height in the boreal mixedwood forest of Quebec (Canada). Data presented as mean ± standard deviation.

Plantation age	**Observed tree height, cm**	**Predicted tree height, cm**	**p-value**
6	126 ± 15	144 ± 64	0.39
7	189 ± 35	178 ± 79	0.65
8	205 ± 47	214 ± 94	0.76
9	236 ± 57	251 ± 109	0.67
10	275 ± 76	290 ± 124	0.72
11	283 ± 85	329 ± 139	0.36
12	278 ± 89	368 ± 155	0.10
13	380 ± 130	409 ± 170	0.60

Table D3 Results of student t-test comparing mean difference in tree heights between species per plantation age, in the boreal mixedwood forest of Quebec (Canada). Data presented as mean ± standard deviation and sample size. Bold indicates significant statistical differences (α = 0.05).

Plantation age	**White spruce tree height, cm (n)**	**Black spruce tree height, cm (n)**	**p-value**
6	**119 ± 12 (44)**	**150 ± 26 (122)**	**< 0.01**
7	**153 ± 33 (264)**	**185 ± 49 (189)**	**< 0.01**
8	**164 ± 45 (409)**	**175 ± 45 (187)**	**< 0.01**
9	**183 ± 55 (231)**	**219 ± 52 (136)**	**< 0.01**
10	217 ± 76 (258)	232 ± 75 (129)	0.08
11	200 ± 80 (69)	223 ± 64 (65)	0.07
12	217 ± 86 (115)	204 ± 76 (75)	0.27
13	**295 ± 123 (411)**	**321 ± 112 (239)**	**< 0.01**

Table D4 Model selection results showing permanent physical attributes of the landscape and of the microsite best predicting tree height. Numbers in parentheses refer to the candidate models before selection (Table D1).

Model	**AICc**	**Delta AICc**	**AICc Weight**	**Cum. Weight**
(23)	**32175.08**	**0.00**	**0.95**	**0.95**
(29)	32181.24	6.16	0.04	1.00
(28)	32187.14	12.06	0.00	1.00
(19)	32187.58	12.49	0.00	1.00
(26)	32192.84	17.76	0.00	1.00
(25)	32195.43	20.35	0.00	1.00
(31)	32196.07	20.99	0.00	1.00
(5)	32199.09	24.00	0.00	1.00
(11)	32200.30	25.22	0.00	1.00
(10)	32200.62	25.54	0.00	1.00
(8)	32201.04	25.95	0.00	1.00
(15)	32201.92	26.84	0.00	1.00
(14)	32202.23	27.15	0.00	1.00
(13)	32202.50	27.41	0.00	1.00
(30)	32202.85	27.77	0.00	1.00
(16)	32203.77	28.69	0.00	1.00
(17)	32300.76	125.67	0.00	1.00
(22)	32302.89	127.80	0.00	1.00
(4)	32309.13	134.05	0.00	1.00
(2)	32309.62	134.54	0.00	1.00
(3)	32309.71	134.62	0.00	1.00
(20)	32310.77	135.69	0.00	1.00
(7)	32311.08	136.00	0.00	1.00
(9)	32311.28	136.20	0.00	1.00
(6)	32311.60	136.52	0.00	1.00

(Table D4 suite)

Model	**AICc**	**Delta AICc**	**AICc Weight**	**Cum. Weight**
(12)	32313.16	138.08	0.00	1.00
(21)	32313.86	138.77	0.00	1.00
(27)	32318.62	143.54	0.00	1.00
(18)	32319.64	144.56	0.00	1.00
(24)	32322.53	147.45	0.00	1.00
(1)	32364.46	189.38	0.00	1.00

Table D5 Model selection results showing permanent physical attributes of the landscape and of the microsite best predicting frost damage to foliage. Numbers in parentheses refer to the candidate models before selection (Table D1).

Model	**AICc**	**Delta AICc**	**AICc Weight**	**Cum. Weight**
(21)	**1434.28**	**0.00**	**0.23**	**0.23**
(23)	**1434.32**	**0.04**	**0.23**	**0.46**
(28)	**1435.23**	**0.95**	**0.15**	**0.61**
(18)	**1436.42**	**2.14**	**0.08**	**0.69**
(8)	**1437.08**	**2.80**	**0.06**	**0.74**
(5)	**1437.16**	**2.88**	**0.06**	**0.80**
(14)	1437.51	3.23	0.05	0.84
(11)	1437.63	3.36	0.04	0.89
(27)	1439.43	5.15	0.02	0.91
(29)	1439.53	5.25	0.02	0.92
(10)	1440.41	6.14	0.01	0.93
(13)	1440.65	6.37	0.01	0.94
(19)	1440.65	6.38	0.01	0.95
(16)	1440.85	6.57	0.01	0.96

(Table D5 suite)

Model	**AICc**	**Delta AICc**	**AICc Weight**	**Cum. Weight**
(1)	1441.00	6.72	0.01	0.97
(2)	1441.40	7.12	0.01	0.98
(7)	1441.63	7.36	0.01	0.98
(4)	1441.87	7.59	0.01	0.99
(25)	1442.39	8.11	0.00	0.99
(17)	1443.19	8.91	0.00	0.99
(3)	1444.68	10.41	0.00	1.00
(9)	1444.75	10.47	0.00	1.00
(12)	1444.89	10.61	0.00	1.00
(6)	1444.94	10.66	0.00	1.00
(26)	1445.20	10.92	0.00	1.00
(22)	1446.64	12.36	0.00	1.00
(15)	NA	NA	NA	NA
(20)	NA	NA	NA	NA
(24)	NA	NA	NA	NA
(30)	NA	NA	NA	NA
(21)	NA	NA	NA	NA

BIBLIOGRAPHIE

Andalo, C., Beaulieu, J. et Bousquet, J. (2005). The impact of climate change on growth of local white spruce populations in Québec, Canada. *Forest Ecology and Management,* 205, 169–182.

Antonucci, S., Rossi, S., Deslauriers, A., Lombardi, F., Marchetti, M. et Tognetti, R. (2015). Synchronisms and correlations of spring phenology between apical and lateral meristems in two boreal conifers. *Tree Physiology,* 35, 1086-1094.

Aono, Y. et Kazui, K. (2008). Phenological data series of cherry tree flowering in Kyoto, Japan, and its application to reconstruction of springtime temperatures since the 9th century. *International Journal of Climatology,* 28, 905-914.

Augspurger, C.K. (2009). Spring 2007 warmth and frost: phenology, damage and refoliation in a temperate deciduous forest. *Functional Ecology,* 23, 1031-1039.

Ault, T.R., Henebry, G.M., de Beurs, K.M., Schwartz, M.D., Betancourt, J.K. et Moore, D. (2013). The false spring of 2012, earliest in north American record. *Eos, Transactions, American Geophysical Union*, 94, 181-188.

Barton, K. (2018). *MuMIn: Multi-model inference*. R package version 1.42.1.

Basler, D. (2016). Evaluating phenological models for the prediction of leaf-out dates in six temperate tree species across central Europe. *Agricultural and Forest Meteorology,* 217, 10-21.

Basler, D. et Körner, C. (2012). Photoperiod sensitivity of bud burst in 14 temperate forest tree species. *Agricultural and Forest Meteorology*, 165, 73-81.

Bates, D., Maechler, M., Bolker, B. et Walker, S. (2015). Fitting linear mixed-effects models using lme4. *Journal of Statistical Software*, 67, 1-48.

Beaulieu, J. (2009). Optisource: A tool for optimizing seed transfer. Canadian Forest Service, Ottawa, ON, Canada. 2 p.

Beaulieu, J., Perron, M. et Bousquet, J. (2004). Multivariate patterns of adaptive genetic variation and seed source transfer in *Picea mariana*. *Canadian Journal of Forest Research*, 34, 531–545.

Beckage, B., Osborne, B., Gavin, D.G., Pucko, C., Siccama, T. et Perkins, T. (2008). A rapid upward shift of a forest ecotone during 40 years of warming in the Green Mountains of Vermont. *Proceedings of the National Academy of Sciences of the USA*, 105, 4197-4202.

Bergeron, Y., Drapeau, P., Gauthier, S. et Lecomte, N. (2007). Using knowledge of natural disturbances to support sustainable forest management in the northern Clay Belt. *The Forestry Chronicle*, 83, 326-337.

Bergeron, Y., Harvey, B., Leduc, A. et Gauthier, S. (1999). Stratégies d'aménagement forestier qui s'inspirent de la dynamique des perturbations naturelles : considérations 1'échelle du peuplement et de la forêt. *The Forestry Chronicle*, 75, 55-61.

Bergeron, Y., Vijayakumar, D. B. I. P., Ouzennou, H., Raulier, F., Leduc, A. et Gauthier, S. (2017) Projection of future forest age class structure under the influence of fire and harvesting: implications for forest management in the boreal forest of eastern Canada. *Forestry*, 90, 485–495. doi:10.1093/forestry/cpx022.

Bertin, R. (2008). Plant phenology and distribution in relation to recent climate change. *The Journal of the Torrey Botanical Society*, 135, 126–146.

Beuker, E. (1994). Adaptation to climatic changes of the timing of bud burst in populations of *Pinus sylvestris* (L.) and *Picea abies* (L.) Karst. *Tree Physiol*ogy, 14, 961–970.

Bigler, C. et Bugmann, H. (2018). Climate-induced shifts in leaf unfolding and frost risk of European trees and shrubs. *Scientific Reports*, 8, 9865.

Bigras, J.F. et Hébert, C. (1996). Freezing temperatures and exposure times during bud break and shoot elongation influence survival and growth of containerized black spruce (*Picea mariana*) seedlings. *Canadian Journal of Forest Research*, 26, 1481-1489.

Bonsal, B.R., Zhang, X., Vincent, L.A. et Hogg, W.D. (2000). Characteristics of daily and extreme temperatures over Canada. *Journal of Climate*, 14, 1959-1976.

Bootsma, A. (1976). Estimating minimum temperature and climatological freeze risk in hilly terrain. *Agricultural and Forest Meteorology*, 16, 425-443.

Bronson, D.R., Gower, S.T., Tanner, M. et Van Herk, I. (2009). Effect of ecosystem warming on boreal black spruce bud burst and shoot growth. *Global Change Biology*, 15, 1534-1543.

Brown, A. (2019). Seasonally uneven warming. *Nature Climate Change*, 9, 186.

Brüchert, F. et Gardiner, B. (2006). The effect of wing exposure on the tree aerial architecture and biomechanics of sitka spruce (*Picea sitchensis*, Pinaceae). *American Journal of Botany*, 93, 1512–1521.

Bugmann, H. (2001). A review of forest gap models. *Climatic Change*, 51, 259–305.

Burnham, K.P., Anderson, D.R. et Huyvaert, K.P. (2011). AIC model selection and multimodel inference in behavioral ecology: some background, observations and comparisons. *Behavioral Ecology and Sociobiology*, 65, 23-35.

Caffarra, A. et Donnelly, A. (2011). The ecological significance of phenology in four different tree species: effects of light and temperature on bud burst. *International Journal of Biometeorol*ogy, 55, 711-721.

Cannell, M.G.R. (1984). Spring frost damage on young *Picea sitchensis*. I. Occurrence of damaging frosts in Scotland compared with western North America. *Forestry*, 57, 159-175.

Cannell, M.G.R. et Smith, R.I. (1986). Climatic warming, spring budburst and forest damage on trees. *Journal of Applied Ecology*, 23, 177-191.

Chen, L., Huang, J.G., Ma, Q., Hänninen, H., Rossi, S., Piao, S. et Bergeron, Y. (2018). Spring phenology at different altitudes is becoming more uniform under global warming in Europe. *Global Change Biol*ogy, 24, 3969-3975.

Chen, L., Huang, J.G., Ma, Q., Hänninen, H., Tremblay, F. et Bergeron, Y. (2019). Long-term changes in the impacts of global warming on leaf phenology of four temperate tree species. *Global Change Biol*ogy, 25, 997-1004.

Chuine, I. (2000). A unified model for budburst of trees. *Journal of Theoretical Biology*, 207, 337-347.

Chung, U., Seo, H.H., Hwang, K.H., Hwang, B.S., Choi, J., Lee, J.T. et Yun, J.I. (2006). Minimum temperature mapping over complex terrain by estimating cold air accumulation potential. *Agricultural and Forest Meteorology*, 137, 15-24.

Clark, S., Melillo, J., Mohan, J. et Salk, C. (2014). The seasonal timing of warming that controls onset of the growing season. *Global Change Biology*, 20, 1136-1145.

Clark, J.S., Salk, C., Melillo, J. et Mohan, J. (2014). Tree phenology responses to winter chilling, spring warming, at north and south range limits. *Functional Ecology*, 28, 1344-1355.

Clark, J.S., Bell, D.M., Kwit, M., Stine, A., Vierra, B. et Zhu, K. (2012). Individual-scale inference to anticipate climate-change vulnerability of biodiversity. *Philosophical Transactions of the Royal Society B: Biological Sciences*, 367, 236-246.

Clements, J.R., Fraser, J.W. et Yeatman, C.W. (1972). Frost damage to white spruce buds. *Canadian Journal of Forest Research,* 2, 62-63.

Cooke, J.E.K., Eriksson, M.E. et Junttila, O. (2012). The dynamic nature of bud dormancy in trees: environmental control and molecular mechanisms. *Plant, Cell and Environment*, 35, 1707-1728.

Côté, J.-F., Fournier, R.A., Luther, J.E., et van Lier, O.R. (2018). Fine-scale three-dimensional modeling of boreal forest plots to improve forest characterization with remote sensing. *Remote Sensing of Environment*, 219, 99-114.

D'Orangeville, L., Houle, D., Duchesne, L., Phillips, R.P., Bergeron, Y. et Kneeshaw, D. (2018). Beneficial effects of climate warming on boreal tree growth may be transitory. *Nature Communication*, 9, 3213.

Dehayes, D.H., Dickmann, D.I. et Lemmien W.A. (1980). Management of exotic timber trees in temperate regions of Eastern North America: An assessment. *Forest Ecology and Management,* 3, 31-44.

de Montigny, L.E. et Weetman, G.F. (1990). The effects of ericaceous plants on forest productivity. In The silvics and ecology of boreal spruce. Titus, B.D., Lavigne, M.B., Newton, P.F. et Meades, W.J. Canadian Forest Service, Forestry Canada, St. John's, Newfoundland. pp. 83-90.

Dhont, C., Sylvestre, P., Gros-Louis, M.C. et Isabel, N. (2010). *Field Guide for identifying apical bud break and bud formation stages in white spruce.* Ressources naturelles Canada, Service canadien des forêts, Centre de foresterie des Laurentides. ISBN: 978-1-100-93942-1.

Dormling, I. (1988). Frost resistance during bud flushing and shoot elongation in *Picea abies*. *Silva Fennica*, 16, 167-177.

Du, J., Li, K., He, Z., Chen, L., Zhu, X., et Lin, P. (2019). Age-mediation of tree-growth responses to experimental warming in the northeastern Tibetan Plateau. *Ecology and Evolution*, 9, 2242-2254.

Dugas, C., (1975). Le climat et son influence sur l'agriculture abitibienne. Sud de la baie de James et partie de l'enclave argileuse de l'Objibway. Collection Nordicana (Volume 39), Centre d'études nordiques, Université Laval, Québec, Canada. 140 pp. doi: 10.5885/464018ND-DEA2492A1.

Dy, G. et Payette, S. (2007). Frost hollows of the boreal forest as extreme environments for black spruce tree growth. *Canadian Journal of Forest Research*, 37, 492-504.

Environment Canada. (2019a). *Barrage Angliers weather station, normal 1981-2010*.http://climate.weather.gc.ca/climate_normals/results_1981_2010_f.html?searchType=stnProv&lstProvince=QC&txtCentralLatMin=0&txtCentralLatSec=0&txtCentralLongMin=0&txtCentralLongSec=0&stnID=5976&dispBack=0. [accessed accessed 1 April 2018].

Environment Canada. (2019b). *Mont-Brun weather station, normal 1981-2010.* http://climate.weather.gc.ca/climate_normals/results_1981_2010_f.html?searchType=stnProv&lstProvince=QC&txtCentralLatMin=0&txtCentralLatSec=0&txtCentralLongMin=0&txtCentralLongSec=0&stnID=5988&dispBack=0. [accessed 1 April 2018].

Environment Canada. (2019c). *Sunset calculator*. https://www.nrccnrc.gc.ca/eng/services/sunrise/advanced.html. [accessed 1 April 2018].

Environment Canada. (2019d). Earlton weather station. http://climate.weather.gc.ca/climate_data/hourly_data_f.html?hlyRange=2008-11-20%7C2019-03-16&dlyRange=2008-11-20%7C2019-03-17&mlyRange=%7C&StationID=47687&Prov=ON&urlExtension=_f.html&searchType=stnProx&optLimit=specDate&Month=7&Day=6&StartYear=1840&EndYear=2018&Year=2018&selRowPerPage=25&Line=0&txtRadius=25&optProxType=navLink&txtLatDecDeg=47.695&txtLongDecDeg=79.848888888889&timeframe=1

Environment Canada. (2019e). Rouyn A weather station. https://meteo.gc.ca/past_conditions/index_f.html?station=yuy

Estiarte, M. et Peñuelas, J. (2015). Alteration of the phenology of leaf senescence and fall in winter on deciduous species by climate change: effects on nutrient proficiency. *Global Change Biology,* 21, 1005-1017.

Fenton, N.; Lecomte, N.; Légaré, S. et Bergeron, Y. (2005). Paludification in black spruce (*Picea mariana*) forests of eastern Canada: Potential factors and management implications. *Forest Ecology and Management*, 213, 151–159.

Fløistad, S.I. et Granhus, A. (2010). Bud break and spring frost hardiness in *Picea abies* seedlings in response to photoperiod and temperature treatments. *Canadian Journal of Forest Research*, 40, 968-976.

Franklin, J. F. (1993). Preserving biodiversity: species, ecosystems or landscapes. *Ecological Applications*, 3, 202-205.

Fu, Y.H., Piao, S., Delpierre, N., Hao, F., Hänninen, H., Liu, Y., Sun, W., Janssens, I.A. et Campioli, M. (2017). Larger temperature response of autumn leaf senescence than spring leaf-out phenology. *Global Change Biology*, 24, 2159-2168.

Fuchigami, L.H. et Nee, C.C. (1987). Degree growth stage model and rest-breaking mechanisms in temperate woody perennials. *Horticultural Science,* 22, 836-845.

Gärtner, S.M., Lieffers, V.J. et Macdonald, S.E. (2011). Ecology and management of natural regeneration of white spruce in the boreal forest. *Environmental Review*, 19, 461-478.

Gauthier, S., Vaillancourt, M-A., Leduc, A., De Granpré, L., Kneeshaw, D., Morin, H., Drapeau, P. et Bergeron, Y. (2008). Aménagement écosystémique en forêt boréale. Presse de l'Université du Québec.

Glerum, C. et Farrar, J.L. (1966). Frost ring formation in stems of some conifer species. *Canadian Journal of Botany*, 44, 879–886.

Glerum, C. (1973). Annual trends in frost hardiness and electrical impedance for seven coniferous species. *Canadian Journal of Plant Science*, 53, 881-889.

Groot, A. et Carlson, D.W. (1996). Influence of shelter on night temperatures, frost damage, and bud break of white spruce seedlings. *Canadian Journal of Forest Research*, 26, 1531-1538.

Grossnickle, S.C. (2000). *Ecophysiology of northern spruce species. The performance of planted seedlings*. NRC Research Press, Ottawa, ON.

Groupe de travail sur la définition du rendement durable. (2015). Du rendement soutenu au rendement durable. Direction de la recherche forestière et Bureau du forestier en chef, 1-37.

Grueber, C.E., Nakagawa, S., Laws, R.J. et Jamieson, I.G. (2011). Multimodel inference in ecology and evolution: challenges and solutions. *Journal of Evolutionay Biology*, 24, 699-711.

Gurskaya, M.A. et Shiyatov, S.G. (2002). Formation of two xylem frost injuries in one annual ring in siberian spruce under conditions of western Siberian forest-tundra. *Russian Journal of Ecology*, 33, 73–79.

Hannerz, M. (1999). Evaluation of temperature models for predicting bud burst in Norway spruce. *Canadian Journal of Forest Research*, 29, 9-19.

Hannerz, M. (1994). Predicting the risk of frost occurrence after budburst of Norway spruce in Sweden. *Silva Fennica*, 28, 243-249.

Hänninen, H. (2006). Climate warming and the risk of frost damage to boreal forest trees: identification of critical ecophysiological traits. *Tree Physiology,* 26, 889–898.

Hänninen, H. (2016). *Boreal and temperature trees in a changing climate, modelling the ecophysiology of seasonality*. Helsinki, Finland, Springer.

Hänninen, H. et Tanino, K. (2011). Tree seasonality in a warming climate. *Trends in plant science*, 16, 412-416.

Heide, O.M. (2003). High autumn temperature delays spring bud burst in boreal trees, counterbalancing the effect of climatic warming. *Tree Physiology*, 23, 931–936.

Hjelm, K., Nilsson, U. et Örlander, G. (2012). A comparison of long-term effects of scarification methods on the establishment of Norway spruce. *Forestry*, 86, 91-98.

Hocevar, A. et Martsolf, J.D. (1971). Temperature distribution under radiation frost conditions in a central Pennsylvania valley. *Agricultural and Forest Meteorology*, 8, 371-383.

Huang, J., Tardif, J.C., Bergeron, Y., Denneler, B., Berninger, F. et Girardin, M. (2010). Radial growth response of four dominant boreal tree species to climate along a latitudinal gradient in the Eastern Canadian boreal forest. *Global Change Biology*, 16, 711–731.

Hufkens, K., Friedl, M.A., Keenan, T.F., Sonnentag, O., Bailey, A., O'Keefe, J. et Richardson, A.D. (2012). Ecological impacts of a widespread frost event following early spring leaf-out. *Global Change Biology*, 18, 2365-2377.

Hunter, A.F. et Lechowicz, M.J. (1992). Predicting the timing of budburst in temperate trees. *Journal of Applied Ecology,* 29, 597–604.

Inouye, D.W. (2008). Effects of climate change on phenology, frost damage, and floral abundance of montane wildflowers. *Ecology,* 89, 353-362.

IPCC. (2018). Allen, M.R., Dube, O.P, Solecki, W., Aragón-Durand, F., Cramer, W., Humphreys, S. et al. 2018. *Global Warming of 1.5°C. An IPCC Special Report on the impacts of global warming of 1.5°C above pre-industrial levels and related global greenhouse gas emission pathways, in the context of strengthening the global response to the threat of climate change, sustainable development, and efforts to eradicate poverty*.

Jeong, S.J., Ho, C.H., Gim, H.J. et Brown, M.E. (2011). Phenology shifts at start *vs*. end of growing season in temperature vegetation over the Northern Hemisphere for the period 1982-2008. *Global Change Biology*, 17, 2385-2399.

Jeong, D., Sushama, L., Tefera Diro, G.T. et Khaliq, M. N. (2016). Projected changes to winter temperature characteristics over Canada based on an RCM ensemble. *Climate Dynamics*, 47, 1351–1366.

Kollas, C., Körner, C. et Randin, C.F. (2014). Spring frost and growing season length co-control the cold range limits of broad-leaved trees. *Journal of Biogeography,* 41, 773–783.

Körner, C. (2016). Plant adaptation to cold climates. *100 Research,* 5, 2769.

Körner, C., Basler, D., Hoch, G., Kollas, C., Lenz, A., Randin, C.F., Vitasse, Y. et Zimmermann, N.E. (2016). Where, why and how? Explaining the low-temperature range limits of temperate tree species, *Journal of Ecology,* 104, 1076–1088.

Körner, C., Basler, D. (2010). Plant science. Phenology under global warming. *Science*, 327, 1461-1462.

Laamrani, A., Valeria, O., Bergeron, Y., Fenton, N., Cheng, L.Z. et Anyomi, K. (2014). Effects of topography and thickness of organic layer on productivity of black spruce boreal forests of the Canadian Clay Belt region. *Forest ecology and management*, 330, 144-157.

LaMarche, V. C., Jr., et K. K. Hirschboeck (1984), Frost rings in trees as records of major volcanic eruptions, Nature, 307, 121–126, doi:10.1038/ 307121a0.

Lang, W., Chen, X., Qian, S., Liu, G. et Piao, S. (2019). A new process-based model for predicting autumn phenology: How is leaf senescence controlled by photoperiod and temperature coupling? *Agricultural and Forest Meteorology*, 268, 124-135.

Langvall, O., et Örlander, G. (2001). Effects of pine shelterwoods on microclimate and frost damage to Norway spruce seedlings. *Canadian Journal of Forest Research*, 31, 155-164.

Langvall, O. et Löfvenius, M.O. (2002). Effect of shelterwood density on nocturnal near-ground temperature, frost injury risk and budburst date of Norway spruce. *Forest Ecology and Management*, 168, 149-161.

Langvall, O., Nilsson, U. et Örlander, G. (2001). Frost damage to planted Norway spruce seedlings –influence of site preparation and seedling type. *Forest Ecology and Management*, 141, 223-235.

Laughlin, G.P. et Kalma, J.D. (1987). Frost hazard assessment from local weather and terrain data. *Agricultural and Forest Meteorology*, 40, 1-16.

Leboeuf, A. et Pomerleau, I. (2016). Guide d’utilisation des produits dérivés du LiDAR. Ministère des Forêts, de la Faune et des Parcs, Secteur des forêts, Direction des inventaires forestiers.

Lenz, A., Hoch, G., Körner, C. et Vitasse, Y. (2016). Convergence of leaf-out towards minimum risk of freezing damage in temperate trees. *Functional Ecology*, 30, 1480-1490.

Li, P., Beaulieu, J., Daoust, G. et Plourde, A. (1997). Patterns of adaptive genetic variation in eastern white pine (*Pinus strobus*) from Quebec. *Canadian Journal of Forest Research*, 27, 199–206.

Lieffers, V.J. et Stadt, K.J. (1994). Growth of understory of *Picea glauca*, *Calamagrostis canadensis* and *Epilobium angustifolium* in relation to overstory light transmission. *Canadian Journal of Forest Research*, 24, 1193-1198.

Lindkvist, L. et Lindqvist, S. (1997). Spatial and temporal variability of nocturnal summer frost in elevated complex terrain. *Agricultural and Forest Meteorology*, 87, 139–153.

Linkosalo, T., Häkkinen, R. et Hänninen, H. (2006). Models of the spring phenology of boreal and temperate trees: is there something missing? *Tree Physiology,* 26, 1165–1172.

Liu, Q., Fu, Y.H., Zhu, Z., Liu, Y., Liu, Z., Huang, M., Janssens, I.A. et Piao, S. (2016). Delayed autumn phenology in the Northern Hemisphere is related to change in both climate and spring phenology. *Global Change Biology,* 22, 3702-3711.

Liu, Q., Piao, S., Janssens, I.A., Fu, Y., Peng, S., Lian, X., Ciais, P., Myneni, R.B., Peñuelas, J. et Wang, T. (2018). Extension of the growing season increases vegetation exposure to frost. *Nature Communication,* 9, 426.

Loarie, S.R., Duffy, P.B., Hamilton, H., Asner, G.P., Field, C.B. et Ackerly, D.D. (2009). The velocity of climate change. *Nature,* 462, 1052-1055.

Löf, M., Dey, D.C., Navarro, R.M. et Jacobs, D.F. (2012). Mechanical site preparation for forest restoration. *New Forests*, 43, 825-848.

Lu, P. et Man, R. (2011). Assessment of assisted migration effects on spring bud flush in white spruce (*Picea glauca* [Moench] Voss) seedlings. *Forestry Chronicle,* 87, 391-397.

Lu, P., William, L., Parker, H., Cherry, M., Colombo, S., Parker, W.C. Man, R et Roubal, N. (2014). Survival and growth patterns of white spruce (*Picea glauca* [Moench] Voss) rangewide provenances and their implications for climate change adaptation. *Ecology and Evolution*, 4, 2360–2374.

Ma, Q., Huang, J.G., Hänninen, H. et Berninger, F. (2019). Divergent trends in the risk of spring frost damage to trees in Europe with recent warming. *Global Change Biology*. 25, 351-360.

Man, R., Colombo, S., Lu, P. et Dang, Q.L. (2016). Effects of winter warming on cold hardiness and spring budbreak of four boreal conifers. *Botany*. 94, 117-126.

Man, R., Lu, P. et Dang, Q-L. (2017). Insufficient chilling effects vary among boreal tree species and chilling duration. *Frontiers in Plant Science*, 8, 1354.

Man, R. et Lu, P. (2010). Effects of thermal model and base temperature on estimates of thermal time to bud break in white spruce seedlings. *Canadian Journal of Forest Research*, 40, 1815–1820.

Man, R. et Lieffers, V.J. (1999). Effects of shelterwood and site preparation on microclimate and establishment of white spruce seedlings in a boreal mixedwood forest. *The Forestry Chronicle*, 75, 837-844.

Man, R., Kayahara, G.J., Dang, Q.-L. et Rice, J.A. (2009). A case of severe frost damage prior to budbreak in young conifers in Northeastern Ontario: consequence of climate change? *The Forestry Chronicle*, 85, 453-462.

Marchand, W., Girardin, M.P., Hartmann, H., Gauthier, S. et Bergeron, Y. (2019). Taxonomy, together with ontogeny and growing conditions, drives needleleaf species' sensitivity to climate in boreal North America. *Global Change Biology, 25*, 2793-2809.

Marris, E. (2009). Planting the forest for the future. Nature, 459, 906–908.

Mazerolle, M.J. (2017). AICcmodavg: Model selection and multimodel inference based on (Q)AIC(c). R package version 2.1-1. https://cran.r-project.org/package=AICcmodavg.

McKenny, D.W., Pedlar, J. et O’Neill, G.A. (2009). Climate change and forest seed zones: Past trends, future prospects and challenges to ponder. Forestry Chronicle, 85, 258–265.

Messier, C. et Kneeshaw, D. (1999). Thinking and acting differently for sustainable management of the boreal forest. *The Forestry Chronicle*, 75, 929-938.

Messier, C., Titler, R., Kneeshaw, D.D., Gelinas, N., Paquette, A., et autres. (2009). TRIAD zoning in Quebec: Experiences and results after 5 years. *Forestry Chronicle*, 85, 885-896.

Morin, X. et Chuine, I. (2014). Will tree species experience increased frost damage due to climate change because of changes in leaf phenology? *Canadian Journal of Forest Research*, 44, 1555–1565.

Morin, X., Lechowichz, M.J., Augspurger, C., O’Keefe, J., Viner, D. et Chuine, I. (2009). Leaf phenology in 22 North American tree species during the 21st century. *Global change Biology*, 15, 961-975.

Mullin, R.E. (1963). Planting check in spruce. *The Forestry Chronicle*, 39, 252-259.

Nagel, L.M., Palik, B.J., Battaglia, M.A., D'Amato, A.W., Guldin, J.M., Swanston, C.W., Janowiak, M.K., Powers, M.P., Joyce, L.A., Millar, C.I., Peterson, D.L., Ganio, L.M., Kirschbaum, C., et Roske, M.R. (2017). Adaptive silviculture for climate change: A national experiment in manager-scientist partnerships to apply an adaptation framework. *Journal of Forestry*, 115, 167-178. doi: 10.5849/jof.16-039.

Numainville, G. et Desponts, M. (2004). *Les stades de débourrement des bourgeons foliaires de l’épinette noire*. Guide nº 7. Gouvernement du Québec, Ministère des Ressources naturelles, de la Faune et des Parcs.

O’Neill, G.A., Ukrainetz, N.K., Carlson, M., Cartwright, C.V., Jaquish, B.C., King, J.N., Krakowski, J., Russell, J.H., Stoehrm M.U., Xie, C.-Y. et Yanchuk, A.D. (2008). Assisted migration to address climate change in British Columbia: recommendations for interim seed transfer standards. Technical Report, Research Branch, British Colombia.

O’Reilly, C. et Parker, W.H. (1982). Vegetative phenology in a clonal seed orchard of *Picea glauca* and *Picea mariana* in northwestern Ontario. *Canadian Journal of Forest Research*, 12, 408-4013.

Oke, T.R. (1987). *Boundary layer climates*. Cambridge University Press, Cambridge, UK.

Olson, M.S., Levsen, N., Soolanayakanahally, R.Y., Guy, R.D., Schroeder, W.R., Keller, S.R. et Tiffin, P. (2013). The adaptive potential of *Populus balsamifera* L. to phenology requirements in a warmer global climate. *Molecular Ecology*, 22, 1214–1230. doi: 10.1111/mec.12067.

Olsson, C., Olin, S., Lindström, J. et Jönsson, A.M. (2017). Trends and uncertainties in budburst projections of Norway spruce in Northern Europe. *Ecology and Evolution*, 7, 9954-9969.

Örlander, G. (1993). Shading reduces both visible and invisible frost damage to Norway spruce seedlings in the field. *Forestry*, 66, 27-36.

Pacala, S.W., Canham, C.D., Saponara, J., Silander, J.A., Kobe, R.K. et Ribbens, E. (1996). Forest models defined by field measurements: Estimation, error analysis and dynamics. *Ecological Monographs*, 66, 1-43.

Park, A, Puettmann, K., Wilson, E., Messier, C., Kames, S. et Dhar, A. (2014). Can boreal and temperate forest management be adapted to the uncertainties of 21st century climate change? *Critical Reviews in Plant Sciences*, 33, 251-285.

Parmesan, C. et Yohe, G. (2003). A globally coherent fingerprint of climate change impacts across natural systems. *Nature*, 421, 37-42.

Partanen, J., Koski, V. et Hänninen, H. (1998). Effects of photoperiod and temperature on the timing of bud burst in Norway spruce (*Picea abies*). *Tree Physiology*, 18, 811-816.

Payette, S. et Delwaide, A. (2018). Tamm review: The North-American lichen woodland. *Forest Ecology and Management*, 417, 167-183.

Payette, S., Delwaide, A. et Simard, M. (2010). Frost-ring chronologies as dendroclimatic proxies of boreal environments. *Geophysical Research Letters*, 37, L02711.

Payette, S., Delwaide, A., Morneau, C. et Lavoie, C. (1996). Patterns of tree stem decline along a snow- drift gradient at tree line: a case study using stem analysis. *Canadian Journal of Botany*, 74, 1671–1683.

Pedlar, J., McKenneym D.W., Beaulieu, J., Colombo, S., McLachalan, J.S. et O'Neil, G.A. (2011). The implementation of assisted migration in Canadian forests. For. Chron. 87:766 –777.

Pereg, D. et Payette, S. (1998). Development of black spruce growth forms at treeline. *Plant Ecology*, 138, 137-147.

Perrin, M., Rossi, S. et Isabel, N. (2017). Synchronisms between bud and cambium phenology in black spruce: early-flushing provenances exhibit early xylem formation. *Tree physiology*, 37, 593-603.

Piao, S., Friedlingstein, P., Ciais, P., Viovy, N. et Demarty, J. (2007). Growing season extension and its impact on terrestrial carbon cycle in the Northern Hemisphere over the past 2 decades. *Global Biogeochemical Cycles*, 21, GB3018.

Plasse, C. et Payette, S. (2015). Frost hollows of the boreal forest: a spatiotemporal perspective. *Journal of Ecology*, 103, 669-678.

Polgar, C.A., Gallinat, A. et Primack, R.B. (2013). Drivers of leaf-out phenology and their implications for species invasions: insights from Thoreau’s Concord. *New Phytologist*, 202, 106-115.

Polgar, C.A. et Primack, R.B. (2011). Leaf-out phenology of temperate woody plants: from trees to ecosystems. *New Phytologist*, 191, 926-941.

Prégent, G., Picher, G. et Auger, I. (2010). *Tarif de cubage, tables de rendement et modèles de croissance pour les plantations d’épinette blanche au Québec*. Mémoire de recherche forestière no 160, Ministère des Ressources naturelles et de la Faune, Direction de la recherche forestière.

Purves, D.W., Lichstein, J.W, Strigul, N. et Pacala, S.W. (2008). Predicting and understanding forest dynamics using a simple tractable model. *Proceedings of the National Academy of Science of the United States of America*, 105, 17018-17022.

R Development Core Team. (2018 et 2019). R: A language and environment for statistical computing. R Foundation for Statistical Computing, Vienna, Austria. Website http://www.R-project.org.

Régnière, J., St-Amant, R. et Béchard, A. (2014). *BioSIM 10 user’s manual*. Natural Resources Canada, Canadian Forest Service, Laurentian Forestry Centre. Inf. Rep. LAU-X-137E.

Repo, T. (1992). Seasonal changes of frost hardiness in *Picea abies* and *Pinus sylvestris* in Finland. *Canadian Journal of Forest Research*, 22, 1949-1957.

Robeson, S.M. (2004). Trends in time-varying percentiles of daily minimum and maximum temperature over North America. *Geophysical Research Letters*, 31, L04203.

Rossi, S. (2015). Local adaptations and climate change: converging sensitivity of bud break in black spruce provenances. *International Journal of Biometeorology*, 59, 827-835.

Rossi, S. et Bousquet, J. (2014). The bud break process and its variation among local populations of boreal black spruce. *Frontiers in Plant Science,* 5, 574.

Rossi, S. et Isabel, N. (2016). Bud break responds more strongly to daytime than night-time temperature under asymmetric experimental warming. *Global Change Biology*, 23, 446-454.

Rossi, S. et Isabel, N. (2017). The timing of bud break in warming conditions: variation among seven sympatric conifer species from Eastern Canada. *International Journal of Biometeorology,* 61, 1983-1991.

Rossi, S., Girard, M. et Morin, H. (2014). Lengthening of the duration of xylogenesis engenders disproportionate increases in xylem production. *Global Change Biology*, 20, 2261-2271.

Rowlandon, T., Berg, A.A., Roy, A., Kim, E., Lara, R.P., Powers, J., Lewis, K., Houser, P., McDonald, K., Toose, P., Wu, A., De Marco, E., Derksen, C., Entin, J., Colliander, A., Xu, X., et Mavrovic, A. (2018). Capturing agricultural soil freeze/thaw state through remote sensing and ground observations: a soil freeze/thaw validation campaign, *Remote Sensing of Environment*, 211, 59-70.

Sanchez-Pinto, L.N., Venable, L.R., Fahrenbach, J. et Churpek, M.M. (2018). Comparison of variable selection methods for clinical predictive modeling. *International Journal of Medical Informatics*, 116, 10-17.

Saucier, J.-P., Robitaille, A. et Grondin, P. (2009). *Cadre bioclimatique du Québec*. In Manuel de foresterie, 2nd edition. Edited by R. Doucet and M. Côté. Ordre des ingénieurs forestiers du Québec, Éditions Multimondes, Québec, QC. pp. 186-205.

Saucier, J-P., Baldwin, K., Krestov, P. et Jorgenson, T. (2015). Boreal forests. Dans K. S.-H. Peh, R. T. Corlett et Y. Bergeron (dir.), Routhledge Handbook of Forest Ecology (p. 7-29), New-York: Routhledge Taylor & Francis group.

Saucier, J. P., Bergeron, J. F., Grondin, P. et Robitaille, A. (1998). Les régions écologiques du Québec mériodional : un des éléments du système classification écologique du territoire mis au point par le ministère des Ressources naturelles du Québec. *L'aubelle*, 1-8.

Schliep, E.M., Gelfand, A.E. et Clark, J.S. (2015). Stochastic modeling for velocity of climate change. *International Biometric Society Journal of Agricultural, Biological, and Environmental Statistics*, 20, 323–342.

Schweingruber, F.H. (2007). *Wood structure and environment*. Springer series in wood science, Springer-Verlag Berlin.

Simard, M.; Lecomte, N.; Bergeron, Y.; Bernier, P.Y. et Paré, D. (2007). Forest productivity decline caused by successional paludification of boreal soils. *Ecological Applications*, 17, 1619–1637.

Snyder, R.L., Spano, D., Cesaraccio, C. et Duce, P. (1999). Determining degree-day thresholds from field observations. *International Journal of Biometeorology*, 42, 177-182.

Soil Classification Working Group. (1998). *The Canadian System of Soil Classification*. 3rd ed. Agriculture and Agri-Food Canada. Publication 1646.

Soolanayakanahally, R.Y., Guy, R.D., Silim, S.N. et Song, M. (2013). Timing of photoperiodic competency causes phenological mismatch in balsam poplar (*Populus balsamifera* L.). *Plant, Cell and Environment.* 36, 116-127.

Sutinen, S., Partanen, J., Viherä-Aarnio, A. et Häkkinen, R. (2012). Development and growth of primordial shoots in Norway spruce buds before visible bud burst in relation to time and temperature in the field. *Tree Physiology*, 32, 987-997.

Sutinen, S., Roitto, M. et Repo, T. (2015). Vegetative buds, needles and shoot growth of Norway spruce are affected by experimentally delayed soil thawing in the field. *Forest Ecology and Management*, 336, 217–223.

Sutton, R.F. (1993). Mounding site preparation: A review of European and North American experience. *New Forests*, 7, 151-192.

Sylvestro, R., Rossi, S., Zhang, S., Froment, I., Huang, J.G. et Saracino, A. (2019). From phenology to forest management: ecotypes selection can avoid early or late frosts, but not both. *Forest Ecology and Management*, 436, 21-26.

Tang, J., Körner, C., Muraoka, H., Piao, S., Shen, M., Thackeray, S.J. et Yang, X. (2016). Emerging opportunities and challenges in phenology: a review. *Ecosphere*, 7, e01436.

Tebaldi, C., Hayhoe, K., Arblaster, J.M. et Meehl, G.A. (2006). Going to the extremes, an intercomparison of model-simulated historical and future changes in extreme events. *Climatic Change,* 79, 185–211.

Thiffault, N. et Hébert, F. (2017). Mechanical site preparation and nurse-plant facilitation for the restoration of subarctic forest ecosystems. *Canadian Journal of Forest Research*, 47, 926-934.

Thiffault, N., Hébert, F. et Jobidon, R. (2012). Planted *Picea mariana* growth and nutrition as influenced by sylviculture x nursery interactions on an ericaceous-dominated site. *Silvæ Fennica*, 46, 667-682.

Thiffault, N., Titus, B.D. et Munson A.D. (2004). Black spruce seedlings in a *Kalmia-Vaccinium* association: microsite manipulation to explore interactions in the field. *Canadian Journal of Forest Research*, 34, 1657-1668.

Tolvanen, A., et Kubin, E. (1990). The effect of clear felling and site preparation on microclimate, soil frost and forest regeneration at elevated sites in Kuusamo. *Aquilo, Serie Botanica*, 29, 77–86.

Veillette, J.J. (1994). Evolution and paleohydrology of glacial Lakes Barlow and Ojibway. *Quaternary Science Review*, 13, 945–971.

Vepakomma, U., St-Onges, B. et Kneeshaw, D. (2011). Response of a boreal forest to canopy opening: assessing vertical and lateral tree growth with multi-temporal lidar data. *Ecological applications*, 21, 99-121.

Villeneuve, I., Lamhamedi, M.S., Benomar, L., Rainville, A., DeBlois, J, Beaulieu, J., Bousquet, J., Lambert, M.-C. et Margolis, H. (2016). Morpho-physiological variation of white spruce seedlings from various seed sources and implications for deployment under climate change. *Frontiers in Plant Science*, 7, 1450.

Vitasse, Y., Lenz, A., Hoch, G. et Körner, C. (2014). Earlier leaf-out rather than difference in freezing resistance puts juvenile trees at greater risk of damage than adult trees. *Journal of Ecology*, 102, 981–988.

Vitasse, Y., Signarbieux, C. et Fue, Y.H. (2018). Global warming leads to more uniform spring phenology across elevations. *Proceedings of the National Academy of Sciences U.S.A.*, 115, 1004–1008.

Vitra, A., Lenz, A. et Vitasse, Y. (2017). Frost hardening and dehardening potential in temperate trees from winter to budburst. *New Phytologist*, 216, 113-123.

Vyse, A. (1981). Growth of young spruce plantations in interior British Columbia. The *Forestry Chronicle*, 57, 174-180.

Wallace, J.M. et Hobbs, P.V. (2006). *Atmospheric science an introductory survey*. Elseviewer, London, U. K.

Walther, G.R., Post, E., Convey, P. et autres (2002). Ecological responses to recent climate change. *Nature*, 416, 389–395.

Wang, Y., Case, B., Rossi, S., Zhu, L., Liang, E. et Ellison, A. (2019). Frost controls spring phenology of juvenile Smith fir along elevational gradients on the southeastern Tibetan Plateau. *International Journal of Biometeorology*, 63, 963-972.

Wang, P., Zhao, T., Shi, J., Hu, T., Roy, A., Qiu, Y. et Lu, H. (2019). Parameterization of freeze/thaw discrimination function algorithm using dense in-situ observation network data. *International Journal of Digital Earth*, 12, 980-994.

Zuur, A., Ieno, E.N., Walker, N., Saveliev, A.A. et Smith, G.M. (2009). *Mixed effects models and extensions in ecology with R*. Springer-Verlag New York.